Synthesis and Design of Distillation based Separation Schemes

Bek-Pedersen, Erik

Publication date:
2003

Document Version
Publisher's PDF, also known as Version of record

Synthesis and Design of Distillation based Separation Schemes

Ph.D. Thesis

Erik Bek-Pedersen
CAPEC
Department of Chemical Engineering
Technical University of Denmark

October 2002

Preface

This thesis is submitted as partial fulfillment of the requirements for the Ph.D.–degree at Danmarks Tekniske Universitet (Technical University of Denmark).

The work has been carried out at Institut for Kemiteknik (Department of Chemical Engineering) from September 1999 to October 2002 under the supervision of Professor Rafiqul Gani.

I would like to thank all the students and co-workers at the Computer Aided Process Engineering Center (CAPEC) at the Department of Chemical Engineering at Technical University of Denmark with whom I have worked during my time in CAPEC. I am grateful for the many good and fruitful discussions about the work and research, and the contributions to an inspiring atmosphere and a good social climate. I would like to express my gratitude to Professor Rafiqul Gani for giving me the opportunity to work on an interesting project, and for his inspiration and cooporation on the research presented in this thesis. His involvement, encouragement and inspiration has been very helpful and doing this Ph.D. project under his supervision has been rewarding. I am grateful for Danmarks Tekniske Universitet for providing the funding of this project.

Finally I would like to thank my family and friends for their support and understanding, throughout the project. There have been times when moral support was needed, and I have had little time for other things than work. This is gratefully acknowledged.

København, October 2002

Erik Bek-Pedersen

Abstract

This thesis describes a new driving force based approach to the synthesis, design and operation of separation processes. Based on the definition of driving force, as the difference in composition between two co-existing phases, simple and highly accurate methods for synthesis and design have been developed. These methods consequently exploit the differences in compositions between two co-existing phases, and rely on these differences for identification of separation feasibility and the synthesis and design of the corresponding feasible separation techniques. The concept of a maximum driving force (its size and relative location) has been introduced as a design and operational parameter. On the basis of this parameter, a large number of methods for the solution of separation synthesis and design/operation problems have been developed. This includes methods for the synthesis of separation schemes for distillation columns, hybrid separation schemes, and the design/operation of simple, complex and reactive distillation columns, as well as the retrofit of distillation columns. By targeting the separation operation at the largest driving force, synthesis/design corresponding to the easiest separation and the near optimal energy consumption are obtained. Thus, near optimal solutions are obtained through simple, visual techniques without performing any rigorous mass or energy balance calculations. The methods proposed for synthesis and design have been tested and verified thoroughly in a series of case studies and application examples, primarily involving separation systems with various types of distillation operations.

Resumé på dansk

I forbindelse med design af kemiske procesanlæg er anvendelse af seperationsprocesser ofte påkrævet. Seperation kræver som hovedregel altid energi for at indtræffe. Derfor er det ved valg af seperationsmetode, såvel som ved design af seperationsanlæg vigtigt at overveje hvilke seperationsmetoder der anvendes, da den økonomiske forskel (energiforbruget) på drift mellem to seperationsmetoder kan være ganske betydelig. Det er væsentligt i denne sammenhæng at seperationen kan ske med mindst mulig energi i den daglige drift. I forbindelse med design af seperationsanlæg (destillationsanlæg) er der en række parametre man kan variere, som har relativ stor indflydelse på energiforbruget, for eksempel har reflux forhold og placering af fødebund stor indflydelse på energiforbruget.

Denne afhandling beskriver en ny metodik til at udvikle og designe seperationsprocesser. Baseret på definitionen af drivende kræfter i seperationsprocesser som forskellen i sammensæning mellem to sameksisterende faser, er der udviklet en række metoder til at designe og udvikle seperationsanlæg. Disse metoder er baseret på kendskabet til fasesammensætninger, og udnytter forskellen i fasesammensætningen mellem nøglekomponenter i de enkelte seperationsenheder til at fastlægge design og operationsforhold. Metodikken i denne afhandling er baseret på drivende kræfter er blevet anvendt til lœsning af en række problemstillinger angående seperationsanlæg. Metoderne baserer sig på enkel visuel forståelse af fasesammensætningerne og simple beregninger. På denne baggrund kan en række problemer løses, og de opnåede løsninger er tilmed optimale (eller tæt på) med hensyn til energiforbrug. De udviklede metoder benytter sig af størrelsen på den største drivende kræft, og dennes relative position som design parametre. Eksempler på typer af design der er udviklet løsningsmodeller til er; simple destillationskolonner, komplicerede destillationskolonner, herunder reaktive destillationskolonner. Der er udviklet metoder til bestemmelse af rækkefølgen af destillationskolonner, og hvordan destillation som proces mest hensigtsmæssigt kan kombineres med andre processer udfra et energimæssigt synspunkt. Ideen i de udviklede metoder er at de tager udgangspunkt i den største drivende kræft, fordi denne er tæt forbundet med hvor nemt det er at foretage en seperation, og dermed også med den mængde energi seperationen kræver. Ved at tage udgangspunkt i den største drivende kræft som parameter, opnås det design der kræver mindst energi til drift. I denne afhandling er den primære seperationsmetode der er behandlet destillation. Anvendelsen af den udviklede metodik er belyst ved en række eksempler som er løst ved brug af de udviklede metoder.

Contents

Appendices

List of Figures

List of Tables

1

INTRODUCTION

Separation of chemical species is an operation that can be found in almost all chemical process plants. Synthesis of separation processes can be described as the determination of the set of separation tasks that needs to be performed by a corresponding set of separation techniques and their sequences in order to achieve a desired separation. The design and operation of a separation technique refer to the determination of the values of a set of design variables and the condition of operation so that the corresponding separation tasks can be achieved. Therefore, given the composition of the mixture to be separated and the specifications of the desired products that need to be separated from the mixture, the objective is to identify the best process flowsheet that performs the necessary separation tasks. In addition, appropriate and consistent design and operating conditions must be determined as part of the lay-out of the process.

The methodologies usually applied in separation synthesis can be categorized in three main approaches:

Those that employ heuristic rules: These methods rely on different sets of guidelines, which are based on observations and experiences obtained from existing processes, and are often simple and explicit rules. In distillation synthesis, heuristic rules relate, for example, feed mixtures to the size of the fractions that appear in the top and the bottom products of each split, and/or to the size of the relative volatility between the sets of key compounds. However, such heuristic rules may be contradictory, and they must be considered carefully before application. Heuristic methods may be applied both to the retrofit of existing processes and to the synthesis of new separation flowsheets.

Those that employ mathematical programming techniques: These are mathematical programming-based techniques in separation synthesis that employ numerical (optimisation) methods to determine the best flowsheet. In general, these methods require a significant amount of work to solve the mathematical optimisation problem. When applying this methodology, usually all the alternatives to the separation synthesis are embedded in a comprehensive superstructure. A superstructure contains the alternative separation techniques and combinations of these to be considered in the final design. Then, the optimal solution may be found by searching through all the possible synthesis routes/configurations in the superstructure. The success of this kind of methodology is dependent on a suitable solver to be available as well as to the

representation of alternative solutions embedded in the superstructure, and the level of accuracy in the model for each unit operation. Besides, the alternative solutions considered must be feasible, otherwise an optimum solution cannot be found. The solution of such a mathematical optimisation problem is often highly complex, and requires an extensive effort.

Those that employ thermodynamic insights: These methodologies are based on insights gained from the chemical/physical properties of the mixture compounds in the separation synthesis and design problem, rather than heuristics or mathematical optimisation techniques. Generally it can be said, for these techniques that based on the analysis of the mixture compound properties, feasible separation techniques for each split are identified through established property-separation technique/task relationships. That is, the compound/mixture properties relevant to different separation techniques are estimated and used to generate physically feasible separation flowsheets. The goal of these methodologies is to identify feasible flowsheets and operating conditions, based on thermodynamic properties of the system involved in the separation. An important advantage of these methods is that feasible and accurate flowsheets are generated without the use of rigorous simulation models. Also, these flowsheets may serve as very good initial estimates for the mathematical programming techniques.

The objective of this Ph.D. project is to propose methods for optimal (or near optimal) solutions for the synthesis and design of separation processes in general, and distillation based separation in particular. Since separation processes usually make use of some kind of driving force to achieve the desired separation, it is advantageous to perform a driving force analysis at the earliest possible stage in the synthesis/design of a separation process. The methods developed in this thesis are based on the definition of driving force as the difference in composition between two co-existing phases, and emphasis has been placed on optimal solutions with respect to energy consumption. With this definition of driving force, the synthesis/design approach developed in this thesis, is based on the actual thermodynamic behaviour of the separation processes, and using this approach, the largest possible driving force can be identified and utilized in the design. Previously developed methods for separation synthesis and design have not tried to maximise the driving force. The results of this Ph.D. project show how this approach based on the difference in composition between two co-existing phases in a rapid and visual way (without performing any rigorous mass and/or energy balance calculations) leads to optimum (or near optimum) design of separation processes.

The driving forces can be generated or caused by various techniques related to different chemical/physical properties. The driving force, defined in this thesis for distillation and evaporation as the difference in composition between the vapour phase and the liquid phase, is generated by the addition/removal of energy. A good indication of the size of the driving force can be obtained by observing the differences of properties such as the boiling point and vapour pressure of the key compounds in the separation task. When the driving force becomes small, separation becomes difficult and at zero driving force no sepa-

ration can take place, whereas when the driving force approaches a maximum, separation becomes the easiest. This feature is a consequence of the driving force being inversely proportional to the energy added to the system to create and maintain the two-phase (often vapour-liquid) system.

The developed framework of synthesis/design algorithms thus represents a new, simple but accurate, thermodynamically consistent and flexible but generalized framework for synthesis/design of separation processes. This development closes a gap in the synthesis and design of separation systems, since not only feasible, but also optimum (or, at least, near optimum) solutions can now be found on a very simple basis, applying a thermodynamic insight based approach rather than rigorous mathematical optimisation. An important feature of the methods in this driving force based framework is that they can at a very early stage of the process design phase provide near optimum solutions and thereby help to obtain highly reliable predictions of optimal design solutions. In this way complex optimisation problems, where very large superstructures needs to be searched can be avoided, as is shown on the basis of some examples in chapter 5. In a schematic form of the framework of driving force methods for synthesis and design, it is outlined what inputs are required for each algorithm, and what is the output from the corresponding algorithms (presented in chapter 4). The algorithms are verified in chapter 5 on a large range of application examples, where it is illustrated how simple, visual and easy it is to implement each method.

The thesis comprises a total of six chapters. Chapter 2 covers the theoretical background of the thesis. Different problem formulations in synthesis and design are discussed here, together with a selection of state-of-the-art solution methods reported in the open literature. In chapter 3, a problem formulation of the synthesis/design methods considered in this thesis is given, and a brief introduction of some methods and tools applied to the solution of the problems is also given. The basic principles of the driving force concept, and the algorithms developed on this basis are presented in chapter 4. The application of the different driving force based algorithms to a range of illustrative application examples are presented in chapter 5. Finally, chapter 6 gives a short summary of the thesis together with some concluding remarks. The future directions and application of the driving force concept is also briefly discussed.

2

THEORETICAL BACKGROUND

2.1 Introduction

There are many issues one could consider regarding choice and layout of unit operations, in order to make appropriate decisions in the synthesis and design of chemical process flowsheets. In the process of generating a design for a manufacturing facility, it is important to make correct decisions at an early stage of the design phase. A chemical process flowsheet consists of, among other things, a reaction part and a separation part, on which integrated mass and energy networks may be applied. The important steps in process synthesis are:

1. Reactors and reaction network synthesis.
2. Separation system synthesis.
3. Mass and energy integrated networks, *e.g.* heat exchanger networks (HEN).

The issue of recycle streams within the flowsheet is also important, and may significantly affect other design decisions and variables, such as size of equipment and stream compositions. In order to maintain a high production rate, recycling of effluent streams from the reactor and downstream separation units may be introduced. However, it is obvious that the recycling of streams cause larger mass flows, which lead to larger units within the recycle loop.

When exploring possible synthesis routes for a given product, the first step in all operations is to gather information, for example, properties of pure compounds and/or mixtures involved in the process. Also, the use of alternative feasible reaction schemes, solvents, separation techniques need to be considered. Biegler *et al.* (1997) state the elementary steps of flowsheet synthesis as:

1. Gathering information.
2. Representation of alternatives.

3. Assessment and evaluation of preliminary designs.

4. Generating and searching among these alternatives.

In this thesis, the focus is on the separation synthesis part of the flowsheet, in particular, separation by distillation. Besides distillation columns, hybrid separation schemes, where distillation is combined with other separation techniques are also considered, as well as reactive distillation where reaction and separation are taking place in the same distillation column. Considering the separation part of a flowsheet, the unit operations can be dealt with individually or simultanously, and be designed to be part of an integrated mass and/or energy network.

The objective of this chapter is to give an overview of the important issues related to separation synthesis, as well as to present methods for the synthesis of separation processes. A brief overview of the current state of the art on separation synthesis and design and some related topics is given in this chapter.

2.2 Separation system synthesis

This section deals with the synthesis of separation schemes. The main focus is on the topics in the field of synthesis that are relevant to this thesis, *i.e.*, mainly distillation based separation systems.

A separation problem is defined by the feed stream(s) and the final products. The problem may have one feed stream or multiple feed streams from different sources. The products can be of high purity (pure compounds) or of low purity (fractions of compounds).

> *The problem is to determine the separation tasks, the techniques employed to perform the tasks and the sequence of the tasks that would achieve the desired separation.*

The problem stated above is one formulation of the separation problem. Other similar formulations are given by *e.g.* Jaksland *et al.* (1995), Hostrup (2001) and Barnicki and Fair (1990). Hostrup (2001), for example, emphasizes the consideration of different potential separation techniques and determination of appropriate operating conditions for the feasible (and optimal) separation technique. Barnicki and Fair (1990) state that for a given mixture, and knowing the properties of the mixture and the desired specifications, a limited number of feasible (optimium) process designs can be selected from a great variety of separation methods.

In this section, different approaches to separation synthesis, such as heuristic, insights based approaches, graphical approaches and optimisation are described.

2.2.1 Heuristic approaches

The most commonly used approach is the heuristic approach of various types. Heuristic approaches give guidelines or rules of how to compose chemical flowsheets relying on experience. A number of heuristic methods in separation synthesis have been reported in the open literature, and a brief overview will be given below.

Douglas (1985) presents a general hierachical decision framework, where the separation task is divided into two levels, namely one level for vapour recovery and one level for liquid recovery. Based on this information, heuristic rules seek to guide the user through the selection of separation tasks (what separations are to be performed) and techniques (which separation techniques should be employed). Barnicki and Fair (1990, 1992) have proposed a task-oriented knowledge-based approach to the separation synthesis problem. This approach is also based on the phase identity of the feed mixture (vapour or liquid phase). The *selector module* in the knowledge based system then selects the separation techniques for each sub-task, based on process characteristics and pure compound properties. Chen and Fan (1993) have proposed a heuristic synthesis procedure with special emphasis on stream splitting, where only sharp separations are assumed. More recently McCarthy *et al.* (1998) have proposed an automated procedure for product separation synthesis. To begin with, the procedure employs an in-depth tree search in order to locate solutions and the unit operation design variable discretisation to reduce the search space. Then, based on the stream specifications, alternative separation methods are proposed based on different splits and mixers, until the final products have been achieved, thus avoiding mapping into an a priori generated superstructure.

A topic that attracted a lot of attention in the literature published until the 1970's is the heuristic rules for separation synthesis where only distillation columns are considered. Hendry and Hughes (1972), Thomson and King (1972), Heaven (1970) have, among many others, studied the relative cost of different sequences of simple distillation columns. They all lead to heuristic rules suggesting how to sequence distillation trains. Similar sets of heuristic rules are, for example, given by King (1980) and Smith (1995), while a thorough review of the methods is given by Nishida *et al.* (1981).

2.2.2 Insights based approaches

Insights based approaches to synthesis and design are methods that are relying on physical/chemical insights to identify feasible process flowsheets, rather than employing heuristics or optimisation. The insights based techniques are thus relying on thermodynamic data of mixture compounds in the synthesis as well as the design and analysis of feasible solutions to chemical process flowsheets.

A synthesis approach based on thermodynamic insights has been proposed by Jaksland (1996). Jaksland applies thermodynamic insights combined with a set of rules related to physio-chemical properties to choose separation techniques

and to generate separation sequences. These rules are relating the ratio of different properties of mixture compounds to a selection of relevant separation techniques, thus exploiting the feasibility of different techniques for the particular mixture. The method employs two main levels. In the first level differences in compound properties are calculated as ratios for a wide range of properties. These ratios are then used for initial screening among a large number of separation techniques to identify those that are feasible. In the second level a more detailed analysis of the mixture is applied for further screening. This also covers separation techniques which make use of solvents, that are identified according to a molecular design framework adapted from Gani *et al.* (1991). After this stage, in the second (higher) level suggestions for the sequencing of the separation tasks with the corresponding relevant separation techniques, as well as determination of the conditions of operation are also included.

The synthesis approach of Jaksland (1996) has been further extended by Hostrup (2001), who proposes an integrated approach to the solution of process synthesis, design and analysis problems. The integrated concept combines thermodynamic insights with structural optimisation techniques and consists of a problem formulation step, an optimisation step and a validation/analysis step. In this way Hostrup (2001) takes advantage of optimisation techniques to compare the alternative synthesis routes generated by thermodynamic insights.

2.2.3 Graphical approaches

Synthesis/design as well as the analysis using graphical (visual) techniques, provide an intuitive understanding of the process behaviour. The advantage of graphical approaches is especially noticeable, when phenomena like azeotropes and distillation boundaries are present in the mixture to be separated. Then, the use of visual techniques for the synthesis of separation processes can form an excellent basis for understanding the behaviour of the process.

A number of researchers have developed graphical tools for the synthesis of distillation based separation processes and a selection of these are discussed here. Graphical synthesis methods are mainly based on triangular diagrams with residue curve maps or distillation line maps. Such an approach to synthesis has been reported by Malone and Doherty (1995), who developed a comprehensive synthesis framework employing triangular diagrams, and implemented it in a computer program called MAYFLOWER, where residue curve maps are combined with heuristic rules in a hybrid synthesis approach. Apart from simple distillation, MAYFLOWER also considers complex distillation columns and liquid-liquid extraction as possible separation alternatives. The method allows for the use of recycle streams to cross distillation boundaries within the flowsheet, in order to reach pure compound properties. Bossen *et al.* (1993) have developed computational tools for synthesis as well as design algorithms for the separation (distillation) of ternary azeotropic mixtures. This approach relies on the identification of azeotropes and distillation boundaries in ternary diagrams, and based on the analysis of this information a number of synthesis

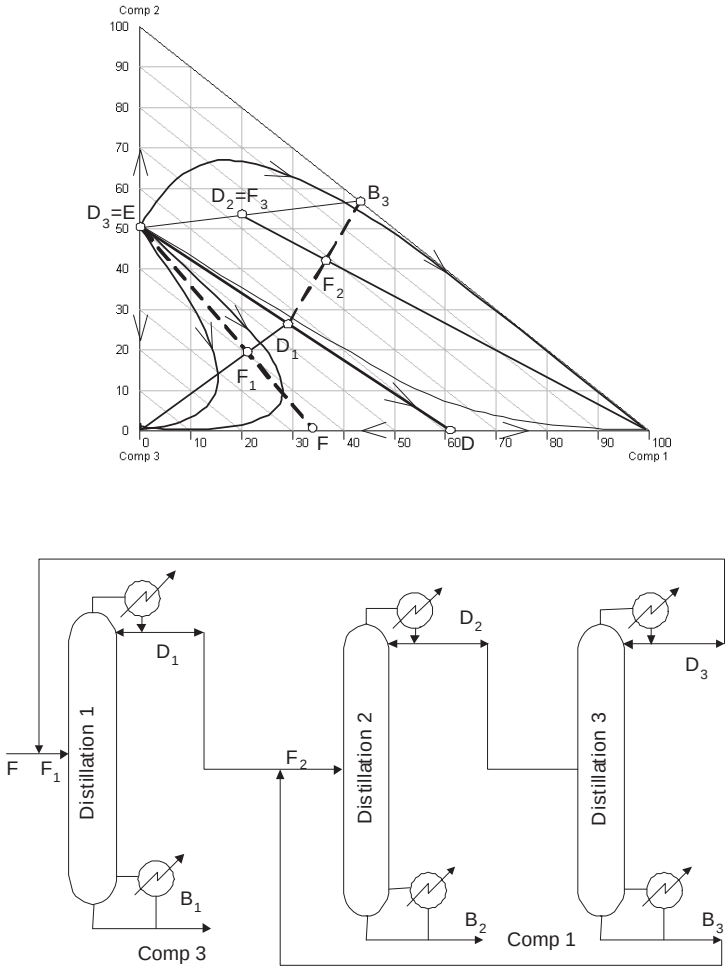

Figure 2.1: Distillation sequence with recycle for entrainer-based separation of a binary azeotropic mixture.

and design rules are proposed. Stichlmair and Herguijuela (1992) also developed a generalised synthesis approach for the distillation of ternary azeotropic mixtures, based on distillation lines. Here, they combined entrainer properties with the properties of the azeotropic mixture to formulate some criteria for the selection of entrainers in order to be able to bypass azeotropic points and for the crossing of distillation boundaries in ternary azeotropic mixtures. In this approach hybrid schemes employing decantation, absorption, extraction and membrane permeation apart from distillation are also considered as means to produce pure compound products. Another approach of the graphical type has

been developed by Laroche *et al.* (1992). They present a method for the selection of entrainers to *break* binary azeotropic mixtures, and propose a method to predict possible (feasible) combinations of distillation flowsheet sequences and alternative solvents. Extensive work on this topic has also been done by the group of Westerberg, (*e.g.* Wahnschafft *et al.* (1991), Wahnschafft *et al.* (1992b), Wahnschafft *et al.* (1993)), who developed a program called SPLIT. In this program, recycle streams within the flowsheet are allowed in order to cross distillation boundaries. Peterson and Partin (1997) developed what they call *Temperature Sequences*, which is a method to charaterize distillation boundary maps for ternary systems, based on boiling points of the pure compounds present in the feed mixture and azeotropic data. The method lists all the possible temperature sequences for a given boundary map. The technique is then applied for initial screening of distillation sequences. The work of Petlyuk (*e.g.* Petlyuk (1997) and Petlyuk and Danilov (1998)) on composition regions in ternary diagrams is also useful in the synthesis of azeotropic distillation schemes.

A thorough review on azeotropic distillation has been given by Widagdo and Seider (1996), where a similar example to the one shown in figure 2.1 is also given. This figure illustrates how distillation line diagrams serve as a tool for the synthesis of distillation column schemes.

Finally, in some cases azeotropic points are sensitive to pressure changes. This is the basis of another distillation based separation technique called *pressure-swing distillation*. This technique can be applied to recover two pure compound products from a binary azeotropic mixture, without the use of an entrainer or another external source (for example a membrane). The concept of pressure-swing distillation is illustrated in figure 2.2, where it can clearly be seen how the composition of the azeotrope is moving with the change of pressure. In this figure, it is also shown how the corresponding separation scheme is obtained, taking advantage of the pressure sensitivity of the azeotrope. Knapp and Doherty (1992) give a list of binary mixtures with pressure sensitive azeotropes.

2.2.4 Optimisation approaches

The objective for using optimisation in separation synthesis is to find the best solution, usually among a number of candidate separation schemes. In order to be able to solve the synthesis problem through optimisation, it is essential that models for the unit operations involved have been formulated, and that an appropriate solver is available, so that a mathematical programming (optimisation) problem can be defined and solved.

When applying optimisation to the synthesis of separation processes, it usually involves structural optimisation decisions. A general formulation of this kind of problem is given by Biegler *et al.* (1997) as:

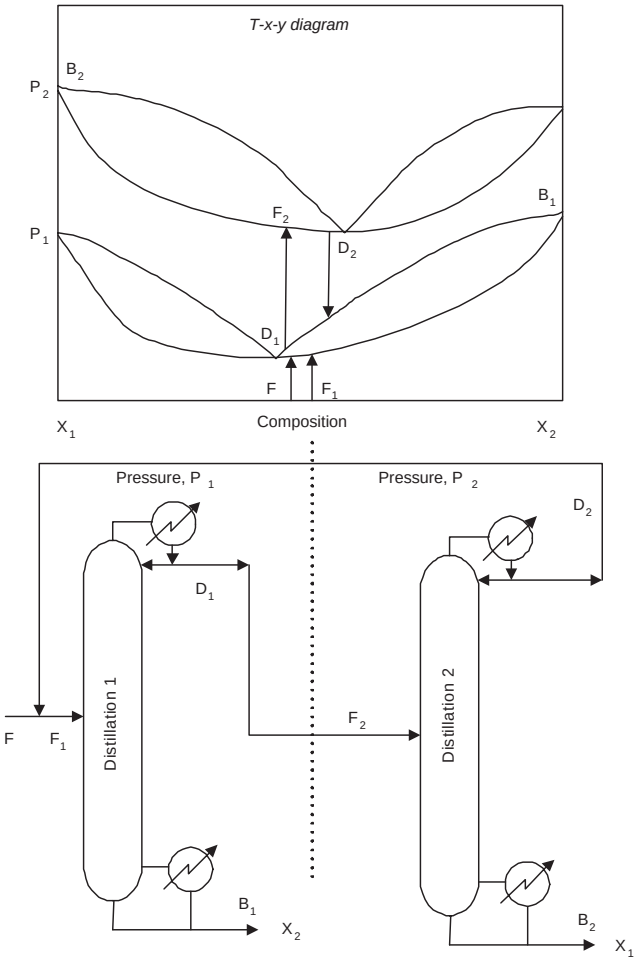

Figure 2.2: Pressure-swing distillation for the separation of minimum boiling azeotrope; (a) *txy* diagram at two pressures; (b) corresponding distillation sequence.

$$\begin{aligned} \min_{x,y} \quad & Z = C(x,y) \\ s.t. \quad & h(x) = 0 \\ & g(x,y) \leq 0 \\ & x \in X \quad y \in \{0,1\}^m \end{aligned} \tag{2.1}$$

The continuous design variables, x, are optimised so that the minimum value of $Z(x)$ has been deduced and still meet the criteria of the constraints, $g(x)$

and $h(x)$. The discussion in this section deals specifically with the different approaches that apply optimisation techniques in separation synthesis as reported in the open literature. The theory of structural optimisation techniques is further treated in section 3.4.2.2,

Structural optimisation techniques have been employed to large numbers of problems involving separation synthesis. Common to all of them is that they are for the most part limited to sequences of distillation columns only. The application of the structural optimisation approach is relying on the derivation of an appropriate superstructure of feasible solutions. A superstructure is a collection of several alternative (separation) process design/synthesis possibilities, and it is essential that the formulation of this superstructure is as comprehensive as possible. Otherwise, the real optimal solution may not be incorporated in the search space. This is often an issue, for example, when complex distillation columns are considered in the superstructure, whether all feasible complex column configurations are considered. The question of possible recycle streams within the superstructure is also an important issue that may cause the superstructure to be defective.

Another question that also needs to be taken into consideration is how rigorous the models of the individual columns/unit operations are, as it is crucial for the solution of the optimisation that the models in the superstructure are consistent and correct. In the paper of Andrecovich and Westerberg (1985), for example, where a *mixed integer linear programming* (MILP) formulation for the synthesis of distillation sequences is proposed, the method is only valid for ideal mixtures, and all splits are calculated by linear equations. A more thorough general approach to this problem has been developed by Aggerwal and Floudas (1990), where non-sharp separations are included and a *mixed integer non-linear programming* (MINLP) problem is solved.

A unified approach has been developed by Hu *et al.* (1991). They generate a superstructure of simple, as well as a large variety of complex distillation columns. The superstructure is formulated and solved as a MINLP problem. The different columns are calculated by short-cut design procedures, employing Underwood's method (see section 2.3.1.2) and thereby limiting the procedure to nearly ideal mixtures. A similar type of work has been carried out by Yeomans and Grossmann (1999). Here non-linear short-cut models are applied for calculation of the individual distillation columns. They operate in two different ways to generate a superstructure, one is the *state task network* (STN) and the other is the *state equipment network* (SEN). Each method defines a superstructure, the STN method links each state in the separation with a task and equipment (distillation column), while the SEN method has the possibility of employing every column for different separation tasks. Complex columns are, however, not represented in the superstructure. Ismail *et al.* (1999) developed a modular synthesis framework for homogenous azeotropic distillation. Here, entrainer and alternative distillation column sequences are explored simultanously in a single optimisation problem. The method employs a multi-purpose mass/heat exchange module to investigate simultanously, separation units and heat and

mass exchange possibilities. In this way optimal separation schemes are identified together with the entrainers.

2.2.4.1 Generation of superstructures

Generating a superstructure for a process flowsheet is in principle difficult. Even for the separation synthesis part of the flowsheet, there are large numbers of alternatives to take into account. Heuristic rules are often applied to reduce the size of the related structural optimisation problem (*e.g.* Kocis and Grossmann (1989)). However, when dealing only with sharp separations (often performed by distillation columns only) the size of the problem is clear, as there is the need for a minimum of one separation unit to perform one split between two adjacent key compounds. So, the minimum number of separation units will be *N-1* for an N-compound mixture. This can be represented as a symmetric binary separation tree (Stephanoloulos and Westerberg, 1976). Figure 2.3 shows a separation superstructure for a five-compound separation. A root node is introduced to represent the feed mixture. The intermediate nodes of the binary tree represent distinct separation tasks, while the terminal nodes represent product targets. Thomson and King (1972) proposed an expression to calculate the number of possible sequences for this kind of superstructure of binary splits. The formula (equation 2.2) states that there are S_R possible separation sequences for NC products.

$$S_R = \frac{[2(NC-1)]!}{NC!(NC-1)!} \tag{2.2}$$

Equation 2.2 has been applied for the calculation of the number of possible distillation column sequences for different numbers of compounds in table 2.1. As can be noticed, even when only sharp splits and only one type of unit operations (*i.e.* distillation columns) are considered, the number of alternatives in the superstructure rapidly increase with the number of compounds to be separated.

NC	S_R
2	1
3	2
4	5
5	14
6	42
8	429
10	4862
20	$1.767 \cdot 10^9$

Table 2.1: Variation in the number of possible sequences of distillation columns as a function of the number of compounds to be separated.

It follows clearly that if the superstructure is expanded further to include for

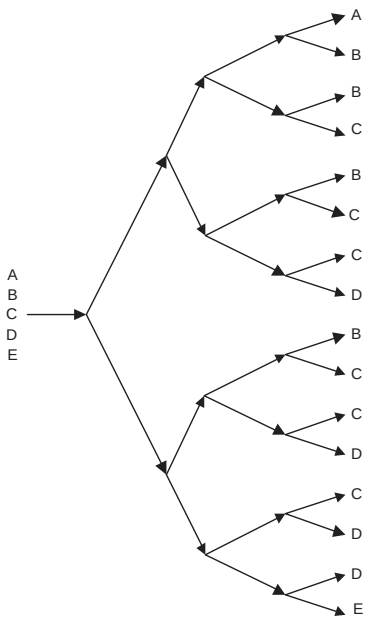

Figure 2.3: Superstructure for the separation of a five-compound mixture.

example non-sharp separations, complex columns and other separation techniques than distillation, the size and complexity of the problem will become immense. Formulating a superstructure model and solving the corresponding MINLP optimisation problem directly are very large tasks, both mathematically and computationally. Therefore, if the superstructure is large and detailed, it is advantageous to identify the structure of the MINLP problem and exploit it so as to reduce the computational costs and increase the reliability of the solution.

2.3 Design of separation systems

The objective in this section is to cover some of the techniques related to the design of the individual separation units in the process flowsheet. The focus here is on distillation columns and the separation systems involving distillation, and also briefly covers hybrid separation schemes and reactive distillation. In the context of this thesis mainly empirical and graphical design methods are considered, as the methods developed in this thesis are of this type (in contrast to mathematical programming methods). Some other approaches, such as optimisation are also briefly mentioned. Although a large number of publications exist on empirical and graphical design methods, an attempt will be made to cover the state of the art for non-rigorous design techniques of distillation

columns.

2.3.1 Distillation column design techniques

Distillation columns have been designed for centuries. Many models of distillation columns have been developed over the last century, and now rigorous computer aided models are available in almost any commercial simulation software package. However, there is still a need for simple distillation models with good accuracy for various reasons. In the open literature, no models have yet been reported that give near optimum designs with respect to energy consumption, without performing rigorous calculations. Some empirical relations for design have been proposed, but they assume ideality of the mixture to be separated. Also, consider for example the case where a distillation column is part of structural optimisation problem. Here it is important that the column does not have to be calculated rigorously, which will lead to high computation time. Besides, it is an advantage for the initialisation of a simulation model to know the approximate numerical values of minimum flows in the column for the initialisation of rigorous simulation calculations.

Calculations for steady-state distillation columns are in most cases based on vapour-liquid equilibrium data. Experimental determination and especially estimation of such data is crucial to the accuracy of the design. The objective in the design of distillation columns is to match the desired product purities as well as keeping the operating costs low. Since the operating costs are proportional to the energy consumption, the aim is to design distillation columns that consume the least energy possible. Rapid and reliable calculation of minimum energy requirement for a specified sharpness of a separation is therefore an important task. In this context, an overview of the existing simple design methods will be given in this section.

2.3.1.1 Pinch zones

In distillation, a pinch zone is defined as a region where separation is limited because infinitesimal concentration changes occur between the vapour and the liquid phases. In order for a separation to occur in this zone, a large number of stages is required, and in the extreme case, even an infinite number of stages are needed to perform the desired separation. Therefore, identification of pinch zones in distillation columns is important. In a simple distillation column where all compounds are present in both products, and when the operating lines intersect on the equilibrium curve, there is an indication of a pinch zone around the feed tray. This is shown by McDonough and Holland (1961) and illustrated in figure 2.4.

Shiras *et al.* (1950) classified multicomponent systems as having either one (*class 1*) or two pinch points (*class 2*). For *class 1* separations, all the compounds in the feed distribute to both the bottom and the distillate products. The single pinch point in this case occurs at the feed stage, as in binary dis-

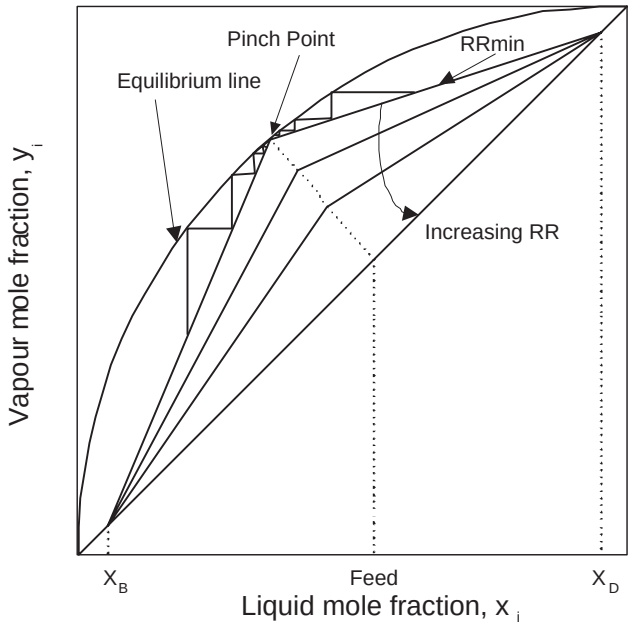

Figure 2.4: Pinch point indication for binary distillation in a McCabe-Thiele diagram with varying RR (RR = reflux ratio).

tillation, and can occur when narrow boiling mixtures are distilled and the separation between the key compounds is non-sharp. In this context, King (1980) defines key compounds as those that 'appear to a significant extent in both products' of the column, whereas compounds boiling lower than the light key or higher than the heavy key are 'relegated almost exclusively to one product or the other'. In the case of *class 2* separations, one or more compounds appear in only one of the products. If neither the distillate nor the bottom product contains all the feed compounds, two pinch points occur away from the feed stage, one on each side of the feed stage in the distillation column.

2.3.1.2 Empirical design methods

A number of empirical correlations for the calculation of distillation columns have been developed over the time. They still play an important role in modern design techniques, since they provide important design parameters, usually based on very little information. A brief overview of the most predominant methods is given below.

The most well-known method is Underwood's method. It has been described in its original version in five publications (Underwood, 1932, 1945, 1946a, 1946b, 1948). Underwood's method gives a general solution to the problem

of minimum reflux ratio for the separation by distillation. It is based on the assumptions of constant molar overflow and constant relative volatility, and thus in reality only applies to ideal mixtures. Underwood's method uses two parameters, φ and ψ for the rectifying and stripping sections respectively. The equations proposed by Underwood are

$$\sum_{i=1}^{NC} \frac{\alpha_i x_{D,i}}{\alpha_i - \varphi} = RR + 1 \tag{2.3}$$

and

$$\sum_{i=1}^{NC} \frac{\alpha_i x_{B,i}}{\alpha_i - \psi} = -S \tag{2.4}$$

Each of the equations 2.3 and 2.4 have as many solutions as there are compounds in the mixture, for a given product composition ($x_{D,i}$, $x_{B,i}$) and reflux ratio (RR). Underwood states that at least one common root, θ exists (where $\theta = \varphi = \psi$). The common root(s) may then be found by multiplication of 2.3 and 2.4 with D and B, respectively, and inserted into the overall column mass balance $x_{F,i}F = x_{D,i}D + x_{B,i}B$ to obtain equation 2.5.

$$\sum_{i=1}^{NC} \frac{\alpha_i x_{F,i}}{\alpha_i - \theta} = 1 - q \tag{2.5}$$

Here q is the liquid fraction of the feed and θ is a common root. To find the minimum reflux ratio, it is necessary to evaluate the common roots of equation 2.5 and putting the value of θ into equation 2.3, to find the minimum reflux ratio. The method requires that the value of θ lies between the values of α for the key compounds of the separation.

Several people have developed similar types of methods, or extended Underwood's method. A few examples of this kind are given below. Glinos and Malone (1984) give an approximate solution to the Underwood equations for ternary mixtures and propose the use of pseudocompounds for multicomponent mixtures. Cerda and Westerberg (1981) developed another method for calculation of the reflux ratio, where it is assumed that for sharp multicomponent separations, the two pinch points always occur two stages above and two stages below the feed stage, which is often not the case. Lestak *et al.* (1989) point out that some of the equations of Cerda and Westerberg (1981) are contradictory with respect to operation with total or partial reboiler and condenser.

Another approach for the determination of distillation design variables is the approach based on the Gilliland correlation (Gilliland, 1940). The Gilliland correlation relates the reflux ratio to the number of stages for the separation between two compounds in a binary mixture or two key compounds in a multicomponent mixture. A plot of the Gilliland correlation in linear coordinates is given in figure 2.5.

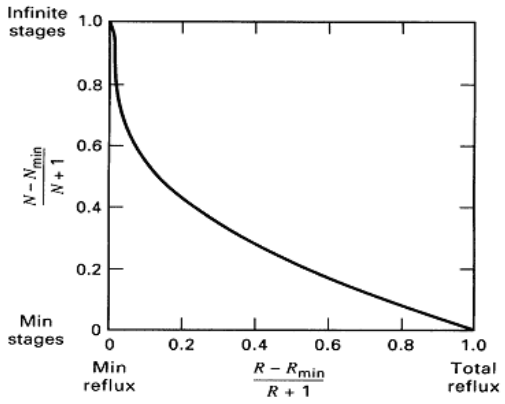

Figure 2.5: Gilliland correlation with linear coordinates.

The Gilliland correlation is useful in the preliminary design of binary and multicomponent separations. As can be seen in figure 2.5, a small increase in the ratio of reflux ratio to minimum reflux ratio causes a large decrease in the number of stages, but further changes in reflux ratio have little effect on the number of stages. Robinson and Gilliland (1950) extended the Gilliland correlation to take the feed condition into account, by utilizing the parameter q (degree of vapourisation). Implicit in the application of the Gilliland correlation is the specification that the theoretical stages are distributed optimally between the rectifying and the stripping sections, for example by using equation 2.6. Martin and Brown (1939) suggest that the optimum feed stage can be located from the ratio of stages above the feed to stages below the feed, by assuming that the ratio is the same as the ratio determined by the Fenske equation (Fenske, 1932) to each of the two sections. This leads to equation 2.6.

$$\frac{N_R}{N_S} \cong \frac{(N_R)_{\min}}{(N_S)_{\min}} = \frac{\log[(x_{LK,D}/z_{LK,F})(z_{HK,F}/x_{HK,D})]}{\log[(z_{LK,F}/x_{LK,B})(x_{HK,B}/z_{HK,F})]} \frac{\log(\alpha_B \alpha_F)^{1/2}}{\log(\alpha_D \alpha_F)^{1/2}} \tag{2.6}$$

Seader and Henley (1998) report that this equation is not very reliable. It is best with symmetrical feeds and separations, (*i.e.* equimolar feed composition and the same product purities). According to Seader and Henley (1998), a better approximation of the optimum feed stage location can be made by employing the empirical equation of Kirkbride (1944):

$$\frac{N_R}{N_S} = \left[\left(\frac{z_{HK,F}}{z_{LK,F}} \right) \left(\frac{x_{LK,B}}{x_{HK,D}} \right)^2 \left(\frac{B}{D} \right) \right]^{0.206} \tag{2.7}$$

Another comparison of equation 2.6 and equation 2.7 has been performed by Oliver (1966) where it was also found that the Kirkbride equation (equation

2.7) was superior to the Fenske equation (equation 2.6).

2.3.1.3 Graphical design methods

Graphical methods are important for design and synthesis of distillation columns, as they can provide highly valuable visual representation of the operation of the process. Through graphical design methods, feasibility and operational constraints as well as operating conditions can be exploited in an intuitive way. Therefore, graphical design techniques play an important role in the design of distillation columns.

One of the most well-known design techniques is the graphical McCabe-Thiele method (McCabe and Thiele, 1925). This approach can determine the number of theoretical stages as well as the feed stage location and reflux ratio. It is based on the knowledge of the feed composition, the desired product compositions and it requires reliable phase composition data at the given pressure of operation. Figure 2.6 illustrates how the operating lines and equilibrium curve together constitute the McCabe-Thiele diagram, and how they are related to design variables such as product compositions and reflux ratio. Figure 2.4 provides another example of McCabe-Thiele diagram that shows the operating lines for different values of reflux ratios.

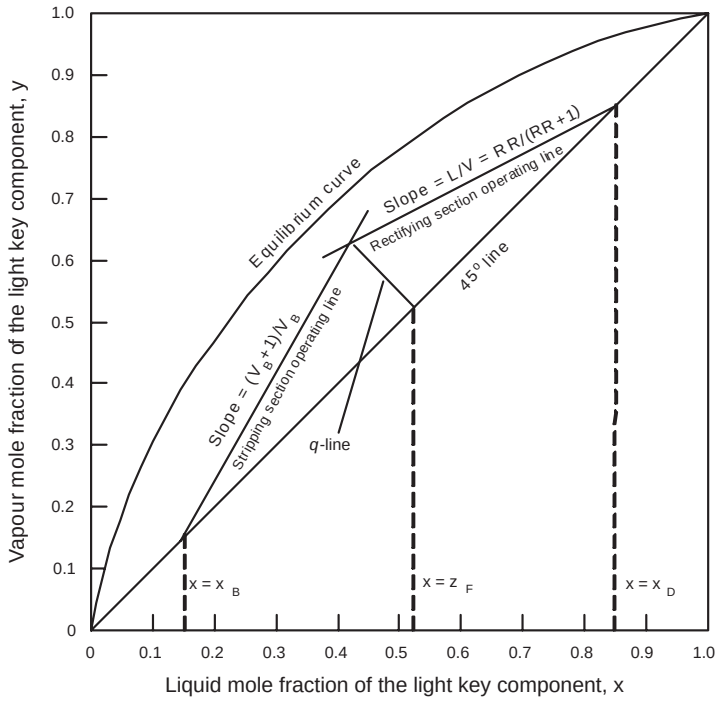

Figure 2.6: McCabe-Thiele diagrams with operating lines.

The McCabe-Thiele method is based on the assumption of *constant molar overflow* (constant molar vapour and liquid flow rates in each section of the column) and is generally useful for the visualisation of design decisions related to distillation columns. However, since the method was published in 1925, a significant number of alternative methods (graphical, empirical and numeric) have been developed that are more efficient and reliable. The McCabe-Thiele method is also capable of predicting the number of *ideal* equilibrium stages necessary for a given separation at a given reflux. Figure 2.4, illustrates how the method also gives the minimum reflux, corresponding to the pinch point at the feed stage. This corresponds to an infinite number of stages, whereas the operation at total reflux corresponds to operating lines coinciding with the diagonal in the diagram, and the minimum number of stages. The method is still widely used, although mainly for generating quick initial designs.

Another classical graphical design approach is the Ponchon-Savarit method (Ponchon (1921) and Savarit (1922)). Ponchon and Savarit developed a design method based on an enthalpy concentration diagram, where both enthalpy and mass balances are considered together with the thermodynamic equilibrium. The method does not give the same intuitive graphical description as the McCabe-Thiele method. For this reason, and also due to the existence of much more accurate rigorous models (also employing enthalpy balances), it is not very commonly used anymore. Recently, however, Reyes *et al.* (2000) extended the method to handle ternary mixtures.

The visual (graphical) design tool that is most extensively used nowadays is triangular diagrams, which are used for systems of three (or more) compounds. Triangular diagrams have been developed initially for graphical analysis, because they can provide valuable insights and design assistance for a variety of unit operations, including distillation columns. For ternary distillation, the distillate and bottom products of a distillation column have to meet two conditions (Stichlmair and Herguijuela (1992)). The first is the simple linear mass balance (equation 2.8) and the second is the complex internal concentration profile (equation 2.9).

$$\begin{aligned} F &= D + B \\ F \cdot x_{Fi} &= D \cdot x_{Di} + B \cdot x_{Bi} \end{aligned} \tag{2.8}$$

$$x_{i,n} = f(x_{Fi}, p_i^0, \gamma_i, T, P, n_1, n_2, RR, D/F, ...) \tag{2.9}$$

The convergence of the above equations is often difficult and cumbersome, and solving these equations efficiently requires complex computer programs. To avoid this at an initial design stage, a number of authors have presented methods for prediction of feasible product (regions) in ternary distillation without performing rigorous design calculations. In general, these methods rely on operating at total reflux, but some authors have also treated the case of separation at finite reflux. A short introduction and overview is given below.

Distillation lines are calculated by stepping off equilibrium stages in a column at total reflux from a given feed location, and they show the feasible distillate

and bottom product regions at total reflux. When operating at total reflux, the composition profile in the column is identical to the corresponding distillation line. This means that the bottom and distillate products need to lie on the same distillation line, which have to pass through the feed composition F in order to match the material balance.

Sometimes distillation lines are confused with residue curves. They differ from distillation lines in the way that where the distillation line is calculated for a continuous process, the residue curve is calculated for a batch process (Seader and Henley (1998)) and in principle is tracing of the composition of the residue of a simple Rayleigh batch distillation in time. Seider *et al.* (1999) point out that the two types of lines/curves do not coincide, and if the assumption is made that they do coincide, significant errors may be produced. An example of a ternary system where distillation lines and residue curves are compared is given in figure 2.7, which shows an example given by Fidkowski *et al.* (1993). The dashed lines are distillation lines and the solid lines are residue curves. Note the difference between the two types of lines is pronounced where extensive curvature is exhibited. It is evident that the distillation lines are limiting the composition range more than the residue curves. Widagdo and Seider (1996) comment that distillation lines should be used rather than residue curves, for analysis as well as design purposes, as they in general match *reality* better.

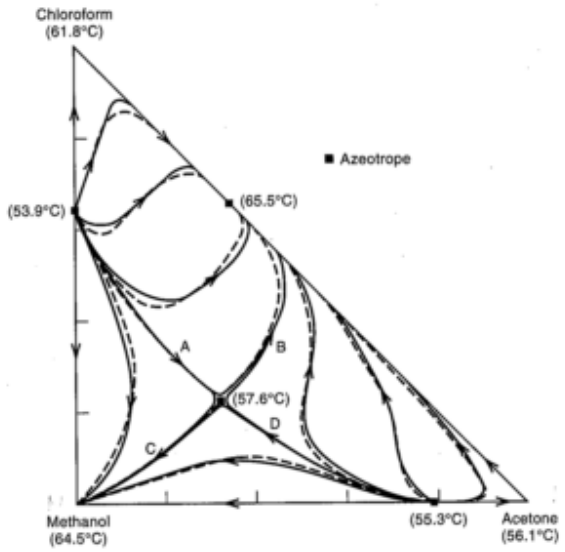

Figure 2.7: Comparison of residue curves (solid) and distillation curves (dashed) [Fidkowski *et al.* (1993)].

Fixed points are important properties of triangular diagrams. These are points where the change in liquid composition with respect to time is zero,

(*i.e.* $dx/dt=0$). This occurs in connection with pure compound vertices and azeotropic points. The behaviour of residue curves in the vicinity of fixed points depends on their stability. In the case where all residue curves are directed towards a fixed point, it is called a *stable node*, as illustrated in figure 2.8a, and when all the curves are directed away from the point, it is called an *unstable node* (figure 2.8b), and in case some curves are directed away and some towards the point, it is called a *saddle* (figure 2.8c).

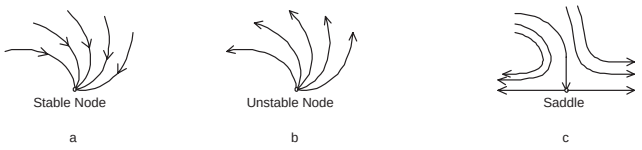

Figure 2.8: Stability of residue curves for ternary systems near *fixed points*.

In the case of a zeotropic (non-azeotropic) ternary distillation, there is only one distillation region, (Seader and Henley, 1998). An example is given in figure 2.9, which is similar to an example given by Stichlmair and Herguijuela (1992). Figure 2.9a shows the possible distillate and bottom fractions. Note the straight lines passing through F, to illustrate alternative products. The straight lines are represented by equation 2.8. Figure 2.9b illustrates the regions of possible (feasible) bottom and distillate products, denoted by B and D, for a specified feed composition, F. The regions are limited by the distillation line also passing through F and the straight mass balance lines passing through F. Note, only the low-boiling compound (Comp 2) and the high-boiling compound (Comp 3) can be separated as a pure compound in only one column.

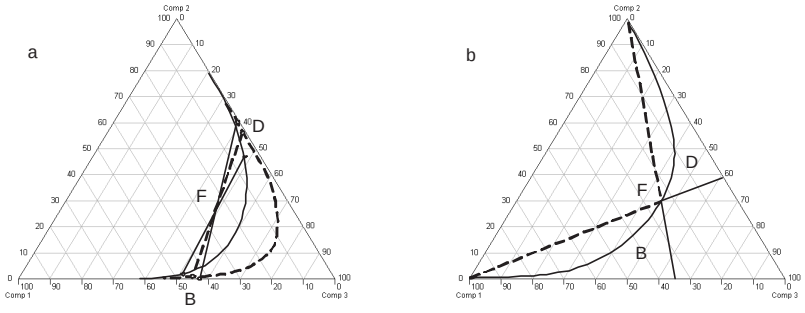

Figure 2.9: Separation region of a ternary zeotropic mixture; (a) determination of possible top and bottom fractions; (b) feasible separation regions.

Two examples of ternary azeotropic systems are given by Seader and Henley (1998) from where figure 2.10 is adapted. Figure 2.10a has two distillation regions caused by two minimum boiling azeotropes, and figure 2.10b shows

four distillation regions caused by two minimum boiling binary azeotropes, one maximum boiling azeotrope and one ternary azeotrope.

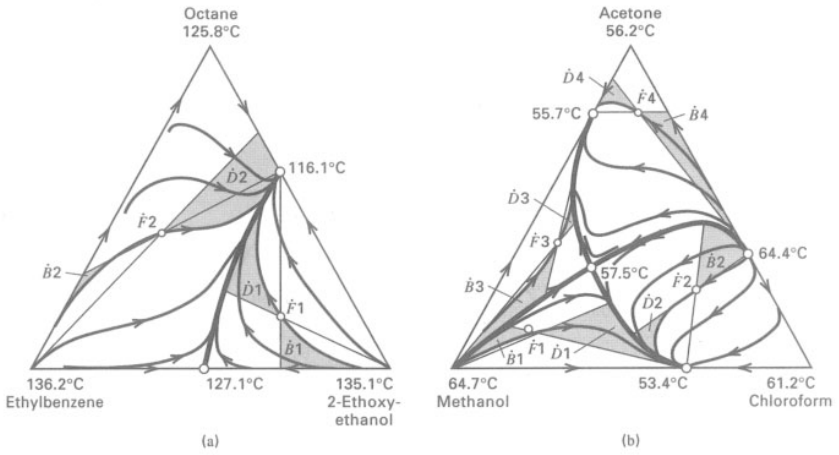

Figure 2.10: Product composition regions for given feed compositions: (a) ternary mixture with two minimum boiling azeotropes; (b) ternary mixture with three binary azeotropes and one ternary azeotrope [(Seader and Henley, 1998)].

In figure 2.10, the achievable product compositions are indicated by the shaded regions showing feasible distillate and bottom products, for the given feeds. As can be seen, all the feed, bottoms and distillate points on the mass balance lines lie within the same distillation boundary line.

In some cases it is possible to cross the distillation boundary at total reflux. This happens when the distillation boundary line is highly curved. Then it is possible to have the feed on one (convex) side of the distillation boundary line, and the distillate and bottom products on the other (concave) side of the distillation region.

An example of this is given in figure 2.11, which illustrates an example given by Widagdo and Seider (1996). The distillation boundary is between the points K and L, forming two regions. Two distillation curves are indicated, a and b, one in each region. As illustrated in figure 2.11, the feed F_1 can be separated into products B_1 and D_1, and also products B_2 (or B_3) and D_2. The feed F_2 can be separated into B_4 and D_4. A detailed treatment of product composition regions is given by Fidkowski *et al.* (1993), Wahnschafft *et al.* (1992a), Stichlmair *et al.* (1989), Widagdo and Seider (1996), Safrit and Westerberg (1997) and by Petlyuk and Danilov (2001). Unlike binary systems, ternary systems may be separated in higher purities with a lower reflux ratio. This was shown by van Dongen and Doherty (1985) and Laroche *et al.* (1992). Fidkowski *et al.* (1993) and Wahnschafft *et al.* (1992a) have developed methods to

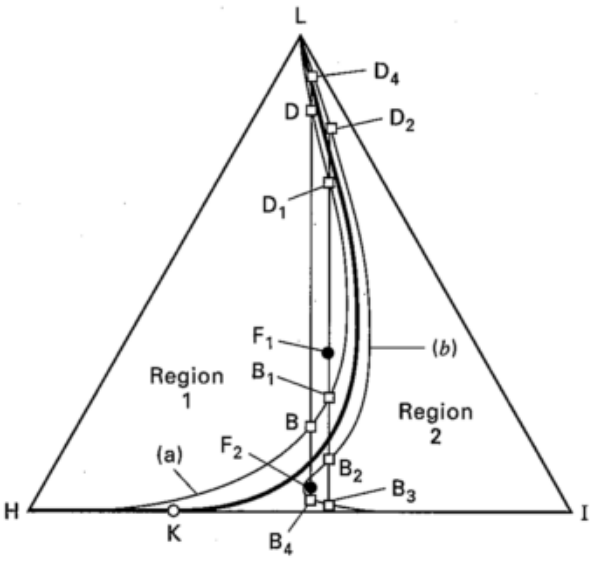

Figure 2.11: Feasible and infeasible crossings of distillation boundaries for an azeotropic system [(Widagdo and Seider, 1996)].

estimate the regions of feasible product composition at finite reflux. Fidkowski *et al.* (1993) developed what they call *distillation limits* which extend the feasible region compared to the distillation boundary. Wahnschafft *et al.* (1992a) developed what they call the *feed-pinch-trajectory*. The methods will not be treated in detail here, but common to the two methods is that they extend the region of feasible product compositions in the regions where the residue curves exhibits large curvature. Widagdo and Seider (1996) comment that the *distillation limit* method is the better one of the two.

Residue curve and distillation line maps are mainly used for the design and analysis of ternary systems. Within the group of ternary systems, the methodology is widely applied to search for, or to test candidate entrainers (solvents) for the separation of binary azeotropic mixtures. In case the solvent has a higher boiling point than any of the two feed compounds, and it does not form an azeotrope with any of them or form two liquid phases, the separation method is called *extractive distillation*. Otherwise, if these restrictions to the entrainer are not complied with, the separation is known as *azeotropic distillation* (Seader and Henley, 1998). Other definitions of these terms also exist. Bossen *et al.* (1993) *e.g.* state that the distillation of all (solvent-based) homogenous ternary mixtures is *extractive distillation*, and the term *azeotropic distillation* is only describing heterogeneous systems. In either case, the entrainers are compared using residue curve and/or distillation line maps. The

process of selecting an entrainer, is directly linked to configuring the separation scheme of (usually) two or three distillation columns (see section 2.2.3). Investigation of criteria that define good entrainers in azeotropic or extractive distillation has caught the attention of many researchers, such as Doherty and Caldarola (1985), Stichlmair *et al.* (1989), Foucher *et al.* (1991), Wahnschafft and Westerberg (1993), Laroche *et al.* (1992) and Hostrup *et al.* (1999). One of the most interesting works amongst these is the one by Laroche *et al.* (1992), who did a comprehensive study on the non-linear relationship between reflux rate and the extent of separation, both for heavy, light and intermediate entrainers.

In the case where two liquid phases are formed in an area of the ternary composition space, the process is called a *heterogeneous azeotropic distillation*. In this case, the separation in the liquid-liquid split region is sometimes done by decantation (*e.g.* water-butanol separation), and sometimes there are two liquid phases and one vapour phase in a part of the distillation column (*e.g.* water-ethanol-benzene separation). In some cases heterogeneous azeotropic separation is preferred, as this is a means to overcome an azeotropic point by decantation, rather than by using an entrainer forming a homogenous mixture. It is sometimes easy to "jump" from one distillation region to another, and in this way attain the desired separation. The decantation is usually applied to the distillate of one of the (usually) two columns in the separation sequence. This is illustrated in figures 2.12 and 2.13. Here an example is given of a residue curve map with mass balance lines and the corresponding heterogeneous azeotropic distillation, where ethanol and water are separated by employing benzene as an entrainer. In the notation of figure 2.12, I, II and III refer to distillation regions.

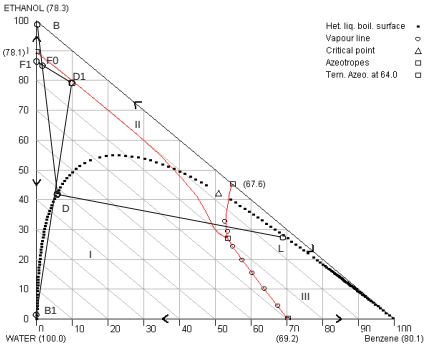

Figure 2.12: Mass balance in ternary diagram for heterogeneous azeotropic distillation.

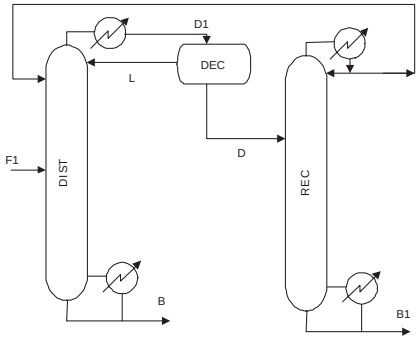

Figure 2.13: The corresponding column sequence for separation.

Different authors have treated the design problem for heterogeneous azeotropic columns, *e.g.* Stichlmair and Herguijuela (1992), Bossen *et al.* (1993). A

comprehensive work has been done by Pham and Doherty (Pham and Doherty (1990a), Pham and Doherty (1990b) and Pham and Doherty (1990c)), and the topic is also covered in the review by Widagdo and Seider (1996).

Another issue in the operation of heterogeneous azeotropic columns is steady state multiplicities. It is essential to be aware when the possibility of more than one steady-state operation point exits, when making design decisions. Magnussen *et al.* (1979) reported three steady states in a column for the separation of water and ethanol, using benzene as an entrainer. Gani and Jørgensen (1994) characterize three types of multiplicity, 1) input multiplicity (a given output can be obtained with multiple input), 2) output multiplicity (a given input has multiple (output) solutions), and 3) state multiplicity (multiple values of internal states exist for the same input and output). The group of Morari has been very active in the field of multiple steady states in azeotropic distillation. Bekiaris and Morari (1996) have developed a method for prediction of steady states in multicomponent mixtures, and they also illustrate the implications which the existence of multiple steady states may cause. Güttinger and Morari (1996) studied multiple steady states in sequences of interlinked columns used for the separation of azeotropic mixtures based on predictive models, and Güttinger *et al.* (1997) did experimental studies of multiple steady states in azeotropic distillation columns.

2.3.2 Complex distillation column design techniques

Distillation configurations with other topological structures than conventional distillation columns (simple distillation columns with one feed stream and two product streams) are often more economical in operation. In the context of this section, the topic is single complex distillation units (columns with side-products/feeds and or thermally coupled columns) only. Topics like heat integration of simple distillation columns and heat pump systems are beyond the scope of this thesis.

It has been shown in different theoretical studies (*e.g.* Petlyuk *et al.* (1965) and Tedder and Rudd (1978)) that differently coupled configurations of distillation columns are capable of saving up to 30% of the energy consumption, or even more compared to conventional sequences of distillation columns. Also, for some coupled (integrated) configurations, there are possibilities of reduced capital cost through the elimination of column shells. Düssel *et al.* (2001) report savings of 42% by operating an actual industrial unit of this kind.

Different configurations of distillation columns have been studied, *e.g.* columns with more than two products, columns with more than one feed, columns with side-rectifier and/or side-stripper, but the configuration that has attracted the most attention (at least from academic researchers) is the fully thermally coupled distillation column (Petlyuk *et al.*, 1965) also known as the *Petlyuk column*. Most of the studies in the literature published are limited to separation of three or four compounds, but the proposed design methods can in some cases be extended to handle mixtures with more compounds. In this section, a brief

overview of design procedures for these types of complex columns is given.

2.3.2.1 Columns with multiple feeds and/or products

Tedder and Rudd (1978) have investigated a number of distillation configurations, including the side-draw arrangements of simple columns. They found that if the intermediate compound was in excess and one of the other compounds was only present in minor quantities, then a configuration with a side-draw distillation column could be applied with advantage. The limits they found are: if there is more than 50% of the intermediate boiling compound in a ternary mixture, and at the same time less than 5% of either the highest or lowest boiling compound, then it may be attractive to use a column with a side-draw. If both bottom and distillate products exceed 5% of the feed mixture, Tedder and Rudd (1978) state that it is difficult to get a pure intermediate product. If less than 5% of the feed mixture is the highest boiling compound (bottom product), then the side-draw should be placed below the feed stage (vapour side-draw), and if less than 5% of the feed mixture is the lightest boiling compound (distillate), then the side-draw should be placed above the feed stage (liquid side-draw). Other authors found other composition limitations for when to consider side-draw columns (*e.g.* Glinos and Malone, 1988). The two possible configurations for distillation columns with side-draws are shown in figures 2.14 and 2.15.

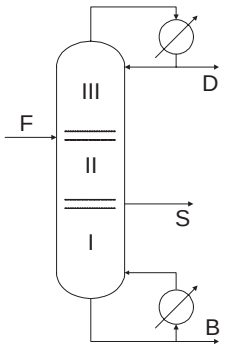

Figure 2.14: Distillation column with side-draw below feed stage.

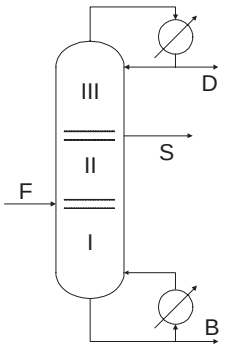

Figure 2.15: Distillation column with side-draw above feed stage.

In the design of this type of columns, the specification for the side-draw stream is essential. Glinos and Malone (1985) mention that the maximum concentration of the intermediate product is not known a priori, but usually a high recovery rate is desired. This is because the product compositions that can be achieved in the distillate and bottom products will be dependent on the flow and/or the composition of the intermediate compound in the side-draw, which is thus an important parameter. Since it is most often desirable to produce pure compound products, Glinos and Malone (1985) state that specification

of a high recovery rate of the intermediate compound in the side-draw should usually be favoured.

The design methods of side-draw columns are for the most part based on Underwood's equations, while some are graphical. In general, these methods try to minimise the vapour flow rate or the reflux ratio. A significant amount of work on this topic has been been carried out by the group of Malone, which has developed iterative short-cut design algorithms for the estimation of essential design parameters (*e.g.* reflux ratio, side-draw location), also including composition of the side-draw stream as variable (Glinos and Malone, 1985 and 1988). The method aims at minimising the vapour rate, and is limited to mixtures with ideal or nearly ideal behaviour. Nikolaides and Malone (1987) extended this work, and developed analytical solutions for the design of columns with multiple feed/side-streams. They developed a method to determine the order of the feed flows into the column in such a way that the smallest feasible reflux ratio is achieved. Meiers *et al.* (1995) also found that an Underwood's equation based method was acceptable for ideal systems, but developed a graphical approach for design of side-draw columns that is applicable to both ideal and non-ideal mixtures. A more thorough design procedure was developed by Rooks *et al.* (1996). They developed a geometric method for the design of side-draw columns, which is applicable to ideal, non-ideal and azeotropic mixtures. This method also provides estimates of utility requirements and formulates some criteria for scenarios when side-draw columns should be favoured. Other cases where side-draws are used are thermally coupled columns, which are distillation columns where heat is transferred between columns via direct contact of vapour and liquid phases. These are treated in section 2.3.2.2

The issue of multiple feeds is mainly relevant in contexts of azeotropic and extractive distillation (see section 2.3.1.3). Levy and Doherty (1986) developed a "boundary value design procedure" for the calculation of minimum reflux ratio in double feed distillation columns, that is applicable to ideal, non-ideal and azeotropic ternary mixtures. Julka and Doherty (1993) extended this method to quarternary and multicomponent mixtures. Wahnschafft and Westerberg (1993) developed a method to assess the feasibility of product specifications in multiple feed columns. The method relies on *fixed point curves*, which are pinch point trajectories in compositions space. These trajectories describe the possible pinch point compositions in each section of the column. Petlyuk and Danilov (1998) also have a method for the design of two feed columns based on trajectories in the compositions space.

2.3.2.2 Thermally coupled distillation columns

Petlyuk *et al.* (1965) introduced the fully thermally coupled distillation column, and found it thermodynamically attractive due to the complete mixing of internal streams and feed streams. They characterise the fully thermally coupled column as a unit performing the separation in $NC(NC-1)$ column sections for a NC-component mixture, with only one reboiler and one condenser. This

shall be compared to $(2NC-1)$ sections for the conventional sequence and one reboiler and one condenser for each column. The key compounds in a Petlyuk column are the two compounds with the highest and lowest volatilities, and every other compound is distributed between the top and the bottom product of each column. Petlyuk *et al.* (1965) developed a mathematical description of the fully thermally coupled system, and compared it to a number of other systems of similar topology. They found that the work of separation is minimal in the fully thermally coupled system, which is thus superiour. The *Petlyuk column* with "main column" and "pre-fractionator" is shown in figure 2.16.

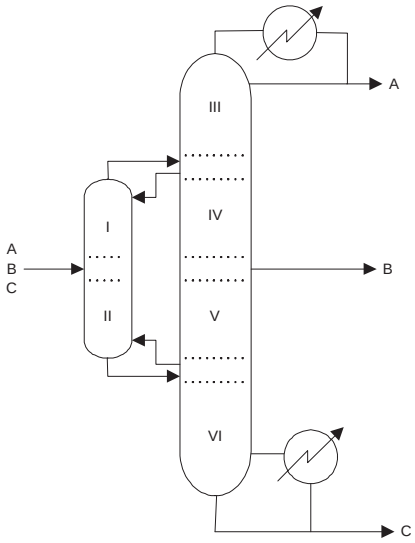

Figure 2.16: Thermally coupled distillation column with pre-frationator (*Petlyuk column*).

The definition of simple conventional columns implies that they have one reboiler and one condenser. If vapour and liquid flows in a column are used to provide some of the necessary heat transfer via direct contact between directly coupled column shells, we are talking about *thermal coupling*. Apart from the *Petlyuk column*, this can be achieved by of coupling simple columns (direct or indirect sequence) or adding a side-rectifier and/or side-stripper. The side-rectifier and side-stripper configurations are shown in figures 2.17 and 2.18.

It is also possible to have intermediate reboiling and condensing in distillation columns, and finally, there is the fully thermally integrated distillation column with a pre-fractionator, a *Petlyuk column*. If the Petlyuk column is built into one shell, it is called a *divided wall column*. A number of other configurations are also possible (see *e.g.* Becker *et al.* (2000), Agrawal and Fidkowski (1999) or Agrawal (2000)). The issue of thermally coupled distillation columns is interesting from an energy consumption point of view, and has attracted a lot of

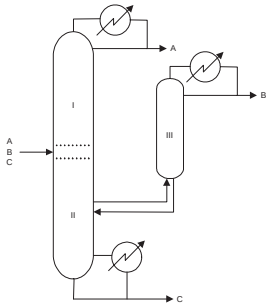

Figure 2.17: Distillation column with side-rectifier.

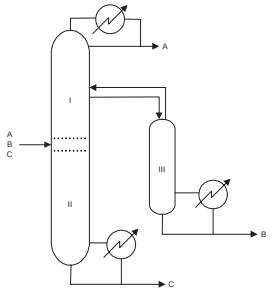

Figure 2.18: Distillation column with side-stripper.

interest from industry and academia. Also the question of which configuration to use under which conditions, and how this limits the operation are interesting issues that need further consideration. Thus, a number of design methods, and analysis tools for this kind of separation schemes are available in the literature published. However, many of the design methods end up in an optimisation approach based on approximate models.

One of the problems related to the operation of thermally coupled columns is the large number of *degrees of freedom*. This is discussed by Rudd (1992) and by Dünnebier and Pantelides (1999), who mention the industry's concern regarding potential control problems of these units related to the many degrees of freedom. The major decision variables related to the Petlyuk column is illustrated in figure 2.19. Wolff and Skogestad (1995) and Halvorsen (2001) show that a sustainable control strategy can overcome these problems. Rudd (1992) and Triantafyllou and Smith (1992) give some ideas to preliminary assumptions that can be made at an early stage in the design (short-cut models).

Some of the solution approaches to the design of thermally coupled columns previously mentioned are of a heuristic character, like for example Tedder and Rudd (1978). Rév *et al.* (2001) did a thorough study, considering a great many different complex distillation schemes. They did calculations, both with short-cut models and with rigorous models, for the purpose of identifying which configurations are more attractive. The study also involved an optimisation and controllability analysis, and ends up giving a set of heuristic rules for the design of different configurations of distillation columns, including guidelines as to the conditions under which each configuration should be applied. Rong *et al.* (2000) studied the separation of five-compound mixtures in a large number of different separation sequences, including thermally coupled columns. The study aims at optimisation of the total annual costs using short-cut models for the design. The authors have then considered eight superiour flowsheets, which they compared to real mixtures applying rigorous thermodynamics. This leads to seven heuristic rules of how to synthesise multicomponent thermally coupled distillation systems. Kaibel *et al.* (1990) give a set of guidelines for synthesis

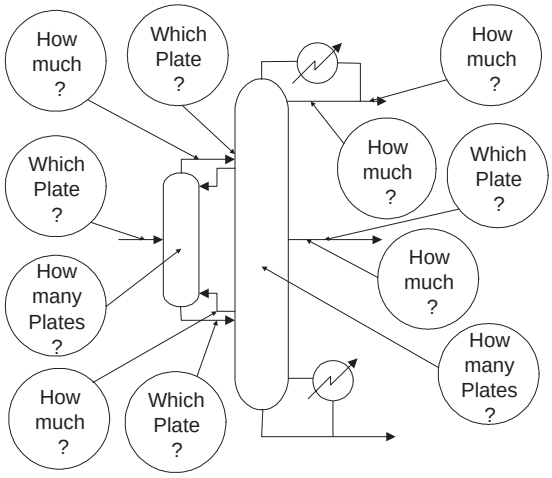

Figure 2.19: *Degrees of freedom* for fully thermally coupled distillation column.

of integrated distillation column flowsheets based on simplified process models aimed at minimising the thermodynamic (exergy) loss in the separation.

Fidkowski and Królikowski (1987) developed analytical expressions for four different types of thermally coupled systems, including columns with side-strippers as well as Petlyuk columns. These expressions can be used to detect minimum vapour flows, and thus can be used to compare the different configurations. The methodology is based on Underwood's equations, and is limited to ideal systems. Fidkowski and Agrawal (2001) extended this approach to handle four or more compounds. However, it is still only applicable to ideal systems where constant relative volatility can be assumed and Underwood's equations are applied. The separation of quarternary mixtures in this kind of complex columns was found to require significantly less energy than conventional configurations. Carlberg and Westerberg (1989a) also used Underwood's equations as basis for a *Temperature-Heat-Diagrams* method for the design of Petlyuk columns, and Carlberg and Westerberg (1989b) used the same approach for the design of columns with side-strippers/rectifiers. Glinos and Malone (1988) applied Underwood's equations to a number of alternative configurations, and compared the minimum vapour flows in order to identify regions of optimality for the different lay-outs considered. Halvorsen (2001) proposes a design procedure for Petlyuk columns based on minimum vapour flows using Underwood's equations, which is applicable to multicomponent mixtures separated into three products. Triantafyllou and Smith (1992) present a design approach based on a model where three simple models constitute the Petlyuk column and applied the standard Fenske-Underwood-Gilliland short-cut techniques to obtain the design.

A more detailed approach is presented by Dünnebier and Pantelides (1999).

They developed a method for optimal design of distillation columns based on mathematical optimisation and the use of detailed models for distillation columns. The method is capable of designing simple as well as complex configurations. The approach implies use of detailed superstructures, and allows for simultaneous determination of the design and the operational characteristics of the individual columns. Another detailed design and optimisation approach has been developed by Hernández and Jiménez (1999). This work is based on a dynamic model, which uses the two recycle streams (going from the main column back to the prefractionator, (see figure 2.16)) as search variables to minimise the reboiler heat duty. Kim (2001) has also developed a rigorous model for the design of Petlyuk columns, and compares the results of this model to a conventional sequence of distillation column. Shah and Kokossis (2001) use what they call "knowledge-based models" for analysis and design of various complex distillation schemes. Based on simple mathematical models, a supestructure is generated, based on which different "hybrid tasks" are defined in order to rank the alternatives by optimisation.

Another alternative complex distillation configuration is applying intermediate reboilers and condensers, or simply pumparounds (where liquid is withdrawn from the column, cooled and returned). This option may be advantageous to use in the retrofit design of existing columns, or when space (column height) is limited. Although the problem is of significant industrial interest, only few publications on this topic have been published in the open literature recently. King (1980) deals with this issue to some extent and shows how this kind of operation appears graphically in a McCabe-Thiele diagram. Terranova and Westerberg (1989) developed a *Temperature-Heat-Diagrams* based method for columns with intermediate heat exchange. Agrawal has also worked with this topic (Agrawal and Herron, 1998), and developed a set of heuristic rules for the placement and use of intermediate heat exchangers, that are all based on the feed mixture composition. The objective of this method is to identify the thermodynamically most efficient configuration for heat removal/addition at intermediate locations in a distillation column. Finally, also Aguirre *et al.* (1997) developed a method for the placement of inter-coolers and inter-reboilers on distillation columns, based on optimisation techniques.

2.3.3 Hybrid separation systems involving distillation

When a distillation column (or another type of separation unit) is associated with another separation process/unit to achieve a specified separation the separation scheme may be called a *hybrid separation scheme*. This kind of separation scheme becomes attractive if a separation is difficult or even impossible to achieve with conventional distillation, or simply because it is more efficient and thus can save energy.

Most often hybrid separation schemes are used for the separation of azeotropic mixtures, mixtures having eutectic points (in solid separation), or to perform a separation of close-boiling mixtures. Some of these processes may be con-

sidered to belong to the category of hybrid processes, but are treated in the context of other sections in this chapter. These are, for example, pressure-swing distillation, extractive distillation and reactive distillation. Extractive - and pressure-swing distillation are, in this thesis, considered *enhanced distillation* and are treated as distillation in section 2.3.1.3. Reactive distillation is treated as a separate topic in section 2.3.4.

Some of the separation processes that are commonly used in association with distillation in hybrid separation schemes are listed below:

- Absorption
- Adsorption
- Crystallisation
- Membrane Permeation
  - Pervaporation
  - Reverse Osmosis
- Evaporation
- Liquid-Liquid Extraction

The search for improvements of separation technology increases, partly due to the focus on environmental issues (such as for example emissions of undesired compounds) and the desire to keep energy consumption at a low level. Hybrid separations can be considered in many contexts and for a very wide spectrum of possible applications (*e.g.* separation of azeotropic mixtures, waste water treatment). Since the primary interest in this thesis is separation by distillation, only hybrid separation schemes involving distillation are discussed. Application of hybrid separation schemes is limited by the performance of the *substitute technique* to distillation (*i.e.* whether an alternative separation technique is known to be capable of performing the desired separation). This makes the solution approach very specific to the mixture (system) being separated, as the substitute techniques rely on system specific data, such as membrane material and permeability for pervaporation.

The application of hybrid separation schemes as an alternative to distillation is dependent on the feasibility and performance of, for example, a specific membrane to attain the desired products. The publications on *hybrid separation* are, however, still limited. A short overview of recent publications is given here.

One of the most well-known distillation-membrane hybrid separation schemes is the dehydration of ethanol by pervaporation. This process is treated by Sander and Soukop (1988), who represent a company that built a commercial scale hybrid separation plant, and operated it parallel to an entrainer-based distillation plant. They found the process economically attractive, but

also emphasized that the potential saving could increase radically with better performing membranes. Szitkai *et al.* (2002) also worked on the distillation-pervaporation ethanol dehydration system, where they developed a superstructure and applied a MINLP optimisation technique, and thereby improved operation of an actual plant. Another interesting pervaporation-distillation system was investigated by Hömmerich and Rautenbach (1998), who designed and simulated hybrid processes for the separation of MTBE from methanol. Two alternative configurations were studied together with the conventional separation scheme, and both alternatives were found to be more attractive than the conventional process.

Pressly and Ng (1998) have developed a method for the screening of alternative processes and break-even cost analysis of membrane-distillation hybrid schemes. The method is based on a general cost model for distillation as well as one for membranes. In this way, a break-even price for the cost of a membrane is calculated. The system deals with binary mixtures, which are classified in terms of difficulty of separation. A large number of possible combinations of distillation and membrane units are proposed in this work. Al-Rabiah *et al.* (1999) studied a number of distillation-membrane hybrid separation schemes for ethane/ethylene separation, and made a cost evaluation of the alternatives proposed. Al-Rabiah *et al.* (1999) concluded that there was a large saving potential compared to the use of conventional distillation, especially by using a parallel configuration, where a membrane unit is performing an intermediate separation.

Other authors have also treated this problem as an optimisation problem, with very specific models for the membrane. An example is Brusis *et al.* (2000), where optimisation was applied to a synthesis/design problem for an azeotropic mixture. The superstructure here incorporated membrane separation.

Berry and Ng (1997) have developed a procedure for the design of crystallisation-distillation hybrid separation schemes. This approach combines the two separation techniques, so that feasible separation schemes are generated and a break-even analysis can be performed for alternative solutions. Stepanski and Haller (2000) have developed an industrial crystallisation-distillation hybrid process for the recovery of m-xylene from a mixture of xylene isomers, which they claim to be very economical.

Myasnikov *et al.* (2002) proposed a hybrid process, integrating distillation, pervaporation as well as crystallisation. The basis of their approach is the the solid-liquid-vapour equilibrium phase diagram. For different organic and aqueous-organic mixtures, pilot plants were constructed, and high purity products were obtained, from binary mixtures (including some of azeotropic and eutectic composition).

Another promising hybrid separation scheme was developed by Zhou *et al.* (1995). They added an adsorbent to a part of the distillation column to bypass azeotropic points. This was found to be very energy-effective, and high purity products were obtained. Experimental work with *adsorptive distillation* had been done with a number of azeotropic mixtures.

Some of the references treated in the previous sections of this chapter also deal with hybrid separations schemes. Stichlmair and Herguijuela (1992) give examples of hybrid separation schemes. The separation task involves the mixture of ethanol and water, for which they propose flowsheets where distillation is combined with decantation (heterogeneous azeotropic distillation), absorption, extraction and pervaporation in order to obtain pure water and pure ethanol. Another example is provided by Malone and Doherty (1995), who propose a flowsheet for the separation of a mixture of acetic acid and water by liquid extraction with chloroform.

2.3.4 Reactive distillation

Over the last couple of decades, *reactive distillation*, which may be called a hybrid reaction-separation process, has attracted a lot of attention. It has been found that this single unit where reaction and separation occurs simultaneously is sometimes at least as efficient as a traditional series of reaction and separation units. In the context of this thesis, the application of this combined reaction-separation process is considered for reactive systems limited by chemical equilibrium, where it has been applied successfully, for example to the methyl acetate and methyl-tert-butyl ether (MTBE) production treated by *e.g.* Agreda *et al.* (1990) and Smith and Huddleston (1982).

The increasing interest in reactive distillation has been accompanied by the development of various simulation algorithms related to the study of operation and control of the process (*e.g.* Abufares and Douglas (1995), Monroy *et al.* (2000)). Most of the existing work on the design of reactive distillation columns is based on the use of the transformed composition variables proposed by Doherty (Barbosa and Doherty 1988a and 1988b), Doherty and Buzad (1992), Ung and Doherty (1995) and also Bessling *et al.* (1997)). A similar approach has been proposed by Espininosa *et al.* (1993), Espininosa *et al.* (1995) and Espininosa *et al.* (1996). Espininosa *et al.* (1999) extended this methodology to reactive distillation columns, where the reaction takes place in both a reactor, and a reactive distillation column (finishing column). Barbosa and Doherty (1988a) developed a technique for the design of single-feed and double-feed (Barbosa and Doherty, 1988b) reactive distillation columns, assuming constant molar overflow.

Espininosa *et al.* (1993) proposed to use Ponchon-Savarit diagrams in the transformed composition enthalpy space to simultaneously account for heat and mass balance under the assumption of reaction equilibrium. Doherty and Buzad (1992) continued their studies with kinetically controlled reactions in terms of the Damköhler number. Another approach to reactive distillation column design has been proposed by Gumus and Ciric (1997), where the design problem is formulated as a mixed integer non-linear bi-level optimisation problem.

Pérez-Cisneros *et al.* (1997) developed a design method for reactive distillation systems. This method is based on the use of *chemical elements*, for the calculation of mass balances and the minimisation of Gibbs free energy. The

element approach reduces the number of variables in the reactive system and thus allows for the visualisation of element phase diagrams for design purposes.

Recently, Lee *et al.* (2000) proposed graphical methods to illustrate how to distribute reaction zones in a reactive distillation column based on the difference points concept. Such points are referred to as the points of intersection of the reactive operating lines and the 45-degree line of a xy phase diagram. Despite the extension of the difference points concept to consider the heat effect in a reactive distillation column, such methods while easy to apply for two-compound reactive systems, (*i.e.*, isomerization reactions), become considerably difficult for the problems of higher dimension (three or more compounds).

Kenig *et al.* (1999) developed an integrated computer aided tool for the synthesis and design of reactive distillation columns. It is a rate-based approach that employs Maxwell-Stefan equations for the calculation of multicomponent mass transport, and it provides a large variety of reactions and mass transfer correlations as options to choose from. This tool has been applied to the ethyl acetate production (Kenig *et al.*, 2001). An extensive study of this problem was carried out, in which experiments were also performed to validate the computational predictions. Górak and Hoffmann (2001) developed a rigorous dynamic non-ideal stage model based on Maxwell-Stefan equations, which was tested and compared to pilot plant experiments for the synthesis of methyl acetate.

Recently Taylor and Krishna (2000) made a review in which the modeling of reactive distillation, and the developments of reactive distillation processes are covered in detail.

2.4 Analysis of separation systems

Analysis of separation systems is treated in this thesis due to the close interaction of analysis with design and synthesis. The analysis of a given process is dependent on a model of the process/system being available. In general, once the process (model) is known, analysis can be performed on the process (model). Analysis can then be performed with respect to *e.g.* feasibility or operability. The term operability refers to the ability of a plant (design) to operate under nominal design conditions and conditions different from the nominal design.

Analysis is usually performed using systematic tools and methods. Simulation and optimisation tools are frequently used for the analysis of separation processes. They normally provide rapid calculation of unit operation models, and are useful to find solutions to form the background for the analysis of the process with respect to changing constraints/specifications of the unit operations and/or separation task. These tools are treated separately in chapter 3. In the context of this chapter, operability (including controllability) as long as it is related to analysis will be covered. This topic is presented in the way it will be used in conjunction with the design and synthesis methods in this thesis.

The interaction between analysis and design/synthesis is not always distinct,

and some of the methods covered in the section on design techniques (section 2.3.1), are also highly related to analysis.

2.4.1 Operability of separation systems

The term, *operability* is commonly used to describe the ability of a plant to perform satisfactorily under normal and abnormal nominal design conditions. During operation, changes may occur in disturbance levels, feed/product specifications, product distribution and demand, and the plant needs to remain operable under all these conditions. The major objectives to be achieved when applying the term "operability" may be outlined as the following (Grossmann and Morari, 1983):

- Feasibility of steady state operation for a range of different feed conditions and plant parameter variations.
- Fast and smooth changeover and recovery from process disturbances.
- Safe and reliable operation despite equipment failures.
- Easy start up and shut down.

In the above outline, only the first two items are relevant to "normal" operating conditions, and only these two items, and their interaction with design are addressed here.

The first issue in the outline, feasibility of the separation at various feed conditions and/or plant parameters, deals with the capability of a separation unit to perform a separation task satisfactorily. It can, however, also be treated as a flexibility problem, where different mathematical techniques can be employed in order to determine the design. The main feature of these techniques is to "overdesign" or "underdesign" the unit operations, so that they can operate at a fixed degree of flexibility, often a set of predefined *worst case scenarios*. Flexibility is not treated in this thesis, but the topic is treated in detail by Biegler *et al.* (1997). The second issue in the outline, recovery form disturbances is dealing with controllability and resiliency. This is discussed in the following section.

2.4.1.1 Controllability/resiliency of distillation columns

When a chemical process plant is designed, it is designed to operate at a given steady state point, and it is important that it can operate at this steady state point, or within a certain margin of it, regardless of disturbances. When the design is made, it is assumed that the operation runs at this desired operating level. Nevertheless, it may happen that the dynamics of a process behaves in such a way that the nominal steady state of the process is difficult to maintain and perhaps the control system cannot keep the operation at the desired steady state point. For that reason, dynamic simulations to mimic the behaviour of

the process in a time scale is often advantageously employed before finalising a plant design. However, it is tedious to make dynamic simulations of all designs, and thus is it an advantage to employ short-cut controllability analysis tools at a fairly early stage of the synthesis/design process. According to Seider *et al.* (1999), controllability and resiliency issues should already be considered at the basic design stage. These are for example:

- Adequate disturbance resiliency, *i.e.* ability to reject disturbances quickly enough to meet specifications.
- Insensitivity to model uncertainty, *i.e.* ability to control easily and provide adequate closed-loop performance, relatively insensitive to model uncertainties.

The term resiliency refers to the fact that some processes are easier to control than others, and some choices of manipulated and controlled variables produce systems are easier to control than others. This inherent property is called resilience.

To measure controllability, there are a number of possibilities. First, there is the *Relative Gain Array*, RGA, developed by Bristol (1966). The RGA is easy to calculate, and requires only steady state gain information. Bristol proposed a measure for multiple-input multiple-output (MIMO) systems,

$$\frac{\text{Process gain as seen by given controller with all other loops open}}{\text{Process gain as seen by given controller with all other loops closed}}$$

For a two-input two-output system a matrix of the above gain ratios may be calculated from the open loop steady state gains. This is done by multiplying the elements of the open loop gain matrix with the elements of a matrix, which is the transposed of the inverse of the open loop gain matrix, *i.e.* if

$$\mathrm{y} = \mathrm{G}(0)\mathrm{u} \tag{2.10}$$

where y are the outputs, $G(0)$ the steady state gains and u the inputs of the sytem, then

$$\Lambda = \mathrm{G} \times (\mathrm{G}^{-1})^{\mathrm{T}} \tag{2.11}$$

If the diagonal elements of this matrix are close to unity, then the system may be tuned to react quickly to disturbances in any inputs. The RGA matrix (Bristol, 1966) has the property, that the elements of any row sums to one, and so does the elements of any column. This means, that for a two-input two-output system $\lambda_{11} = \lambda_{22}$, and $\lambda_{12} = \lambda_{21}$. It can also be shown, that if the diagonal elements are positive, then the system is closed-loop stable with a set of single loop controllers. Reversely, if these elements are negative then no single loop controllers may stabilize the system for the given pairing of inputs

and outputs. Generally, the closer the diagonal elements are to one, the easier is the system to control. This corresponds to RGA coefficients close to unity in equation 2.12.

$$\Lambda = \begin{bmatrix} \lambda_{11} & \lambda_{12} \\ \lambda_{21} & \lambda_{22} \end{bmatrix} \tag{2.12}$$

The RGA matrix can easily be calculated from a linearised state space model. With this information, the RGA matrix for a given configuration can be obtained fast, and comparisons of different control configurations can be made.

Other measures of controllability and resiliency are the *Disturbance condition number*, DCN, introduced by Skogestad and Morari (1987), and the *Disturbance cost*, DC, introduced by Lewin (1996). DCN defines a quantity for the identification of the most problematic disturbance direction, whereas the DC gives a direct indication of the feedback effort required to reject disturbances.

Another related issue is the interaction of design and control. It is clear that the control strategy necessarily must reflect the unit designs in the flowsheet (and the corresponding degrees of freedom), in order to maintain operability. Besides, the literature on control strategies and plantwide control systems (*e.g.* Stephanopoulos (1984)), deals with another strategy which proposes simultanous design and control. A methodology for simultaneous design and control under uncertainty has been presented by Bansal *et al.* (2000a), where a very large complex mixed-integer dynamic model is optimised, in circumstances of parametric uncertainties. Other articles treating the interaction of design and control are for example Bansal *et al.* (2000b), or for reactive distillation systems, Georgiadis *et al.* (2002).

2.5 Concluding remarks

In this chapter, a selection of methods reported in the relevant literature for synthesis and design of separation processes have been described. These methods can in general be categorized as either heuristic approaches, insights based approaches, or mathematical optimisation approaches. Some of the methods take advantage of more than one of these approaches in a larger synthesis/design framework. This is, for example, when a heuristic method is used to generate a superstructure with alternative solutions, which then forms the basis for an optimisation study, or heuristic rules are proposed based on numerous optimisation studies of existing plants.

The heuristic methods are often based on a limited number of operational data, and are thus limited to only specific types of operations. If the methods are broader and several heuristic rules are proposed, they may become contradictory. Since heuristic rules are based on observations made on existing plants, the application of heuristic methods exclude alternative new ideas for solutions. Insights based methods are useful for the identification of feasible separation methods to perform a given separation task, as they are based on

the properties of the mixture compounds to be separated. Methods based on (thermodynamic) insights are however not likely to predict optimal solutions, unless an optimisation layer is added to the method. Another similar approach is the employment of graphical methods for synthesis and design. These methods are useful to exploit the behaviour of binary and ternary mixtures, and the feasibility of separations can be predicted on this basis, but at present it is difficult to predict optimality with respect to energy consumption from these methods. The same applies to empirical methods. Although they do predict optimal solutions for the distillation column designs, they rely on constant relative volatility, and are therefore limited to ideal systems only. Mathematical programming techniques are widely used to identify optimal solutions. These solutions are based on mathematical models of the unit operations involved, and the optimality of the solutions are dependent on a solver being available and the level of accuracy in each separation unit model. Besides, a superstructure of alternative solutions needs to be generated prior to solving the problem, and the different alternative solutions (and combinations of these) must be considered when solving the problem. This is often a long and cumbersome process.

Considering the current state of the art, it is obvious that an approach that is able to predict optimal (or near optimal) solutions to synthesis and design problems at a very early stage of the design phase is missing. There is no current method available that can give optimal (or near optimal) solutions to these types of problems without relying on some kind of optimisation or comparison with similar existing separation processes. This is true both for the synthesis of separation schemes, as well as for the design of individual simple and complex separation units. A method based on thermodynamic insights, which can efficiently predict near optimal solutions to separation synthesis and design problems in general, as well as predict controllability, has not been developed yet. Such a method, that relies on chemical/physical properties of the mixture to be separated, and which is capable of predicting energy efficient solutions to separation problems is a desired one in the state of the art. In this case, a method taking the actual thermodynamic behaviour into consideration could not only achieve better solutions, but the solutions could be found very early in the design phase. This method would not only exploit feasible solutions, as the current insights based methods do, but it would also make an associated optimisation problem redundant, or at least very well defined and much easier to solve, since only feasible solutions would be considered and the predicted solution suggested by the new hybrid method would be close to the actual optimal solution (if it is not the optimal solution). Since a method based on actual thermodynamic behaviour does not make any assumptions as to phase behaviour, the solutions would also reflect the *real* system. In this way highly accurate and consistent optimal (near optimal) solutions for separation synthesis and design problems could be obtained for existing and new separations schemes, with very little effort.

3

PROBLEM DEFINITION AND SOLUTION PROCEDURES

3.1 Introduction

In order to conceive a good design for a chemical plant, it is important to ensure that it can operate according to the design specifications. This implies that the design is properly conceived, and that the methods and tools applied for synthesis and design are reliable and predictive. For example, it is important to have some knowledge about the properties and behaviour of the compounds involved in a separation process in order to design the process properly. Also, in order to finalize and/or validate the design, simulation and optimisation of the separations taking place in the chemical plant need to be efficient, reliable and trustworthy.

It is the objective of this chapter to present the problem formulation step, and to cover the most important methods and tools that are needed in order to assist the solution to the problem, and mimic the behaviour of a chemical separation process as well as possible. This implies verification of proposed solutions to synthesis and design problems, as it is relevant to problems treated in this thesis.

In this chapter, a definition of the synthesis and design problems considered in this thesis is given first. The objective of this is to define the problems involved in the solution and/or validation procedure, and to explain the steps necessary to solve them. This is followed by a short description of some methods and tools that are used to solve the problems, and to validate the solutions. The basis of process models is formed by the properties of the compound mixture. Property prediction methods and property retrieval are treated in a section, which will cover single compounds and their mixtures as well as solvent design and selection. The use and availability of databases in the context of properties are also covered here. Simulation as a tool for synthesis and design is described, and the different approaches to simulation are briefly covered (including some simulation packages that have been used in this thesis). The same goes for

optimisation, where the basic theory is outlined for continuous and discrete optimisation techniques. The optimisation tools used in this thesis are also described briefly.

3.2 Problem formulation

The objective of this thesis is to develop simple accurate solution methods for separation synthesis and design problems in the chemical industry. The solution methods are generally based on phase composition data for the compound mixture to be separated and should not require a great effort to be applied and implemented. In this section, the problem formulation step of the synthesis and design methods developed in this thesis are described, and so are the methods and tools necessary to solve the synthesis/design problem and to verify the solution.

Equilibrium based separation processes (distillation) are by definition limited by equilibrium which can be described by thermodynamic models. In non-equilibrium processes, sometimes models may be available (*e.g.* for rate-based distillation), but often this is not the case, and experimental data are usually necessary in order to obtain phase composition data. In case an entrainer is added to a mixture to "change the phase behaviour", this entrainer must be selected on the basis of some selection criteria. In any case, the problem is to retrieve/generate the data necessary for the calculation of phase composition diagrams, whether in equilibrium or not. This is described in section 3.3, where prediction of properties relevant to phase composition data, and storage/retrieval of such data are described, as well as solvent selection and design. In order to employ the methods developed in this thesis, it is necessary that accurate phase composition data should be available, and that they in some cases should be calculated with a solvent (entrainer) present in the system. For separation techniques relying on non-equilibrium data, retrieval of relevant phase-composition data is important. In order to validate solutions proposed by the methods developed, rigorous mass/energy balance calculations by simulation and optimisation are employed. The methods for simulation and optimisation are described in section 3.4.

3.3 Property prediction and retrieval

It is evident that methods and tools for design and analysis of chemical processes are dependent on the availability of accurate property data. If there are no experimental data, or models available for a given compound, it is not possible to predict its behaviour, either as a pure compound or in a mixture with other compounds. Simple examples are the reliability of binary vapour liquid equilibrium data for distillation analysis and design, or distillation line maps for ternary mixtures. In both cases the phase diagrams are completely dependent on availability of physical property data and model parameters for the

calculation of accurate phase equilibrium diagrams and distillation line maps. Another example is in membrane separation, where it is important to know how the membrane interacts thermodynamically with the compounds in the mixture to be separated. In any case, it is clear that the predictivity of the behaviour of chemical compounds is indeed relying on physical properties and/or parameters for predictive methods. In general, such data can be obtained from two sources, namely: databases and literature, where experimental data are reported, or predictive methods are referred to.

As an illustrative example of the importance of reliable properties, Wakeham *et al.* (2001) made a study on the consequences of property errors in the design of distillation columns. They used a number of different predictive methods for the estimation of normal boiling points as well as critical temperatures and pressures. These estimated values were used for phase equilibrium model calculations, and thus in the design of distillation columns in a commercial simulator (HYSIS). The results showed significant deviations on the phase diagrams between the different predictive methods, as well as in the design of the distillation columns.

3.3.1 Databases

Databases for properties of compounds and mixtures are standard tools for storing and retrieving knowledge, such as information of actual experimentally obtained values of thermophysical data. The commercial process simulators (*e.g.* HYSIS, Pro/II, ASPEN) all have their own built-in databases. However, these databases - although comprehensive - do not contain data for all compounds and mixtures. Therefore, there is a market for databases containing very large collections of property data and highly accurate data. Some of the well-known databases, of which the first two are public domain, are:

- CAPEC database (Nielsen *et al.*, 2001). This database contains pure compound data, mixture properties, and solubility data. The compound properties in this database are divided into primary, secondary and functional properties. The database contains data for over 13.000 pure compounds, together with several thousand binary and ternary data sets.

- The NIST Chemistry Webbook (Linstrom and Mallard, 2001) is an internet site that provides access to a very wide range of thermophysical data from NIST as well as other places. At the current stage, the database contains data for over 40.000 compounds.

- The DIPPR database (Thomson and Larsen, 1996) is a research project sponsored by the American Institute of Chemical Engineers. It contains a large set of chemical and physical as well as environmental data. The database contains data for more than 1500 pure compounds and over 2000 sets of data for mixtures.

- The DECHEMA vapour-liquid data collection (Gmeling and Onken, 1977), contains in its present form 4.2 million sets of data for 122.000 pure compounds and mixtures.

Besides the databases, it should be noted that experimental data are published in many journals, for example, *Journal of Chemical Engineering Data* and *Fluid Phase Equilibria*.

3.3.2 Pure compound property prediction

Predictive methods for the estimation of properties often become necessary when the needed property data are not available in a database, since most experiments are expensive to conduct. Therefore, methods for the estimation of physical properties are valuable. Property prediction methods are typically based on property/structure relationships where the unknown properties are calculated by the use of a suitable mathematical relation, given the molecular structure of the compound. Properties can be divided into two classes: primary properties (predicted purely on the basis of the molecular structure) and secondary properties (function of primary properties and/or temperature and pressure) (Jaksland, 1996).

A large number of methods for the prediction of properties are methods based on the Group Contribution Approach (GCA). In this approach, compounds are defined in terms of a set of predefined groups, that together form the given compound. Knowing the identity of the predefined groups that together constitute the compound (molecule), properties can be calculated by equations of the following type:

$$f(x) = \sum_i N_i C_i \tag{3.1}$$

In equation 3.1, $f(x)$ is the given property and C is the contribution of group i, which occurs N_i times. Different GCA methods have been developed by many researchers. Examples are Lydersen (1955), Joback and Reid (1987) or van Krevelen (1990). A severe problem of these methods is that they are not capable of distinguishing between different structural isomers. This problem is to some extent overcome in the method of Constantinou and Gani (1994), in which a second order group has been added, which takes sub-structures into account. More recently Marrero and Gani (2001) have developed a method which enables consideration of taking third order groups into account, to distinguish between many more isomers and at the same time improve the accuracy of the predicted properties.

Some of the GCA methods mentioned above (including Marrero and Gani (2001)) have been incorporated in a computer program called *ProPred* (Marrero, 1998) where the property prediction features are utilized.

In case no GCA methods are available, numerous empirical correlations for property estimation can be used. These methods are based on the knowledge

of other properties (*e.g.* boiling point, critical values, etc). Reliable sources for property correlations and their use are Poling *et al.* (2000) and Lyman *et al.* (1990). In this Ph.D. work, GCA methods have been applied for the estimation of properties of compounds where no data were found in the open literature.

3.3.3 Prediction of mixture properties

As in the case of pure compound properties, mixture properties also need to be estimated when they are not available in a data collection. The methods used for calculating, correlating and predicting mixture behaviour for separation, and especially distillation design purposes are related to two-phase vapour liquid equilibria. To perform mixture property estimation, a number of methods have been developed, and a concise overview is given here. The methods most frequently used can be divided into the following categories:

- Equations of State (EOS) model the pressure-volume-temperature relationship of a fluid (pure compound or mixture). EOS models are used for the prediction/calculation of vapour and liquid fugacities, which may be used to predict vapour-liquid phase equilibrium. This type of models may be divided into virial equations of state (applies only to gasses) and cubic equations of state (applies to both vapour and liquid phases for non-polar mixtures). EOS models are often used in the ϕ-ϕ approach since an EOS is applied to calculate both the vapour and the liquid phase fugacities (and compositions). Examples of this type of models are the Peng-Robinson EOS (Peng and Robinson, 1976) and the Soave/Redlich-Kwong EOS (Soave, 1972).

- Methods for prediction of activity coefficients, γ, of compounds in liquid mixtures are based on excess Gibbs energy for modelling the liquid phase behavior. The corresponding vapour phase is modelled by use of an EOS. This approach is often called the γ-ϕ approach referring to an activity coefficient model is applied to calculate the liquid phase, and an EOS is applied to calculate the vapour phase fugacity coefficient. Some of the most well-known equations employing activity coefficients are the ones by Wilson (Wilson, 1964), NRTL (Renon and Prausnitz, 1968) and UNIQUAC (Abrams and Prausnitz, 1975). One special model of this type is the UNIFAC model (Fredenslund *et al.*, 1977), which is a GCA based method, in contrast to the molecular based methods mentioned above. The UNIFAC method is thus, as the above mentioned methods based on experimental data, but the interaction among the compounds involved is taken into account by structural fragments (groups) contributions, *i.e.* the interaction parameters in the mixture are calculated based on the summation of the contributing groups.

Gani and O'Connell (1989) developed an expert system, "Thermodynamic Model Selection", which assists the user in selecting the optimal property and

phase equilibria models. Provided the mixture compounds, the type of problem and the expected operating range are given, a set of selection indices guides the user to choose appropriate thermodynamic models. In this thesis, thermodynamic models of the types mentioned above have been used frequently to obtain phase composition data for the application of the methods developed.

3.3.4 Solvent selection and design

Solvents are widely used in separation processes. In this thesis, solvents are mainly relevant to azeotropic mixtures, and are used to separate two compounds forming an azeotrope. To accomplish such a separation, a solvent is added to the mixture in an extractive or azeotropic distillation column.

For the particular problem of the separation of mixtures, where solvents (entrainers) are involved, for example, extractive distillation processes, the issue of solvent selection is very important in order to select solvents that are capable of producing feasible designs. Molecular design methods have the ability to predict/design compounds that match desired properties (constraints), for example, total miscibility or no azeotropes formed with either of the mixture (solute) compounds.

Generally, the solution of a computer aided molecular design (CAMD) problem involves finding the molecules of the desired type(s), *e.g.* alcohols, having the desired properties *e.g.* boiling point and solubility.

Several design approaches have been proposed for solving CAMD problems and these approaches can be categorized into three groups:

1. Mathematical programming, employing a numerical optimisation method. Examples of this approach are given by Vaidyanathan and El-Halwagi (1994), Duvedi and Achenie (1997) and Pistikopoulos and Stefanis (1998).

2. Stochastic optimisation, employing a numerical stochastic optimisation method is, for example, described by Venkatasubramanian *et al.* (1995) and Marcoulaki and Kokossis (1998).

3. Enumeration techniques, employing a solution approach where molecules are first generated, and then tested. Approaches of this kind have been developed by *e.g.* Gani *et al.* (1991), Joback and Stephanopoulos (1995) and Friedler *et al.* (1998)

Common to all the different techniques is the objective to find one or more compound(s) or compound mixture(s) fulfilling the requirements formulated by the constraints (property targets). A thorough review of CAMD methods is given by Harper and Gani (2000).

In the context of this thesis, the CAMD technique used for solvent identification and validation is the multi-level CAMD framework of Harper (2000), which is a hybrid method employing aspects of enumeration and mathematical programming techniques. This approach is based on the generation of molecules on the basis of fragments (groups), which are systematically linked

by a rule based approach guaranteeing only feasible compounds to be formed. A computer aided molecular design (CAMD) program has been developed, *ProCAMD* (Harper and Hostrup, 2002). In this way screening of candidate solvents can be performed rapidly, and also new solvents can be generated, on the basis of the groups considered.

3.4 Simulation and optimisation in process synthesis and design

In the design and synthesis of chemical processes and process flowsheets, simulation as well as optimisation are powerful and very widely used tools. Simulators provide fast automated calculations of mass and energy balances, and a great number of models are available to mimic the behaviour of chemical unit operations and the thermodynamic behaviour of fluids involved. These models can be of more or less rigorous character, and often the user can choose between different models, depending on the level of accuracy and amount of information desired. It is often the case that simulation software packages have a built-in optimisation module. This tool allows for the model equations in the simulator to be solved in such a way that a given objective function is minimised (or maximised), in order to identify the optimal operating point, expressed in terms of the objective function.

In this thesis simulation and optimisation have been widely used to analyse and/or validate different design and synthesis results obtained by the methods developed. Different simulation and optimisation software tools have been used in this context. Some of the simulation/optimisation tools used are commercial software packages with graphical user interface and other useful features. Amongst them are the well-known ASPEN (Aspen Technology Inc.) and Pro/II (Simulation Science Inc.). From the academic world, the ICAS package (CAPEC, Technical University of Denmark) has been widely used. Examples of other commercial simulators (not used in this thesis) are HYSIS from Hyprotech Ltd., D-Spice from Fantoft Process Technologies AS and gPROMS from Process Systems Enterprise Ltd. Examples of other academic simulation/optimisation tools are ASCEND (Carnegie-Mellon University) and IMPROVE (RWTH-Aachen).

In this section, the concept of how simulation and optimisation are designed is described, as well as how these tools are used in this thesis for separation synthesis and design.

3.4.1 Simulation

Process simulators may be used in different ways in synthesis and design, depending on the level of knowledge that is available a priori, and on what is to be investigated. For example, when a flowsheeting problem is to be solved, it is normal that all input information is available, so the model equations can be

solved. As to this kind of problem, the input is known and the output information is determined. If, on the other hand, some input information (usually the feed stream) is known, and the desired output is also known, the task is to find specifications for the operating conditions to meet the output criteria, and thus the problem becomes a "specifying a design" problem. In case of a synthesis problem, a flowsheet is determined and then for given input information, the design/specifications of the individual unit operations are determined, so that the desired output criteria are met. Therefore, in the case of the three types of problems mentioned above, simulation needs to be performed to solve them.

A process simulator, as a tool for design and synthesis, may be constructed in different ways. Common to all types is that they consist of an input section in which the user defines the problems and gives the unit specifications, and an output section in which the simulation results of the simulation are presented. Between the input and the output, the simulator performs calculations based on the input decisions made, and the built-in calculation models. Process simulators may then be classified as either *sequential modular* or *equation oriented*. The sequential modular approach simulates (calculates) one unit model at the time according to a *flowsheet decomposition approach* while simulators employing the equation oriented approach assemble the process equations (unit models, streams, connectivity, thermodynamics) and solve them simultaneously. The popular commercial simulation software packages ASPEN, HYSIS and Pro/II are all of the sequential modular type (only referring to steady state simulation options).

Simulation may be performed at steady state, where one steady state point of operation is reached, or it may be performed in dynamic mode, which involves changes with respect to time. Dynamic simulation is often used as a means of analyzing or verifying the controllability and/or disturbance resiliency of a process. Dynamic simulation requires more information (input) from the user than steady state simulation. First of all, dynamic model equations require accumulation terms to be added to mass and energy balances, so that holdups based on the sizes of the equipment can be calculated. Also, to analyze controllability of a given system, a control system must be given as input. Tuning and altering the control system is one of the main objectives when performing dynamic simulations, as performance of the control system can be optimised by this means. This is done with respect to user defined set-point and disturbance variable changes. The initial starting point for a dynamic simulation is usually a steady state operating point. Dynamic simulation may be performed using both a sequential modular approach or a equation oriented approach.

3.4.2 Optimisation

In this section the objective is to give an overview of how separation synthesis and design problems can be solved and/or verified by mathematical optimisation techniques. For the synthesis of separation schemes, it is evident, that

once a number of process alternatives are available, and it is uncertain which alternative is the better choice, it is interesting to evaluate them in a systematic manner to identify which is the optimum one. In case a separation scheme has been determined, and the operating conditions leading to the best performance of the process is sought, optimisation may also be employed. The search for optimum solutions may be carried out in terms of trial and error calculations. However, defining a mathematical programming problem and solving it may be a much more efficient approach. The optimisation problem of separation processes may be stated as:

> *Provided a system (feed mixture) or a separation process is given, find the best solution to this separation process within constraints of operation.*

The 'best solution' is quantified by an *objective function*, a mathematical expression, which describes what is to be optimised by decision variables. In chemical process industries the objective function is usually concerned with minimising the operational costs and/or maximising profitability. The values of the objective function are then found by manipulating design variables, within the *constraints* of operation. These are typically items like product purity, operation variables (*e.g.* reflux ratio, reaction temperature, etc.) related to performance and operation, known as *inequality constraints*, or mass and energy balances equations that need to match as well as equilibrium conditions, etc., known as *equality constraints*. Different methods for the solution of optimisation problems exist, depending on the formulation of the optimisation problem. The common ones are unconstrained optimisation, linear programming (LP), non-linear programming (NLP), mixed integer linear programming (MILP), mixed integer nonlinear programming (MINLP) and dynamic optimisation. In process engineering, practically all optimisation problems are constrained, and only these will be dealt with here.

3.4.2.1 Optimisation of continuous processes

When optimising variables that are continuous, the mathematical formulation of the optimisation problem is as follows:

$$\begin{aligned} \min_{d} \quad & f(x) \\ s.t. \quad & g(x) = 0 \\ & h(x) \leq 0 \end{aligned} \tag{3.2}$$

The optimiser adjusts the continuous design variables, d, until the minimum value of $f(x)$ has been found within the space constrained for the search, *i.e.* the *feasible region* which is limited by equality constraints $g(x)$, and inequality constraints $h(x)$. In case f, g and h are all linear, equation 3.2 corresponds to a LP problem. LP problems are in general easy to solve, and a global optimum

can be found. The *Simplex algorithm* by Hillier and Lieberman (1986) is commonly applied to solve this kind of problem. However, much more common is a scenario in which at least one of f, g and h is not linear, and the problem becomes a NLP problem. These problems are more difficult to solve, and the guarantee that the solution is a global optimum and not a local optimum is often difficult to verify. Local optimum solutions can be defined as satisfying the *Kuhn Tucker* optimality conditions. Biegler *et al.* (1997) gives a detailed description and derivations of the Kuhn Tucker conditions. The Kuhn Tucker optimality conditions have formed the basis of the popular process optimisation algorithm known as *Successive Quadratic Programming* (SQP). Different variations of the SQP algorithm have been developed, one example is the algorithm by Bossen (1995).

3.4.2.2 Optimisation with structural alternatives

If the optimisation problem contains integer (often binary 0-1) variables, *i.e.* structural decision variables such as for example choice of alternative separation units, the problem is either of the linear MILP type or the non-linear MINLP type. This type of optimisation is often based on a predefined superstructure, as a point of reference for alternative solutions, in order to find the optimum. A general mathematical formulation of this problem was given previously in chapter 2, as stated below:

$$\begin{aligned} \min_{x,y} \quad & Z = C(x,y) \\ s.t. \quad & h(x) = 0 \\ & g(x,y) \leq 0 \\ & x \in X \quad y \in \{0,1\}^m \end{aligned} \tag{2.1}$$

The standard solution method of MILP problems is the *branch and bound method* (Nemhauser and Wolsey, 1988). This method solves relaxed LP problems to identify the optimum solution by the use of bounds in a tree of binary variables. This is done for each 0-1 combination, and the solution can be found efficiently by solving successive LP problems. Taking non-linearities into account when dealing with MINLP problems, however, makes it more difficult to solve the optimisation problem. Two commonly used methods to solve these kind of problems exist. One is the *Generalized Benders Decomposition* (GDP) (Geffrion, 1972) and the other is the *Outer-Approximation* (Duran and Grossmann, 1986). Both methods are used to solve an alternative sequence of MILP and NLP sub-problems. The optimum solution is found and the search terminates when the predicted lower bound coincides or exceeds the current best upper bound. More information on this topic is given by *e.g.* Biegler *et al.* (1997) and Floudas (1995).

3.5 Integration of tools

As stated in chapter 2 and the previous sections of this chapter, there are different problems that require a solution in order to make synthesis and design decisions for separation systems in chemical plants, regardless whether well-known existing methods are applied, or the methods developed in this thesis are applied. In order to solve these individual problems, a large number of different tools are often required. To ease the task of doing these different operations, it is asset for the design engineer to have all the necessary tools available in an integrated environment, where they can all communicate with each other, thus gaining large synergy effects from data exchange. The advantages of such integrated systems are not limited to just communication between the tools, they may also assist the user in generation of process alternatives, as for example if an azeotrope is identified in a mixture, some tool in the integrated system may then suggest use of one or more solvent(s), that are capable of 'breaking' the azeotrope. The synthesis tool may then be involved to generate process schemes with solvent based distillation column and solvent recovery columns, or membrane based separation is suggested, and the database is consulted to check whether membrane processes are known for this mixture. At this stage, for example, simulations can be made for the different process alternatives, and an optimisation problem can be formulated and solved. The compounds and their properties will be the same for all these operations.

Many simulation software packages have additional tools integrated to it. Almost all commercial simulators, for example, have an integrated optimisation module. Further, ASPEN has a tool for design of azeotropic distillation schemes called SPLIT (see also section 2.3.1.3). HYSIS has a module for generation of alternative column sequences, including complex columns, which also suggests which alternatives are better for a given feed mixture. Thermodynamic models are always incorporated in simulation packages, and some provide the option to perform dynamic simulation/optimisation in addition to steady state simulation. However, when using most of the available simulation packages, there are still a lot of tools, or information that the user needs to find elsewhere.

3.5.1 ICAS - Integrated computer aided system

Within the CAPEC research group at Technical University of Denmark, a integrated computer aided system (ICAS) has been developed for process synthesis, design, analysis, etc. The individual computational tools are included as toolboxes, where the user then can move from one toolbox to the other during the solving of problems. From any toolbox, it is then possible to invoke a simulation engine, to perform steady state and/or dynamic simulation. In this way the interlinking of the tools necessary are logically reflecting the steps of solving a process synthesis problem, starting from a given feed mixture, generating alternative synthesis routes and ending up with a sophisticated optimal design. With respect to the methods developed in this thesis, some of them

are implemented in ICAS, as described in section 4.9.

Some of the features available in ICAS as toolboxes are:

- Property prediction: The CAPEC database with numerous reported experimental results, Propred for pure component property prediction, TML for mixture property prediction and model parameter estimation, and TMS for thermodynamic model selection.
- Modelling: ModDev for computer aided model generation, MoT for model analysis, translation and solution, as well as addition of user defined models.
- Process synthesis and design: CAPPS for computer aided flowsheet (alternatives) generation, PDS for the design of conventional, reactive and azeo-tropic distillation columns, ProCAMD for solvent search and design.
- Reactions: The CAPEC database with chemical reaction data, ReacPar for kinetic model parameter estimation and RAS for reaction path synthesis.
- Simulation: ICASsim for steady state simulation and DYNSIM for dynamic simulation. BRIC is for batch operation records and simulation.
- Control: Design and analysis of control systems, including a toolbox (MPC) for model predictive control.

More information on ICAS is available from Gani (2002).

4

THE DRIVING FORCE APPROACH TO SYNTHESIS AND DESIGN

4.1 Introduction

In this chapter, the driving force concept and driving force based methods for the synthesis and design of separation processes developed in this Ph.D. project are presented. The approach to separation synthesis and design problems considered in this thesis, is based on the definition of driving forces as the difference in chemical/physical properties between two co-existing phases. The approach is thus a *thermodynamic insights based* approach, utilizing property data to predict optimum or near optimum configurations of separation flowsheets.

In this chapter, the driving force concept is introduced first, and a definition of driving force is given. The methods developed are then presented, and they are divided into methods related to either a synthesis, design, analysis or retrofit problem. Each of these topics are treated in a separate section in this chapter, and the specific methods and algorithms for the solution to each type of problem are then presented in a sub-section. The methods are then further incorporated in an integrated approach, utilizing all the developments in a comprehensive framework for the synthesis and design of separation processes. Finally, computational tools developed to enable the user to get useful and fast calculation of results of the algorithms are presented, and a discussion of the methods developed is given.

4.2 Definition of driving force

Different definitions of driving forces exist in chemical engineering, such as the classical textbook definition by Chilton and Colburn (1935), where the driving force in distillation is defined as the difference between actual concentrations

for substances and their equilibrium concentrations.

In this thesis the term "driving force" (denoted F_{Di}) is based on a new definition, which is given below, together with an explanation.

$$F_{Di} = y_i - x_i = \frac{x_i \beta_{ij}}{1 + x_i(\beta_{ij} - 1)} - x_i \tag{4.1}$$

The definition of driving force is the difference in compositions of compound i in two co-existing phases that may or may not be in equilibrium. β_{ij} is a parameter (relative separability) that may or may not be composition dependent and provides a measure of the driving force. The parameter β_{ij} is obtained from a model describing the differences in composition between two co-existing phases, or measured composition data. As the size of the driving force for a given separation approaches zero, separation of the species involved becomes difficult, because there is less difference in composition between the bulk phases. On the other hand, as the driving force increases in size, the separation becomes easy due to the large difference in composition between the phases. The difference in composition may be due to the thermodynamic equilibrium between the two phases as in the case of distillation. But transport mechanisms other than thermodynamic equilibrium can also cause driving forces, and make separations take place. These are for example diffusion or convection. The transport mechanism is illustrated in figure 4.1, where the transition between two bulk phases and the mechanisms of composition differences is illustrated. The transition between the two bulk phases that cause the composition difference, as it is illustrated in figure 4.1 may occur due to either thermodynamic equilibrium (possibly with reaction) and/or some other transport mechanism.

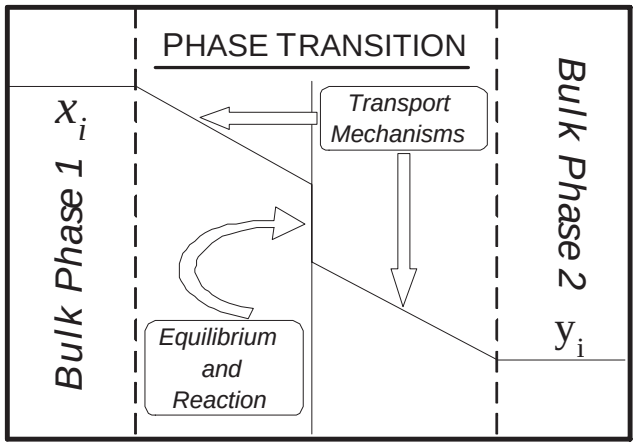

Figure 4.1: Mechanisms of phase composition differences.

4.2.1 Separation mechanisms

The generation of a two-phase separation and a composition dependent driving force can be achieved in different ways and by different separation principles. Two phases can be created in many ways - addition of energy, MSA, creating a barrier, force-field, etc., each defining a corresponding separation mechanism.

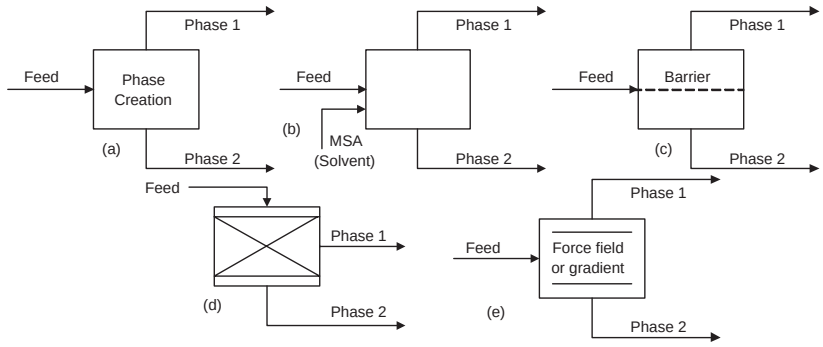

Figure 4.2: Categories of separation mechanisms [Seader and Henley (1998)].

In figure 4.2a, a second phase is created to generate separation of one or more compounds from a feed mixture. This operation requires energy input. The typical example of this type of process is separation by flash, by evaporation or by distillation. Another separation mechanism is illustrated in figure 4.2b, which is also relevant to some form of distillation. Here a solvent/entrainer is added, which affects the phase equilibrium by selectively dissolving one of the mixture compounds. Apart from extractive/azeotropic distillation, the concept is also applied to liquid-liquid extraction. The opportunity of using a semi-permeable membrane, or some other technique based on a separation barrier is illustrated in figure 4.2c. Solid agents may also be used to generate separation, as shown in figure 4.2d, where some typical processes are adsorption and chromatography. Finally, figure 4.2e shows how separation may be caused by some external force or field. Examples are centrifugation or electrolysis, where an electric force is combined with a membrane.

4.2.2 Driving forces for separations

In all cases of separation, the driving force concept may be applied to illustrate and compare feasibility of separation techniques. As mentioned previously in section 4.2, when the driving force decreases, separation becomes difficult, and the separation becomes infeasible when the driving force approaches zero. When the driving force approaches its maximum value, the separation becomes very easy, and the energy necessary to maintain the two-phase system is at a minimum. This is so because, in separation processes where energy is required, the driving force is inversely proportional to the energy added to the system to

create and maintain the two-phase (for example vapour-liquid) system. Therefore, synthesis and design of separation processes, such as distillation, where the largest driving force has been utilized may lead to highly energy efficient flowsheets and separation unit designs. Thus, from an operational point of view, a process should be designed/selected to operate at the highest possible driving force. Note that this is true irrespective of whether the separation process is rate-based or equilibrium-based since the driving force can be calculated from the measured or estimated composition data. Considering driving forces based on different sets of properties (or based on different solvents), a set of feasible separation techniques for a specified separation task can be identified.

The starting point for driving force based methods is first of all the availability of phase composition data, and secondly the graphical representation of these phase composition data. The driving force as defined in equation 4.1, is a general model, independent of whether x_i and y_i are related by equilibrium or not. For a process, where vapour and liquid compositions are in equilibrium, however, β_{ij} may be replaced by α_{ij},

$$\beta_{ij} = \alpha_{ij} = \frac{y_i/x_i}{y_j/x_j} = \frac{y_i(1-x_i)}{x_i(1-y_i)} \tag{4.2}$$

Thus, the well-known relative volatility expression leads to the driving force for equilibrium based distillation. Note in this context, the *relative separability* factor β_{ij} can be fitted to any two phase binary mixture data, whether in equilibrium or not (compound j is the reference key compound).

The model equation (4.1) is differentiated with respect to composition in order to obtain the value of x_i where F_{Di} has its maximum value, *i.e.* where the largest driving force is achieved. Then for a constant value of β_{ij}, the derivative of F_{Di} with respect to x_i becomes:

$$\frac{\partial F_{Di}}{\partial x_i} = \frac{\beta_{ij}}{(1 - x_i + \beta_{ij}x_i)^2} - 1 \tag{4.3}$$

Naturally, x_i is limited to values between 0 and 1, and therefore only positive values of equation 4.3 are of interest. This expression may now be used to identify the location of the maximum driving force, $F_{Di}|_{max}$, which is known as the point $x_i|_{max}$. For a constant value of β_{ij}, this becomes:

$$x_i|_{max} = \frac{\sqrt{\beta_{ij}} - 1}{\beta_{ij} - 1} \tag{4.4}$$

Since β_{ij} is greater than 1 for $F_{Di} > 0$, $x_i|_{max}$ in equation 4.4 is always positive and less than 1.

For visualisation purposes, the driving force, F_{Di} may be plotted as a function of liquid (or vapour) composition. A plot of driving force, F_{Di} versus composition, x_i for a constant $\beta_{ij} = 3$ is shown in figure 4.3. It can be seen that F_{Di} in this case is a convex function with respect to x_i with a well-defined

maximum, and, as $x_i \rightarrow 0$ or 1, $F_{Di} \rightarrow 0$. In figure 4.3, $F_{Di}|_{max}$ and $x_i|_{max}$ are denoted as D and D_x respectively.

Note that the maximum driving force can only be employed if the two product compositions lie on either side of $x_i|_{max}$.

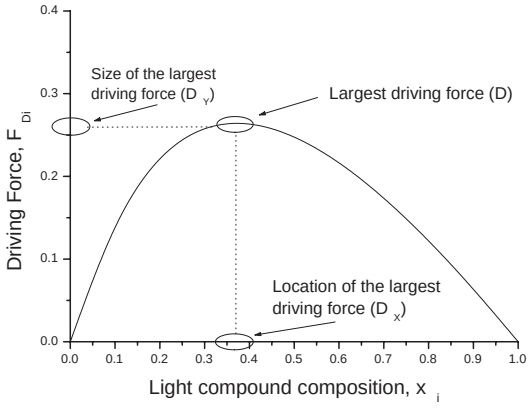

Figure 4.3: Driving force as a function of composition for $\beta_{ij} = 3$.

4.3 Synthesis of separation schemes

For the generation of separation schemes, the driving force approach has been applied to develop separation synthesis techniques. The idea of maximising the driving force has been applied to the generation of distillation column sequences as well as hybrid separation schemes, and methods have been developed for these two types of synthesis problems and are presented in sections 4.3.1 and 4.3.2.

4.3.1 Distillation trains

In order to determine the optimum, or near optimum sequence of a distillation train, a new method has been developed. Based on the driving force approach, an algorithm is proposed that in a simple way provides for the most energy efficient sequence of simple conventional distillation columns in order to obtain the specified product streams. The new algorithm is valid for basically all types of systems, ideal as well as non-ideal, and it is independent of the feed mixture composition. In order to apply it only appropriate and accurate thermodynamic properties that properly describe the phase behaviour of the adjacent key compounds in the feed mixture are required.

For a mixture of NC compounds, the total number of adjacent pairs of key compounds is $NC-1$, and the minimum number of separation tasks is also $NC-1$. To apply the driving force based algorithm to generate a sequence of distillation columns for separation of a multicomponent mixture, the algorithm outlined in the following section is proposed.

4.3.1.1 Algorithm for the generation of distillation trains

This algorithm provides a driving force based solution to the problem of synthesizing a distillation train. Input data to this algorithm are the identity of the compounds in the feed mixture and vapour-liquid phase compositions. The algorithm determines the $NC-1$ separation tasks (that is adjacent pairs to separate) and the sequence in which they should occur. The method is outlined in the step-by-step form below.

1. List all the compounds in the mixture, NC, according to their relative separability, β_{ij} (or relative volatility).
2. Rank the compounds by normal boiling points. Retrieve the vapour-liquid data available for each binary pair of adjacent key compounds in the $NC-1$ splits.
3. Calculate the driving force diagrams for the binary pairs of key compounds, all at the same pressure (usually atmospheric pressure). In total, $NC-1$ driving force curves are calculated. Set $k=1$.
   - 3.1 If a binary pair forms an azeotrope, multiply the maximum driving force for this pair by a penalty factor, $\left(\left(\frac{\mathrm{D_{y,min}}}{\mathrm{D_{y,max}}}\right)\cdot D_{y,azeotrope}\right)$ in order to make its value the smallest among all the binary pairs.
4. For the split k, select the adjacent pair having the largest driving force.
5. Add a distillation column for the separation task k.
6. Remove the split between the selected adjacent pair from the list. Set $k=k+1$, and repeat the algorithm from step 4 until only one split remains to be allocated. Otherwise, go to step 7.
7. For each column of the distillation flowsheet, the feed stage location may now be determined, if desired by the algorithm described in section 4.4.

This algorithm is referred to in this thesis as algorithm S1. The algorithm is presented as a block diagram in figure 4.4.

4.3.1.2 Evaluation of driving force based distilaltion sequencing

The application of algorithm S1 is illustrated in figures 4.5 and 4.6, where driving force curves for four different values of β_{ij} are plotted, and the corresponding distillation sequence is given. In this case the algorithm predicts that,

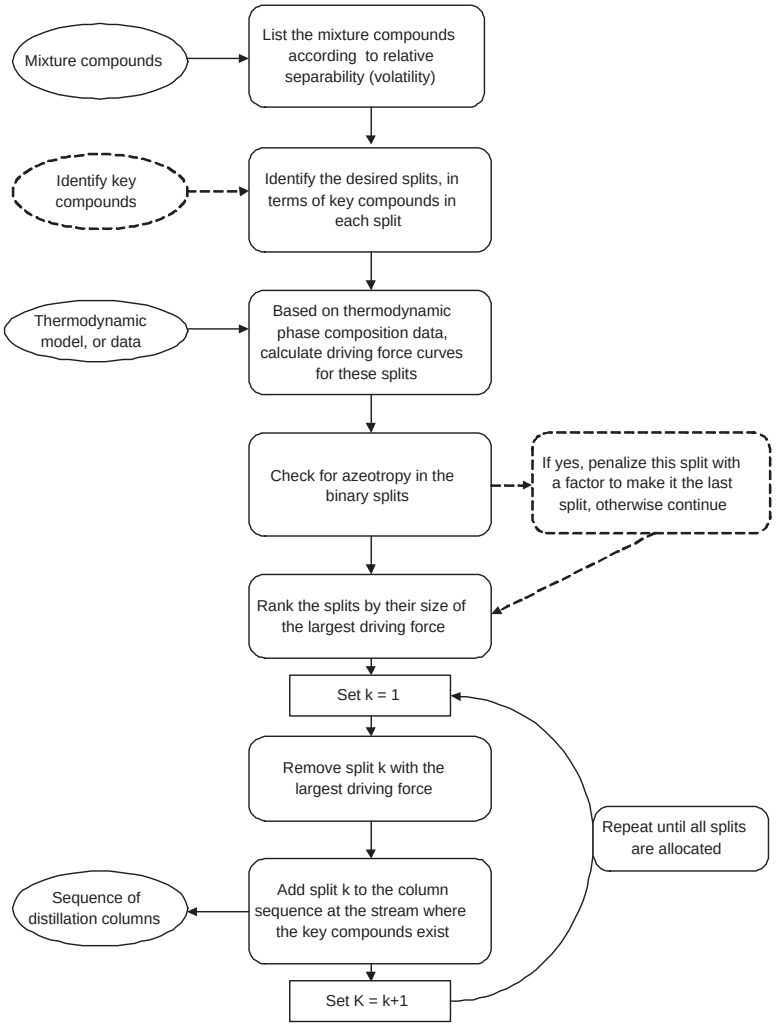

Figure 4.4: Block diagram of the distillation column sequencing algorithm (algorithm S1).

curve 1 represents the first separation task with the largest value of maximum driving force, *i.e.* the first distillation column in the sequence, then followed by the second column performing the separation task of curve 2, then curve 3, and at the end comes the last separation task which is the most difficult represented by curve 4.

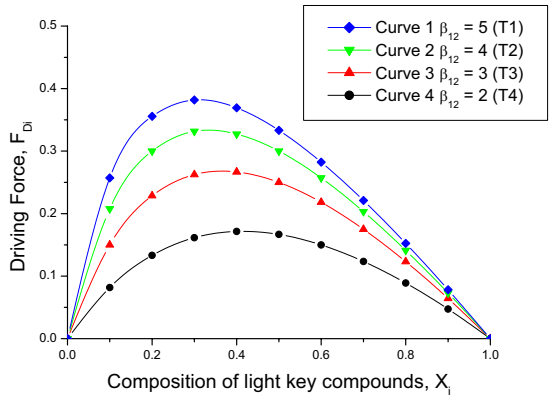

Figure 4.5: Driving force as the function of composition for different values of β_{12}.

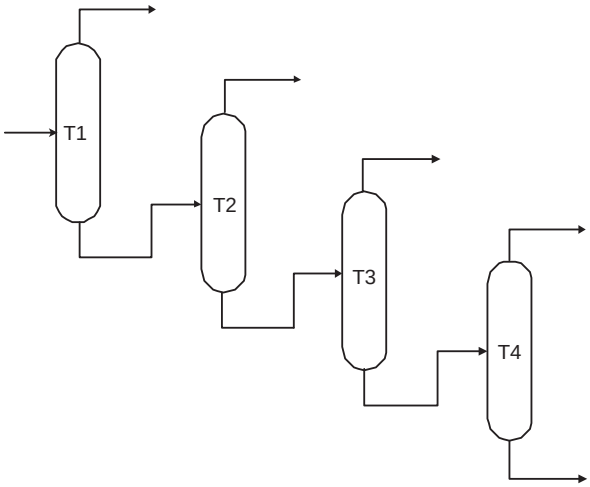

Figure 4.6: Distillation sequence corresponding to the driving force diagrams from figure 4.5.

By following this method, the total driving force that will be utilized, is the largest possible. This is because the largest flow rate is in the first column,

where the largest driving force exist, and the smaller the flows in the columns, the smaller the driving force. In this way the easiest separation is achieved for the total separation sequence, and in the columns with the largest driving force (and largest flows), the least energy is required.

The algorithm is limited to non-azeotropic mixtures. If an azeotropic mixture is selected as the separation task, one of the products is at the azeotropic composition, which limits further separation through simple distillation columns. However, this problem may be resolved by placing the binary pair forming an azeotrope as the last separation and then employing a solvent-based or hybrid separation technique (see algorithm S2 in section 4.3.2).

In case the mixture is not to be separated into pure compounds, but into fractions of more than one compound (for example a fraction of close boiling isomers), the key compounds are identified according to the desired splits. The driving force diagrams only have to be calculated for the binary adjacent pairs of key compounds and the direction of the relevant separation tasks is determined by algorithm S1, starting from step 2.

Although there seem to be no constraints in the proposed new algorithm, practical constraints must be taken into consideration when appropriate. Some practical constraints that may be relevant are listed below. Constraints are individual to each system, and it should be noted that only a few obvious constraints are listed below.

- Safety considerations might dictate that a hazardous compound must be removed early.
- Reactive and heat sensitive compounds must be removed early.
- Corrosive compounds should be removed early, to minimise the use of expensive materials.
- Compounds that are difficult to condense should be removed in the first column, in order to minimise the use of refrigeration and allow for lower pressures in the distillation column sequence.

4.3.2 Hybrid separation

When different separation techniques are considered, it is possible on the basis of driving forces to identify a set of feasible separation methods for a specified separation task. Based on driving force diagrams, flowsheet alternatives can be generated and visualized. By using this approach it is possible to identify cases where a single separation technique is unable to perform a specified separation task. In these cases, feasible flowsheet alternatives of hybrid separation schemes can be generated.

Some reasons to apply hybrid separation schemes are outlined below, while typical processes where hybrid separation schemes are employed are listed in table 4.1.

1. Desired separation cannot be attained in one separation unit.

2. Environmental constraints cannot be satisfied with conventional separation techniques.

3. Energy utilization is too high, *i.e.*, the driving force is too low.

In all the above cases, hybrid separation schemes become attractive, either because the desired separation is not feasible in a single unit, or because the separation becomes difficult or energy inefficient in a given unit operation. An example is the case where the driving force is higher for a membrane process compared to distillation in the separation of two close-boiling compounds, thus it is advantageous to employ a hybrid separation scheme.

Process type	Hybrid scheme
Purification beyond azeotrope	Distillation and membrane
Purification beyond eutectic point	Crystallisation and distillation/extraction
Removal of undesired compounds	Distillation/extraction and external agent based separation
Reactor effluent separation	Combined reaction and separation hybrid units

Table 4.1: Candidate processes for hybrid separation schemes

4.3.2.1 Algorithm for the generation of hybrid separation schemes

The problem this algorithm solves is the identification of the optimal separation sequence(s) for a given separation task, based on a driving force analysis. As input to the algorithm, are the phase composition data for the compounds to be separated, for as many separation methods as there are considered. The algorithm determines feasible solutions based on these data, as well as the solution(s) with the greatest possible driving force. The method consist of five steps, as outlined below:

1. Collect and/or generate phase composition data of the mixture to be separated for as many separation methods as desired (or available).

2. Calculate the driving forces of the alternative separation techniques considered. Plot all corresponding driving force curves in a single driving force diagram.

3. Screen for feasible solutions. Compare the driving force curves for the individual separation techniques, and combine them to generate all feasible combinations/solutions.

4. Identify the solution(s) with the greatest possible maximum driving force. This method (or, these methods) is the optimum solution.

5. Evaluate the alternatives from step 4 (if desired, also step 3). Compare the optimum (feasible) solutions in terms of costs for equipment and costs associated to the operation.

This algorithm is later on in this thesis referred to as algorithm S2. The algorithm is presented in the form of a block diagram in figure 4.7.

The method can be considered iterative. If it is found that the considered techniques do not provide an acceptable solution, or the accuracy or the amount of the data available is improved, the procedure can be repeated.

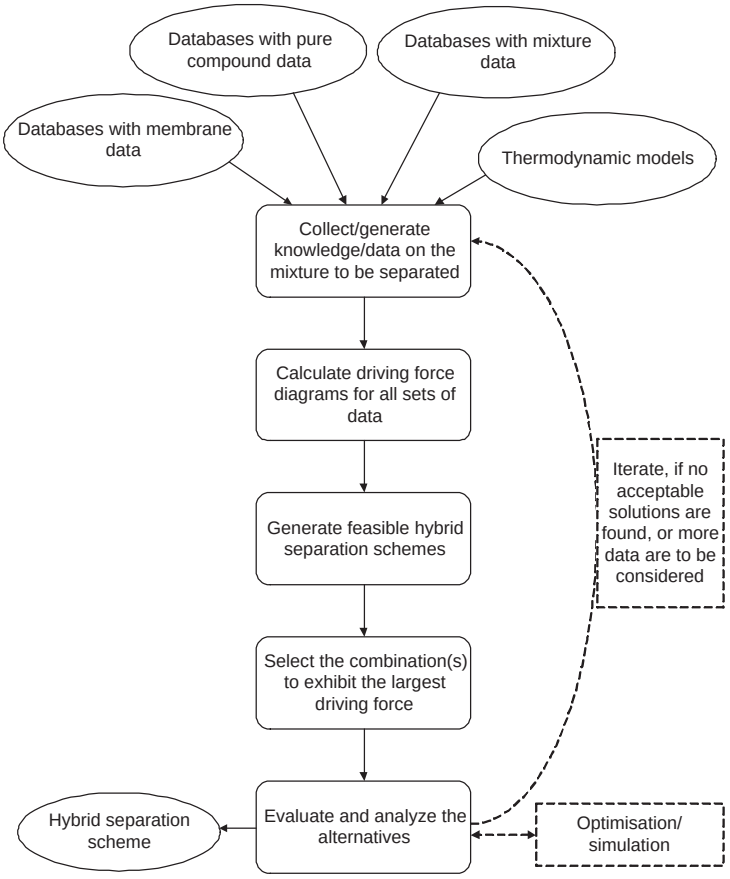

Figure 4.7: Block diagram of the method for the generation of hybrid separation schemes (algorithm S2).

4.3.2.2 Evaluation of driving force based hybrid separation schemes

Figure 4.8 indicates the case where different separation techniques are compared. Data for a given separation has been collected for different separation techniques, and driving force plots have been made for distillation, pervaporation and extractive distillation. If it is desired to perform the separation in the $[0; 1]$ composition range, how should the separation techniques be combined? The first thing to notice is that there are three possible (feasible) combinations. 1) Distillation and pervaporation. 2) Extractive distillation and pervaporation. 3) Extractive distillation. It is clear from visual observation that distillation combined with pervaporation exhibits the largest driving force, and should thus be preferred (step 4). In step 5 of the algorithm, in the evaluation of feasible combinations of unit operations, it must be kept in mind that the extractive distillation operation requires at least one extra column for solvent regeneration. In figure 4.9, the flowsheet exhibiting the greatest possible driving force among the separation methods considered in figure 4.8, is shown. It is clear that distillation should be applied in the lower composition range, and pervaporation should be applied in the higher composition range.

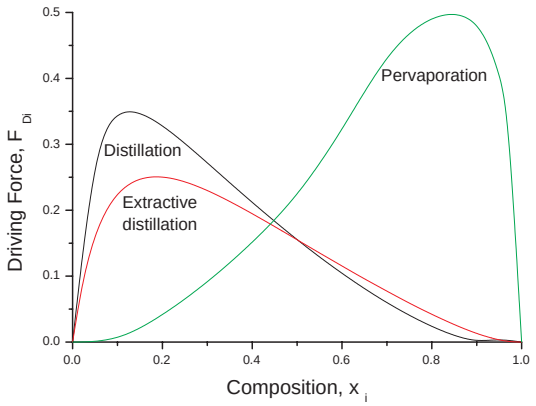

Figure 4.8: Driving force diagrams for alternative separation methods for binary azeotropic mixture.

Applying the driving force approach to hybrid separation problems generates feasible and often optimal solutions to the synthesis problem. This is clear in terms of energy consumption, since choosing separation techniques exhibiting a great driving force requires low energy consumption. The method, however, is strictly dependent on the user having phase composition data sources or tools to obtain such data for alternative separation techniques. For example, if distillation is considered, either measured vapour liquid phase composition data are required, or reliable thermodynamic model parameters are required

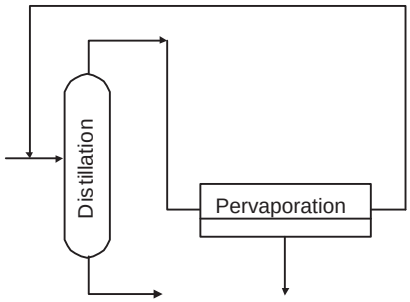

Figure 4.9: Hybrid separation scheme for the separation of azeotropic mixture (for mixture considered in figure 4.8).

to verify whether distillation is a feasible option at all, and then compare it to other separation techniques. Feasibility of membrane separations are more difficult to predict, and the capability of a given membrane to perform the separation is dependent on measured data.

When calculating the driving force diagram for a binary mixture with a solvent added, as in the case of extractive distillation in figure 4.8, the phase compositions are calculated on a solvent free basis. In this way the choice of solvent can be related to the driving force, and the visualisation of the desired separation will then be based on the binary mixture. The following equations define the driving force on a solvent free basis.

$$FD_i = |y'_i - x'_i| \tag{4.5}$$

where,

$$y'_i = \frac{y_i}{1 - \sum_j^S y_j} \tag{4.6}$$

and

$$x'_i = \frac{x_i}{1 - \sum_j^S x_j} \tag{4.7}$$

In equation 4.6 and 4.7, the summations are made for all the solvents in the mixture.

In this approach to the synthesis of hybrid separation schemes, the visualisation of driving force curves for alternative separation techniques allows for an easy prediction of feasible alternatives, and often even the optimal combination.

4.3.2.3 Driving force analysis based on properties

When considering alternative separation techniques such as membranes and different types of distillation in a hybrid separation scheme, the driving force

shows the behaviour of the system in terms of composition changes, as it is illustrated in figure 4.8. In distillation, the driving force occurs due to differences in normal boiling points and is represented by relative volatility, while in other separation techniques driving forces are represented by their corresponding relative separability parameters. Table 4.2 gives a list of separation techniques often applied in hybrid separation schemes, where the efficiency criteria (causing the driving forces) are given for each technique. The limitations are also listed (where the driving force becomes zero). In all the types of separation, the driving force is a function of composition and equation 4.1 can be employed as the model. Different types of driving forces, however, also exist for different separation techniques, where the type of property is related to one or more specific separation technique(s). The separation technique may be based on a *primary* property or a *secondary* property. For the initial evaluation of separation techniques, the properties may be considered as indicators of feasibility of a separation technique, *i.e.* to indicate whether a driving force exists for a related separation technique for a specified mixture. In order to conduct this initial comparison of separation techniques, a parameter, PF_{Di} (*property driving force*), is defined, highlighting the differences in a given property between two compounds.

$$PF_{Di} = \frac{|p_i - p_j|}{p_j} \tag{4.8}$$

In equation 4.8, p_i and p_j are pure compound properties of compounds i and j, in the mixture to be separated, which can be related to one or more separation technique(s). A relevant property is, for example, normal boiling point for distillation. Very close boiling compounds have very close normal boiling points, and distillation is less attractive as the separation technique for such a mixture, whereas large differences in van der Waals volume would indicate that pervaporation is a good choice as the separation technique, provided a suitable membrane can be found.

The property driving force, PF_{Di}, is not directly comparable to the driving force as defined in equation 4.1, F_{Di}, and therefore the two driving forces should be compared on different scales. Figure 4.10 highlights the comparison of different property-based driving forces as defined by equation 4.8. Difference in molar volume is applied as a separation criterion in different membrane processes, van der Waals volume is applied in different separation techniques, amongst them adsorption and pervaporation, and finally melting point difference is exploited in crystallisation.

4.4 Design of distillation columns

Consider the situation where a given mixture is to be separated by distillation to some specified product purity requirements. The design of the distillation column to perform this task typically involves the determination of variables

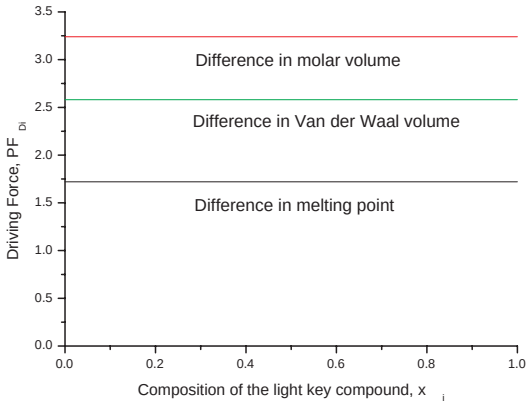

Figure 4.10: Property driving force diagrams for alternative separation methods based on primary properties.

Unit Operation	Efficiency Criteria	Limitations
Distillation	Large difference in volatility	Azeotropy
Membrane	Large difference in size/volume	Low flux
Crystallisation	Large difference in melting point	Eutectic mixtures
Extraction	Solvent breaks azeotropes, eutectic points, increases volatility	Suitable solvents (MSA)

Table 4.2: Candidate unit operations in hybrid separation schemes.

like the number of stages, feed plate location, reflux ratio. Preliminary values of these design variables are often determined by trial and error calculations using for example a simulation engine, or the McCabe-Thiele method in its modern version (see *e.g.* Seader and Henley (1998)). Since distillation is a very energy intensive process, it is desirable to determine the values of these design variables corresponding to a minimum in terms of costs of operation.

In this section the driving force approach has been applied to the design of distillation columns. The objective of a driving force based design is to design the distillation column to operate at the maximum driving force, *i.e.* utilize the largest possible area of the driving force diagram. This simple and visual approach is the basis for the determination of important distillation column design variables, which in this section are determined by introducing the location and the size of the maximum driving force, D_x and D, as parameters.

Then D_x and D are related to the feed stage location and the reflux ratio.

At first, the approach is applied to the simple distillation column with one feed and two products, which also serves as a 'base-case', in which the design concept and procedure are explained in detail. Afterwards, driving force methods for more specialized applications are presented. These show different types of complex distillation columns as well as reactive distillation columns.

4.4.1 Design of simple distillation columns

The starting point for the design of a simple distillation column is the vapour-liquid data, visualised in a driving force diagram, where the driving force between the vapour and liquid composition is plotted as a function of composition. A driving force diagram together with the distillation design parameters are illustrated in figure 4.11.

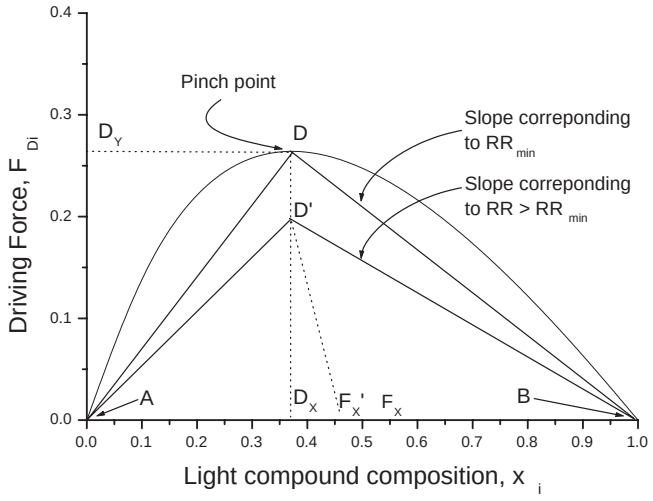

Figure 4.11: Driving force diagram with illustration of the distillation design parameters.

4.4.1.1 Algorithm for design of simple distillation columns

Consider the design problem defined as,

> *Given a mixture to be separated into two products in a distillation column with N plates. What is the optimal (with respect to the costs of operation) feed plate location and the corresponding reflux ratio for different product purity specifications?*

The solution involves the following steps:

1. Generate or retrieve from a database, the vapour-liquid data for the binary system. For a multicomponent system, select the two key compounds to define the "split" and use them as the binary *key* mixture.
2. Compute F_{Di} using equation 4.1 and plot F_{Di} as a function of x_i, where i is the light key compound.
3. Identify the points D and D_x (graphically or using equation 4.4).
4. For a given number of stages, N, determine the feed stage, N_F from $\mathbf{N_F = (1 - D_x)N}$.

Additional steps have been added to the algorithmic procedure for the positioning of the feed stage location in order to deal with the situations where either the feed mixture is diluted, or the desired product specifications are of a non-sharp character. The conditions under which these additional steps are employed is outlined in table 4.3. The steps are given in algorithmic form as the following.

5. If condition 1 or condition 2 in table 4.3 is satisfied go to step 6. Otherwise stop (or go to step 7).
6. If condition 1 is satisfied, go to 6.1, else go to 6.2.
   - 6.1 If condition $1a$ is satisfied, then relocate N_F between 5 and 10% up in the column.
     Else condition $1b$ is satisfied, then relocate N_F between 5 and 10% down in the column.
   - 6.2 If condition $2a$ is satisfied, then relocate N_F 10% down.
     Else, if condition $2b$ is satisfied, then relocate N_F 5% down.
     Else, if condition $2c$ is satisfied, then relocate N_F 5% up.
     Else, if condition $2d$ is satisfied, then relocate N_F 10% up

It is clear that the above algorithm is very simple and needs very few calculations. The algorithm is valid for any value of N where the specified separation is feasible. Therefore, iterations can be made over the number of stages in the column, N. The value of N_F is re-calculated for each value of N, and if the separation is feasible with this number of stages, the value of N_F can be obtained as described above. In case azeotropes are present in the binary mixture, it is important that this is reflected in the choice of the desired products A and B, so that the product compositions are feasible, *i.e.* lies within the convex driving force curve between two end points (where the driving force is zero).

Normally, with the values of N, N_F, product purities (A and B) and feed condition specified, q, the design of a distillation column can be verified through

Condition 1	
a)	$x_{HK,Z} < 0.8$ and $D_x < 0.7$
b)	$x_{LK,Z} < 0.8$ and $D_x > 0.3$
Condition 2	
a)	$\frac{1-x_{LK,D}}{1-x_{HK,B}} < 0.01$ and $D_x < 0.7$
b)	$\frac{1-x_{LK,D}}{1-x_{HK,B}} < 0.1$ and $D_x < 0.7$
c)	$\frac{1-x_{HK,B}}{1-x_{LK,D}} > 0.1$ and $D_x > 0.3$
d)	$\frac{1-x_{HK,B}}{1-x_{LK,D}} > 0.01$ and $D_x > 0.3$

Table 4.3: Conditions of distillation column feed and products that require a scaling factor to be included in the design procedure.

rigorous simulation/optimisation, or further analysed in terms of controllability and operation. For the simulation model, however, it is a good idea to have good estimates for the reflux ratio (since it will be calculated) and a guarantee that the desired separation is feasible. Therefore, values of reflux ratios are needed to start the validation related simulations. For specified product purities, the following alternative steps are employed for the determination of N_F, N and RR.

7. If the product specifications are given, locate the points A and B. Determine the slopes of the lines AD and BD. Determine the corresponding RR_{min} (and RB_{min}).

8. Choose a value of $C = RR/RR_{min}$ to locate the point of intersection, D' (see figure 4.11). Draw the operating lines for the rectifying and stripping sections and determine the number of plates in the same way as in the McCabe-Thiele method.

The algorithm presented here in this thesis is referred to as algorithm D1. The algorithm is presented as a block diagram in figure 4.12.

4.4.1.2 Evaluation and comments on the algorithm for design of simple columns

Figure 4.13 illustrates how the driving force diagram is utilized in the design of a simple distillation column as described above, in order to obtain the maximum driving force, and especially how the connection between the relative position of the maximum driving force, D_x is correlated with the feed stage location, N_F.

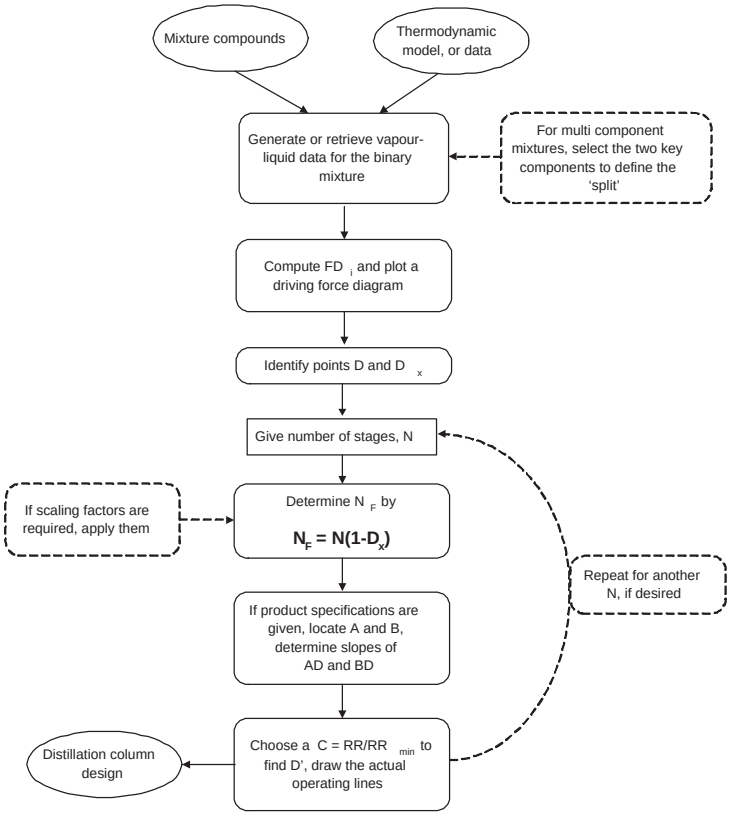

Figure 4.12: Block diagram for the driving force based design procedure for simple distillation columns (algorithm D1).

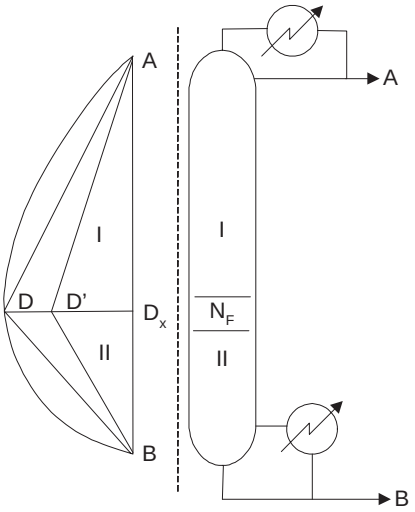

Figure 4.13: Illustration of how the driving force diagram is applied for distillation column design.

The driving force method presented here, proposes that if the feed plate is located on the relative position of the maximum driving force, point D_x, then the resulting design of the distillation column corresponds to a minimum (or close to the minimum) with respect to costs of the operation (energy consumption). The basis for this hypothesis is explained in the following proof for the case of constant β_{ij}.

Considering the points A and B (see figure 4.11) as points representing the specified compositions for the distillate and bottom products of the distillation columns respectively. According to the driving force method, the corresponding operating lines for the rectifying and stripping sections must intersect on the line $D - D_x$. Intersection at point D for a saturated liquid mixture corresponds to the maximum driving force and to the minimum reflux ratio while at the total reflux condition, the two operating lines both have a slope equal to zero (similar to the McCabe-Thiele method). If the actual feed is to the right of D_x (saturated liquid feed) and between the points D_x and F_x, (denoted F'_x in figure 4.11) it indicates an unsaturated feed, while F_x indicates a saturated vapour feed. The location of F_x on the x-axis is determined by the vapour-liquid relation below.

$$F_x = \frac{D_x \beta_{ij}}{1 + D_x(\beta_{ij} - 1)} \tag{4.9}$$

A point of intersection to the left of $D - D_x$ means a higher reflux ratio but lower reboil ratio while a point of intersection to the right of $D - D_x$ means lower reflux ratio but higher reboil ratio. The sum of the angles defined by BAD and

DBA in figure 4.11 is the largest for all other pinch conditions (the operating lines intersecting on the F_{Di} versus x_i surface). For this reason, this operating point signifies the lowest operational costs (lowest energy consumption) and the maximum total driving force. Since the actual reflux ratio is proportional to the minimum reflux ratio, the locus of points given by $D - D_x$ contains the locus of the points of intersection corresponding to the maximum actual driving force with the reflux ratio being $RR_{min} < RR < RR_{total}$. This phenomenon is also true if β_{ij} is not constant. Note that location of the feed point on $D-D_x$ also determines the corresponding reflux (and reboil) ratios and product compositions (or number of plates).

4.4.2 Design of complex distillation columns

Design of distillation columns based on the driving force approach, is not limited to simple configurations. The concept of the maximum driving force leading to the easiest separation, may also be applied to the design of distillation columns of a more complex character. Distillation columns consist of one or more rectifying and stripping sections, where two key compounds are separated, and the fundamental principle, to look at what specific separation is taking place in between two key compounds can be applied. In the simple conventional distillation column, there is only one separation task with two outlet products being separated in one rectifying and one stripping section.

Driving force based design methods for design of columns with one side-draw are presented, in section 4.4.2.1 below, and for the design of thermally coupled columns in section 4.7.

4.4.2.1 Columns with side-draw

A method for the design of distillation columns with a side-draw has been developed based on the driving force approach. The fundamental idea is (as defined in the concept of driving forces) to achieve a design that uses the largest possible driving force. Columns with three products are usually employed for the separation of mixtures with three or more compounds. So, based on the knowledge of the three key compounds (or four, if the side-draw contains more than one compound), two driving force diagrams need to be generated, one for the binary pair of light key and the intermediate key (a), and another one for the binary pair of the intermediate key and the heavy key (b). These two diagrams are combined in a 'merged' driving force diagram which forms the basis for the column design. In order to do this, the first step is to compare the relative sizes of the maximum driving force, D_y for the binary pairs (a) and (b). The diagram with the highest value of D_y represents the section where the feed enters the column. This means, when diagram (a), has the highest value, the feed enters between the light key compound and the intermediate key compound, and the side-draw is below the feed stage, and vice versa. Having this knowledge, the two driving force diagrams are combined to form one diagram. This is done

so that the two graphs intersect as closely as possible to the D_y point for the driving force curve with the smallest D_y (denoted 2). At this point the curve with the highest D_y (denoted 1) takes over and performs the remaining separation. The x-axis is then re-scaled to fit the $[0;1]$ composition space.

4.4.2.2 Algorithm for the design of distillation columns with side-draw

To solve the design problem for one distillation column with three products (side-draw column), the following algorithm is proposed. The algorithm requires two driving force diagrams between the two sets of binary key compounds. The algorithm then determines the location of the feed stage, as well as the side-draw stage and the minimum reflux ratio. The algorithm is outlined here:

1. List the three key compounds according to their boiling points.
   No. 1 is the lightest boiling
   No. 2 is the intermediate boiling
   No. 3 is the heaviest boiling

2. Generate or retrieve vapour liquid phase composition data for compounds 1 and 2, and for compounds 2 and 3.

3. Check if compound No. 1 and No. 2, or No. 2 and No. 3 form an azeotope. If no: go to step 4, otherwise, if yes: Stop.

4. Calculate and plot the *two* driving force diagrams corresponding to the *two* sets of vapour liquid phase composition data.

5. Determine which of the *two* plots exhibits the larger driving force.

6. Configure the column accordingly.

   6.1 If the largest driving force occurs between compounds no. 1 and 2, then the feed should be between the top and the side-draw in the column.

   6.2 Else, if the largest driving force occurs between compounds no. 2 and 3, then the feed should be between the bottom and the side-draw in the column.

7. Give the number of plates, N, in the column.

8. Generate the joint driving force curve such that the largest total driving force is achieved.

   8.1 If the feed is introduced between the top and the side-draw, then the driving force curves should be joined such that the largest driving force is in the top of the column.

8.2 Else, if the feed is introduced between the bottom and the side-draw, then the driving force curves should be joined such that the largest driving force is in the bottom of the column.

9. Calculate the minimum reflux ratio required in the column.

10. Give specifications on the products. Note that the size of the side-draw must be consistent with the overall mass balance of the column.

11. From the joint driving force curve, determine the near optimum position of the side-draw stage, D_s.

    11.1 Locate the point D_s, where the two driving force curves intersect.

    11.2 Calculate the near optimum position of the side-draw stage from $\mathbf{N_S = N(1 - D_S)}$.

12. From the binary driving force plot that exhibits the largest driving force, locate the near optimum feed stage location.

    12.1 Locate the point D_x, the position on the x-axis corresponding to the largest driving force.

    12.2 If the feed is introduced above the side-draw, then calculate the near optimum feed stage from $\mathbf{N_F = N_S(1 - D_x)}$. (Note N_S is used instead of N because there are only N_S stages in the section.)

    12.3 Else, if the feed is introduced below the side-draw, then calculate the near optimum feed stage from $\mathbf{N_F = N_S + (N - N_S)(1 - D_x)}$.

The algorithm presented here is in this thesis referred to as algorithm D2. The algorithm is presented as a block diagram in figure 4.14.

4.4.2.3 Evaluation of the algorithm for the design of columns with side-draw

The concept is illustrated in figure 4.15, where the greatest maximum driving force is between the intermediate and the heavy key compounds, and a 'merged' driving force design has been generated. In case the greatest maximum driving force should be between the light key and the intermediate key compounds, the intersection of the two curves would have been at the lower range of the composition scale (x-axis), and the side-draw stage would have been below the feed stage. The side-draw stage is located at the relative location where the intersection takes place, which is characterised by point D_s in figure 4.15b. After the location of the side-draw, the feed stage is located. This is done on the basis of the 'original' driving force diagram for the binary pairs (1) or (2), as illustrated in figure 4.15a. The calculation of the actual position of the feed stage must reflect the number of stages where this separation takes place, *i.e.* between either the reboiler and the side-draw (as in the case of figure 4.15), or the condenser and the side-draw, otherwise the relative distance between the side-draw stage and the feed stage is not maintained.

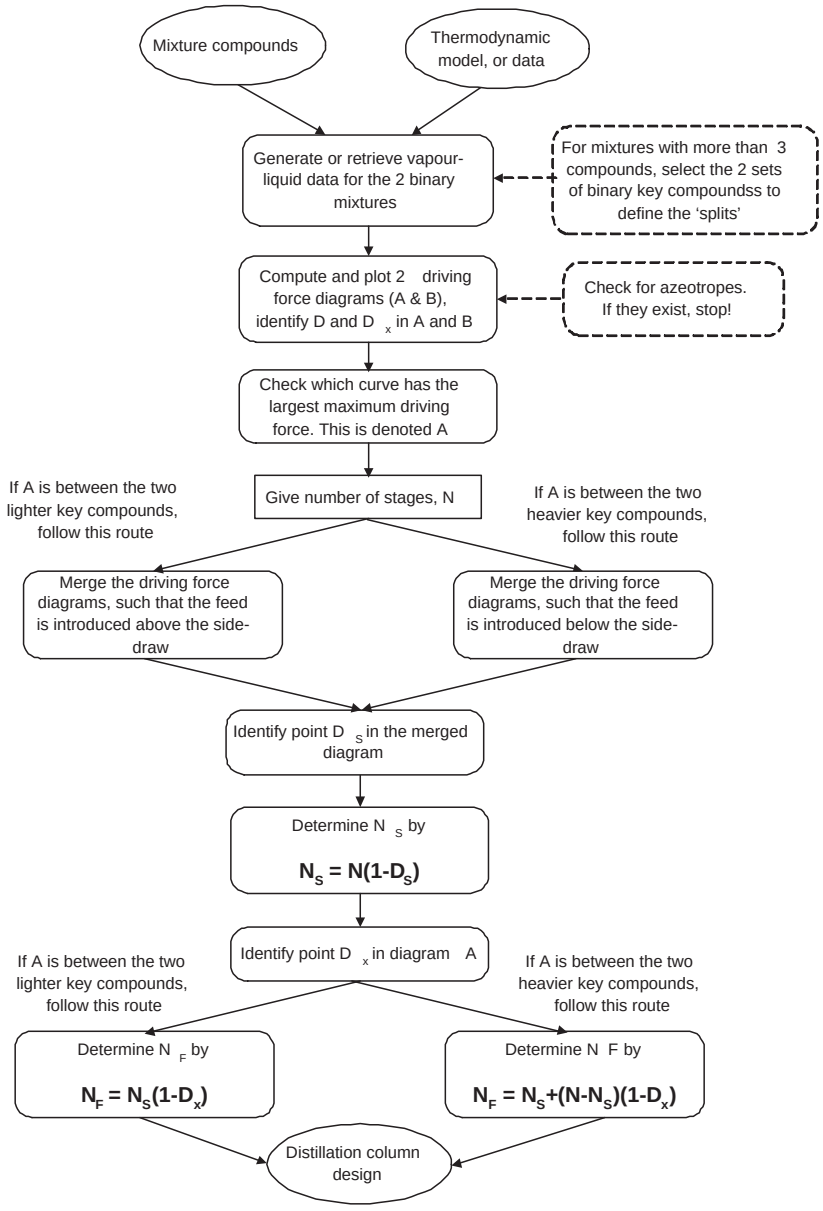

Figure 4.14: Block diagram for the driving force based design procedure for distillation columns with side-draws (algorithm D2).

4.4.3 Design of reactive distillation columns

The objective of the method developed here is to introduce a design method for reactive distillation columns that is simple and easy to use and similar

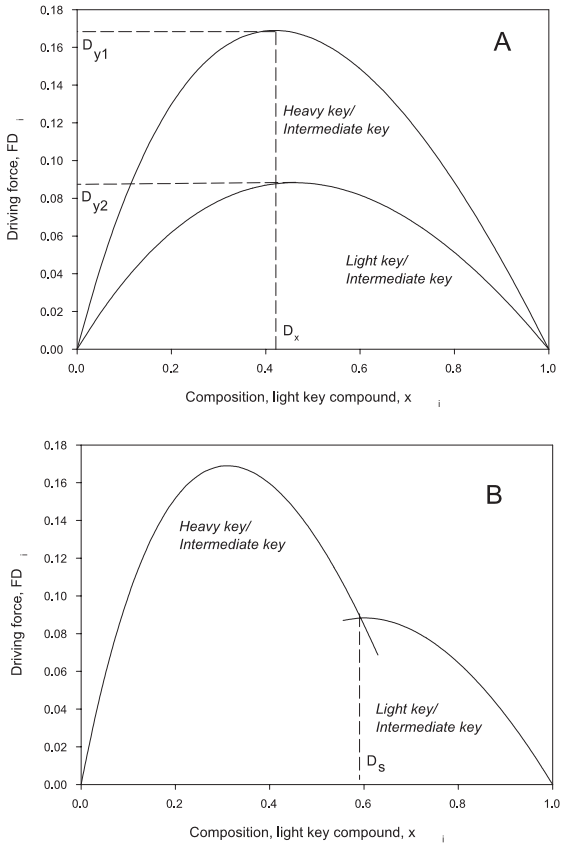

Figure 4.15: Example of the driving force diagram for the design of distillation columns with side-draws.

in its concept compared to the non-reactive distillation design method. In order to do this, the method relies on the *element* concept (Pérez-Cisneros *et al.*, 1997), which significantly reduces the dimension and complexity of the intrinsic calculation problem. This concept allows for the calculation of *binary element* systems, which may be ternary or higher in terms of mixture compounds. Therefore, in order to produce an energy efficient design, the driving force approach has, on this basis been extended to include reactive systems.

4.4.3.1 *Element* balances and equilibrium conditions

In the design of reactive distillation columns operating under equilibrium conditions, the computation of the chemical-physical equilibrium (CPE) is an important step. In this thesis the *element* concept (Pérez-Cisneros *et al.*, 1997),

is used as a tool for a multicomponent CPE problem to be transformed into a phase equilibrium problem for a (binary) mixture of *elements* (which is fully representing the system). In the *element* based approach, the CPE problem is solved by minimising the Gibbs energy of the reactive system.

$$\min G(n) = \sum_{\gamma=1}^{NP} \sum_{i=1}^{NC} n_i^{\gamma} \mu_i^{\gamma} \tag{4.10}$$

Subject to the M constraints:

$$\sum_{\gamma=1}^{NP} \sum_{i=1}^{NC} A_{j,i} n_{i,}^{\gamma} - b_j = 0, \qquad \text{j} = 1, 2...\text{M} \tag{4.11}$$

Here $G(n)$ is the total Gibbs energy of a system containing NC species and NP phases. Equation 4.11 represents the M independent *element* mass balances, with the coefficient A_{ji} being the number of times the reaction invariant *element* j is present in molecule i. The solution of this constrained optimisation problem can be obtained through the Lagrange multiplier formulation where the relation between the Gibbs free energy and the Lagrange multipliers is exploited for a robust method of solution (Pérez-Cisneros *et al.*, 1997). Thus, a fully consistent thermodynamic description of a chemically equilibrated phase can be obtained in terms of b, the (*element*) composition vector, and the corresponding *element* potential vector (see Pérez-Cisneros *et al.* (1997)). The information about the chemical phase equilibrium can be used in binary (or ternary) visual design procedures, including the driving force approach as described in the next section.

A classical example of reactive distillation is the synthesis of Methyl tert-Butyl Ether (MTBE). The compound as well as the *element* stochiometry is given in equation 4.12.

$$\begin{gathered} Methanol + iButene \rightleftarrows MTBE \\ A + B \rightleftarrows AB \end{gathered} \tag{4.12}$$

The *element* stochiometry for this system is given below in table 4.4.

$Compound$	$iButene$ C_4H_8	$Methanol$ CH_3OH	$MTBE$ $C_4H_9OCH_3$
Element			
A	1	0	1
B	0	1	1

Table 4.4: Stochiomertry for the reactive MTBE system in terms of compounds and *elements*.

4.4.3.2 Design of reactive distillation columns through the driving force approach

Since a reactive equilibrium curve is the locus of points in both chemical and physical equilibrium, it gives for an *element* liquid composition W_A^L the corresponding equilibrium vapour composition W_A^V, and vice versa. A reactive equilibrium stage p is represented as a point on the reactive equilibrium curve where W_A^L, p and W_A^V, p are the liquid and vapour *element* compositions leaving the stage. The reactive equilibrium curve is then constructed by sequential computation of reactive bubble points. An example of a reactive equilibrium curve is shown in figure 4.17.

Since the method proposed is an extension of the method for simple distillation columns, to include reactive systems, the driving force model equation (given in equation 4.1) is rewritten here in terms of *elements*.

$$F_{Di}^b = W_i^V - W_i^L = \frac{W_i^L \alpha_{ij}^b}{1 + W_i^L(\alpha_{ij}^b - 1)} - W_i^L \tag{4.13}$$

The concept of operating at the maximum driving force, based on the model in equation 4.13, also form the basis for extension of the design method for non-reactive systems to reactive distillation columns. The location of the maximum driving force can be obtained from the derivative of the driving force model with respect to the liquid *element* composition. The derivative with respect to W_i^L, for a constant value of α_{ij}^b is given in the following equation.

$$\frac{\partial F_{Di}^b}{\partial W_i^L} = \frac{\alpha_{ij}^b}{(1 - W_i^L - W_i^L \alpha_{ij}^b)^2} - 1 \tag{4.14}$$

The driving force design method for reactive (as well as non-reactive distillation) systems requires that data for their vapour-liquid behaviour are available, and that they are "converted" into a binary *element* representation for the two key *elements*. This is because the driving force approach is based on the principle of separation between two key compounds (*elements*). Note that the *element* based driving force diagram fully incorporates the extent of reaction on the *element* basis, and therefore, it can be applied to the design of reactive distillation columns.

4.4.3.3 Algorithm for design of reactive distillation columns

The objective of the method presented here is to solve the design problem for reactive distillation columns, so that they consume the least energy, and at the same time provide the desired separation. The algorithm proposed here is for the design of reactive distillation columns, for which the full reactive separation system can be expressed in terms of a binary pair of *elements*. Having obtained information about the corresponding vapour liquid *element* phase composition data, a driving force diagram is generated and visually or numerically estimates for design parameters like *element* reflux ratio and feed stage location for a

reactive distillation column are obtained. A description of the driving force based reactive distillation design algorithm is given below:

1. Check if the reactive separation can be exploited on the basis of two *elements* (possibly with inerts). If yes, go to step 2, otherwise stop.
2. Generate or retrieve vapour-liquid *element* data at the desired operating pressure.
3. Calculate the corresponding *element* driving force diagram.
4. Identify the area of operation on the driving force diagram.
   - 4.1 Rescale the x-axis accordingly, so that the area of operation covers the $[0;1]$ composition space.
5. Determine or specify the condition of the feed, q.
6. Identify the points D and D_x.
   - 6.1 Determine N_F from $\mathbf{N_F} = (\mathbf{1} - \mathbf{D_x})\mathbf{N}$.
   - 6.2 Give the product specifications and locate the points A and B. Determine the slopes of the lines AD and BD. Determine the corresponding RR_{min}.

The algorithm presented here is in this thesis referred to as algorithm D3. The algorithm is presented as a block diagram in figure 4.16.

4.4.3.4 Evaluation and comments on the algorithm for the design of reactive distillation columns

Figures 4.17, 4.18 and 4.19 illustrate the important steps of the driving force based algorithm for the design of reactive distillation columns. At first, the vapour-liquid data are generated on the *element* basis, then transformed into a driving force diagram. The range of operation is identified, and the design can be performed within this range of operation. It shall be emphasized that the re-scaled x-axis in figure 4.19 is only to be used for visualisation purposes and determination of D_x, since mass balance related calculations (like calculation of reflux ratio) must be performed on the basis of actual (*element*) compositions (as in figure 4.18).

This simple method has been developed to serve as a tool for the design of reactive distillation columns. However, reactive distillation columns are complex processes where both reaction and separation take place, and many aspects of operation must be taken into account. Therefore, this algorithm is a tool that should not be used alone, since practical constraints, like the determination of operating pressure with different catalyst, the dependency of the extent of reaction to the number of reactive stages, etc. are also important issues. However, this algorithm provides a simple method to obtain the preliminary values for some of the important variables that are important to maintain the operating costs in terms of energy consumption at minimum.

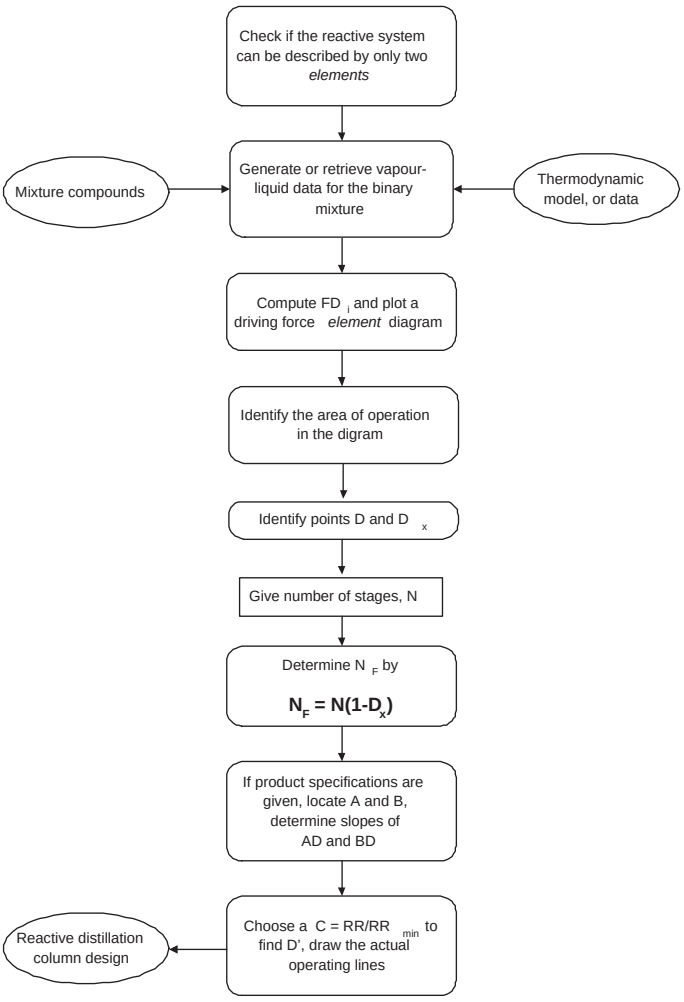

Figure 4.16: Block diagram for the driving force based design procedure for reactive distillation columns (algorithm D3).

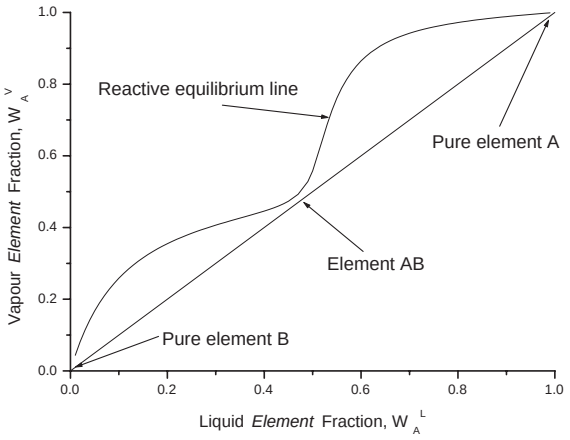

Figure 4.17: Reactive phase diagram for a binary *element* system.

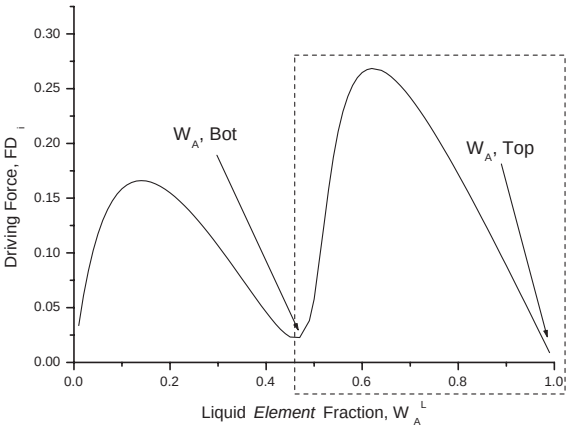

Figure 4.18: Reactive driving force diagram for a binary *element* system with an indication of the operating range.

4.4.4 Allocation of distillation column operating pressure

Since distillation columns in chemical plants are energy intensive operations, and energy consumption in distillation columns is highly sensitive to the operating pressure The choice of the pressure in distillation columns is an essential part of process design and analysis.

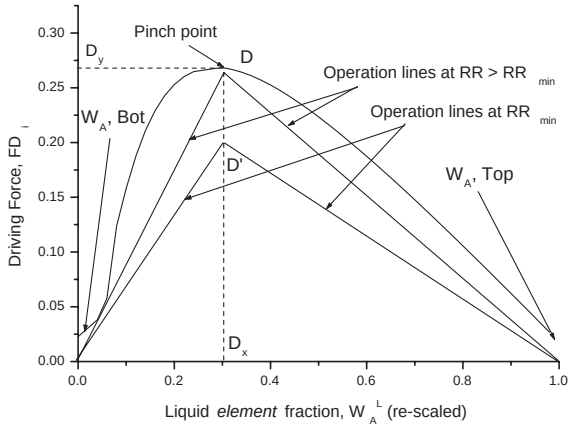

Figure 4.19: Reactive driving force diagram for the operation range of a binary *element* system with an indication of the design parameters.

The method is based on the knowledge of the driving force diagrams of the binary set of key compounds in each distillation column belonging to a distillation train. By means of an iterative technique, the proposed method aims to determine the column pressures leading to near minimum energy consumption in each column while matching the product purity specifications. This is done by the determination of the operating pressure in each column using a driving force based technique (described below).

Although the algorithm is intended for sequences of distillation columns, it can also be applied to parts of column sequences, or even to a single distillation column. The method requires the use of an appropriate thermodynamic model for the calculation of the vapour liquid phase composition data. For each separation that is performed, there is the option of varying the three intensive variables T, P and $\underline{x}$. From the phase rule, it is given that, once two of the intensive variables are fixed, the third one can be calculated. The method proposed here requires calculation of bubble point pressures at specified temperatures for all possible compositions, $\underline{x}$.

4.4.4.1 Algorithm for the allocation of distillation column operating pressure

The algorithm presented in this section has been developed for the determination of operating pressures in the columns of a distillation train. For the application of this driving force based method for the determination of distillation column pressures, it is necessary that the distillation column sequence has already been determined. This could for example have been done by the method

presented in section 4.3.1 (algorithm D1). Besides, an appropriate thermodynamic model for the prediction of mixture bubble points must be available. The driving force approach developed here can then be applied step-wise, as outlined below:

1. Determine the thermal condition of the feed stream to the first column in the distillation sequence, and its temperature T_b.
2. Calculate data for the *pxy* phase diagram for the two key compounds in the distillation column at the temperature determined in step 1.
3. Draw the driving force diagram from the data calculated in step 2, together with the bubble point *vs.* composition diagram (the driving force diagram, in this case is $|y_i - x_i|$, *i.e.* the horizontal distance from the dew point line to the bubble point line in the *pxy* phase diagram, as a function of the mole fraction of the light key compound).
   - 3.1 Identify point D at the relative location in terms of the composition, D_{xi}, where the driving force reaches its maximum.
   - 3.2 Identify the bubble point pressure 'intersecting' the $D - D_x$ line. The operating pressure of the condenser in the distillation column should correspond to this bubble point pressure.
4. Calculate the *pxy* pasee diagram for the two *key* compounds in the following distillation column at different temperatures. The temperature is selected, at which the *pxy* diagram reaches the bubble point pressure identical to the reboiler pressure of the previous column.
   - 4.1 Repeat step 3 for the two key compounds in the second column.
5. Repeat step 4 successively for all the remaining distillation columns in the sequence.
6. Evaluate the results. If the pressure in one or more of the columns in the sequence results in a high vacuum in the condenser, consider starting at a higher pressure in the first column. If the final condenser pressure in the last column is higher than ambient pressure and the separation can be performed at ambient pressure, consider starting at a lower pressure in the first column.

The algorithm presented here is in this thesis referred to as algorithm D4. The algorithm is presented as a block diagram in figure 4.20.

4.4.4.2 Evaluation and comments on the algorithm for pressure allocation

The fundamental concepts of the method are illustrated in two figures. Figure 4.21 is a *pxy* phase diagram, as it is proposed to generate at a given temperature, T_b, whereas in figure 4.22, the driving force diagram for the phase diagram

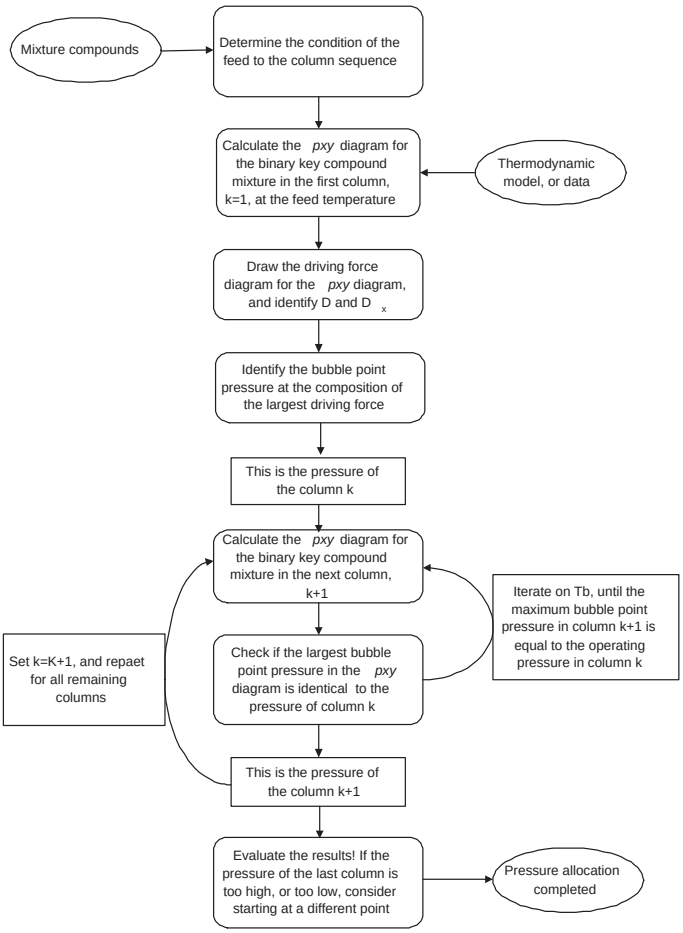

Figure 4.20: Block diagram for the driving force based procedure for pressure allocation in distillation trains (algorithm D4).

in figure 4.21 has been generated and plotted together with the bubble point curve. Here, the pressure that should be applied in the column is indicated, and also what should be the pressure in the column following next in the sequence.

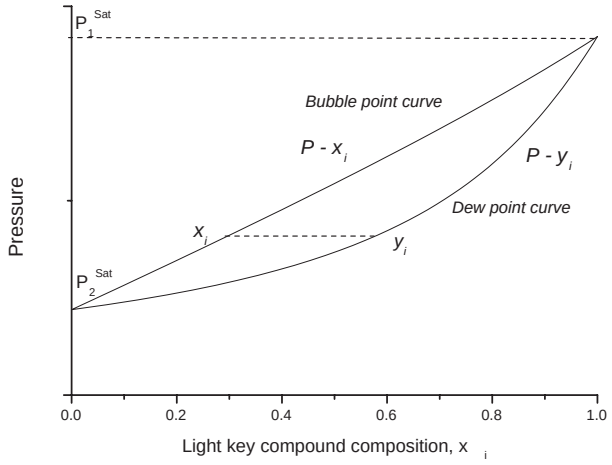

Figure 4.21: A *pxy* diagram for the compounds i and j at bubble point temperature, T_b.

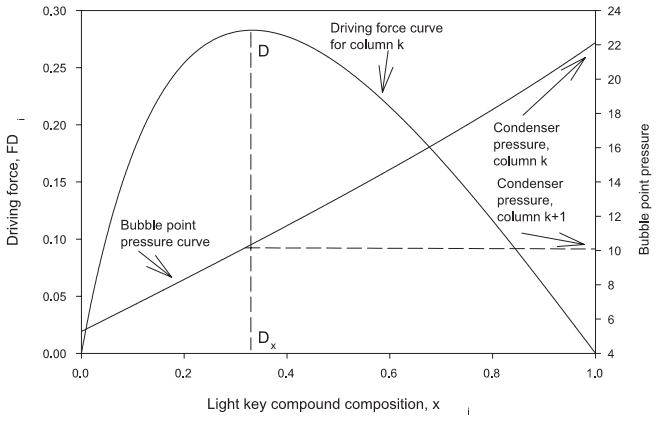

Figure 4.22: Driving force diagram for the compounds i and j, and correponding bubble point curve at temperature T_b.

4.5 Analysis of distillation column operation

The driving force approach is useful not only for synthesis and design problems. It is also useful for analysis and validation purposes. Given a separation system, the feasibility of this design can be verified or analysed further by means of the driving force approach. The methods developed in the previous sections of this chapter provide valuable insights for this purpose. Consider, for example, the situation where a separation of a binary mixture with an azeotrope is to be conducted. A driving force analysis of this separation in which different solvents are compared, in different amounts, as described in section 4.3.2, is highly valuable. In this way, it cannot only shown which solvents make the separation feasible, but also *how* feasible they are, *i.e.* which solvent exhibits the maximum driving force, and how much solvent is needed to perform the separation. An example of the verification of a given distillation based separation scheme is given in section 5.4.1.

The analysis of operation in terms of controllability and resiliency is covered in the following section.

4.5.1 Controllability analysis of distillation columns

It is usual that process design and process control problems are dealing with variables like temperature, pressure and composition (intensive variables). In terms of separations and thermodynamics, it is desired that these intensive variables are different for the compounds to be separated (*i.e.* a large driving force exists). In the field of control, the same intensive variables are measured (or controlled) variables. Therefore the sensitivity of temperature, pressure and composition related to other properties play a major role. The intensive properties can be measured and used to estimate other variables such as enthalpy, density and volume. In this way, the intensive process variables determine the dependency of the constitutive variables (*e.g.* properties) which often affects the design and control of a process (distillation column).

By using the driving force approach to solve the design problem, insights can be gained in terms of controllability and resiliency related to the design problem using the visualisation features of the driving force approach, and the design and control problems may be solved in an integrated manner.

As previously explained in this chapter, distillation columns should be designed to make use of the maximum total driving force, in order to achieve a specified separation with the least energy input. From a control point of view, this design means that greater percentage changes in the manipulative variables can be accommodated for the needed control action. Identification of the most sensitive stage temperatures and stage compositions for control are related to the derivatives of the driving force with respect to temperature and composition. Clearly, for the methanol-water system shown in figure 4.23, composition control or temperature control is feasible, since composition and temperature are sensitive with respect to the driving force (difference in composition). In

this context, it should be mentioned that in design, the relative location of the maximum driving force, D_x with respect to composition is important, and in control, it is the location of the greatest values of the derivatives of the driving force with respect to manipulative (internal) variables that is important.

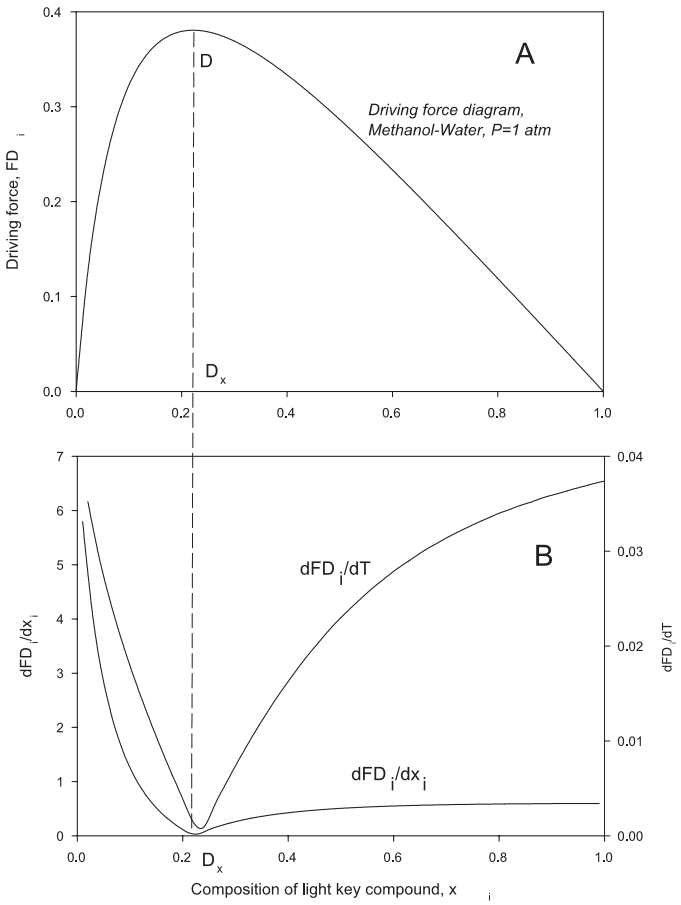

Figure 4.23: A: Driving force diagram for the separation of methanol and water by distillation, B: Corresponding derivatives of the driving force with respect to composition and temperature.

Furthermore, in this thesis, RGA analysis has been used for the comparison of controllability/resiliency properties of different distillation configuration. RGA analysis, and properties of RGA are described in section 2.4.1.1, and an example of the application of RGA analysis to a driving force based design is given in section 5.4.3.

4.6 Retrofit design of distillation columns

A retrofit distillation problem deals with the use of an existing column, in which it is desired to perform another separation than the column was originally designed for. When a retrofit problem for a distillation column is solved, it may therefore be considered as a *reverse* synthesis/design problem. A simple procedure for retrofit synthesis has been developed, based on the driving force design procedure. The procedure involves use of table 4.5, where precalculated values of corresponding numbers of ideal equilibrium stages in distillation columns, (minimum) reflux ratios as function of maximum driving force and product purities are tabulated. In table 4.5, also actual reflux ratios are listed where a value for $C = 1.5$ has been applied, and C is in this case the multiplication factor of RR to RR_{min}. Also figure 4.24 is used in the retrofit method, which contains calculated data for corresponding values of maximum driving force and location of this driving force. Using this method, it is easy to evaluate whether a given mixture can be separated in a given column, or to investigate what *range* (in terms of relative volatility) of mixtures can be separated in a given column.

4.6.0.1 Algorithm for retrofit of distillation columns

The procedure proposed here, is for solving of retrofit problems for existing distillation columns, which are desired to employ for a separation different from what it was designed for. The starting point in a retrofit problem is the knowledge of an existing column with a known number of stages and some desired product purities. It is then determined what mixtures that can be separated into desired products in the given column and the condition of operation. Therefore it is the "reverse" of a distillation column design problem where provided a given feed mixture, the design of the column and the condition of operation is determined.

The specified data or information is taken to table 4.5, and the corresponding minimum reflux can be found together with the equivalent size of the maximum driving force. In table 4.5, tabulated values of the variables for ideal separations by distillation are given, and when the size of the driving force is known, the range of relative volatilities, α_{ij} can be deduced from figure 4.24. The principle is to move from the right side of table 4.5 towards the left side. This can be done by following the algorithm outlined below.

1. Determine desired products, in terms of purities.
2. Find the value of $F_{Di}|_{max}$ and the number of stages [table 4.5].
3. Find the corresponding range of α_{ij} [figure 4.24].
4. Find, RR_{min} [table 4.5].
5. Check for mixtures with these properties.

This algorithm is denoted algorithm R1 in the remaining part of this thesis.

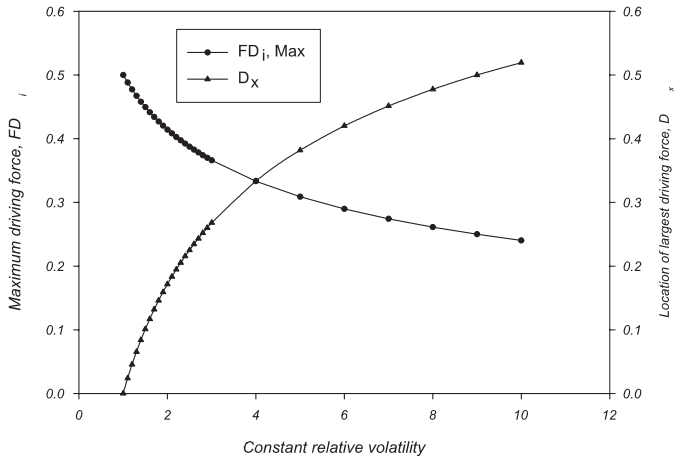

Figure 4.24: Plot of maximum driving force and its corresponding location as function constant of relative volatility.

4.7 Design of thermally coupled distillation columns

A method for design of thermally coupled distillation columns has been developed. The objective of the design method is to use the maximum driving force to verify and/or produce a near minimum energy consumption design for thermally coupled distillation columns, *"Petlyuk columns"*. The advantage of a Petlyuk distillation column configuration is that it can separate three compounds in two distillation columns, which are interlinked so that there is only one reboiler and one condenser and therefore requires less energy than conventional distillation columns. The reboiler and condenser are parts of the "main column" and the additional column is known as the "pre-fractionator". The Petlyuk column arrangement is illustrated in figure 4.25. The two interlinked distillation columns may be divided into six column segments (equivalent to $NC(NC-1)$, where NC is the number of compounds being separated) with one reboiler and one condenser. The separations occur between the three compounds A, B and C, where A is the most volatile and C is the least volatile. The pre-fractionator (sections I and II) is used for the separation of the key compounds A and C with the intermediate, B, being distributed (*i.e.* a "sloppy split"). Here compounds A and C are key compounds in terms of top and bottom products. B is the key in terms of which compound is distributing. In the

$F_{Di}\|_{Max}$	$X_{LK,Dist}$	$X_{LK,Bot}$	RR_{min}	$RR_{min} \cdot C$	N_{ideal}
0.045	0.995	0.005	9.89	14.83	96
	0.98	0.02	9.56	14.36	71
	0.95	0.05	8.90	13.35	54
	0.90	0.10	8.22	12.33	41
0.065	0.995	0.005	7.33	11.00	67
	0.98	0.02	7.10	10.65	50
	0.95	0.05	6.64	9.96	38
	0.90	0.10	6.64	8.58	29
0.101	0.995	0.005	4.50	6.74	44
	0.98	0.02	4.35	6.52	33
	0.95	0.05	4.05	6.08	25
	0.90	0.10	3.56	5.33	19
0.146	0.995	0.005	2.92	4.41	31
	0.98	0.02	2.84	4.26	23
	0.95	0.05	2.63	3.95	18
	0.90	0.10	2.29	3.44	14
0.172	0.995	0.005	2.35	3.53	27
	0.98	0.02	2.26	3.40	20
	0.95	0.05	2.09	3.13	15
	0.90	0.10	1.80	2.70	12
0.195	0.995	0.005	2.06	3.09	24
	0.98	0.02	1.89	2.97	18
	0.95	0.05	1.82	2.74	14
	0.90	0.10	1.57	2.35	11
0.225	0.995	0.005	1.73	2.60	21
	0.98	0.02	1.67	2.50	16
	0.95	0.05	1.53	2.30	12
	0.90	0.10	1.37	1.97	9
0.268	0.995	0.005	1.37	2.06	18
	0.98	0.02	1.31	1.97	13
	0.95	0.05	1.20	1.80	10
	0.90	0.10	1.02	1.52	8
0.382	0.995	0.005	0.82	1.23	13
	0.98	0.02	0.78	1.17	10
	0.95	0.05	0.70	1.05	8
	0.90	0.10	0.57	0.86	6
0.478	0.995	0.005	0.54	0.81	10
	0.98	0.02	0.51	0.76	8
	0.95	0.05	0.44	0.67	6
	0.90	0.10	0.34	0.51	5

Table 4.5: Pre-calculated values of reflux ratio, minimum reflux ratio, number of ideal stages, product purities and driving force for ideal distillation.

section pairs of the main column (III and IV) and (V and VI), essentially the binary splits A/B and B/C are performed, respectively.

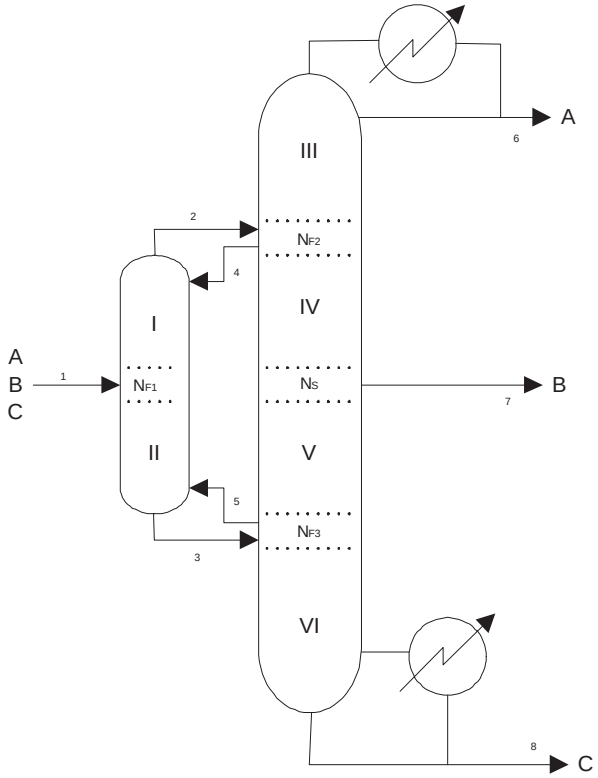

Figure 4.25: Thermally coupled distillation column (*"Petlyuk column"*).

The developed method consists in principle of two parts (sub-algorithms). Sub-algorithm 1 verifies if - for the specified separation problem - the Petlyuk column configuration is feasible. If yes, the two columns are divided into six column segments and sets of "single distillation" column design problems, based on the driving force diagrams of the sets of binary mixtures (A/B and B/C, representing the ternary mixture). For each set of compounds the size of the maximum driving force is identified. The knowledge of these two parameters is used to find the distribution of stages in the main column, *i.e.* the relative sizes of sections III/IV vs. V/VI (see figure 4.25). The distribution is deduced from the interpolation of $F_{Di|Max}$ values of table 4.5. Sub-algorithm 2 (identical to algorithm D1), is employed here for the design of the "single distillations", and the feed stages N_{F2} and N_{F3} are obtained in this way, using the driving force diagrams between compounds A/B and B/C (covering sections III, IV and V, VI) respectively. The feed stage N_{F1} is obtained from a combined driving force curve of compounds A/B for the rectifying section (I) and B/C for the

stripping section (II). Furthermore, values of minimum reflux ratios can be determined.

The fundamentals of the method is the application of the driving force approach to generate a design for the integrated system shown in figure 4.25, in combination with the method for distributing the stages in the main column. The significance of the method lies in the fact that it produces a design for the separation of non-azeotropic mixtures, where near minimum energy consumption is achieved for the given separation. The design is determined in terms of positioning all the feed and product streams, regardless of the number of stages provided in the main column and the pre-fractionator, and it is done on the basis of the knowledge of only the compounds, an appropriate thermodynamic model, and the driving force related design parameters that can be obtained from that knowledge.

4.7.1 Algorithm for design of thermally coupled distillation columns

Given the identity of compounds A, B and C, and an appropriate model for the description of the thermodynamic behaviour of the system, the algorithm presented here determines whether the mixture is suitable for the separation in a Petlyuk distillation column, and in case it is, essential design parameters (position of feed stage, side-draw stage, interlinking streams, and minimum reflux ratio) are determined in such a way that the near optimum design is achieved. The algorithm is outlined below, and the nomenclature refers to figure 4.25.

1. List the compounds in the mixture according to their normal boiling points.

2. Specify the desired products to be obtained from the feed mixture. If there are three desired products (A, B and C, ranked by normal boiling points), Petlyuk configuration may be suitable for separation. Otherwise stop.

3. If products A and C form an azeotrope, Petlyuk configuration cannot be used. Stop.

4. Calculate and plot the two driving force curves between A/B and B/C.

5. If there is a large difference between the size of the maximum driving forces A/B and B/C, (*i.e.* $F_{Di,(A/B)}/F_{Di,(B/C)} \nsim 1$), consider also a sequence of two conventional distillation columns, and/or other alternative configurations.

6. Design the Petlyuk column using the driving force algorithm in a systematic way (employ algorithm D1).

6.1 The pre-fractionator (sections I and II) is designed by combining the driving force curves for A/B and B/C, so that A and C are separated and B is distributed at the top and the bottom. Section 1 (rectifying section) is designed for the separation of A and B using algorithm D1. Section 2 (rectifying section) is designed for the separation of B and C using algorithm D1. The driving force curves for the rectifying and the stripping sections are combined so that the largest area is covered and the feed plate located accordingly. (Note: The x-axis may need to be re-scaled since the x-axis must cover the [0;1] composition range, and the two "half-curves" do not necessarily intersect, but re-scaling takes this into account).

6.2 The main fractionator is designed as two individual columns. Sections III and IV are designed to separate A and B, whereas sections V and VI are designed to separate B and C. The number of stages in the main-fractionator (N_{main}) is distributed relatively between the two column segments (sections III/IV and sections V/VI) based on the interpolation of parameters given in table 4.5. (Knowledge of $F_{Di|Max}$ gives corresponding values of N_{ideal}. The two values of N_{ideal} are then relatively distributed across N_{main}).

6.3 Each of the two columns (sections III/IV and sections V/VI) are designed using algorithm D1, where the feed plates are then located accordingly. This means that, given the number of stages, the feed stages and recycle stages (interlinking stages) are deduced together with minimum reboil and reflux ratios, based solely on the driving force plots. Note: This design step is constrained by the size of the three side-draws and the specified purities of A, B and C. The minimum reflux ratio is obtained from the driving force plots between A/B and B/C respectively.

The algorithm proposed here does not deal with the sizes of the streams connecting the two distillation columns in the configuration. These streams are recycle streams within the configuration. The sizes of these streams determine the reflux and reboil ratios in the pre-fractionator. Therefore there is a minimum to their sizes. However, this issue does not encompass the scope of this algorithm, and is normally treated as a separate constrained optimisation problem. The new method ensures that the optimisation of the sizes of the interlinking streams is done on a near optimal configuration of the Petlyuk column.

The algorithm presented above is denoted as algorithm D5.

4.8 Framework for synthesis and design based on driving forces

The driving force based methods developed and presented in this chapter are combined in a schematic framework for the synthesis, design and retrofit of separation systems. The framework is illustrated in figure 4.26, where it is divided into two levels as described below.

Level 1 In the first level the character of the problem is determined, and it is assigned to one of the three categories; 1) synthesis, 2) design and 3) retrofit. While the retrofit category only has one sub-problem associated to it, the synthesis and design categories have more sub-problems associated.

Level 2 In the second level, individual synthesis, design and retrofit problems are outlined. Each problem has a driving force based algorithm associated to it, which provides for a solution to the specific type of problem. For the individual algorithm, it is then given what is required as input to the algorithm, and what is the output from the algorithm. In this way it is easy to get a clear overview of what is needed to apply the algorithms in a systematic way.

The driving force separation framework presents an overview of the solution techniques that have been developed, and can be presented in algorithmic form. However, in the driving force approach, synthesis, design and retrofit solution methods have been developed, without considering the qualitative comparison of the different design configurations, *i.e.* there are no rules as to when a given distillation configuration should be favoured. For example, there are no means in the methods developed, for the comparison of the separation alternatives for a three compound mixture. There is the opportunity to apply algorithm S1 to find a distillation sequence, and as to each of the two columns algorithm D1 can then be applied to perform the design. There is also the opportunity to apply a complex column with a side-draw (or a thermally coupled distillation column), to perform the separation in a single separation unit. The driving force approach does not indicate which solution is better. A framework is proposed here, where optimum or near optimum separation scheme alternatives can be generated for further comparisons.

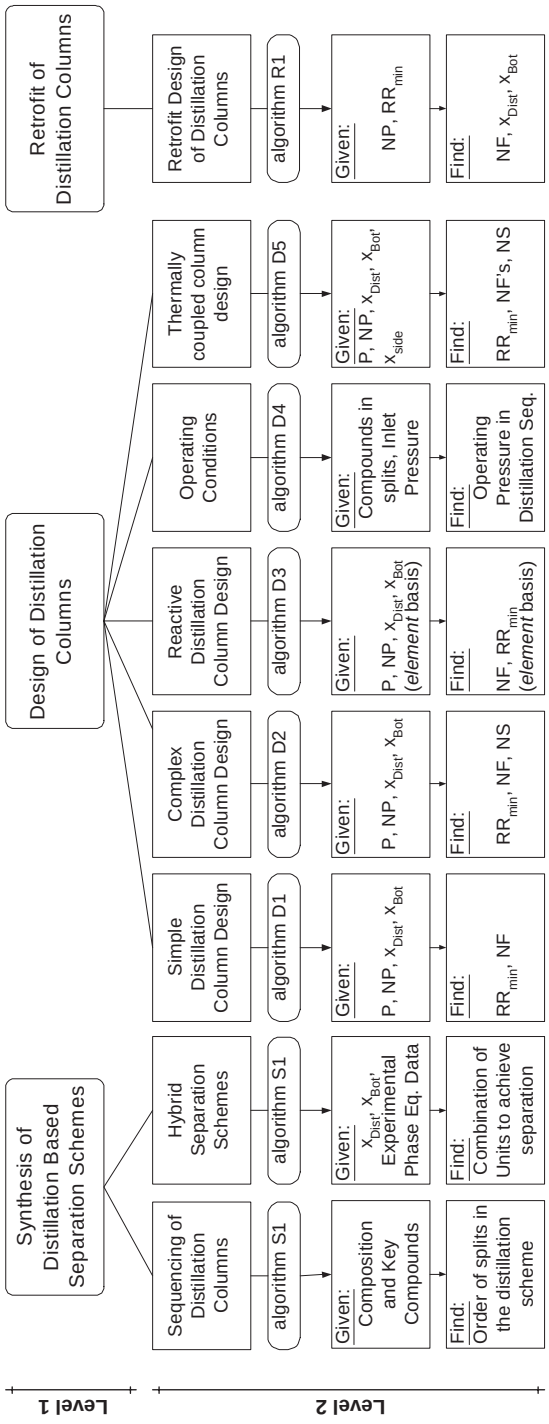

Figure 4.26: Framework of driving force based methods for synthesis, design and retrofit.

4.9 Computational tools

To make the methods developed in this thesis useful and easily accessible, some software tools have been developed. The tools are all made available within the ICAS package (see section 3.5.1), where they can be used in an integrated manner with many other tools. Driving force curves are available in the *property window* in ICAS, which may be used at any time in the synthesis/design procedure. The easy access to these curves is a useful feature, as they can form the basis of an easy and visual design. Driving force based design tools have been implemented in two programs in ICAS, namely Process Design Studio, and the CAPEC database. The software tools are shortly described in this section.

4.9.1 Process Design Studio

Driving force based design tools have been implemented in Process Design Studio. By using this program, generation of driving force curves is possible, based on a selected thermodynamic model. The program also has a tool for the design and analysis of distillation columns, where the driving force approach is one design technique amongst others. Based on the knowledge of the mixture compounds, thermodynamic model data, number of stages and desired products, the program returns values of minimum reflux, and feed stage location.

It is possible in this way to do the analysis of feasible distillation operations, by manipulating the number of stages, the ratio of RR to RR_{min}. Besides, the program can calculate the necessary number of ideal stages, and the user may use this number in his calculation. From Process Design Studio all necessary data for the distillation column can be directly passed to the distillation model in ICASsim, and the simulation can be started from this point, without further specifications.

For the reactive systems, the design tools are based on CPE calculations via the *element* approach. The driving force based design procedure has been implemented in a prototype. Here, the user has the option to manually fix point D_x, where the driving force exhibits the largest value, and force the intersection of the operation lines to be at that point in the McCabe-Thiele design procedure. In this way a driving force based design can be obtained.

4.9.2 CAPEC database

The CAPEC database has been extended to include membrane data, which have been reported in the literature. When doing hybrid separation schemes, and membrane separations are considered, there are limited resources to find data on how the different types of membranes are capable of performing specific separations. In most cases, users are limited to literature searches and to consult membrane vendors. To help the solution of this problem, a database has been built as a part of the CAPEC database (Nielsen *et al.*, 2001). This

database collects data on the differences in composition between the permeate and the retentate, so that driving force diagrams easily can be generated and only require few arithmetic operations and a plotting feature, for visualisation of the data to be used in synthesis of separation schemes. Other information stored in the database is the type of membrane separation and type of membrane material used, as well as the reference. Furthermore, there are options for giving in operating conditions. The database is made so that the user can give input data, and in this way provides data to other users, applying this approach.

4.10 Discussion

By means of a simple definition of driving force, a set of separation synthesis and design methods, mainly for solving problems involving distillation has been developed. Since the easiness of separation is related to the driving force, it is the objective of the methods developed to achieve the easiest separation by maximising the driving force, which should lead to minimum energy consumption, while satisfying purity specifications.

For the synthesis of distillation trains, a method has been developed, where the order of the separation tasks is to be identified. The method is limited to the consideration of the order of the separation tasks only, and does not, in its current form, consider heat integrated networks of distillation columns. This may be considered a disadvantage, as heat integrated networks are frequently applied to save energy in chemical plants. It is, however, believed that the sequence proposed by algorithm S1 is a good candidate sequence, since this algorithm produces (as shown in the examples in section 5.2) optimum, or near optimum sequences of distillation trains with respect to energy efficiency. The important point here is that the optimal network without heat integration can be deduced. Therefore, any subsequent reduction by means of heat integration would be an additional bonus. As pointed out by Freshwater and Ziogou (1976), the sequence where the greatest savings can be achieved by heat integration often already has the lowest energy consumption prior to integration. Therefore, if a heat integrated network is to be synthesized, it is suggested to use the sequence proposed by algorithm S1. The heat integration issue is also relevant to the determination of column operating pressures. A criterion for selection of operating pressure in distillation columns is often the possibility of applying a heat integrated network between the reboilers and the condensers on the distillation columns. This possibility is not taken into account, and is at the current state beyond the scope of this work. What is not considered here, either, is that at different plant sites, there are often different heating/cooling media available at given pressures/temperatures. This may limit the operating range, and also the choice of distillation column pressure, thus implying constraints to the design problem.

The method for the synthesis of hybrid separation schemes is intended to pro-

vide feasible solutions that are near optimum solutions with respect to energy consumption. The method, however, does not consider the costs of alternative separation units/techniques, and does not give a complete overview (comparison) of the costs of separation process units, but only the relative costs in terms of energy consumption.

Although the controllability aspects have not been developed to the extent desired, the objective has been to provide a method that allows for the selection of the control variables as an integrated part of the design, and at the same time exploits the knowledge as to the sensitivity to changes of these variables with respect to design. This makes the selection of what to control and where to control it a decision that is related directly to the phase composition data for the mixture to be separated, the same data that forms the basis for the distillation column design.

The driving force based retrofit method is intended to provide a simple way to get an overview of, for a given distillation column, what are the properties, in terms of the design variables introduced in this thesis (*i.e.* the size of the maximum driving force), required for the mixture to be separated to given products. By solving a "reverse design problem", where the products and the driving force are the known variables, it should be simple to identify what mixtures match the given column. The method, however, in its current version assumes constant relative separability.

5

APPLICATION EXAMPLES

5.1 Introduction

In this chapter the application of the methods in the driving force framework is illustrated by a series of examples. The purpose of the examples is to show the diversity in the types of problems that can be solved using the driving force framework as well as to highlight the feature that the optimum or near optimum synthesis and design of the separation flowsheets can be obtained by employment of the driving force approach, based solely on the knowledge of simple phase composition data.

The examples are based mainly on literature case studies, where previously reported examples are treated from a driving force point of view. In cases where optimisation has already been applied, the results of this optimisation is in this context assumed to represent actual optimum solutions, although the optimisation method and objective function, etc. may not be known in detail. Some examples are generated based on smaller case studies given here for illustrative purposes, and may not previously have been reported in the literature.

All the examples given in this chapter, as well as those not explained in detail in this chapter, are presented in Appendix A in terms of step-by-step application of the corresponding algorithms. In this way, the application and verification of all the algorithms have been illustrated by numerous examples in Appendix A.

In order to make the examples in this chapter easy to follow and easy to compare to the framework described in chapter 4, the individual algorithms will be followed systematically, as stated in the framework in figure 4.26. Some case studies make use of more than one method in the framework, and therefore each example can not always be related to only one procedure (method). Nevertheless, the examples are sub-divided into four main categories, reflecting the sub-sections in chapter 4, but some examples will also cover parts from other sections. The example categories are:

- Section 5.2 deals with synthesis of separation schemes. This covers hybrid

separation schemes and distillation sequences. A number of literature case studies are used as background for these examples, and wherever appropriate, individual distillation column design is also performed.

- Section 5.3 deals with design problems for different types of distillation columns. These are mainly examples of single distillation columns. Simple conventional columns as well as complex and reactive distillation column configurations.
- Section 5.4 contains examples of how the developed driving force approach can be used for the validation of separation flowsheets and operability analysis of distillation columns.
- Section 5.5 gives an example of how the distillation retrofit algorithm based on the driving force approach can be applied.

The problems dealt with in the examples have been solved using mainly thermodynamic data from various simulation packages. The validations are based on the use of simulation and optimisation tools, as described in chapter 3.

5.2 Synthesis of separation sequences

5.2.1 Ethylene plant separation sector

A well-known problem in the petrochemical industry which involves separation of a multicomponent non-azeotropic mixture, is the separation of the reactor effluent in the production of ethylene. This example is based on data obtained from an actual ethylene plant, which was subject to an optimisation study conducted by Hoch and Eliceche (1999). The first unit operation in the separation scheme is a complex demethanizing unit, which is followed by a conventional separation sequence. In the context of this thesis only the conventional separation sequence is relevant, where distillation columns are used as method of separation. The details of the case-study is based on the decription of the process given by Hoch and Eliceche (1999).

5.2.1.1 Problem description

The effluent stream of a demethanizing unit in an ethylene plant needs to be separated by the use of distillation columns. The feed mixture to be separated in the distillation train is the hydrocarbon mixture taken from the reactor in the ethylene plant, from where the bulk of methane had been removed. The objective of the design is to show how the use the driving force based methods provides an energy efficient distillation sequence, as well as near optimum design of the individual columns. The separation scheme contains only conventional distillation columns with one feed and two product streams. The

sequence of the columns in the ethylene plant is given by Hoch and Eliceche (1999) and shown in figure 5.1.

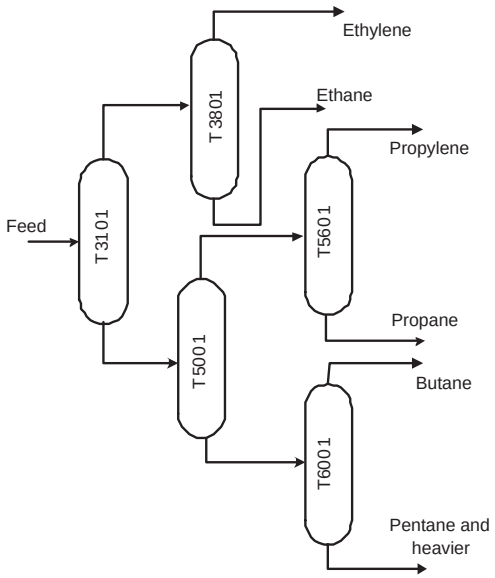

Figure 5.1: Arrangement of distillation columns in the separation sector of ethylene plant.

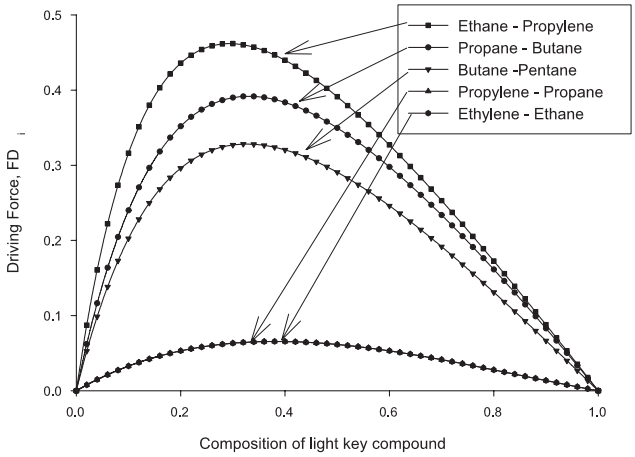

Figure 5.2: Driving force curves for sets of binary compounds at uniform pressure.

The column numbers in figure 5.1 relates to the following distillation column tasks: a) deethanizer (T3101), b) ethylene-ethane splitter (T3801), c) depropanizer (T5001), d) propylene-propane splitter (T5601), e) debutanizer (T6001)

The separation scheme of the ethylene plant was required to produce ethylene with a minimum purity of 99.92 % as the main product. The other products of the recovery section are the following: Ethane, which is recycled to the furnaces. Propylene can be used in the production of polypropylene and propane, butane and pentane can all be used as fuel. The data for the reactor effluent stream in table 5.1 are actual plant data given by Hoch and Eliceche (1999).

Component	Feed flow rate (kg-mole/hr)
Methane	0.105
Ethylene	1038.291
Ethane	650.330
Propine	0.463
Propylene	20.581
Propane	2.386
Butene	22.396
Butane	2.450
Pentane	6.778
Hexane and heavier	8.241
Pressure (bar)	30
Temperature (K)	270

Table 5.1: Feed flow to the separation section of an ethylene plant [Hoch and Eliceche (1999)].

5.2.1.2 Application of driving force based methods

The driving force method for sequencing distillation trains (algorithm S1) is applied to this example, at first to synthesize the distillation train, and then to design the individual distillation columns by using algorithm D1. In this way a synthesis problem is solved, followed by a design problem for each distillation column.

The first step is, from the feed mixture in table 5.1, to identify the key compounds in the mixture. In this case, these are the product compounds indicated in figure 5.1, *i.e.*, ranked by normal boiling point, ethylene, ethane, propylene, propane, butane and pentane (indicating five separation tasks). The next step is to generate driving force diagrams for the five separation tasks carried out among six key compounds. Based on phase composition calculations made by using the SRK equation of state for both the vapour and the liquid phase at 1 atm. pressure, the driving force diagrams shown in figure 5.2 have been generated.

By applying algorithm S1, to the driving force curves in figure 5.2, it is clear that the binary pair between ethane and propylene reaches the highest value of maximum driving force, indicating that the first split should be between these compounds. This leaves us with two products from the first column that need further separation. One product stream contains ethane and ethylene and the other stream contains propylene, propane, butane and pentane. The separation involving ethane and ethylene is obvious, since one of the products from the first column only contains them. The other stream contains four key compounds that need to be separated. According to figure 5.2, the maximum driving force amongst the remaining three curves is found to be that between propane and butane, thus this separation is allocated next. Now, each of the two products contain binary mixtures, indicating two corresponding separation tasks. This finally leads to the confirmation of the separation scheme in figure 5.1.

	T3101	T3801	T5001	T5601	T6001
N	40	90	29	134	22
N_F	24	60	10	80	9
$P_{cond}[bar]$	26.2	8.8	15.1	16.2	5.1
$\Delta P_{perstage}[mmWC]$	1200-1300	1200-1300	650-1000	51-56	500-600
$Type\ \ of condenser$	Total	Total	Total	Total	Total
$D[kg/h] - Plantdata$	21455.	81704.	9367.4	80834.	940.
$B[kg/h] - Plantdata$	7047.8	20592.	2194.3	4548.	384.
$Performance$	$x_{C_3H_6+C_3H_8,D}$	$x_{C_2H_4,D}$	$x_{C_4H_8+C_4H_{10},D}$	$x_{C_3H_6,D}$	$x_{C_4H_8+C_4H_{10},B}$
$SpecificationI$	0.002740	0.9992	0.00035	0.75	0.0178
$Performance$	$x_{C_2H_4+C_2H_6,B}$	$x_{C_2H_4,B}$	$x_{C_3H_6+C_3H_8,B}$	$x_{C_3H_8,B}$	B_{C_5/f_5}
$SpecificationII$	0.00009	0.006	0.004	0.85	0.98

Table 5.2: Operation conditions of distillation columns in ethylene plant [Hoch and Eliceche (1999)].

The design of the individual distillation columns now remains to be determined. These designs are done through algorithm D1, which requires driving force curves at the actual operating pressure and the number of plates as specified data. The number of plates together with some other design parameters are given by Hoch and Eliceche (1999) and shown in table 5.2.

It follows from table 5.2, the columns operate at very different pressures. Since algorithm D1 is based on driving force diagrams at actual operating pressure, these diagrams must be generated. In this case, uniform column pressures are assumed, equivalent to the condenser pressure. The driving force curves at the actual pressures are shown in figure 5.3.

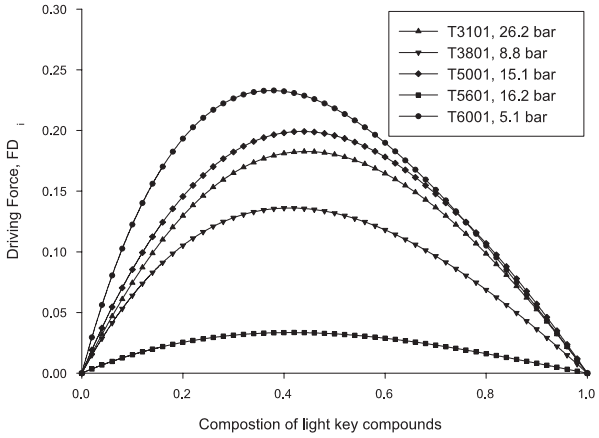

Figure 5.3: Driving force curves at actual operating pressures. The labels on the curves refer to the numbers given in figure 5.1 and in table 5.2.

By following algorithm D1, the minimum reflux ratios and relative feed stage locations can be determined. This is done by the identification of points D and D_x for each of the curves in figure 5.3. These are summarized in table 5.3, where the actual number of stages in each column is also given (see table 5.2). The calculation of the feed stage, N_F is based on the value of N.

	T3101	T3801	T5001	T5601	T6001
D_x	0.47	0.42	0.46	0.44	0.38
N	40	90	29	134	22
N_F	21	52	15	75	13
RR_{min}	3.0	2.1	13.6	1.8	1.7

Table 5.3: Feed locations and minimum reflux ratios of distillation columns as according to algorithm D1.

5.2.1.3 Results and discussion

The synthesis problem and the design problems have been solved by driving force based methods. Hoch and Eliceche (1999) formulated an equivalent design problem as the one solved by algorithm D1, but in terms of a non-linear optimisation problem. As to the optimisation problem, the objective was to minimise the distillate and reflux flow rates. At first the feed plate locations in the distillation columns remained fixed, and afterwards the feed plate locations was also regarded as a variable. As the study was conducted for an actual plant, the column sequence was known, and therefore not subject to this optimisation study. However, it is assumed that the plant built was based on some kind of investigation of the alternative distillation column sequences (14 alternatives, as it is found in table 2.1), and therefore, the column sequence proposed by algorithm S1 is in this context considered to be confirmed as the optimum sequence.

The feed locations obtained from the optimisation study are given in table 5.4. The relative savings in operating costs between "original" feed location, and the optimised feed location are also given. Furthermore, the feed locations, according to algorithm D1 are shown in the same table, and the relative deviation of these feed plate locations from the optimised feed locations found by Hoch and Eliceche (1999) are also shown.

Column	T3101	T3801	T5001	T5601	T6001
Original feed location, N_F (Hoch and Eliceche (1999))	24	60	10	80	9
Optimised feed location, N_F (Hoch and Eliceche (1999))	18	68	14	68	13
Energy Saving [%]	3.12	0.82	57.24	2.37	5.04
N_F predicted by algorithm D1	21	52	15	75	13
Deviation of algorithm D1 from optimum	7 %	18 %	3 %	4 %	0 %

Table 5.4: Comparison of the original N_F in the plant to the optimum positions of N_F found by Hoch and Eliceche (1999) and the positions of N_F found by algorithm D1.

The results presented in table 5.4 confirms algorithm D1 as a tool for determination of the optimum relative position of the feed stage in a distillation

column. Especially when comparing the results in table 5.3 with the original feed stage locations of the plant and the optimised feed locations given in table 5.4, the reliability of the new method for the prediction of the relatively optimal position of the feed position is clear. It should be noted that no simulations have been carried out at this stage, and the product compositions are assumed identical to the specifications (given in table 5.2) given by Hoch and Eliceche (1999). The solution of the optimisation of the distillate flow rate and the reflux ratio with respect to N_F performed by Hoch and Eliceche (1999) is assumed to represent the actual optimum solution.

As a consequence of this, the question of scaling the feed stage location can only be taken into account based on the performance specifications in table 5.2. In general, the optimisation results seem to be close to the predictions according to algorithm D1, except for the ethane-ethylene splitter (T3801). The reason for this is discussed below, where each column is treated separately.

T3101, Deethanizer column The feed stage in the deethanizer column predicted by algorithm D1 deviates by 7 % from the actual optimum feed location. The predicted position is right between the actual position in the plant and the optimum location found by Hoch and Eliceche (1999), and the predicted feed location lies within the 10 % margin of algorithm D1. As it can be seen in table 5.2, there is a much stricter performance specification at the bottom than for the distillate. This indicates that a scaling factor should be applied to the feed stage, to predict the optimum feed stage location. The scaling factor would in this case be number 2c in table 4.3, which would move the feed stage higher up in the column. Hoch and Eliceche (1999) compare the operating cost to different feed stage locations. This comparison shows a saving of less than 1.0 % if the feed introduction to the column is relocated from the stage predicted by algorithm D1 ($N_F = 21$), without a scaling factor to the actual optimum stage ($N_F = 18$). So, even though there is a difference in the feed stage location of 7 %, the saving of energy is less than 1 %.

T3801, Ethane-Ethylene splitter This column is the one where the predicted feed location is the relatively least accurate compared to the actual optimum feed location. It can be noticed from the performance specifications for the column in table 5.2, that there is a stricter specification for the ethylene product in the distillate than there is for the ethane product at the bottom. The scaling factor associated with algorithm D1 would therefore move the feed down in the column. The feed location as predicted by algorithm D1 without a scaling factor is reasonable in terms of operating costs, even though the position is 18 % away from the optimum location. This follows from the comparison in the paper by Hoch and Eliceche (1999) with the operating costs compared to the feed stage location for this column. It shows a difference in operating costs from $N_F = 52$ to $N_F = 68$ of 2.6 %.

T5001, Depropanizer column The depropanizer column is the column in the sequence in which the biggest relative energy saving is achieved as a result of the optimisation by Hoch and Eliceche (1999). As it can be seen from the performance specifications in table 5.2, the recovery rates for the distillate and for the bottoms are nearly the same, and algorithm D1 does not require the use of scaling factors. As it is seen in table 5.4, algorithm D1 predicts a feed location only one stage below the optimum feed stage location. This indeed is very much closer to the optimum solution than the original location in the plant, and since Hoch and Eliceche (1999) show a reduction of 57 % in operating costs by relocating the feed location in the column, this clearly shows the accuracy of the driving force based method. In this connection, it also worth noticing that an illustration of operating costs as a function of feed location in the paper by Hoch and Eliceche (1999), only shows a slight difference in operating costs occurs between the optimum feed stage location and the feed stage location obtained by algorithm D1.

T5601, Propane-Propylene splitter This column is the column with the greatest number of stages in the sequence. The objective of the column is to split propane and propylene. The two performance specifications for the column are listed in table 5.2, where it is seen that the two performance specifications are of the same order of magnitude, but slightly stricter at the bottom. This indicates an optimum feed location slightly above the one predicted by algorithm D1, without the use of scaling. However, at the same time, there is significantly more propylene than propane in the column feed, indicating the feed should be lower in the column. The optimisation result of Hoch and Eliceche (1999) suggests re-locating the feed stage by 9 % from the original location. This re-location corresponds to a saving of 2.4 % of the operating cost. Algorithm D1 predicts a feed location between the original feed location in the plant and the optimum feed location, 3 % from the optimum feed location. Whereas the scaling factor related to performance specification would imply that it should move up in the column, towards the optimum solution, the other scaling factor related to dilution proposes movement in the opposite direction.

T6001, Debutanizer column From this column, the optimisation study of Hoch and Eliceche (1999) suggests a feed stage location four stages from the original location. This corresponds to a relative movement of 18 %. As it can be seen from table 5.2, the performance specifications for this column are the same order of magnitude for the distillate and the bottom, just one is a composition specification and one is a recovery specification. Algorithm D1 predicts a location of the feed stage in this column exactly at the same stage that was found in the optimisation study by Hoch and Eliceche (1999).

The optimisation study by Hoch and Eliceche (1999) show that the two columns, T3101 and T3801 together consume more than 90 % of the total

energy during normal operation. On this basis, the advantage of applying the pressure allocation method, algorithm D4 for the overall flowsheet is moderate, because the pressures in these two columns cannot be lowered due to the large amount of light compounds. The condenser temperatures are already below -10^oC, and the costs of cooling utilities in this temperature range is very high. If, anyhow, algorithm D4 is applied, rigorous simulations with Pro/II show that a reduction in the energy consumption of approximately 55 % can be achieved. This reduction is achieved by lowering the condenser pressure in the deethanizer (T3101) to 16 bar and the condenser pressure in the ethylene-ethane splitter (T3801) to 5.5 bar (found through algorithm D4). Another possibility is to apply algorithm D4 to the system, starting from the bottom stream of the deethanizer (T3101). But the incentive of such an application is almost negligible, when there is only a basis for a reduction of the energy consumption in a part of the sequence that consumes less than 10 % of the total energy. The biggest advantage can be achieved by lowering the pressure in the propylene-propane splitter (T5601), where the most stages are. Here a reduction of 36 % in the operating costs of this column can be achieved by lowering the condenser pressure to 4.7 bar as the application of algorithm D4 to this column predicts, and still achieve a bubble point temperature higher than the bubble point temperature in the condenser of column T3101.

At this point it is clear that a synthesis problem, solved by algorithm S1, has determined the optimal distillation column sequence for separation of the feed composition in table 5.1 into individual compounds. The optimal distillation sequence was found strictly on basis of vapour-liquid phase composition data of the compounds to be separated. Furthermore, each column has been designed by algorithm D1, which has confirmed its ability to predict the near optimal design of distillation columns, also solely based on the vapour-liquid data for the mixture compounds at the actual operating pressures. Hoch and Eliceche (1999) performed an optimisation study on the flowsheet studied in this example by solving a complex mathematical problem. Almost the similar results were obtained by using algorithm S1 and algorithm D1, without performing any simulation or optimisation.

5.2.2 Separation of hydrocarbon mixture

This example deals with the separation of a mixture of hydrocarbons. The example is given by Shah and Kokossis (1997), who developed a conceptual programming method and applied it to the separation of eight hydrocarbon compounds into their individual constituent compounds. The authors have not described the example in detail, but here it is used as an example and treated by the driving force method for the synthesis of distillation trains (algorithm S1). The results are then compared to the results of the optimisation reported by Shah and Kokossis (1997).

5.2.2.1 Problem description

In this example, an aromatic-paraffin mixture with eight compounds is to be separated into its constituent pure compound products in a sequence of simple distillation columns (Shah and Kokossis, 1997). The feed mixture is given in table 5.5.

The application of the driving force based method for the synthesis of distillation trains requires the generation of driving force diagrams between the key compounds, which means that seven driving force diagrams need to be generated for the seven pairs of key compounds, indicating the separation tasks (splits) for each column.

Compounds	Feed composition (kmole/hr)
2,2-Dimethyl-propane (A)	32.51
i-Pentane (B)	59.97
n-Pentane (C)	62.71
2,2-Dimethyl-butane (D)	6.64
2,3-Dimethyl-butane (E)	10.80
2-Methyl-pentane (F)	62.71
n-Hexane (G)	39.62
Benzene (H)	80.33

Table 5.5: Feed mixture to distillation sequence, ranked by normal boiling points [Shah and Kokossis (1997)].

5.2.2.2 Application of the driving force method for distillation sequencing

The synthesis of a distillation column sequence can be obtained by the application of algorithm S1. The binary pairs to be split in each column are identified by ranking the normal boiling points as shown in table 5.5. Based on phase composition calculations using the SRK equation of state, driving force diagrams at atmospheric pressure have been generated, as shown in figure 5.4. The curve labels in figure 5.4 refer to the compounds in table 5.5 and the columns where the splits are performed.

Note here that *n-hexane* and *benzene* form a binary azeotrope, but this split has a driving force which is the third greatest of them all. As dictated by algorithm S1, the split is therefore removed from its third position and placed at the end of the sequence, by multiplying D_y with a penalty factor = 0.11 (obtained from step 3.1 in algorithm S1 applied to the curves in figure 5.4). In this way, step by step application of algorithm S1 leads to a ranking of the splits by the size of their maximum driving forces, and the lay-out of the separation scheme can be deduced. This is shown in figure 5.5.

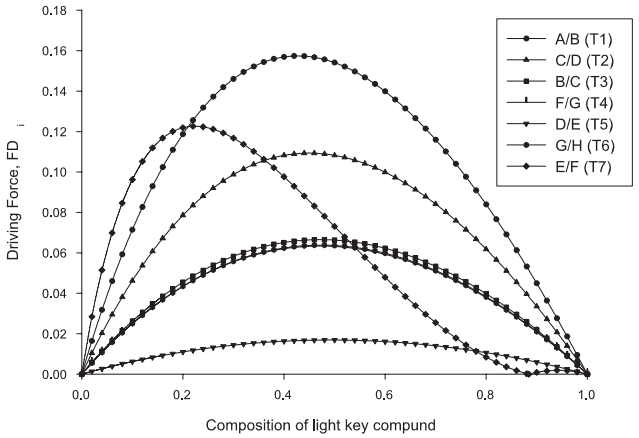

Figure 5.4: Driving force curves for adjacent key compounds.

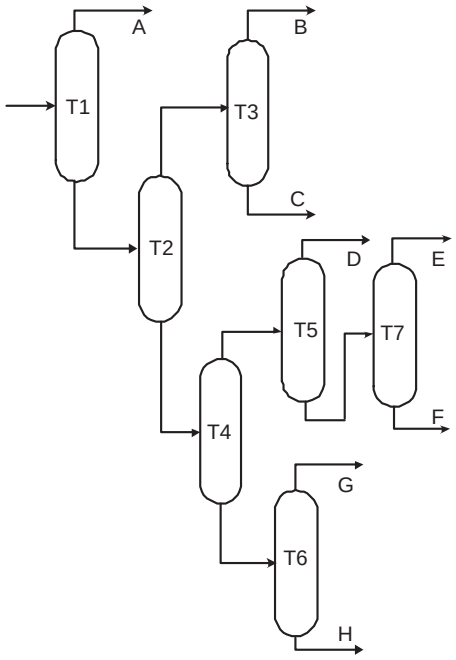

Figure 5.5: Sequence of distillation columns proposed by algorithm S1.

5.2.2.3 Discussion of results

The distillation train proposed by algorithm S1 differs from the flowsheet proposed as optimal by Shah and Kokossis (1997). They reported the flowsheet

given in figure 5.6 to be optimal. However, the optimisation study by Shah and Kokossis (1997) is based on constant relative volatilities, which may not lead to the actual optimum solution. Therefore rigorous simulations of the two alternative flowsheets have been performed with Pro/II, to verify which one is superiour. As input for the simulations, the information in table 5.6 is used. The design specifications, like number of stages, reflux ratios and feed stage locations applied have in all cases been obtained directly from algorithm D1. The specifications have been determined in order to produce reasonably pure products. Based on this information, both alternative flowsheets have been simulated and it was found that the flowsheet obtained from the driving force based algorithm requires less energy (approximately 8 %) than the flowsheet found by Shah and Kokossis (1997). Since the optimisation study by Shah and Kokossis (1997) is performed with very approximate models for the splits, it is likely that the solution they found is not the actual optimum flowsheet. In this context, it is important to note, however, that the driving force based flowsheet has been obtained visually, and without doing any detailed simulation or optimisation.

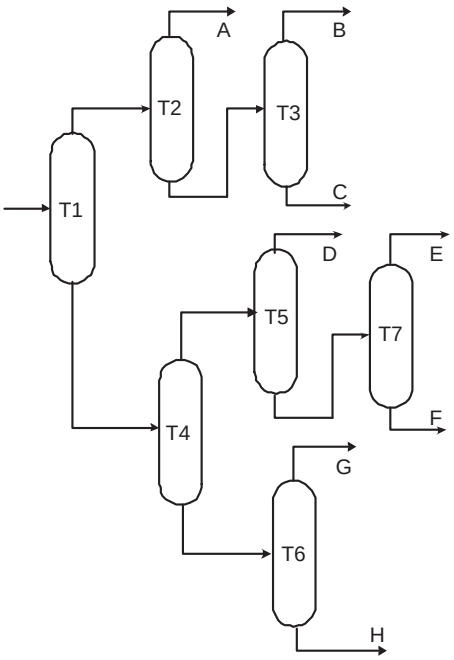

Figure 5.6: Sequence of distillation columns proposed by Shah and Kokossis (1997).

Column	Separation task	N	N_F	RR	Specification I	Specification II
T1	A/B	27	12	16.72	Recovery of A = 0.997	B through H = 0.998
T2	C/D	38	15	2.85	Recovery of B+C = 0.9998	Recovery of D through H = 0998
T3	B/C	61	30	8.42	Recovery of B = 0.9855	Recovery of C = 0.985
T4	F/G	63	38	10.14	Recovery of D through F = 0.995	Recovery of G+H = 0.995
T5	D/E	64	28	60.51	Recovery of D = 0.994	Recovery of E+F = 0.995
T6	G/H	44	39	18.08	Recovery of G = 0.985	Recovery of H = 0.92
T7	E/F	138	73	596.0	Recovery of E = 0.98	Recovery of F = 0.99

Table 5.6: Specifications on the optimum flowsheet as used for simulation. The letters refer to compound identities listed in table 5.5.

5.2.3 Separation of Methanol and MTBE

A simple example of separation of a binary mixture with an azeotrope has been presented by Sano *et al.* (1995). The mixture is the classical methanol-MTBE mixture. Sano *et al.* (1995) studied the separation of this mixture by pervaporation using a silicate membrane. The pervaporation data of Sano *et al.* (1995) are given in figure 5.7 together with vapour liquid equilibrium data, which have been obtained based on the UNIFAC liquid activity coefficient model for the liquid phase and the ideal gas model for the vapour phase.

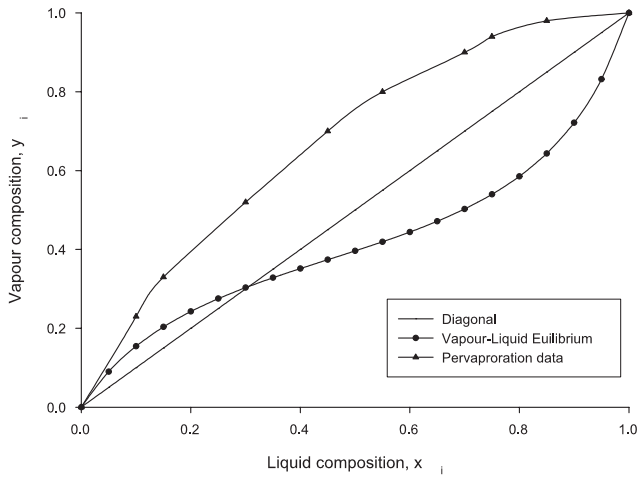

Figure 5.7: Pervaporation and vapour liquid phase composition diagram for methanol - MTBE separation (Sano *et al.*, 1995).

5.2.3.1 Problem description

In order to apply the driving force methods for synthesis of hybrid separation schemes, the driving force curves have to be calculated, for a number of separation techniques and are shown in figure 5.8. Here, pervaporation data are given, together with vapour liquid equilibrium data, as applied in the distillation at two different pressures, and extractive distillation, where binary data on a solvent free basis are exploited. The solvent in this case is toluene, which was identified using the $ProCAMD$ program.

5.2.3.2 Application of the driving force method for synthesis of hybrid schemes

Once the phase composition data for the mixture to separate have been found, and driving force curves have been generated, the comparison of separation techniques can start. From figure 5.8, it can be seen that there are a number of feasible solutions that can be generated. First of all, pervaporation, in principle can be applied within the whole separation spectrum. However, in reality, flux limitations makes this alternative impossible, but pervaporation can be applied in combination with any of the other separation techniques. Extractive distillation, on the other hand can be applied throughout the whole separation range, although the driving force becomes low at one end. In principle extractive distillation can be applied as the only separation technique, or combined with any of the other separation techniques considered here. The last possibility is to take advantage of the pressure sensitivity of the binary azeotrope, and apply pressure-swing distillation.

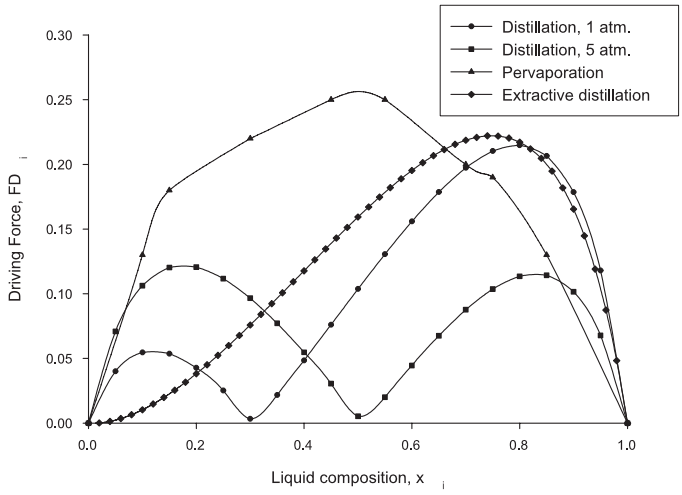

Figure 5.8: Driving force curves for various separation techniques (methanol - MTBE system).

5.2.3.3 Evaluation of results

Examining the curves in figure 5.8, the maximum driving force is from a combination of atmospheric distillation with pervaporation. The benefit, however, of applying distillation to perform part of the separation may seem negligible at a first glance. But since membrane processes are limited by flux and it is virtually impossible to perform the whole separation by use of a membrane,

distillation may be necessary to achieve high-purity products. Consequently, there is a large advantage in combining the two different separation techniques, *i.e.*, employ a hybrid separation scheme. Simulations with Pro/II show that if distillation and pervaporation are combined, at least 34 % energy is saved, compared to any configuration involving two columns (extractive distillation and pressure-swing distillation).

5.3 Design of distillation columns

5.3.1 Design of simple distillation columns

Although a number of distillation column designs are shown in different case-studies in this chapter, a section is here dedicated to illustrating the simple design procedure outlined in algorithm D1. The scope here is to illustrate the design method, and how it applies to binary and multicomponent mixtures covering a wide spectrum of feed compositions.

5.3.1.1 Distillation of methanol and water

This example deals with the classical distillation problem of separating the binary mixture of methanol and water. The data for this system are obtained from vapour liquid compositions, calculated by the UNIFAC model for the liquid phase, and the ideal gas model for the vapour phase. The driving force diagram is shown in figure 5.9.

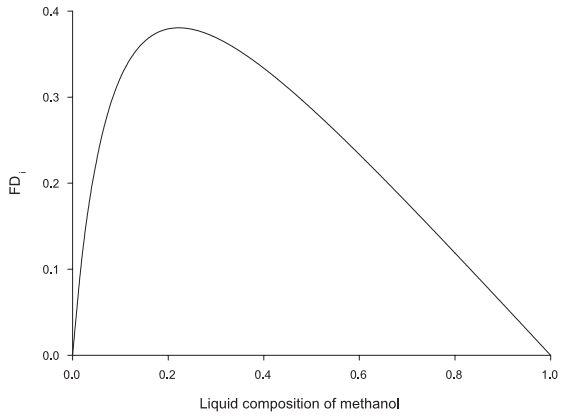

Figure 5.9: Driving force diagram for methanol - water separation.

The point D_x is here identified as $D_x = 0.22$ and the minimum reflux ratio is $RR_{min} = 1.02$. Applying algorithm D1 to this example, assuming 22 equilibrium stages in the column, leads to a prediction of $N_F = 17$.

To verify these results, optimisation with rigorous distillation models in Pro/II have been performed, for a number of different feed compositions. These, together with the optimisation results for verification are given in figure 5.10.

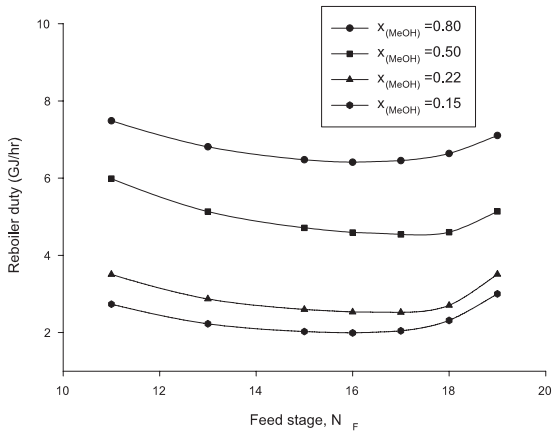

Figure 5.10: Reboiler duty as function of feed stage location for methanol - water separation.

The simulations are performed with equal size specifications of mole fractions for the two products at the top and at the bottom. Note that, for the feed composition $x_{(MeOH)} = 0.15$, scaling factor 1a of algorithm D1 is activated, thereby moving the feed stage 5 % up in the column. Clearly, the predicted value of $N_F = 17$ is confirmed. For two cases, the optimum was found to be stage 16, and in one of these cases, it was already predicted. The reflux ratios for these compositions, were found to be at the actual optimum feed stage locations between 1.24 and 2.12.

5.3.1.2 Distillation of ethanol and toluene

The binary mixture of ethanol and toluene forms an azeotrope, and therefore it cannot be separated into pure products by normal distillation. In this example, pure ethanol will be produced together with a mixture of ethanol and toluene at the azeotropic composition. The azeotropic composition corresponds to an ethanol composition of 0.81 when the operating pressure in the system is P = 1 atm. The thermodynamic model applied for this system is the NRTL model for the liquid phase and the SRK equation of state for the vapour phase. The driving force diagram is shown in figure 5.11.

By following algorithm D1, and taking the azeotrope into account, D_x is found to be 0.12 and the minimum reflux ratio is $RR_{min} = 0.89$. Applying algorithm D1 to this example, and assuming 20 equilibrium stages to be present in the column, algorithm D1 predicts $N_F = 17$.

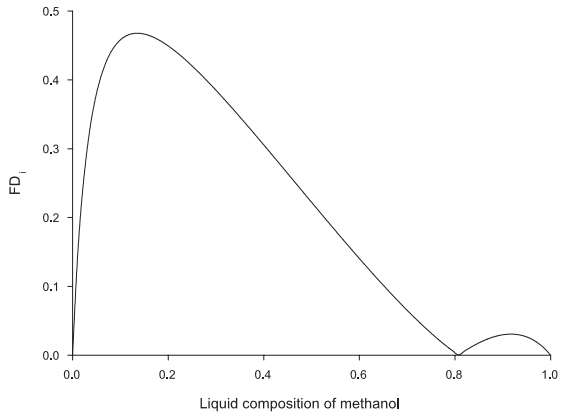

Figure 5.11: Driving force diagram for ethanol - toluene separation.

To verify these results, optimisation using rigorous distillation models in Pro/II has been performed, for different feed compositions. The feed compositions, together with the optimisation results for verification are given in figure 5.12.

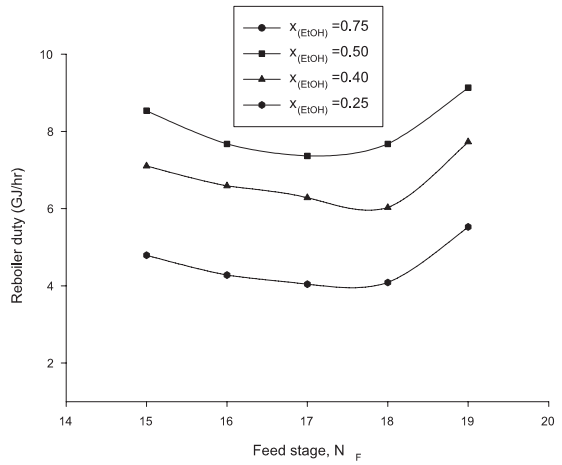

Figure 5.12: Reboiler duty as function of feed stage location for ethanol - toluene separation.

The optimisation is performed employing variations of the feed stage and maintaining the purity specifications in both the top and the bottom. The distillate corresponds to a purity of 80.72 % toluene (very close to azeotropic point) while the bottom corresponds to a purity of 99.9 % ethanol. The results

in figure 5.12 confirm the predicted optimum feed stage location to be $N_F = 17$, except in one case, where it was found to be 18. The reflux ratios in this example ranges from 1.93 to 2.18.

5.3.1.3 Design of deethanizer

Seader and Henley (1998) give an example of a deethanizer, operating at 400 psia. They propose a distillation column with 13 stages where the feed stage is located at $N_F = 7$. The feed composition and condition is given in table 5.7.

Component	lb-mole/hr
C_1	160.0
C_2	370.0
C_3	240.0
C_4	25.0
C_5	5.0
Total Flow	800.0
Physical Condition	
Temperature (^oF)	105
Pressure (psia)	400

Table 5.7: Feed composition and physical condition of the feed to the deethanizer [Seader and Henley (1998)].

The driving force design method has been applied to this example. The split is obviously between ethane and propane. Based on the SRK equation of state for both phases, phase composition data have been calculated and the driving force diagram for these data are shown in figure 5.13.

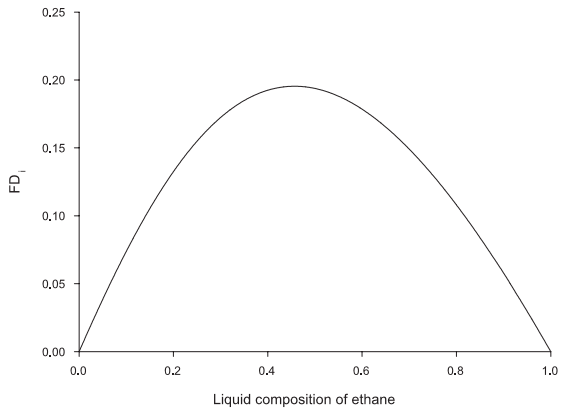

Figure 5.13: Driving force diagram for ethane - propane separation at 400 psia.

From figure 5.13, the relative location of the greatest possible driving force is determined to be $D_x = 0.48$, and along with a number of stages of $N = 13$, this leads to a prediction of an optimum feed introduction at stage, N_F = 6-7 from algorithm D1. Seader and Henley (1998) assumed the feed stage to be at stage 7. This was obtained by drawing a modified McCabe-Thiele diagram, based solely on the key compounds. The modified McCabe-Thiele diagram was made on a basis of rigorous simulation results, as proposed by Scheibel (1946). Seader and Henley (1998) eventually conclude, on the basis of simulations, that a more effective separation between the compounds is achieved by relocating the feed introduction to stage 6. The driving force based method the predicted this result without performing any simulations. Rigorous simulation with Pro/II shows that stage 6 and 7 are equally good feed stage locations.

5.3.2 Design of side-draw distillation columns

5.3.2.1 BTX mixture

This is an example of how algorithm D2 is applied to make a design for distillation columns with side-draws. The feed mixture to be separated in this case is the well-known mixture of benzene, toluene and xylenes. The mixture is treated here using three different feed compositions.

The conditions of operation in this example is at a pressure of 10 atm., and there are 40 stages in the column. Following algorithm D2, the first step is to generate driving force diagrams for the two binary pairs of key compounds. These have been generated based on the SRK equation of state for both phases, and are shown in figure 5.14.

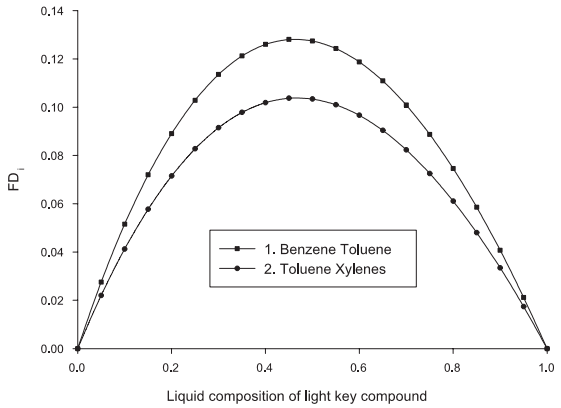

Figure 5.14: Driving force diagrams for benzene - toluene separation and for toluene - xylenes separation at 10 atm.

From figure 5.14, it can be seen that the largest maximum driving force is

between benzene and toluene, which is the binary set of key compounds which is lighter boiling. From algorithm D2, it follows now that the feed should be introduced above the side-draw, and the next task is to generate the joint driving force curve. This comprises both of the curves in figure 5.14, and in such a way that the side-draw will be located below the feed stage. This is seen in the driving force curve shown in figure 5.15. The column configuration is shown in figure 5.16.

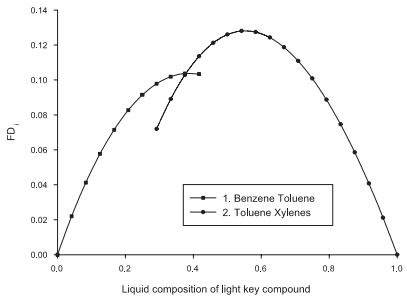

Figure 5.15: Joint driving force diagrams for benzene - toluene and toluene - xylenes separation at 10 atm.

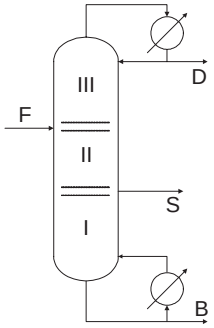

Figure 5.16: Distillation column with side-draw below feed stage, for BTX mixture separation.

The next step involves identification of point D_s, where the two original driving force curves intersect. The point to be identified here is $D_s = 0.38$. According to algorithm D2, with 40 stages in the column, the side-draw should be placed at $N_S = 24$. The feed stage can at this point be located, based on the original driving force diagram in figure 5.14, where curve 1 (with the greatest possible driving force) is applied. It is here identified that $D_x = 0.46$. This corresponds to feed stage, $N_F = 13$.

Rigorous simulation of the system has been performed in Pro/II, at three different feed mixture compositions. The results are outlined in table 5.8.

The specifications were in all the cases consistent, producing a pure benzene product in the distillate, and a near pure (as pure as possible with 40 stages) xylenes product at the bottom. Clearly, the results in table 5.8 confirm that algorithm D2 is indeed capable op predicting near optimum solutions for complex columns with side-draw.

5.3.2.2 Hydrocarbon mixture

Algorithm D2 has been applied here for the separation of a mixture of three hydrocarbons, with the objective to illustrate the driving force based method for the design of distillation columns with side-draws. The feed mixture contains propane, butane and 2,3 dimethylbutane (23MB). This example has been

Composition	Feed 1	Feed 2	Feed 3
Benzene	0.33	0.15	0.50
Toluene	0.33	0.70	0.35
Xylenes	0.34	0.15	0.15
	N_S	N_F	
Algortihm D2	24	13	$\frac{side-draw}{feed}$
Feed 1	23	12	0.33
Feed 2	23	14	0.70
Feed 3	23	11	0.35

Table 5.8: Verification of algorithm D2 for BTX mixture

worked out for two different feed compositions.

In this case, the column operates at 10 atm. pressure and has 36 stages. Again, by following algorithm D2, the first step is to generate driving force diagrams for the two binary pairs of key compounds. In this case, the SRK equation of state for both phases has been applied, and the driving force curves are shown in figure 5.17.

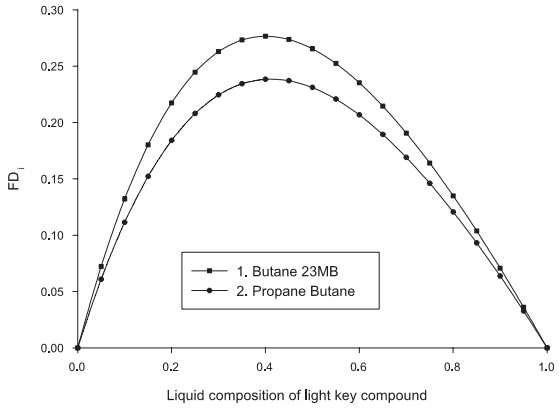

Figure 5.17: Driving force diagrams for benzene - toluene separation and for toluene - xylenes separation at 10 atm.

From figure 5.17, it is clear that the greatest possible driving force is between butane and 23MB. This is the binary set of key compounds which is heavier boiling, and algorithm D2 states therefore that the feed should be introduced below the side-draw. This is then reflected in the joint driving force curve, which in this case is made so that the side-draw will be located above the feed stage. The driving force curve is shown in figure 5.18. The column configuration is shown in figure 5.19.

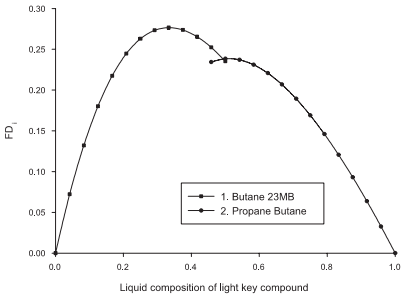

Figure 5.18: Joint driving force diagrams for propane - butane and butane - 23MB separation at 10 atm.

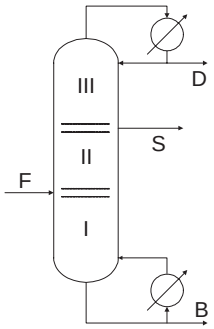

Figure 5.19: Distillation column with side-draw below feed stage, for the hydrocarbon mixture separation.

By following algorithm D2, point D_s can now be identified, where the two original driving force curves intersect. The point is identified here to be $D_s = 0.50$. Employing 36 stages when applying algorithm D2, it proposes that the side-draw should be placed at $N_S = 18$. Now, the feed stage can be located, based on the original driving force diagram in figure 5.17, where curve 1 (with the greatest possible driving force) is applied. It has been found that $D_x = 0.41$, which according to algorithm D2 corresponds to a feed stage, $N_F = 28$.

Rigorous simulation of the system has been performed in Pro/II, for the two different feed compositions. The results are given in table 5.9.

Composition	Feed 1	Feed 2	
Benzene	0.33	0.15	
Toluene	0.33	0.70	
Xylenes	0.34	0.15	
	N_S	N_F	
Algortihm D2	18	28	$\frac{side-draw}{feed}$
Feed 1	18	28	0.33
Feed 2	18	28	0.70

Table 5.9: Verification of algorithm D2 for hydrocarbon mixture.

The column specifications were in both cases consistent, producing a pure benzene product as the distillate, and a nearly pure propane product at the bottom. It is very clear, that the results in table 5.9 confirm that algorithm D2 is indeed capable of predicting near optimum solutions to complex column designs with side-draw accurately.

5.3.3 Design of thermally coupled distillation columns

5.3.3.1 BTX mixture

Seider *et al.* (1999) give a design problem for a Petlyuk column configuration, which is intended to be used for the separation of a BTX mixture (this is, ranked by normal boiling point, benzene, toluene and xylenes). This problem serves here as an example, with conditions slightly different from the ones given by Seider *et al.* (1999), to illustrate how algorithm D5 is applied for the design of thermally coupled columns. The information of the feed mixture composition as well as of the desired products has been collected for this example and is presented in table 5.10.

Compounds	Feed rate (lbmole/hr)	Product purity
Benzene	20	0.995
Toluene	65	0.98
Xylenes	15	0.99

Table 5.10: Feed mixture and desired products for algorithm D5 applied to a BTX mixture separation.

The operating pressure is atmospheric pressure (0 psig), and the feed is mainly vapour (90 %). The number of stages in the main column is 50, and there are 6 stages in the pre-fractionator. The driving force diagrams are calculated, in this case based on the Peng-Robinson equation of state, and they are shown in figure 5.20.

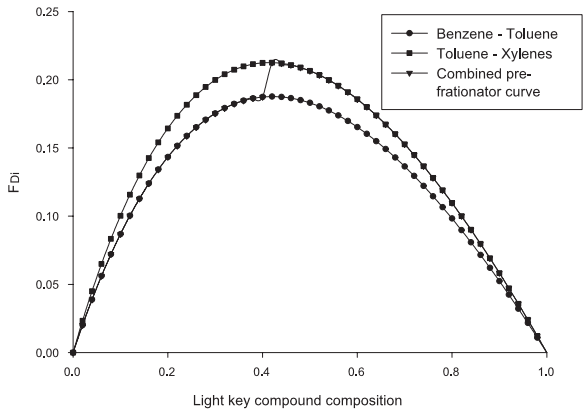

Figure 5.20: Driving force diagrams for the separation of BTX mixture in Petlyuk column.

The parameters obtained from the driving force diagrams are summarized in

tabular form in table 5.11.

Curve	$x_{i\|Max}$	$F_{Di\|Max}$
Benzene-Toluene	0.42	0.21
Toluene-Xylenes	0.42	0.19
Pre-fractionator	0.42 (intersection)	

Table 5.11: Design parameters for algorithm D5 applied to a BTX mixture separation.

Having obtained this knowledge, the design of the Petlyuk column can be made. The first step is to determine the feed stage for the pre-fractionator. Considering the vapour feed mixture, and $x_{i|Max}$ is 0.42 (see table 5.11), the value of $x_{i|Max}$ is estimated to be $x_{i|Max} = 0.55$. This leads to a prediction of the pre-fractionator feed stage, as $N_{F,pre-frac} = 3$. The next step is to determine the distribution between sections III/IV and V/VI, thereby obtaining the side-draw stage. The interpolation of the values of $F_{Di|Max}$ found in table 5.11, in table 4.5 (tabulated values of corresponding N_{ideal} and $F_{Di|Max}$), and by distributing the values for the number of stages over the 50 stages in the main column, leads to $N_S = 24$. Now, for each of the sections, III/IV and V/VI algorithm D1 is applied directly to the relative number of stages in each section (considering that the vapour feed in the top segment of the main column is vapour). The results can be seen in table 5.12, together with a comparison to the actual optimum values, as they are found by optimisation in Pro/II.

Variable	Prediction by algorithm D5	Actual optimum
$N_{F,pre-frac}$	3	4
N_S	24	24
$N_{F,top}$	10	9
$N_{F,bottom}$	39	38

Table 5.12: Comparison of design parameters obtained by algorithm D5 to actual optimums for a BTX mixture separation.

5.3.3.2 Mixture of butanoles

This example deals with the design of a thermally coupled distillation (Petlyuk) column, for the separation of a mixture of s-butanole, i-butanol and n-butanole (outlined by normal boiling point). The example is used as a case-study by Kim (2001), and in this context, it is used as an example for the application of algorithm D5 to design of thermally coupled columns. The information about the feed mixture as well as the desired product purities is presented in table 5.13.

The operating pressure in this case is atmospheric pressure (0 psig), and the feed is partly vapour (50 %). The number of stages in the main column is 72,

Compounds	Feed rate (lbmole/hr)	Product purity
s-Butanol	100	0.98
i-Butanol	100	0.98
n-Butanol	100	0.98

Table 5.13: The feed mixture and desired products for algorithm D5 applied to the separation of a butanoles mixture.

and the pre-fractionator has 20 stages. Based on the UNIQUAC model, the driving force diagrams have been calculated, as they are shown in figure 5.21.

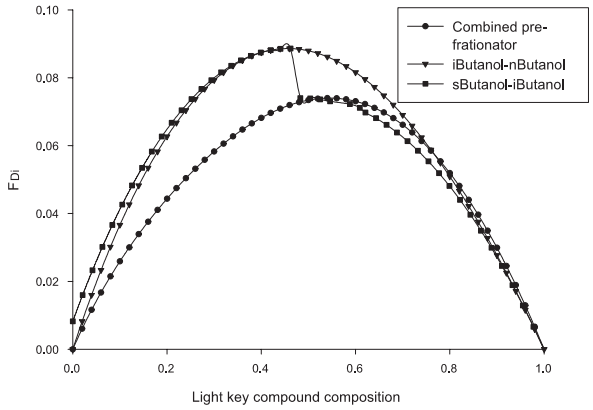

Figure 5.21: Driving force diagrams for the separation of mixture of butanoles in Petlyuk column.

The parameters obtained from diagrams are summarized in tabular form in table 5.14.

Curve	$x_{i\|Max}$	$F_{Di\|Max}$
sButanol-iButanol	0.55	0.074
iButanol-nButanol	0.45	0.089
Pre-fractionator	0.48 (intersection)	

Table 5.14: Design parameters for algorithm D5 applied to the separation of a butanoles mixture.

At this stage, the design of the Petlyuk column can be generated. The first step is to determine the feed stage for the pre-fractionator. The value of $x_{i|Max}$ is 0.48 (see table 5.14), taking the vapourisation into account, it is estimated to be $x_{i|Max} = 0.63$. This leads to a prediction of the pre-fractionator feed stage, as $N_{F,pre-frac} = 7$. The next step is to determine the distribution between

sections III/IV and V/VI, in order to obtain the side-draw stage. Interpolation of the values of $F_{Di|Max}$ found in table 5.14, in table 4.5 and distributing the number of stages over the 72 stages in the main column of this example, leads to $N_S = 41$. Then, for each of the sections, III/IV and V/VI algorithm D1 remains to be applied to the relative number of stages in each section, in order to finalize the design (considering that the vapour feed in the top segment of the main column is vapour). The results are listed in table 5.15, together with a comparison to the actual optimum values (found by optimisation in Pro/II).

Variable	Prediction by algorithm D5	Actual optimum
$N_{F,pre-frac}$	7	7
N_S	40	40
$N_{F,top}$	14	13
$N_{F,bottom}$	57	58

Table 5.15: Comparison of design parameters obtained by algorithm D5 to actual optimums for the separation of butanoles mixture.

Besides, Kim (2001) proposed a design of the Petlyuk column to perform the separation of butanoles. The parameters for this design are $N_S = 31$, $N_{F,pre-frac} = 9$, $N_{F,top} = 10$, $N_{F,bottom} = 57$, and the product purities are in the range of 0.90 to 0.96. Simulation of the design obtained from the driving force based method and the design proposed by Kim (2001), shows an energy reduction of 5 % by using the design obtained from algorithm D5, even when the product purities are significantly lower in the design by Kim (2001).

5.3.4 Design of reactive distillation columns

5.3.4.1 MTBE production

The production of methyl tert-butyl ether (MTBE) through the simultaneous reaction and separation of isobutene with methanol is a well-studied example. Application of algorithm D3 is highlighted by this reactive system. The system can be described on the basis a binary pair of *elements*, thereby reducing the complexity of the system (Pérez-Cisneros *et al.*, 1997).

The *element* stochiometry for this system is given below in table 5.16.

The reaction taking place in terms of compounds and *elements* is given in equation 4.12, which is repeated here in the context of this example.

$$\begin{array}{c} Methanol + iButene \rightleftarrows MTBE \\ A + B \rightleftarrows AB \end{array} \tag{4.12}$$

In order to apply algorithm D3, it is necessary to check whether the reaction-separation system can be exploited on a binary basis, using chemical *elements*. It can be seen in table 5.16 and in equation 4.12 that this is the case, and the vapour liquid *element* composition diagram at P = 1 atm. is shown in figure

Compound / *Element*	*iButene*	*Methanol*	*MTBE*
A	1	0	1
B	0	1	1
Feed composition	0.7	0.3	
Temperature, K		300	
Pressure, atm.		1	
Degree of vaporisation, q		0.83	

Table 5.16: Stochiomertry and feed mixture data for the reactive MTBE system in compounds and *elements*.

5.22. Phase composition calculations are based on the WILSON equation for the liquid phase and the SRK equation of state for the vapour phase.

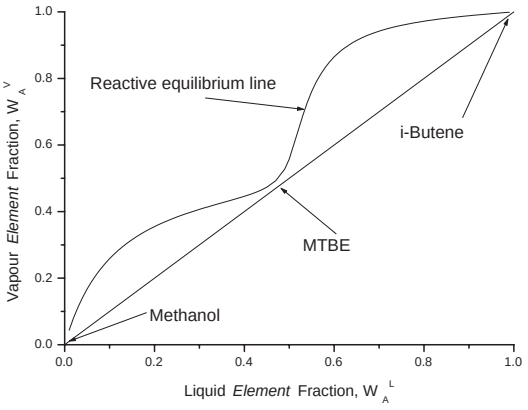

Figure 5.22: Reactive phase diagram for a binary *element* system.

As stated in algorithm D3, the generation of a driving force diagram can be done, when binary vapour liquid composition data are available. The driving force diagram on the basis of the data in figure 5.22 is shown in figure 5.23.

In order to do a design of a reactive distillation column (driving force based, or not), it is necessary at this stage to define the range of the operation desired. For visualisation purposes, this region is re-scaled, to fit the $[0;1]$ composition space, where the points D and D_x are identified. This re-scaled diagram is shown in figure 5.24. It is here emphasized, as also stated in algorithm D3, that the re-scaled diagram is not suitable for mass balance related calculations, like the determination of operating lines and reflux ratio.

Algorithm D3 now dictates to identify point D and D_x. In this case, the determination of D_x must take the vapourisation into account, and it is here

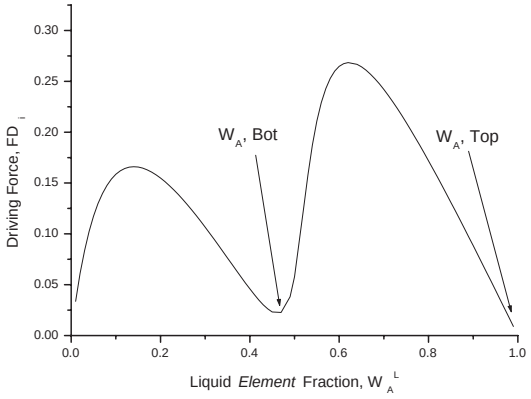

Figure 5.23: Reactive driving force diagram for a binary *element* system with an indication of the desired products.

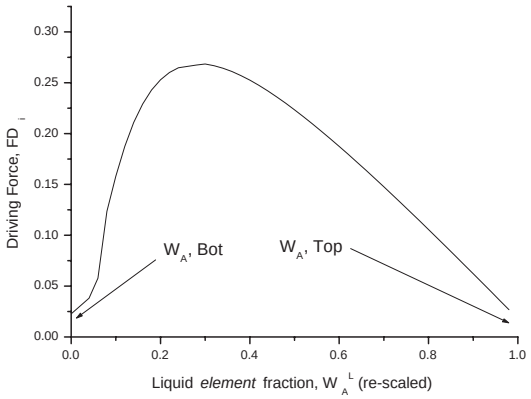

Figure 5.24: Reactive driving force diagram for the operation range of a binary *element* system with an indication of some design parameters.

estimated to be $D_x = 0.38$. The equivalent minimum reflux ratio is found to be $RR_{min} = 0.5$ (*elements* based). Pérez-Cisneros *et al.* (1997) applies this example with the use of 5 equilibrium stages in the distillation. Applying this number for this example, algorithm D3 predicts that the feed stage should be stage 3 in this column. The specifications for the design are high recovery of the MTBE product (and the little content of unreacted methanol) at the bottom (= 0.997), and excess i-butene goes in the distillate, achieved by fixing

the molar reflux ratio at $RR = 2.5$. Rigourous simulations, based on chemical equilibrium in the CPE program and in ASPEN[1] confirm that feed stage, $N_F = 3$ is the optimum with respect to energy.

The objective of the design method is to generate a design that consumes the least energy, and at the same time leads to the desired separation. It is here verified that, from an energy point of view, with consistent design specifications, the actual optimum feed stage matches the prediction.

5.3.4.2 Benzene production

The disproportionation of toluene to produce benzene and *o*-xylene, is an equilibrium limited reaction which could be synthesised by use of reactive distillation. Although benzene is now mostly produced through catalytic reforming (*i.e.*, toluene hydrodealkylation, pyrolysis of gasoline), the complexity of this process is rather high, as illustrated in *e.g.* Petrochemical processes '97 (1997).

The *element* stochiometry for this system is given below in table 5.17.

Compound / *Element*	*Benzene*	*Toluene*	$o-Xylene$
A	1	1	1
B	0	1	2
Feed composition		1	
Pressure, atm.		1	
Degree of vaporisation, q		0	

Table 5.17: Stochiometry and feed mixture data for the reactive Benzene system in compounds and *elements*.

The reaction taking place in terms of compounds and *elements* is the following.

$$\begin{array}{c} 2Toluene \rightleftarrows Benzene + o-Xylene \\ 2AB \rightleftarrows A + AB_2 \end{array} \tag{5.1}$$

It follows clearly from equation 5.1 that the reactive system can be described by a binary set of *elements*. The phase composition data for this reactive system are calculated, using thermochemical and vapour pressure data obtained from the DIPPR data bank. The vapour phase is considered as ideal gas and the NRTL model was used to calculate the activity coefficients of the liquid phase.

The vapour liquid phase composition diagram is given in figure 5.25.

As can be seen in figure 5.25, the diagram only spans over the $[0.33; 1]$ composition range. This is because *element* B cannot be obtained in pure form, as the closest the reaction comes towards pure B is AB_2. The objective in the design of this reactive distillation column is, however, to obtain high purity

[1] All ASPEN results are obtained at UAM, Mexico

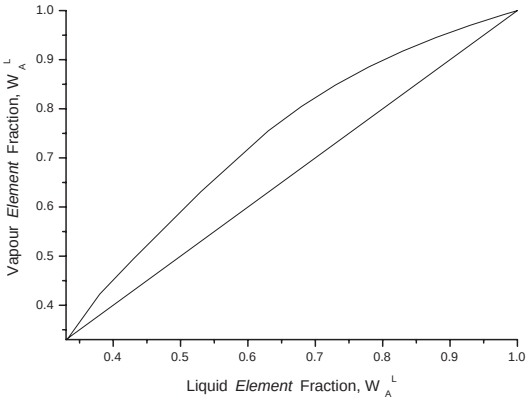

Figure 5.25: Reactive vapour liquid diagram for the binary benzene *element* system.

benzene at the top of the column and a mixture of toluene and *o*-xylene at the bottom.

The driving force diagram can be generated on the basis of the vapour liquid phase composition data, and it is shown in re-scaled format in figure 5.26

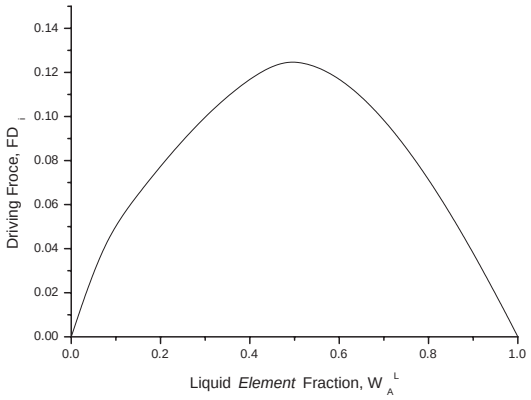

Figure 5.26: Reactive driving force diagram for the binary benzene *element* system.

On this basis, the design can be obtained by following algorithm D3. It is proposed here to employ 13 reactive stages, and D_x is identified as 0.5. Now, it

can be observed from rigourous simulations with ASPEN[2] that moving the feed location and maintaining the heat duty for the reboiler constant, the benzene purity passes through a maximum value, indicating clearly the optimum stage location of the feed at stage 6, thereby exactly matching the prediction. In this case, it was decided to keep the heat duty constant because the reactive system behaves as an isenthalpic system, as pointed out by Stitt (2002) and the heats of vapourisation for the different compounds are closely similar.

5.3.5 Light ends fractionation plant

This example deals with the separation of a feed mixture to a "lights ends fractionating plant". A flowsheet is proposed in the ProVision User's Guide (1994) that separates a given feed mixture into four fractions of alkanes. The separations are all performed by the use of conventional distillation columns. The flowsheet contains a deethanizer column, a depropanizer column and a debutanizer column, as it is shown in figure 5.27.

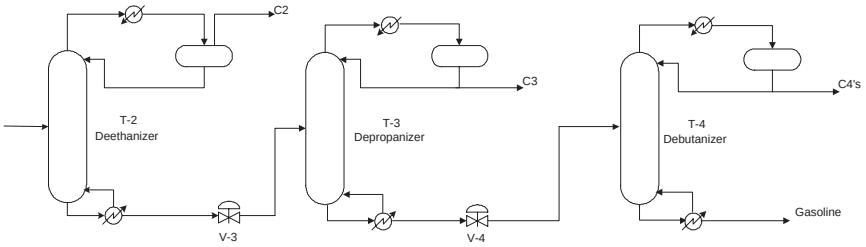

Figure 5.27: Flowsheet for the separation of ethane, propane, butanes and gasoline.

Detailed design specifications for the flowsheet are given in the ProVision User's Guide (1994). Based on the same design criteria, driving force based algorithms have been applied to this feed mixture. For comparison, the flowsheet is simulated with the design parameters in the ProVision User's Guide (1994), and the results of the simulation based on the driving force methods are compared with those reported in the ProVision User's Guide (1994). The thermodynamics used for this process is the Peng-Robinson equation of state for both phases.

5.3.5.1 Description of the fractionation plant

The feed stream consist of two sources, as given in table 5.18. The desired product streams of the separation sequence are ethane, propane, butanes and gasoline, where gasoline, refers to C_5+ compounds.

[2]All ASPEN results are obtained at UAM, Mexico

Component	Feed 1 (kg-mole/hr)	Feed 2 (kg-mole/hr)
Nitrogen	0.0040	0.05
Carbon dioxide	0.0789	0.82
Methane	0.9060	1.82
Ethane	59.1403	56.75
Propane	87.0559	99.88
i-Butane	20.6348	35.41
n-Butane	52.5224	68.10
i-Pentane	10.3454	4.54
n-Pentane	20.9053	21.79
Hexane and heavier	14.1632	13.62
	Physical Condition	
Temperature (^oC)	38.88	38
Pressure (kPa)	3896	4240

Table 5.18: Feed stock compositions for the light ends fractionating plant [ProVision User's Guide (1994)].

The sequence of distillation columns proposed in the ProVision User's Guide (1994) is a direct sequence of conventional distillation columns. The first column is the dethanizer, followed by the depropanizer and the debutanizer, as shown in figure 5.27.

The relevant details of the design for the proposed sequence of distillation columns are given in the ProVision User's Guide (1994), and these data are given in table 5.19, together with the results obtained for the distillation sequence in the ProVision User's Guide (1994).

Condenser Data	T-2	T-3	T-4
Type	Partial	Subcooled	Subcooled
Pressure (kPa)	2930	1758	792
Temperature (C)	–	43.5	43.5
Pressure Data			
Top Tray Pressure (kPa)	2964.5	1792.5	826.5
Column ΔP (kPa)	34.5	34.5	34.5
Results			
Theoretical Stages	25	23	30
Feed stage location	13	11	16
Reflux Ratio	2.738	2.950	1.836
Overhead Product Rate (kmole/hr)	117.30	187.69	177.52
Condenser Duty (GJ/hr)	-2.683	-9.392	-9.066
Reboiler Duty (GJ/hr)	9.124	7.755	7.452

Table 5.19: Column data and results from the ProVision User's Guide (1994).

5.3.5.2 Application of the driving force approach

This example has been subject to the application of three driving force based methods. At first, the sequencing is performed by algorithm S1, then the pressures in the columns within the sequence are allocated by algorithm D4, and finally, the individual columns are designed by algorithm D1.

In order to apply algorithm S1, the driving force diagrams for the binary sets of key compounds must be generated at a uniform pressure. In this case, the three separation tasks are ethane/propane, propane/i-butane and n-butane/i-pentane. The driving force diagrams for the three binary sets of key compounds are shown in figure 5.28.

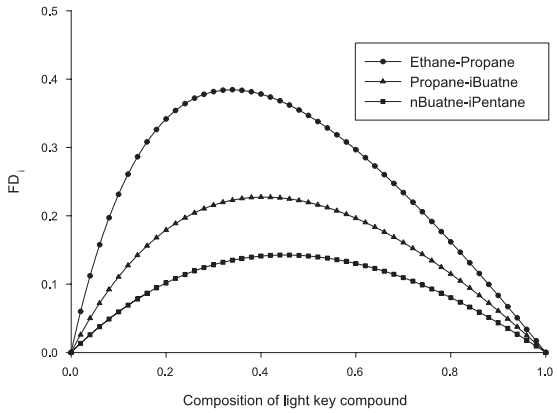

Figure 5.28: Driving force diagrams for the adjacent key components at P = 1000 kPa.

The different sizes of maximum driving force gives a clear picture what the order of the splits should be when algorithm S1 is applied. The first split is ethane/propane (the split with the largest driving force), then followed by propane/i-butane and finally n-butane/i-pentane.

The next step in the design is to determine the operating pressure of the columns in the distillation train by means of algorithm D4. The first step in this algorithm is to calculate the driving force diagram, based on the *pxy* phase diagram for the two key compounds in the deethanizer column, T-2, at the temperature of the feed stream mixture. The temperature is identified to be approximately 38^oC, as given in table 5.18. On the basis of the *pxy* phase diagram, the driving force diagram is calculated. The *pxy* phase diagram together with the bubble point curve is shown in figure 5.29.

Once the driving force diagram for the two key compounds is fixed at the temperature of the feed stream, and the bubble point curve is drawn in the same diagram, the operating pressure can be fixed. The operating pressure

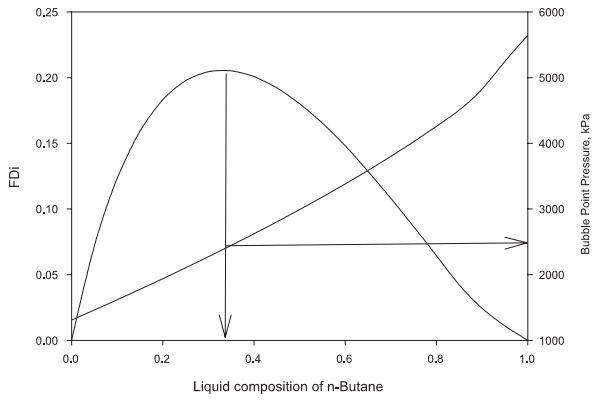

Figure 5.29: Driving force diagram and bubble point pressure for ethane - propane system at T = 38^oC.

is chosen according to algorithm D4, so that it corresponds to the maximum value of the driving force, as indicated in figure 5.29. From here it follows that the condenser pressure of column T-2 should be approximately 2500 kPa.

Now the pressure in the deethanizer column is fixed, the next step is to determine the pressure in the depropanizer column, T-3. This is an iterative process, in which the pxy phase diagram for the two key compounds is computed at varying temperatures. The pxy phase diagram is searched for, which has a bubble point pressure that does not exceed the bottom pressure of the previous column (T-2). The temperature with the bubble point pressure no higher than 2500 kPa is found at 67^oC. For this temperature the driving force diagram from pxy data is calculated, which is shown in figure 5.30.

From the plots in figure 5.30, it is now possible to identify the pressure in the depropanizer, T-3. The pressure is again selected as the point corresponding to the maximum driving force. This leads to a condenser pressure of 1550 kPa in the column.

The procedure is repeated in the last column of the sequence. The temperature corresponding to the maximum bubble point pressure of 1550 kPa is identified to be 100 ^oC. The driving force diagram based on the pxy-diagram are given in figure 5.31.

As it follows from figure 5.31, an operating pressure of 1000 kPa in the debutanizer, T-4 should be selected.

Finally the location of the feed stages in the three individual distillation columns will be determined by algorithm D1. The algorithm requires the driving force for the three binary sets of key compounds, at actual operating pressures. The operating pressures in the three columns are assumed to be uniform, although the actual pressure drop is 34.5 kPa in each column (ProVision User's

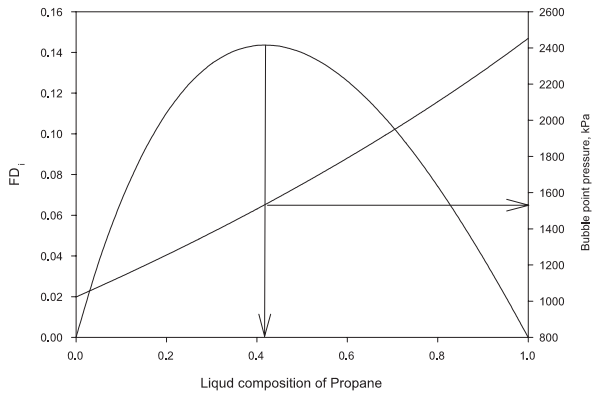

Figure 5.30: Driving force diagram and bubble point pressure for propane - i-butane system at T = 67^oC.

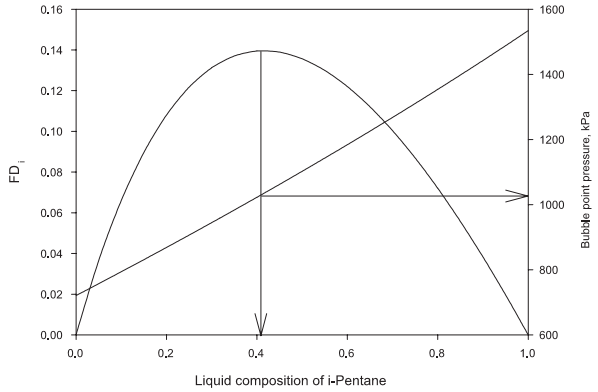

Figure 5.31: Driving force diagram and bubble point pressure for i-propane - i-pentane system at T = 100^oC.

Guide, 1994). The driving force diagrams for the three splits are shown in figure 5.32.

Algorithm D1 is applied to each of the three splits, where the three values of D_x are found in order to determine the feed stages, N_F. The results are shown in table 5.20 together with the corresponding number of stages in each column.

5.3.5.3 Evaluation and discussion of results

The flowsheet for the fractionation plant has been simulated in Pro/II with the design parameters determined by means of driving force based methods. The

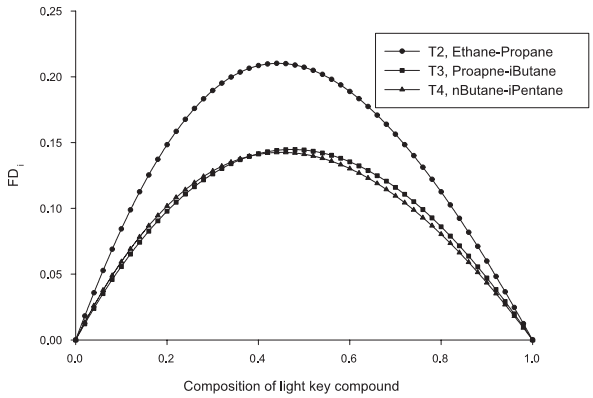

Figure 5.32: Driving force diagrams for adjacent key compounds at operating pressure.

	T-2	T-3	T-4
Pressure, kPa	2500	1550	1000
Number of stages, N	25	23	30
D_x	0.46	0.50	0.46
Feed stage, N_F	13	11	16

Table 5.20: Design data obtained from driving force based methods.

results are compared to the results obtained with the parameters from the ProVision User's Guide (1994). This yields two different but directly comparable simulation results, including the corresponding energy requirements, as shown in table 5.21.

The results confirm that the driving force algorithms achieve the specified separation, as proposed in the ProVision User's Guide (1994). The order, in which the compounds are separated, is validated to be the optimum sequence of the separations by algorithm S1. The feed stage locations throughout the flowsheet are all consistent with the optimum feed locations, according to algorithm D1. With respect to operating pressures, algorithm D4 definitely proposes better column pressures than proposed in the ProVision User's Guide (1994). The two first columns show significant reductions in the energy consumption, thereby reducing the costs of operating the plant. According to the driving force based method, the operating pressure and the operation costs of the third column are higher than in the configuration proposed in the ProVision User's Guide (1994). The reason is that the driving force based method is aiming at a pressure in the last distillation column of the sequence corresponding to atmospheric pressure, due to the costs of operating at vacuum conditions instead of atmospheric pressure.

	Deethanizer, T-2	Depropanizer, T-3	Debutanizer, T-4
Theoretical Stages, N	25	23	30
	Original data from ProVision User's Guide (1994)		
	Condenser pressure		
(kPa)	2930	1758	792
Feed location, N_F	13	11	16
Reboiler Duty (GJ/hr)	10.0159	9.5474	6.5739
	Data obtained from driving force methods		
	Condenser pressure		
(kPa)	2500	1550	1000
Feed location, N_F	13	11	16
Reboiler Duty (GJ/hr)	8.6458	8.8846	7.6059
Difference (Saving, %)	13.68	6.94	-15.70
	Total Saving 3.83 %		

Table 5.21: Comparison of results from the ProVision User's Guide (1994) to driving force based results.

5.4 Analysis of distillation columns

5.4.1 Reverse extractive distillation

Hunek *et al.* (1989) proposed a separation scheme based on reverse extractive distillation, to obtain high purity alcohols from a multicomponent mixture of alcohols and water. Instead of using solvents to break the water-alcohol azeotropes in the mixture, Hunek *et al.* (1989) employed a separation scheme consisting of five distillation columns and one decanter. The feed stream corresponds to the effluent stream from a methanol synthesis plant and is given in table 5.22.

The separation scheme is based on the ability of methanol, which is present in the mixture, to act as an extractive agent separating the azeotropic mixtures of water and light end alcohols. The separation scheme produces high purity methanol, ethanol and i-propanol. Besides, a large quantity of water is produced and a stream containing water from the decanter (liquid-liquid split) is recycled back to the first column (see flowsheet in figure 5.33).

In this case-study the separation scheme proposed by Hunek *et al.* (1989) has been verified by the driving force approach. The thermodynamic model used to describe the phase behaviour is the original UNIFAC (VLE).

5.4.1.1 Problem description

The scope of this process is that the considerable quantity of methanol present in the feed stream is able to take with it the other light alcohols in the top product, thus methanol acts as extractive agent. The bottom product from

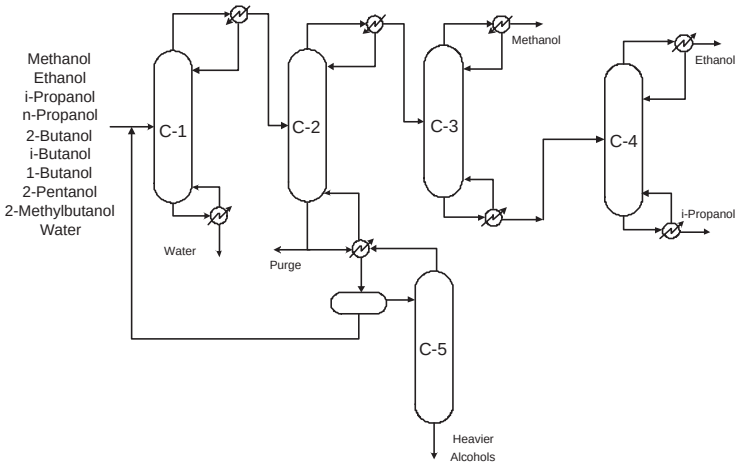

Figure 5.33: Flowsheet for the reverse extractive distillation process proposed by Hunek *et al.* (1989).

Component	Flow in kmole/hr
Water	156824.0
Methanol	1048.8
Ethanol	61.6
i-Propanol	5.9
1-Propanol	12.0
2-Butanol	10.1
1-Butanol	3.3
2-Pentanol	0.5
2-Methylbutanol	1.8
Physical Condition	
T (K)	297.0
P (atm)	1.0

Table 5.22: Feed stream to the reverse extractive separation scheme.

the first column (C1) is mainly water and the large amount of methanol in the top product prevents the formation of azeotropes between water and the light alcohols in the second column (C2), *i.e* methanol modifies the activity coefficients in the liquid phase. In this way, it is possible to get all the alcohols with lower volatility than water to separate from the water and the heavier alcohols. After the reverse extractive distillation process, the separation of methanol, ethanol and i-propanol is done by conventional distillation.

The columns of interest in this flowsheet is especially C1 and C2. These are treated in the following section by using the driving force approach, together

with the conventional simple columns C3 and C4. Column C5 is a special column, introduced only for stripping, and the feed to the column is introduced at the top stage. The description of how to design of this columns is beyond the scope of this thesis.

5.4.1.2 Application of the driving force approach

A driving force analysis is conducted here on the columns C1 and C2. The procedure does not really match any of the algorithmic approaches, presented in the framework in figure 4.26. The objective here is to show the feasiblility of the separation, which is performed in these two columns, and thereby confirm the flowsheet proposed by Hunek *et al.* (1989). Afterwards, the conventional columns C3 and C4 are treated by the driving force methods for the synthesis of distillation trains and the design of distillation columns.

Driving force diagrams for column C1 and column C2 are shown in the figures 5.34 and 5.35. These driving force diagrams are both generated on a methanol free basis, for the compounds relevant. In this case, the scope is the separation of light alcohols from water, and due to the presence of methanol, the azeotropes can be broken. In figure 5.34, the driving force curves have been made for the mixtures of water and ethanol and for water and i-propanol, on a solvent free basis. It is clear from these plots, that methanol can serve as extractive agent in these cases, which breaks the azeotropes.

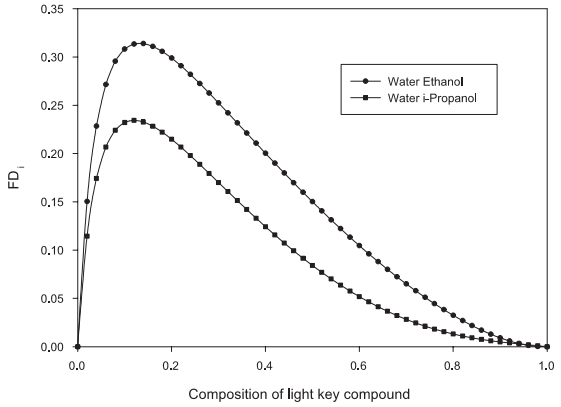

Figure 5.34: Driving force diagram on a solvent (MeOH) free basis for column C1.

In figure 5.35, the same kind of plot is made for column C2. Here, driving force diagrams for all the alcohols present in the column are plotted, on a solvent (methanol) free basis. Here it becomes clear that, in this column, sufficient methanol can completely separate ethanol and i-propanol from water. In this

way, it is easy to purify not only methanol, but also ethanol and i-propanol in a conventional distillation sequence.

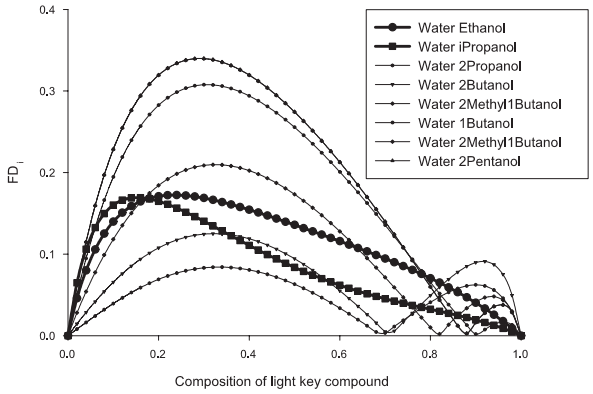

Figure 5.35: Driving force diagram on a solvent (MeOH) free basis for column C2.

Now follows the sequencing and design of columns C3 and C4. Regarding the order of the separations, it can be noticed that the splits are ranked in accordance with algorithm S1. The split in column C3 exhibits a significantly greater maximum driving force than the split in C4. The values of D_y are listed in table 5.23.

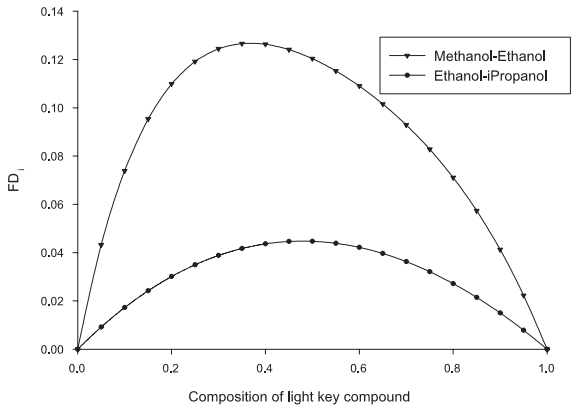

Figure 5.36: Driving force diagram for separations in columns C3 and C4.

Next, the design parameters of the columns C3 and C4 are obtained from the diagrams in figure 5.36. The two values of D_x are listed in table 5.23, together

with the number of stages, as proposed by Hunek *et al.* (1989), and applying algorithm D1, the corresponding feed stages, N_F are found.

Column	Number of stages, N	D_x	D_y	Feed stage location, N_F
C1	23	0.22[1]	0.37[1]	17
C2	40	0.22[1]	0.37[1]	31
C3	30	0.38	0.125	18
C4	60	0.50	0.05	30

Table 5.23: Design parameters for the distillation columns in the separation.

[1] Based on methanol water, see figure 5.38

5.4.1.3 Evaluation and discussion of results

In order to compare the flowsheet with the predictions made by the driving force approach, rigorous simulation of the flowsheet has been performed in Pro/II. The first column, C1 is used for the removal of most of the water, and can as such not be subject to a driving force design with the purpose of applying a driving force based design method, since the definition of the other key compound is difficult. If, however an attempt is made, and methanol is employed as a second key compound, all the scaling possible would be required, since the water content is over 99 % of the total feed mixture. The actual optimum (feasible) feed stage is $N_F = 7$. In column C2, simulations show that the feed consists of about 70 % water. However, if methanol and water are considered to be key compounds, the driving force diagram for methanol water, on an ethanol and i-propanol free basis should form the basis for the design, rather than just methanol and water. The optimum feed stage is $N_F = 20$.

The situation is different in the simple distillation columns, C3 and C4. The clearly obey the driving force procedures for synthesis and design. At first, the order of the splits in the flowsheet by Hunek *et al.* (1989) is confirmed to be identical with the one predicted by algorithm S1, then the individual columns confirm the solutions found by algorithm D1, since optimisation shows that the best feed stage in C3 is 15 and in C4, it is 30.

5.4.2 Separation of effluents from methyl acetate production

Methyl acetate is a commonly used compound in the chemical industry, especially as a solvent. It is produced by esterification of methanol and acetic acid, producing water as side product. The reaction is the following:

$$\text{Methanol} + \text{AceticAcid} \rightleftarrows \text{MethylAcetate} + \text{Water} \tag{5.2}$$
$$CH_3OH + CH_3COOH \rightleftarrows CH_3COOCH_3 + H_2O$$

The mixture to be separated here is the reactor effluent. The desired product specification is 99.9 % pure methyl acetate. It is the objective here to treat the separation sector of the methyl acetate, as proposed by Jaksland (1996). The flowsheet proposed by Jaksland (1996) is given in figure 5.37.

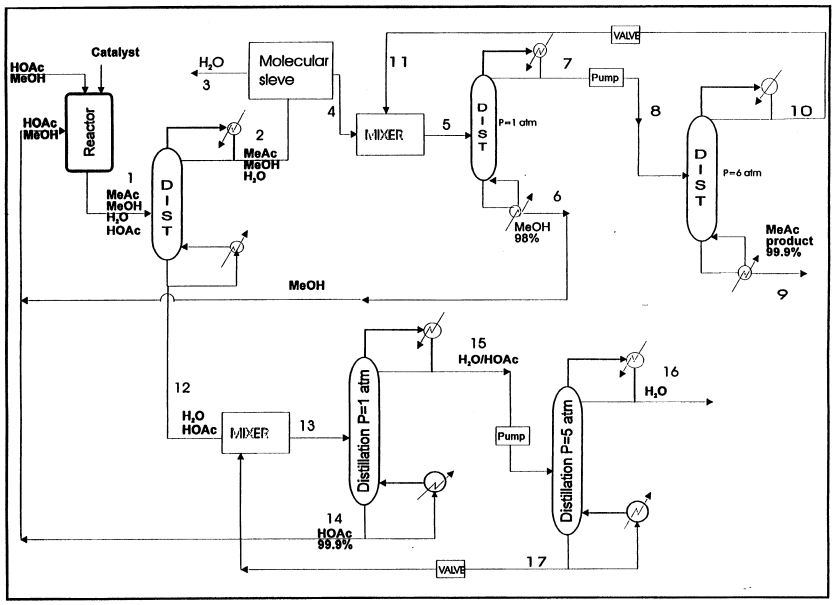

Figure 5.37: Flowsheet for separation of methyl acetate reactor effluent [Jaksland (1996)].

Jaksland (1996) identified a physically feasible flowsheet for the production of methyl acetate and separation of the outlet stream from the reactor into pure products. This flowsheet deviates significantly from conventional flowsheets for the production of methyl acetate (*e.g.* Siirola (1995) proposes to use of a process which involves addition of solvents to break the azeotropes). A short description of the process given in figure 5.37 follows here. Methanol and acetic acid is fed to the reactor together with recycle streams. The effluent stream from the reactor is sent to the first distillation column, where methyl acetate and methanol are separated from water and acetic acid. The mixture of water and acetic acid is sent to a distillation column where water is taken out and acetic acid is recycled. The other mixture of methyl acetate and methanol is sent through a molecular sieve, where the remaining water is removed. Then

the methanol and methyl acetate is separated by pressure-swing distillation. Methyl acetate is the product, and methanol is recycled. The steady-state composition of the reactor effluent for separation is given in table 5.24.

Compound	Flow rate (kg-mole/hr)
Methyl acetate	12.7075
Methanol	70.5672
Water	11.8364
Acetic Acid	37.3263

Table 5.24: Steady-state composition of the reactor effluent of the flowsheet in figure 5.37.

In this example, the separation sequence proposed by Jaksland (1996) will be treated by the driving force approach.

5.4.2.1 Problem description

The separations of the reactor effluent in this case involves six binary pairs, of which two form azeotropes (see table 5.25). The mixtures in the separation tasks are all polar mixtures, deviating strongly from ideal behavior. In this case, NRTL parameters have been applied for the calculation of the liquid phase behaviour. The vapour phase is rather critical, as acetic acid is strongly dimerizing, and is therefore described by the Hayden-O'Connell model for the 2^{nd} virial coefficients, based on chemical theory.

According to Knapp and Doherty (1992), the binary low-boiling azeotrope between methyl acetate and methanol is pressure sensitive, and the application of pressure-swing distillation in this case can save a lot of energy compared to the conventional azeotropic distillation, employing an extractive agent. Knapp and Doherty (1992) also report the other binary azeotrope between methyl acetate and methanol as being pressure sensitive. But Jaksland (1996) chose to use a solvent for this separation, and identified CO_2 as a supercritical solvent, to break the methyl acetate water azeotrope. Since there are no interaction parameters between the $COOH$ and CO_2 groups available, no calculations of this separation can be performed. The separation is therefore performed with a molecular sieve assuming an ideal separation. Since there is no azeotrope between water and acetic acid, pressure-swing distillation has not been applied for this separation, as it has been proposed by Jaksland (1996).

Binary pair	Azeotropic composition , x_i
Methyl acetate / Water	93
Methyl acetate / Methanol	67

Table 5.25: Compositions of azeotropes in the reactor effluent mixture of the methyl acetate production.

To summarize, the separations in the flowsheet given by Jaksland (1996) are listed in table 5.26.

Separation task	Reactor effluent into two streams	Water from methyl-acetate and methanol	Methyl-acetate from methanol	Acetic-acid and water
Applied separation	Distillation	Molecular sieve	Pressure-swing distillation	Distillation

Table 5.26: Applied techniques of separation throughout the flowsheet.

A driving force analysis is performed on the sequence of the three relevant separations. Two of the three separations are treated by the driving force approach, and the results are discussed later in the evaluation in section 5.4.2.3.

5.4.2.2 Application of the driving force approach

Since, in this case, it was not possible to find any data for membrane separation for the mixtures to be separated here, only distillation, extractive distillation and pressure-swing distillation will be considered as separation methods here.

The separation sequence is briefly considered and the designs of different distillation columns are treated by the driving force approach.

On the basis of an appropriate thermodynamic model to describe the vapour liquid phase behaviour, the driving force diagrams can be generated, as shown in the figures 5.38, 5.39 and 5.40. The two diagrams for the pressure swing distillation sequence in figure 5.39 are given at the two pressures considered. Values of relevant design parameters obtained from the driving force diagrams are listed in table 5.27, together with the number of stages in each column employed by Jaksland (1996).

Column	Number of stages, N	D_x	D_y	Feed stage location N_F
Dist 1	22	0.22	0.38	17
Dist 2	20	0.33	0.175	13
Dist 3	20	0.36	0.095	12
Dist 4	40	0.35	0.175	26

Table 5.27: Design parameters for the distillation columns in the separation.

At first, the sequence is considering, according to which the splits are performed in the flowsheet proposed by Jaksland (1996) (see figure 5.37). It is clear when following algorithm S1 that the order of the separations is in accordance with the sequence proposed by the driving force approach, where the split of key compounds in Dist 1 exhibits the greatest maximum driving force. This split leads to two binary pairs, which are then split individually into their constituent compounds. Note here, also the order of the splits in the pressure-swing distillation sequence, where the split with the greatest maximum driving

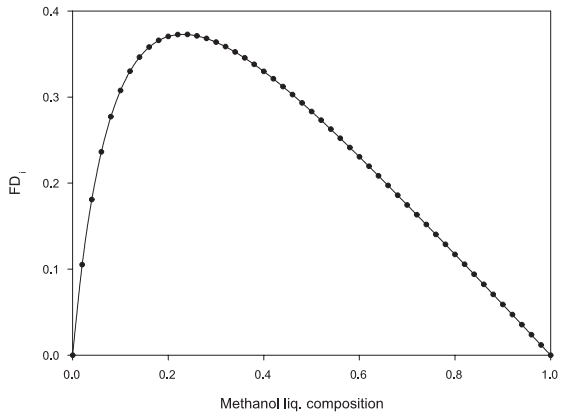

Figure 5.38: Driving force diagram for methanol - water system, at 1 atm.

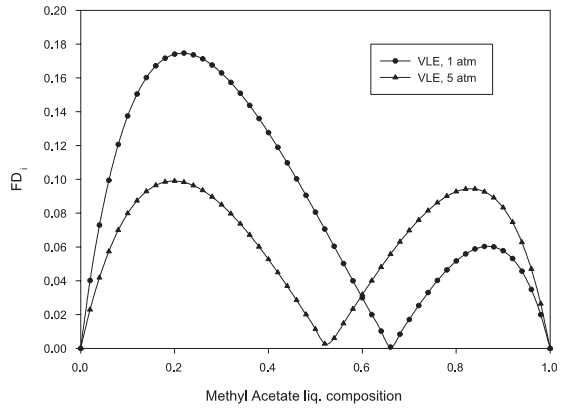

Figure 5.39: Driving force diagram for methyle acetate - methanol system, at 1 and 5 atm.

force is performed first. The relative feed stage locations are predicted by algorihm D1, based on values of D_x and corresponding N_F obtained form figures 5.38, 5.39 and 5.40 and listed in table 5.27. In the following section, the results of the predicted values are dicussed for each column, based on rigorous simulations in Pro/II.

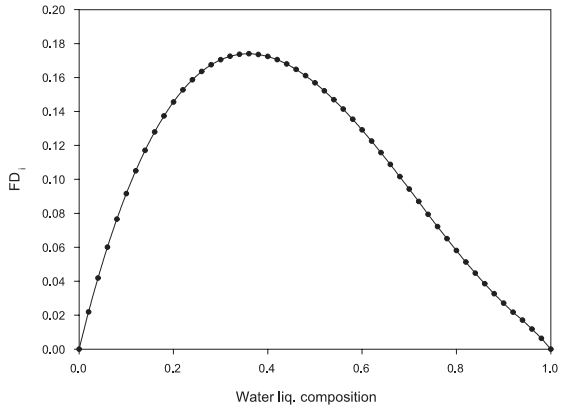

Figure 5.40: Driving force diagram for acetic acid - water system, at 1 atm.

5.4.2.3 Evaluation and discussion of results

In order to compare the results predicted by the driving force based methods, the flowsheet proposed in figure 5.37 has been simulated and the distillation columns have been optimised with respect to feed stage locations. The performance specifications for the four distillation columns in the proposed flowsheet are listed in table 5.28.

	Dist 1	Dist 2	Dist 3	Dist 4
Performance Specification I	$x_{MeAc+MeOH}$ = 0.996	x_{MeOH} = 0.981	x_{MeAc} = 0.999	x_{H_2O} = 0.999
Performance Specification II	$x_{H_2O+AceticAcid}$ = 0.99999	RR = 3.0	RR = 3.0	$x_{AceticAcid}$ = 0.999

Table 5.28: Performance specifications of the converged flowsheet in figure 5.37.

The sequence of the distillation columns will not be discussed in detail. It shall be mentioned that the order of the separations fit the prediction by the driving force method. However, the importance of performing the split in Dist 1, followed by the removal of water from the mixture of methanol and methyl acetate also makes the two next separations much easier. In the following paragraphs, the individual columns are discussed.

Dist 1 This column is the one where the most critical split is performed. The feed to the column is the mixture given in table 5.24, which is a highly complex mixture with multiple azeotropes. Due to the azeotropic behaviour, water goes into the distillate. Apart from this water content in the distillate, the separation into two mixtures for further separation is performed successfully.

The performance specifications between the top and the bottom of the column deviates, due to the water content in the distillate. Algorithm D1 can hardly be expected to predict the feed stage location in this column, as there are multiple azeotropes and distillation boundaries in the mixture. The simulations were unable to converge at the feed stage predicted by algorithm D1 (given in table 5.27), and it was found that simulation was possible when $N_F = 8$ was employed, rather than $N_F = 17$. However, the driving force plot for this column (figure 5.38) is in this case not generated on a solvent free basis, and therefore it does not incorporate the effects of the other compounds in the feed mixture.

Dist 2 and Dist 3 The pressure-swing distillation sequence consists of two columns to break the azeotrope between methanol and methyl acetate. As can be seen in figure 5.39, the location of the azeotropic point moves significantly with changing pressure. In the first column (Dist 2), pure methanol is taken out at the bottom and the azeotropic mixture of methyl acetate and methanol goes in the distillate. In the second column (Dist 3), the azeotropic mixture from the first column enters at 5 atm. By increasing the pressure to 5 atm., the azeotropic point moves and the separation of pure methyl acetate is achievable. As the azeotrope is a low-boiling azeotrope, the methyl acetate goes at the bottom and the mixture with the azeotropic composition goes to the top and is recycled back to the first column (Dist 2). In this way a pure product of methyl acetate is achieved.

Applying algorithm D1 to the data in table 5.27, the near optimum feed stage location in the first distillation column (Dist 2) is predicted to be at stage 13, and by optimisation the optimum stage was found to be number 15. When the method is applied to Dist 3, the near-optimum feed stage was predicted to be stage number 12, which was also found by optimisation to be the optimum. Note that methyl acetate is the heavy key compound in this case.

Dist 4 The last distillation column of the flowsheet is separating water from acetic acid. The separation is approaching pinch condition as the mole fraction of water is approaching unity. Jaksland (1996) proposed the use of pressure swing distillation to produce both pure water and pure acetic acid. With the thermodynamic model applied to this system, it was not possible to detect an azeotrope. It is a fact, however, that acetic acid is strongly dimerizing and the separation can cause difficulties. The application of algorithm D1 predicts the near optimum feed stage location as stage 26, and the optimum feed stage was found to be stage number 26 by optimisation.

5.4.3 Controllability analysis of distillation column

A simple controllability example is given here, to illustrate how a design based on a driving force method is found to be easier to control. The system in this example is distillation of methanol and water, which is separated in a column with 10 stages. Based on a linearised state space model of a dynamic

simulation, values of RGA's are found for different configurations of the column, and different control structures. The system in this example is outlined in table 5.29, together with the specified product purities.

System	
Methanol	50.0 kmole/hr
Water	50.5 kmole/hr
Temperature	300 K
Pressure	1 atm.
Product purities	
Methanol	0.950
Water	0.947

Table 5.29: Dynamic system for RGA analysis.

The first step is to conduct a driving force analysis. A driving force diagram for methanol and water has been generated and D_x has been found (see *e.g.* figure 5.38), where $D_x = 0.22$. Considering the separation to be performed in 10 stages, and applying algorithm D1 to obtain a design, it has been found that the feed should be introduced at feed stage, $N_F = 7$.

The results obtained are outlined in tabular form in the following four tables, together with the specifications that give the required product purities, at the different feed stage locations. In these tables two control configurations are compared, where one is for feed at stage $N_F = 7$, and one is for feed at stage $N_F = 3$. The reason for this, is to compare the design predicted by algorithm D1 to be optimal, to an arbitrarily chosen alternative design.

Feed stage, $N_F = 7$, QB = 3500, L = 37		
RGA	L	QB
$x_{B,Water}$	-0.791242	1.79124
$x_{B,Methanol}$	1.79124	-0.791242

Table 5.30: RGA matrix for $N_F = 7$, QB/L specifications.

Feed stage, $N_F = 3$, QB = 5032, L = 80		
RGA	L	QB
$x_{B,Water}$	-0.919538	1.91954
$x_{B,Methanol}$	1.91954	-0.919538

Table 5.31: RGA matrix for $N_F = 3$, QB/L specifications.

It can be observed from the 4 tables, with RGA matrices that, first of all the energy requirements are much higher for feed introduced at stage $N_F = 3$, than it is for feed stage $N_F = 7$, which is not surprising as this feature has been demonstrated before, and secondly, it can be noticed that the RGA matrix is

Feed stage, $N_F = 7$, QB = 3500, D = 49.7677		
RGA	D	QB
$x_{B,Water}$	0.0409052	0.959095
$x_{B,Methanol}$	0.959095	0.0409052

Table 5.32: RGA matrix for $N_F = 7$, QB/D specifications.

Feed stage, $N_F = 3$, QB = 3500, D = 49.8296		
RGA	D	QB
$x_{B,Water}$	0.0594297	0.94057
$x_{B,Methanol}$	0.94057	0.0594297

Table 5.33: RGA matrix for $N_F = 3$, QB/D specifications.

closer to unity for the feed stage being $N_F = 7$. This indicates for both control configurations that the resiliency (*e.g.* how easy the system is to control) is better for the feed stage predicted by algorithm D1 ($N_F = 3$). Thus, there is a good indication that the design procedure in algorithm D1 also leads to easier controllable systems.

5.5 Retrofit of distillation columns

In this section, an example is given, in which the principles of the retrofit method proposed in algorithm R1 are highlighted. Consider for example a distillation column with 60 equilibrium stages, and assume initially that product purities are desired within a range near 0.995 for both distillate and bottom products. Following algorithm R1, table 4.5 is consulted, and the driving force and minimum reflux matching these criteria are found. For this column, with these purity specifications, the maximum driving force is $FD_{i|max} \simeq 0.07$, and the minimum reflux ratio is $RR_{min} \simeq 6.4$. Now, the corresponding values of α_{ij} can be found in figure 4.24, assuming that α_{ij} is approximately constant. In this case, compound mixtures with values of α_{ij} in the range $\alpha_{ij} \simeq 1.3$-1.4.

Mixture	Pressure [atm.]	$FD_{i\|max}$	α_{ij}
Butane-iButane	5	$\simeq 0.074$	1.33-1.34
Cycloheptanol-Cycleoctanol	5	$\simeq 0.080$	1.33-1.38
1,4Butanediol-1,3Butanediol	15	$\simeq 0.065$	1.24-1.85
Diethyleneglycol-1,6Hexanediol	3	$\simeq 0.07$	1.22-1.34

Table 5.34: Candidate retrofit mixtures.

These criteria cover an extensive number of binary mixtures, and a list with just a few of them is given here, for which the proposed separation is feasible.

In all cases, the feed is introduced in the range of N_F = [33;38], approximately corresponding to a normal design, as carried out by means of algorithm D1. It shall be emphasized that the stages are equilibrium stages, and this must be taken into account when giving the number of stages and/or purity requirements.

6

CONCLUSIONS

6.1 Achievements

In this thesis, the main achievement is the new definition of the driving force and the synthesis/design algorithms that are based on maximizing this driving force. Especially the realisation of how this driving force can be utilized in separation processes introduces a new class of algorithms for separation synthesis and design. This driving force approach to synthesis and design employs thermodynamic insights and fundamentals of separation theory (in terms of the causes of separation). The concept of operating a separation process/scheme at the maximum driving force leads to near optimum solutions, without requirering any rigorous mass and/or energy balance calculations. In the methods developed in this thesis, the size and relative location of the maximum driving force are utilized as design parameters for each separation task. In this way, as it has been shown in this thesis, near optimum separation schemes can be generated, based on phase composition data, thereby enabling important decisions to be made with high reliability at an early stage of the process design.

The driving force approach has been applied to develop methods for synthesis and design, as well as related topics like analysis, retrofit and controllability/operability. The advantages of the methods developed lie in the simplicity of application and implementation, which is visual/graphical (or simple numeric), combined with the accuracy of the results they provide (and the insights gained from the driving force approach). The methods for the design of simple and complex distillation columns are very good examples of this, where it is shown by the algorithms developed, how problems, usually considered as large and complex, through the driving force methods become simple and the visual solution is intuitive. It is very advantageous to be able to predict near optimum solutions to this type of problems on a simple basis, since usually it requires mathematical optimisation based on detailed knowledge to achieve this aim, and the combinatorial aspects, especially of the complex column design problems are rather immense. Highlights of the methods developed are outlined below:

- Synthesis: The driving force methods developed for the synthesis of separation schemes comprise methods for sequencing of distillation columns

and the generation of hybrid separation schemes. As to both methods, it has been shown in this thesis that they lead to optimum or near optimum solutions in terms of energy consumption through the visualisation and comparison of different separation tasks/techniques in driving force diagrams. A number of case-studies have been worked out to illustrate the application of the methods.

- Design: The driving force approach is indeed useful when applied to design of unit operations for separation tasks, and especially when applied to distillation. The method for the design of distillation columns is a very powerful method, that works for virtually all types of distillation, when applied properly. In a simple way, independent of feed composition, this approach makes it possible to predict near-optimum design variables, like feed stage location and reflux ratio that strongly affect the energy consumption in the distillation column, thus making the developed methods highly valuable. The application of the same approach to the design of more complex distillation columns as well as the indication of operating pressures are also very useful. A number of case studies illustrate the high accuracy of the methods proposed.

- Analysis: The concept of driving forces has been found to be a powerful tool also for the analysis of distillation operations. The idea of using driving force diagrams for analysis to predict feasible separations is highly promising, not only for conventional columns, but also for extractive/azeotropic distillation columns, where plots are made on a solvent free basis. This feature is different from existing methods. There also seems to be a clear indication that distillation columns designed to operate at the maximum driving force, are easier to control.

- Retrofit: Retrofit design/analysis through the driving force approach provides a tool that in a simple way predicts feasible separations in given distillation columns. The principle of this method is to solve a 'reverse' design problem, where the number of stages and largest driving force are the known input variables, and feasible mixtures for this column are obtained on this basis.

The methods developed in this thesis have been combined in a framework for the synthesis, design and retrofit of separation synthesis, primarily based on distillation. This framework incorporates individual algorithms to handle subproblems in an integrated manner, whereby it is possible to solve interactively, separation synthesis, design and retrofit problems. The methods are based on driving force curves that have been calculated in accordance with the definition of driving force, as given in this thesis, and they provide useful tools for the generation of feasible process flowsheets and the determination of design and operating conditions. Emphasis has been given in this thesis to separation techniques involving differences in vapour and liquid properties, in particular

distillation. The driving force methods have been applied to a number of case studies, where the usefulness of the approach and the methods derived from it, are highlighted.

6.2 Remaining challenges and future work

The principle of designing separation schemes to operate at the largest driving force leads to feasible and near optimum solutions for separation problems, based on visual intuition and very few calculations, as has been shown in this thesis. The driving force approach, however, can be extended and developed further. The approach is obviously capable of handling many more problems of different kind, since almost all separation techniques rely on differences in composition. The framework can fairly simply be extended to handle more different and more complex configurations of distillation columns (like, for example, columns with side-rectifiers and/or side-strippers, or multiple feed columns), so that the design of these distillation columns can be obtained as easily as the ones presented in this thesis. But the design of unit operations performing other tasks than separation can also be considered.

Another topic that could be addressed is heat-integrated distillation sequences (and columns), where the driving force diagram can be linked to temperature/pressure profiles of the columns, and combinations with heating/cooling duties can also be incorporated in the approach, thereby enabling prediction of heat-integrated column sequences. It can be deducted from literature studies that the sequence found by algorithm S1 is a very good candidate sequence as a basis for heat integration. Several examples of heat-integrated distillation trains, where the sequence (order) of distillation columns has been subject to a structural optimisation problem for the generation of both the sequence, and a corresponding heat integrated network, confirm that the sequence proposed by algorithm S1, is the optimal sequence for the heat integrated network. An example is given in the paper by Yeomans and Grossmann (1999), where two different structural optimisation techniques come up with the same sequence as the driving force approach, for two different feed compositions with the same four compounds in the feed.

An issue that has not been dealt with in this thesis which is highly relevant, is batch processes. It would be obvious to extend the driving force based methodology to also incorporate batch distillation, and develop a procedure for the energy efficient design and/or operation of batch distillation columns.

The issue of scaling factors can also be extended. In this thesis, simple scaling factors have been presented as an improvement in the accuracy of prediction with respect to energy optimality for conventional distillation columns. Development of scaling factors for other types of separation synthesis and design problems can help to provide solutions that are even closer to optimality than the ones presented in this thesis. In this way, it will eventually be possible to predict any separation (distillation) sequence, performance, and design ac-

curately by using a driving force based framework, without even considering rigorous models and mass and energy balance equations. A complete overview of distillation processes can be fitted into such a framework.

In a driving force based separation framework where hybrid separations are dealt with, cost factors could be linked to each type of unit operation, or taken even further, the types of compounds to be separated could be incorporated. In this way, things like the steel type used for manufacture of distillation columns, the cost of specific membranes, etc. could be incorporated in the database and linked to the individual compounds, thereby enabling the user to also get an accurate cost estimate at a very early stage of the design of a process.

Finally, the issue of controllability analysis has only been treated briefly in this thesis. However, the results show a clear tendency that the operation and control of a distillation column is the easiest when operated at maximum driving force. The concept can be extended, to lead to determination of the control structure and perhaps even design of the controllers, based on analysis of the derivatives of driving forces with respect to the candidate control variables.

Appendices

A

Application Examples of Algorithms S1, S2, D1-D5 and R1

This appendix highlights the application of the driving force based methods through a number of illustrative examples. The application of the algorithms to the respective examples are presented in tabular form, and the validation through simulation of each example is also presented. In the heading, the system being separated is given, and in the captions, reference is given to the example sources, which are listed in table A.1. In binary splits of multicomponent mixtures, the key compounds are indicated by bold fonts.

Example number	Description	Source of example
Example 1	Separation of reactor effluent from ethylene plant	Hoch and Eliceche (1999), treated in section 5.2.1
Example 2	Separation of hydrocarbon mixture	Shah and Kokossis (1997), treated in section 5.2.2
Example 3	Separation of Methanol and MTBE	Partly based on Sano *et al.* (1995), treated in section 5.2.3
Example 4	Separation of Methanol and Water	Treated in section 5.3.1.1
Example 5	Separation of Ethanol and Toluene	Treated in section 5.3.1.2
Example 6	Separation by a deethanizer	Seader and Henley (1998), treated in section 5.3.1.3
Example 7	Separation of BTX mixture	Treated in section 5.3.2.1
Example 8	Separation of hydrocarbon mixture	Treated in section 5.3.2.2
Example 9	Reactive distillation of MTBE	Pérez-Cisneros *et al.* (1997), treated in section 5.3.4.1
Example 10	Reactive distillation of benzene	Treated in section 5.3.4.2
Example 11	Light ends fractionation plant	ProVision User's Guide (1994), treated in section 5.3.5
Example 12	Reverse extractive distillation	Hunek *et al.* (1989), treated in section 5.4.1
Example 13	Methylacetate production	Jaksland (1996), treated in section 5.4.2
Example 14	Controllability analysis	Treated in section 5.4.3
Example 15	Retrofit example	Treated in section 5.5
Example 16	Separation of hydrocarbon mixture	
Example 17	Separation of hydrocarbon mixture	Smith (1995)

Example 18	Separation of BTX mixture	Smith (1995) and BELSIM
Example 19	Separation of Ethanol and Water	
Example 20	Separation of Acetic acid and water	sub-part of example 13
Example 21	Separation of hydrocarbon mixture	
Example 22	Separation of hydrocarbon mixture	
Example 23	Separation of alcohol mixture	
Example 24	Reactive distillation of ethylene	
Example 25	Separation of BTX mixture	Seader and Henley (1998) (modified)
Example 26	Separation of Butanoles mixture	Kim (2001)

Table A.1: Overview of examples treated in appendix A.

A.1 Synthesis examples

System: Propane, iButane, nButane, iPentane, nPentane		
Pressure, $P = 1$ atm.		
Algorithm	**Action**	
Step 1,2,3	Retrieve data and calculate driving force curves	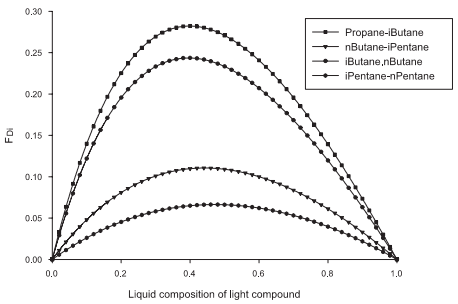
Step 4,5	Rank the splits by size of maximum driving force	$D_{y,Propane-iButane} = 0.28$, $D_{y,nButane-iPentane} = 0.24$, $D_{y,iButane-nButane} = 0.11$, $D_{y,iPentane-nPentane} = 0.07$
Step 6	Draw the flowsheet	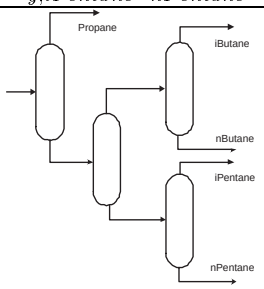
Validation		
Step 1	Originally proposed flowsheet by Smith (1995)	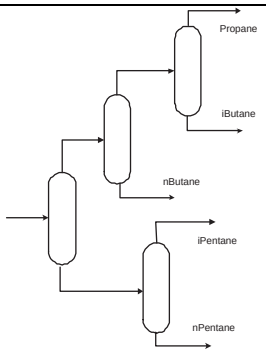
Rigorous simualtion of the alternative flowsheets give:	Original flowsheet: Energy consumption = 243 GJ/hr	Driving force based flowsheet: Energy consumption = 208 GJ/hr

Table A.2: Application of algorithm S1 to example 17.

System: Benzene, Toluenen, EthylBenzene, Xylenes, $C_9's$		
Pressure, $P = 1$ atm.		
Algorithm	**Action**	
Step 1,2,3	Retrieve data and calculate driving force curves	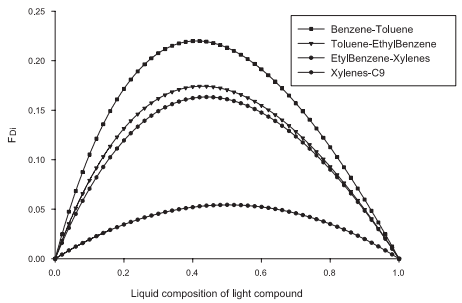
Step 4,5	Rank the splits by size of maximum driving force	$D_{y,Benzene-Toluene} = 0.22,$ $D_{y,Toluene-EthylBenzene} = 0.175,$ $D_{y,EthylBenzene-Xylenes} = 0.16,$ $D_{y,Xylenes-C9's} = 0.055$
Step 6	Draw the flowsheet	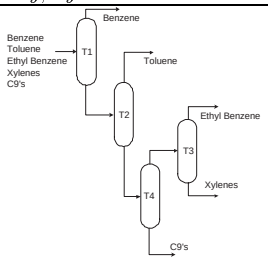
Validation		
Step 1	Smith (1995) and BELSIM found independently of each other, this proposed sequence to be the optimum. This is taken as proof here.	

Table A.3: Application of algorithm S1 to example 18.

System: Ethylene, Ethane, Propene, Propane, Butane, Pentane		
Pressure, $P = 1$ atm.		
Algorithm	**Action**	
Step 1,2,3	Retrieve data and calculate driving force curves	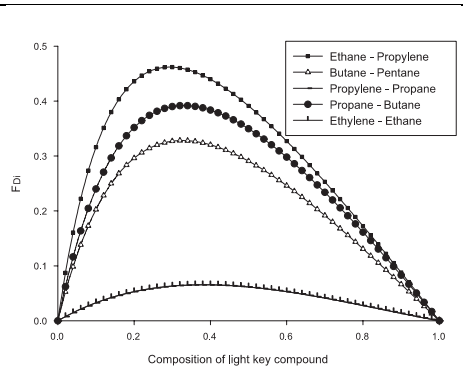
Step 4,5	Rank the splits by size of maximum driving force	$D_{y,Ethane-Propylene} = 0.46,$ $D_{y,Propane-Butane} = 0.39,$ $D_{y,Butane-Pentane} = 0.33,$ $D_{y,Propylene-Propane} = 0.07,$ $D_{y,Ethylene-Ethane} = 0.07$
Step 6	Draw the flowsheet	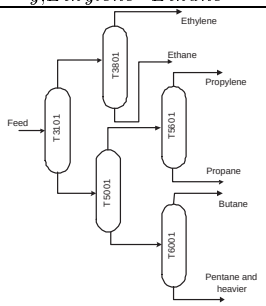
Validation		
Step 1	Hoch and Eliceche (1999) reporeted this proposed sequence to be on an actual industrial size plant. This is taken as proof here.	

Table A.4: Application of algorithm S1 to example 1.

System: Neopentane, iPentane, nPentane, 2,2-MethylButane, 2,3-MethylButane		
2-MethylPentane, Hexane, Benzene		
Pressure, $P = 1$ atm.		
Algorithm	**Action**	
Step 1,2,3	Retrieve data and calculate driving force curves	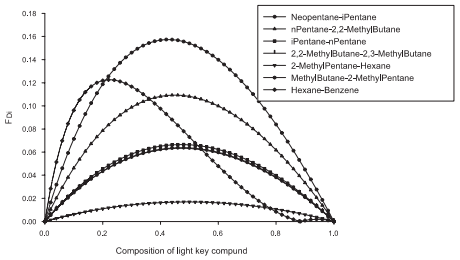
Step 4,5	Rank the splits by size of maximum driving force	$D_{y,Neopentane-iPentane} = 0.16$, $D_{y,nPentane-2,2-MethylButane} = 0.122$, $D_{y,iPentane-nPentane} = 0.119$, $D_{y,2,2-MethylButane-2,3-MethylButane} = 0.066$, $D_{y,2-MethylPentane-Hexane} = 0.06$, $D_{y,2,3-MethylButane-2-MethylPentane} = 0.06$, $D_{y,Hexane-Benzene} = 0.122$
Step 6	Draw the flowsheet	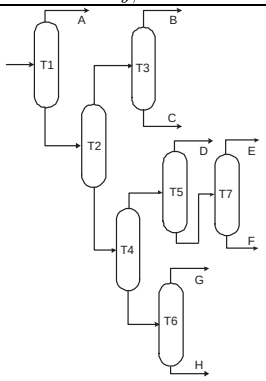

Validation		
Step 1	Originally proposed flowsheet by Shah and Kokossis (1997)	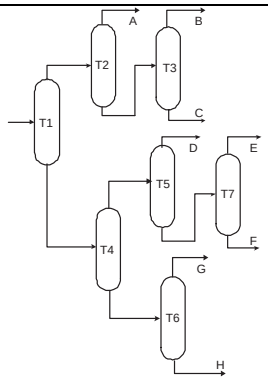
Rigorous simualtion of the alternative flowsheets give:	Original flowsheet: Energy consumption = 311 GJ/hr	Driving force based flowsheet: Energy consumption = 285 GJ/hr

Table A.5: Application of algorithm S1 to example 2.

[1] Note: azeotrope between Benzene and Hexane.

System: Ethane, Propane, iButane, nButane, iPentane+		
Pressure, $P = 1$ atm.		
Algorithm	**Action**	
Step 1,2,3	Retrieve data and calculate driving force curves	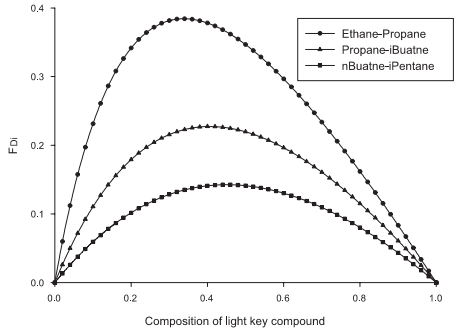
Step 4,5	Rank the splits by size of maximum driving force	$D_{y,Ethane-Propane} = 0.34,$ $D_{y,Propane-iButane} = 0.23,$ $D_{y,nButane-iPentane} = 0.14$
Step 6	Draw the flowsheet	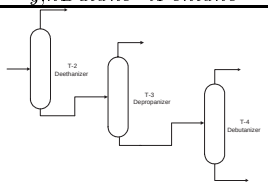
Validation		
Step 1	ProVision User's Guide (1994) reporeted this proposed sequence to be the best. This is considered as proof here.	

Table A.6: Application of algorithm S1 to example 11.

System: Ethanol-Water		
Algorithm	**Action**	
Step 1,2,	Retrieve data and calculate driving force curves	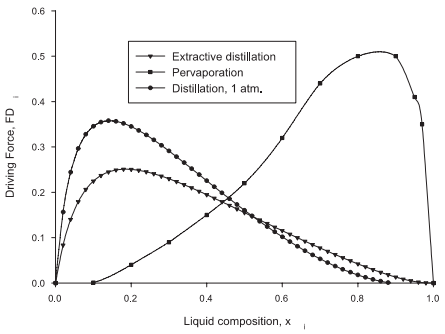
Step 3	Identify feasible paths	1) Distillation and pervaporation, 2) distillation with solvent, 3)distillation with solvent and pervaporation
Step 4	Identify the solution(s) with the largest driving force	Distillation combined with pervaporation is chosen as initial flowsheet
Validation		
Step 1	Identification of alternatives	Distillation + pervaporation Add solvent to distillation
Step 2	Rigorous calculation of energy duties	Distillation and Pervaporation consumes maximum 73 % of the energy for a distillation column and a solvent recovery column

Table A.7: Application of algorithm S2 to example 19.

System: Methanol-MTBE		
Algorithm	**Action**	
Step 1,2,	Retrieve data and calculate driving force curves	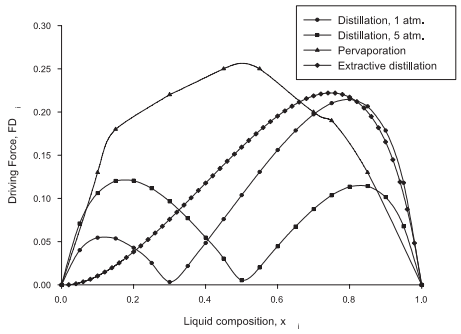
Step 3	Identify feasible paths	1) Distillation and pervaporation, 2) distillation with solvent, 3)distillation with solvent and pervaporation
Step 4	Identify the solution(s) with the largest driving force	Distillation combined with pervaporation is chosen as initial flowsheet
Validation		
Step 1	Identification of alternatives	Distillation + pervaporation Add solvent to distillation
Step 2	Rigorous calculation of energy duties	Distillation and Pervaporation consumes maximum 34 % of the energy for a distillation column and a solvent recovery column

Table A.8: Application of algorithm S2 to example 3.

A.2 Design examples

Feed: Methane (0.20), **Ethane (0.46)**, **Propane (0.30)**, Butane (0.03), Pentane (0.01)		
Pressure, $P = 400$ psia, Number of stages, $N = 13$		
Algorithm	**Action**	
Step 1,2	Calculate driving force curve	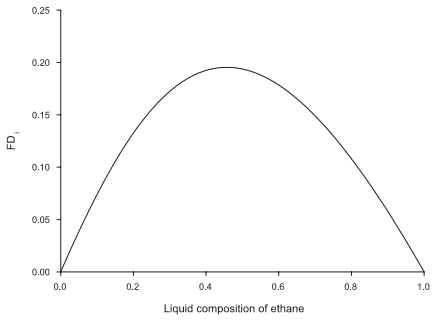
Step 3	Identify D_x	$D_x = 0.48$
Step 4	Determine N_F	$N_F = 13(1 - 0.48) = 6.76$
Step 5	Check for scaling	No scaling
Step 7	Determine RR_{min}	1.81
Step 7a	Give specification 1	$x_{(light \quad compounds)} = 0.9915$
Step 7b	Give specification 2	$x_{(heavy \quad compounds)} = 0.9829$
Validation		
Step 1	Optimisation of N_F, $N_{F,opt}$ = 6-7	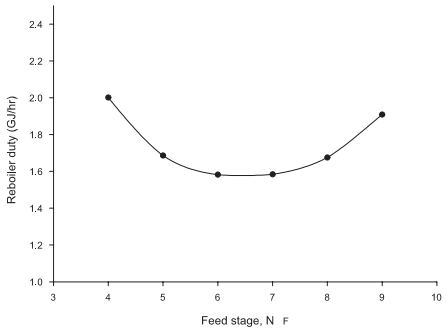
Step 2	Actual RR	1.10

Table A.9: Application of algorithm D1 to example 6.

Feed: **Ethanol-Toluene**, x_{EtOH} = (0.75, 0.50, 0.40, 0.25)		
Pressure, P = 1 atm, Number of stages, N = 20		
Algorithm	**Action**	
Step 1,2	Calculate driving force curve	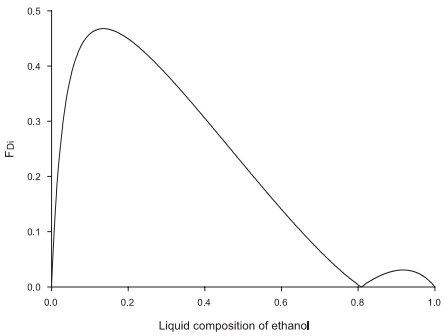
Step 3	Identify D_x	$D_x = 0.12$
Step 4	Determine N_F	$N_F = 20(1 - 0.12/0.81) = 17$
Step 5	Check for scaling	No scaling
Step 7	Determine RR_{min}	0.89
Step 7a	Give specification 1	$x_{Ethanol} = 0.999$
Step 7b	Give specification 2	$x_{Toluene} = 0.8072$
Validation		
Step 1	Optimisation of N_F, $N_{F,opt}$ = 17, 17, 18, 17	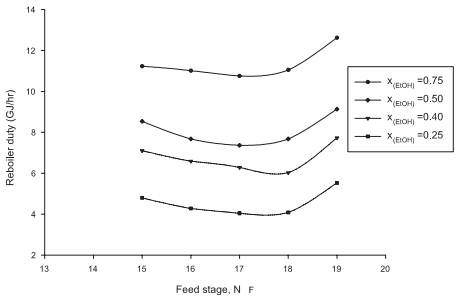
Step 2	Actual RR	1.93, 2.09, 2.10, 2.18

Table A.10: Application of algorithm D1 to example 5.

Feed: **Methanol-Water**, x_{MeOH} = (0.80, 0.50, 0.22, 0.15)		
Pressure, P = 1 atm, Number of stages, N = 22		
Algorithm	**Action**	
Step 1,2	Calculate driving force curve	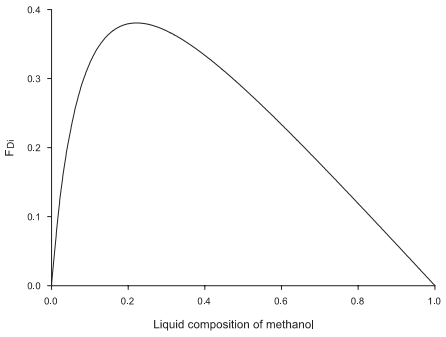
Step 3	Identify D_x	D_x = 0.22
Step 4	Determine N_F	$N_F = 22(1 - 0.22) = 17$
Step 5	Check for scaling	Case 4; factor 1a, N_F = 16
Step 7	Determine RR_{min}	1.02
Step 7a	Give specification 1	$x_{Methanol}$ = 0.9995
Step 7b	Give specification 2	x_{Water} = 0.9995
Validation		
Step 1	Optimisation of N_F, $N_{F,opt}$ = 16, 17, 17, 16	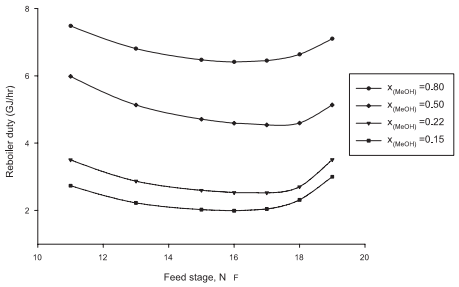
Step 2	Actual RR	1.24, 1.43, 1.84, 2.12

Table A.11: Application of algorithm D1 to example 4.

Feed: **Acetic Acid-Water**, $x_{Acetic} = (0.23)$, (Traces of MeOH and Meac)		
Pressure, $P = 1$ atm, Number of stages, $N = 40$		
Algorithm	**Action**	
Step 1,2	Calculate driving force curve	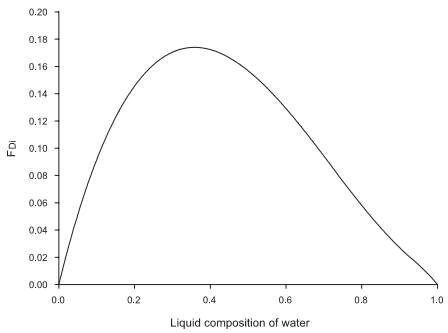
Step 3	Identify D_x	$D_x = 0.35$
Step 4	Determine N_F	$N_F = 40(1 - 0.35) = 26$
Step 5	Check for scaling	No scaling
Step 7	Determine RR_{min}	2.84
Step 7a	Give specification 1	$x_{Acetic} = 0.999$
Step 7b	Give specification 2	$x_{Water} = 0.989$
Validation		
Step 1	Optimisation of N_F, $N_{F,opt} = 26$	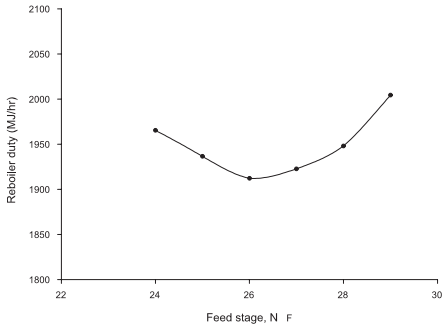
Step 2	Actual RR	3.53

Table A.12: Application of algorithm D1 to example 20.

Feed: C_3 (0.55), iC_4 (0.11), nC_4 **(0.16)**, $iC5$ **(0.04)**, nC_5+ (0.13)		
Pressure, $P = 210$ psia, Number of stages, $N = 22$		
Algorithm	**Action**	
Step 1,2	Calculate driving force curve	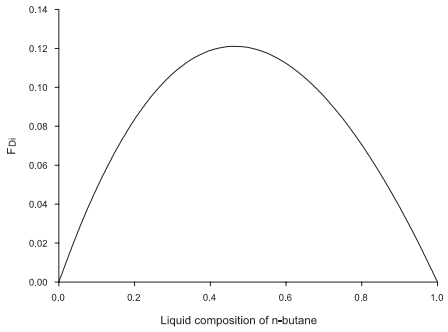
Step 3	Identify D_x	$D_x = 0.46$
Step 4	Determine N_F	$N_F = 22(1 - 0.46) = 11.8$
Step 5	Check for scaling	No scaling
Step 7	Determine RR_{min}	3.53
Step 7a	Give specification 1	$x_{(light \quad compounds)} = 0.98$
Step 7b	Give specification 2	$x_{(heavy \quad compounds)} = 0.95$
Validation		
Step 1	Optimisation of N_F, $N_{F,opt} = 11$	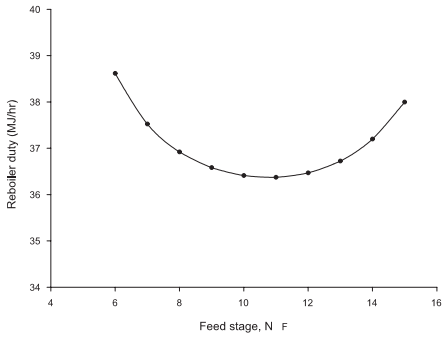
Step 2	Actual RR	0.53

Table A.13: Application of algorithm D1 to example 11.

Feed: (N_2, CO_2, C_1), C_2 **(0.21)**, C_3 **(0.33)**, iC_4 (0.10)		
nC_4 (0.21), iC_5+ (0.114)		
Pressure, P = 415 psia, Number of stages, N = 25		
Algorithm	**Action**	
Step 1,2	Calculate driving force curve	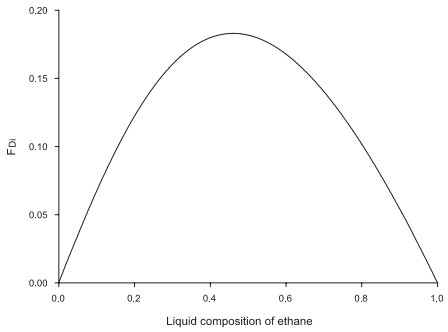
Step 3	Identify D_x	$D_x = 0.46$
Step 4	Determine N_F	$N_F = 25(1 - 0.46) = 13.5$
Step 5	Check for scaling	No scaling [1]
Step 7	Determine RR_{min}	3.53
Step 7a	Give specification 1	C_2/C_3 mole ratio = 0.025
Step 7b	Give specification 2	Composition C_3 = 0.02
Validation		
Step 1	Optimisation of N_F, $N_{F,opt}$ = 10, according to ProVision User's Guide (1994): $N_{F,opt}$ = 13	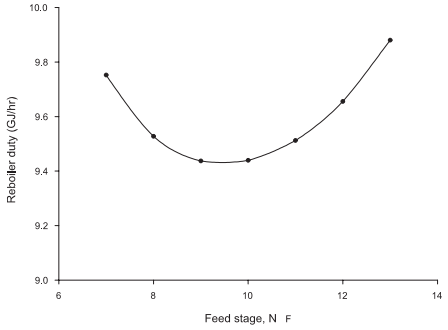
Step 2	Actual RR	3.05

Table A.14: Application of algorithm D1 to example 11.

[1] In principle, no scaling is required simece the light key compostion is 0.21 (and not 0.20). If, however, scaling is applied, the feed is moved 10 % up in the column, and matches the optimum, according to optimisation.

Feed: (N_2, CO_2, C_1), C_2 (0.01), C_3 **(0.41)**, iC_4 **(0.12)**		
nC_4 (0.27), iC_5 (0.03), nC_5 (0.09), C_6+ (0.06)		
Pressure, P = 245 psia, Number of stages, N = 23		
Algorithm	**Action**	
Step 1,2	Calculate driving force curve	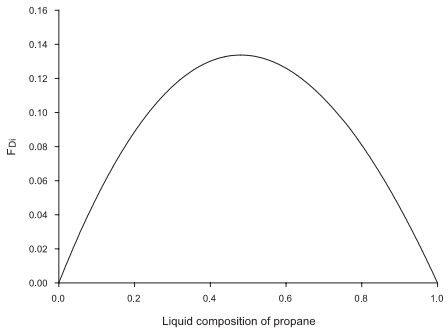
Step 3	Identify D_x	$D_x = 0.48$
Step 4	Determine N_F	$N_F = 23(1 - 0.48) = 11.5$
Step 5	Check for scaling	No scaling
Step 7	Determine RR_{min}	2.70
Step 7a	Give specification 1	Composition $C_3 = 0.02$
Step 7b	Give specification 2	Composition $iC_4 + nC_4 = 0.02$
Validation		
Step 1	Optimisation of N_F, $N_{F,opt} = 11$, according to ProVision User's Guide (1994): $N_{F,opt} = 11$	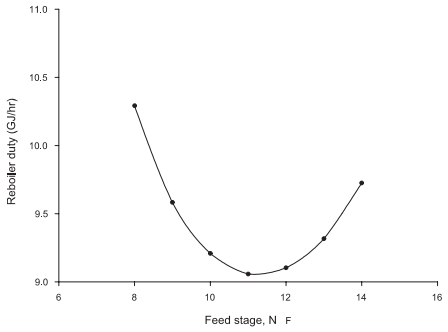
Step 2	Actual RR	3.44

Table A.15: Application of algorithm D1 to example 11.

Feed: (N_2, CO_2, C_1, C_2) (0.01), C_3 (0.02), iC_4 (0.202),		
nC_4 **(0.45)**, iC_5 **(0.06)**, nC_5 (0.16), C_6+ (0.105)		
Pressure, P = 105 psia, Number of stages, N = 30		
Algorithm	**Action**	
Step 1,2	Calculate driving force curve	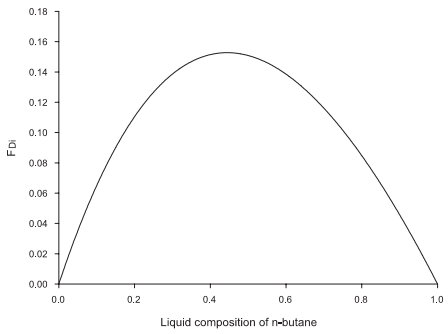
Step 3	Identify D_x	$D_x = 0.47$
Step 4	Determine N_F	$N_F = 30(1 - 0.47) = 16$
Step 5	Check for scaling	No scaling
Step 7	Determine RR_{min}	2.50
Step 7a	Give specification 1	Composition $iC_5 = 0.0025$
Step 7b	Give specification 2	Composition $nC_4 = 0.01$
Validation		
Step 1	Optimisation of N_F, $N_{F,opt} = 17$, according to ProVision User's Guide (1994): $N_{F,opt} = 16$	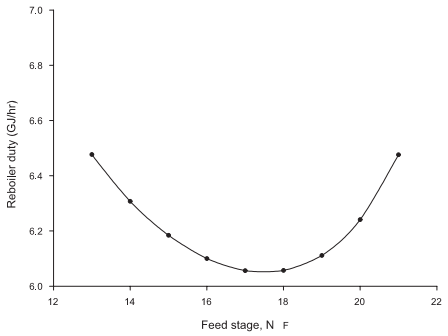
Step 2	Actual RR	1.27

Table A.16: Application of algorithm D1 to example 11.

Feed: ($Methane$), $Ethylene$ **(0.613)**, $Ethane$ **(0.384)**		
($Propadien\ Propylene$, $Propane$)		
Pressure, $P = 8.8$ atm, Number of stages, $N = 90$		
Algorithm	**Action**	
Step 1,2	Calculate driving force curve	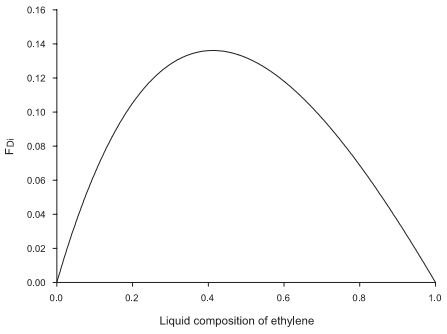
Step 3	Identify D_x	$D_x = 0.42$
Step 4	Determine N_F	$N_F = 90(1 - 0.42) = 52$
Step 5	Check for scaling	No scaling [1]
Step 7	Determine RR_{min}	3.4
Step 7a	Give specification 1	Composition $C_2H_4 = 0.9992$
Step 7b	Give specification 2	Composition $C_2H_4 = 0.006$
Validation		
Step 1	Optimisation of N_F, $N_{F,opt} = 68$	Hoch and Eliceche (1999) (p.339)
Step 2	Actual RR	2.91

Table A.17: Application of algorithm D1 to example 1.

[1] Note, in this column, that purity constraints are very close to enforce scaling factor 2b to applied. Note also that the difference from feed on stage 68 to feed on stage 52 is as low as 2.6 %.

Feed: (*Methane*), *Ethylene* (0.59), *Ethane* **(0.37)**, (*Propadien*)		
Propylene **(0.01)** , (*Propane*, *Butene*, *Pentane*)		
Pressure, $P = 26.2$ atm, Number of stages, $N = 40$		
Algorithm	**Action**	
Step 1,2	Calculate driving force curve	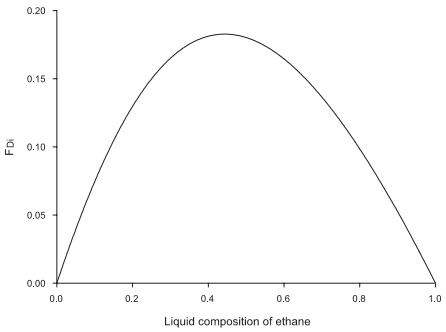
Step 3	Identify D_x	$D_x = 0.465$
Step 4	Determine N_F	$N_F = 40(1 - 0.465) = 21$
Step 5	Check for scaling	Scaling [1]
Step 7	Determine RR_{min}	3.4
Step 7a	Give specification 1	Composition C_2H_4 + $C_2H_6 = 0.00009$
Step 7b	Give specification 2	Composition C_3H_6 + $C_3H_8 = 0.00274$
Validation		
Step 1	Optimisation of N_F, $N_{F,opt} = 18$	Hoch and Eliceche (1999) (p.339)
Step 2	Actual RR	0.39

Table A.18: Application of algorithm D1 to example 1.

[1] The column feed has a large majority of light compounds. Therefore, condition 1b is activated, and the feed stage should be 5% lower in the column. At the same time, there is a larger purity demand to the purity of the bottom product. There is a indication from the results of Hoch and Eliceche (1999) that the scaling factor for purity is dominant to the scaling factor for composition.

Feed: (*Ethylene*, *Ethane*), *Propylene* **(0.88)**, (*Propadien*)		
Propane **(0.11)**, (*Butene*, *Pentane*)		
Pressure, $P = 16.2$ atm, Number of stages, $N = 134$		
Algorithm	**Action**	
Step 1,2	Calculate driving force curve	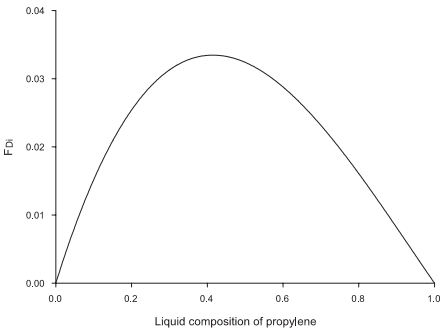
Step 3	Identify D_x	$D_x = 0.44$
Step 4	Determine N_F	$N_F = 134(1 - 0.444) = 75$
Step 5	Check for scaling	Scaling [1]
Step 7	Determine RR_{min}	3.82
Step 7a	Give specification 1	Composition $C_3H_6 = 0.75$
Step 7b	Give specification 2	Composition $C_3H_8 = 0.85$
Validation		
Step 1	Optimisation of N_F, $N_{F,opt} = 68$	Hoch and Eliceche (1999) (p.339)
Step 2	Actual RR	27.11

Table A.19: Application of algorithm D1 to example 1.

[1] The column feed has a majority of light compounds. Therefore, condition 1b is activated, and the feed stage should be 5% lower in the column. At the same time the performance specification is stricter in the bottom, indicating a feed higher in the column. According to Hoch and Eliceche (1999) the optimum feed stage is higher than the prediction, indicating scaling on product specification is superiour to scaling for diluted feed mixture.

Feed: (*Ethane*, *Propadien*), *Propylene* (0.28), *Propane* **(0.035)**		
1 − *Butene* **(0.382)**, *Butene* (0.04), (*Pentane*, *Hexane*)		
Pressure, $P = 15.1$ atm, Number of stages, $N = 29$		
Algorithm	**Action**	
Step 1,2	Calculate driving force curve	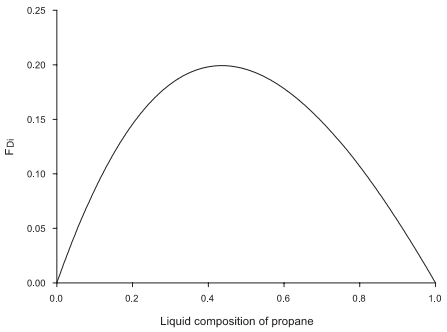
Step 3	Identify D_x	$D_x = 0.46$
Step 4	Determine N_F	$N_F = 29(1 - 0.46) = 15$
Step 5	Check for scaling	No scaling
Step 7	Determine RR_{min}	1.75
Step 7a	Give specification 1	Composition $C_4H_8 + C_4H_{10} = 0.00035$
Step 7b	Give specification 2	Composition $C_3H_6 + C_3H_8 = 0.004$
Validation		
Step 1	Optimisation of N_F, $N_{F,opt} = 15$	Hoch and Eliceche (1999) (p.339)
Step 2	Actual RR	4.10

Table A.20: Application of algorithm D1 to example 1.

Feed: ($Propadien$, $Propylene$, $Propane$), $1-Butene$ (0.557), $Butane$ **(0.06)**, $Pentane$ **(0.17)**, $Hexane$ (0.21)		
Pressure, $P = 5.1$ atm, Number of stages, $N = 22$		
Algorithm	**Action**	
Step 1,2	Calculate driving force curve	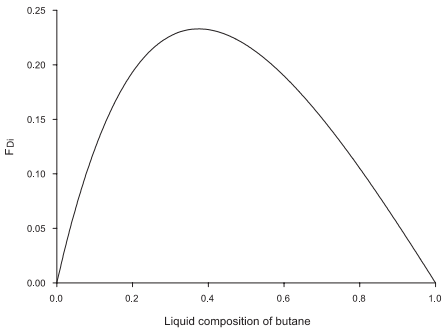
Step 3	Identify D_x	$D_x = 0.38$
Step 4	Determine N_F	$N_F = 22(1 - 0.38) = 13$
Step 5	Check for scaling	No scaling
Step 7	Determine RR_{min}	1.78
Step 7a	Give specification 1	Composition C_4H_8 + C_4H_{10} = 0.0178
Step 7b	Give specification 2	BC_5/fC_5 = 0.98
Validation		
Step 1	Optimisation of N_F, $N_{F,opt} = 13$	Hoch and Eliceche (1999) (p.339)
Step 2	Actual RR	1.33

Table A.21: Application of algorithm D1 to example 1.

System: Propane (1), Butane (2), 2,3-DimethylButane (3)		
Pressure, $P = 10$ atm., Number of stages, $N = 36$		
Algorithm	**Action**	
Step 1,2,3,4,5	Retrieve data and calculate driving force curves and determine which split has the larger driving force, and determine D_x for this curve, $D_x = 0.46$	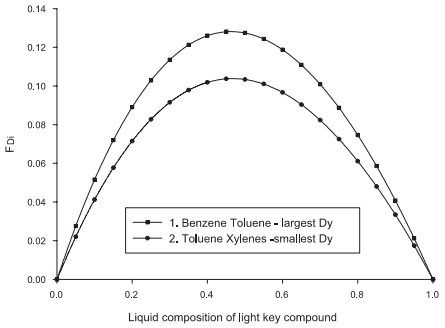
Step 6,7,8	Configure the column as feed above side-draw, or side-draw above feed and ghenerate the 'merged driving force diagram', and determine D_s, $D_s = 0.38$.	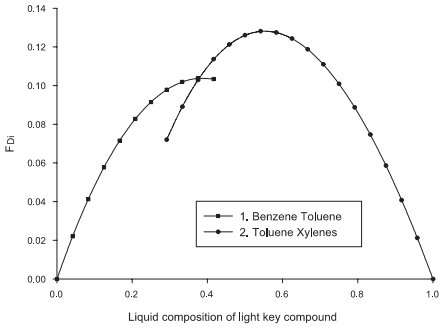
Step 9	Determine RR_{min}	3.28
Step 10a	Give specification 1	Composition $Benzene = 0.995$
Step 10b	Give specification 2	Composition $Xylenes = 0.92$
Step 10c	Determine side-draw	Side-draw = Composition $Toluene \cdot Feed$
Step 11	Calculate N_S	$N_S = 40$(1-0.38) = 24
Step 11	Calculate N_F	$N_S = 24$(1-0.46) = 12

Table A.22: Application of algorithm D2 to example 8.

Validation		
Feed(1,2,3) = (0.33, 0.33, 0.34)	Feed(1,2,3) = (0.15, 0.70, 0.15)	Feed(1,2,3) = (0.50, 0.35, 0.15)
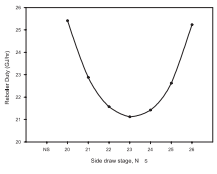	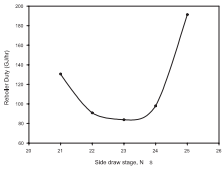	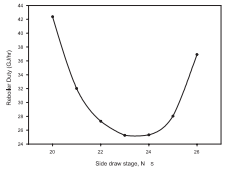
Optimum $N_S = 23$	Optimum $N_S = 23$	Optimum $N_S = 23$
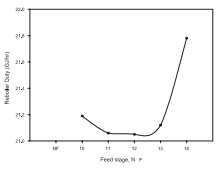	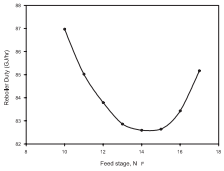	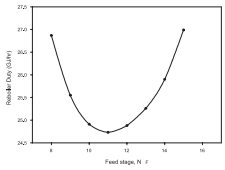
Optimum $N_F = 12$	Optimum $N_F = 14$	Optimum $N_F = 11$
$RR/V/F$= 21.7/7.13	$RR/V/F$= 222.5/32.7	$RR/V/F$= 18.3/9.2

Table A.23: Validation of algorithm D2 to example 8, see table A.22.

System: Pentane (1), Hexane (2), Heptane (3)		
Pressure, $P = 5$ atm., Number of stages, $N = 36$		
Algorithm	**Action**	
Step 1,2,3,4,5	Retrieve data and calculate driving force curves and determine which split has the larger driving force, and determine D_x for this curve, $D_x = 0.45$	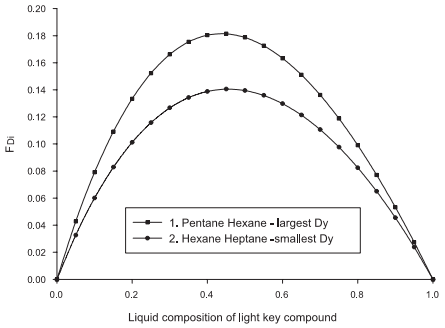
Step 6,7,8	Configure the column as feed above side-draw, or side-draw above feed and generate the 'merged driving force diagram', and determine D_s, $D_s = 0.32$	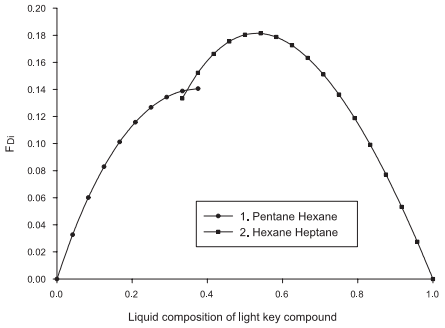
Step 9	Determine RR_{min}	2.02
Step 10a	Give specification 1	Composition $Pentane = 0.998$
Step 10b	Give specification 2	Composition $Heptane = 0.85$
Step 10c	Determine side-draw	Side-draw = Composition $Hexane \cdot Feed$
Step 11	Calculate N_S	$N_S = 36(1\text{-}0.32) = 24$
Step 11	Calculate N_F	$N_S = 24(1\text{-}0.45) = 13$

Table A.24: Application of algorithm D2 to example 16.

Validation		
Feed(1,2,3) = (0.33, 0.33, 0.34)	Feed(1,2,3) = (0.20, 0.70, 0.10)	Feed(1,2,3) = (0.05, 0.90, 0.05)
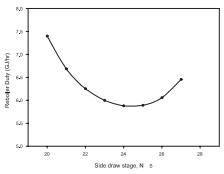	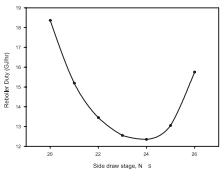	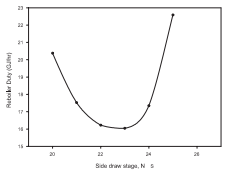
Optimum $N_S = 24$	Optimum $N_S = 24$	Optimum $N_S = 23$
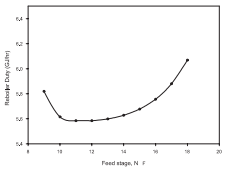	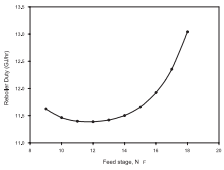	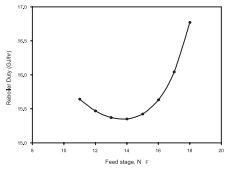
Optimum $N_F = 12$	Optimum $N_F = 12$	Optimum $N_F = 14$
$RR/V/F$= 4.69/1.67	$RR/V/F$= 20.6/4.06	$RR/V/F$= 116.7/5.78

Table A.25: Validation of algorithm D2 to example 16, see table A.24.

System: Propane (1), Butane (2), Heptane (3)		
Pressure, $P = 5$ atm., Number of stages, $N = 20$		
Algorithm	**Action**	
Step 1,2,3,4,5	Retrieve data and calculate driving force curves and determine which split has the larger driving force, and determine D_x for this curve, $D_x = 0.30$	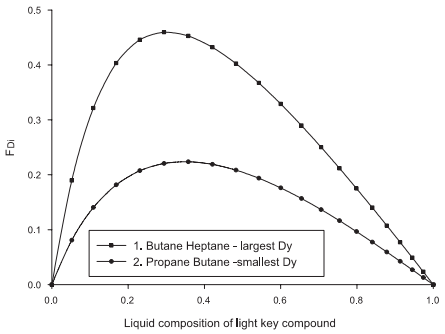
Step 6,7,8	Configure the column as feed above side-draw, or side-draw above feed and generate the 'merged driving force diagram', and determine D_s, $D_s = 0.52$	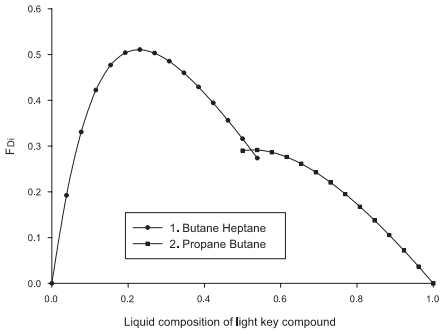
Step 9	Determine RR_{min}	1.97
Step 10a	Give specification 1	Composition $Propane = 0.9050$
Step 10b	Give specification 2	Composition $Heptane = 0.9999$
Step 10c	Determine side-draw	Side-draw = Composition $Butane \cdot Feed$
Step 11	Calculate N_S	$N_S = 20(1\text{-}0.52) = 9.6$
Step 11	Calculate N_F	$N_S = 11(1\text{-}0.30) + 9 = 16.7$

Table A.26: Application of algorithm D2 to example 21.

Validation		
Feed(1,2,3) = (0.33, 0.33, 0.34)	Feed(1,2,3) = (0.20, 0.60, 0.20)	Feed(1,2,3) = (0.10, 0.80, 0.10)
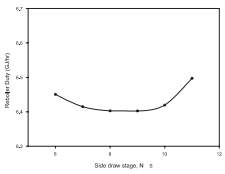	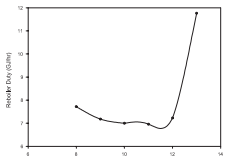	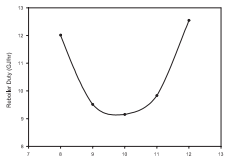
Optimum $N_S = 9$	Optimum $N_S = 11$	Optimum $N_S = 10$
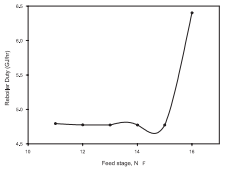	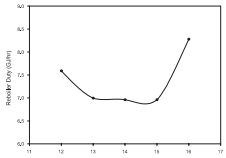	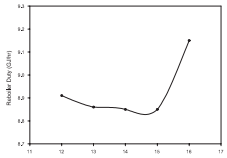
Optimum $N_F = 15$	Optimum $N_F = 15$	Optimum $N_F = 15$
$RR/V/F$= 5.44/1.79	$RR/V/F$= 17.05/3.41	$RR/V/F$= 47.63/4.76

Table A.27: Validation of algorithm D2 to example 21, see table A.26.

System: Propane (1), Butane (2), 2,3 DimethylButane (23DB) (3)		
Pressure, $P = 10$ atm., Number of stages, $N = 36$		
Algorithm	**Action**	
Step 1,2,3,4,5	Retrieve data and calculate driving force curves and determine which split has the larger driving force, and determine D_x for this curve, $D_x = 0.41$	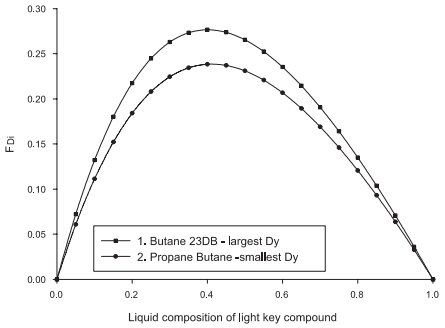
Step 6,7,8	Configure the column as feed above side-draw, or side-draw above feed and generate the 'merged driving force diagram', and determine D_s, $D_s = 0.50$	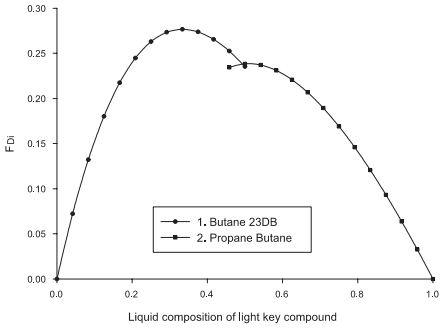
Step 9	Determine RR_{min}	1.51
Step 10a	Give specification 1	Composition $Propane = 0.90$
Step 10b	Give specification 2	Composition $Heptane = 0.998$
Step 10c	Determine side-draw	Side-draw = Composition $Butane \cdot Feed$
Step 11	Calculate N_S	$N_S = 36(1\text{-}0.50) = 18$
Step 11	Calculate N_F	$N_S = 11(1\text{-}0.41) + 18 = 28$

Table A.28: Application of algorithm D2 to example 22.

Validation	
Feed(1,2,3) = (0.33, 0.33, 0.34)	Feed(1,2,3) = (0.15, 0.70, 0.15)
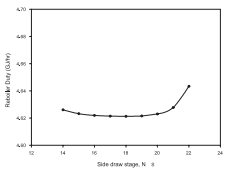	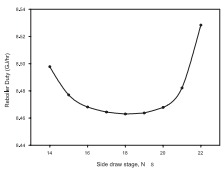
Optimum $N_S = 18$	Optimum $N_S = 18$
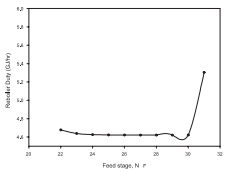	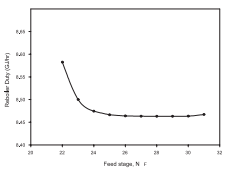
Optimum $N_F = 28$	Optimum $N_F = 28$
$RR/V/F$= 8.88/2.27	$RR/V/F$= 34.0/5.09

Table A.29: Validation of algorithm D2 to example 22, see table A.28.

System: iButanol (1), Butanol (2), Pentanol (23DB) (3)		
Pressure, $P = 1$ atm., Number of stages, (1) $N = 36$, (2) $N = 50$		
Algorithm	**Action**	
Step 1,2,3,4,5	Retrieve data and calculate driving force curves and determine which split has the larger driving force, and determine D_x for this curve, $D_x = 0.41$	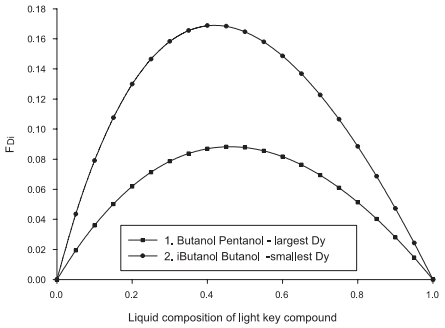
Step 6,7,8	Configure the column as feed above side-draw, or side-draw above feed and generate the 'merged driving force diagram', and determine D_s, $D_s = 0.58$	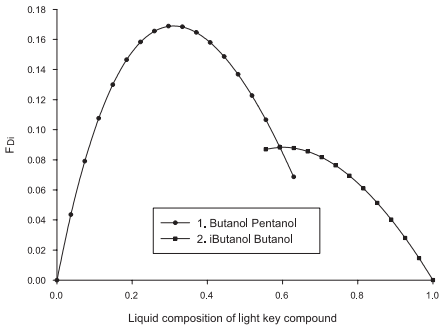
Step 9	Determine RR_{min}	5.21
Step 10a	Give specification 1	Composition $iButanol = 0.999$
Step 10b	Give specification 2	Composition $Pentanol = 0.85$
Step 10c	Determine side-draw	Side-draw = Composition $Butanol \cdot Feed$
Step 11 (1)	Calculate N_S	N_S = 36(1-0.58) = 15
Step 11 (1)	Calculate N_F	N_S = 21(1-0.41) + 15 = 27
Step 11 (2)	Calculate N_S	N_S = 50(1-0.58) = 21
Step 11 (2)	Calculate N_F	N_S = 29(1-0.41) + 21 = 38

Table A.30: Application of algorithm D2 to example 23.

Validation	
Feed(1,2,3) = (0.33, 0.33, 0.34)	Feed(1,2,3) = (0.15, 0.70, 0.15)
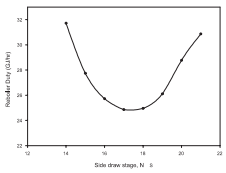	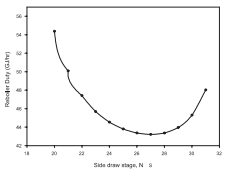
Optimum $N_S = 17$	Optimum $N_S = 27$
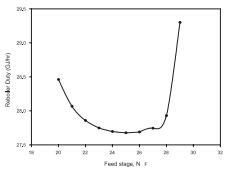	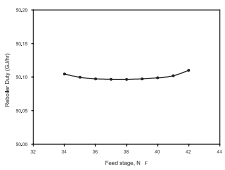
Optimum $N_F = 25$	Optimum $N_F = 38$
$RR/V/F$= 16.3/5.34	$RR/V/F$= 66.6/10.0

Table A.31: Validation of algorithm D2 to example 23, see table A.30.

Sytem: MTBE synthesis from Methanol and iButene		
Pressure, $P = 1$ atm, Number of stages, $N = 5$		
Algorithm	**Action**	
Step 1,2,3	Retrieve data and calculate driving force curve	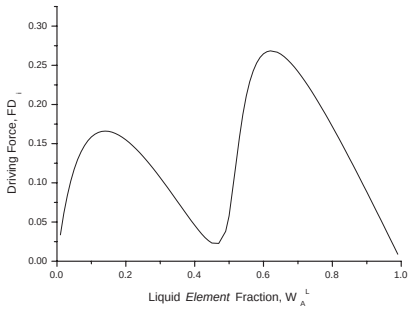
Step 4	Identify area of operation	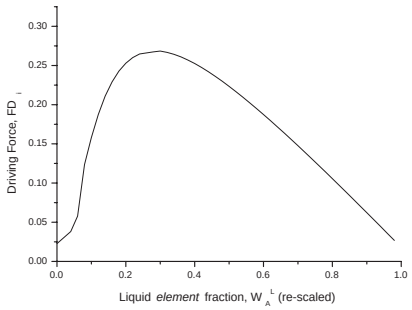
Step 5	Determine feed condition, q	$q = 0.83$
Step 6	Identify D, D_x	$D = 0.27$, $D_x = 0.38$
Step 6.1	Determine N_F	$N_F = 3$
Step 6.2	Determine RR_{min}	$RR_{min} = 0.5$
Validation		
Step 1	Optimisation of N_F, $N_{F,opt} = 3$	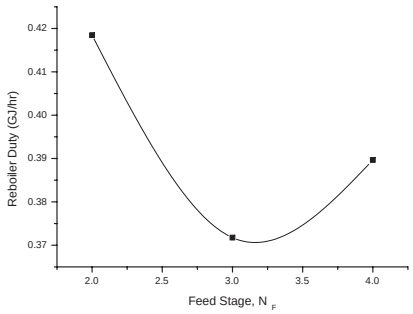
Step 2	Actual RR	$RR = 2.50$ (molar)

Table A.32: Application of algorithm D3 to example 9.

Sytem: Ethanol synthesis from Ethylene and Water		
Pressure, $P = 35$ atm, Number of stages, $N = 9$, (3 reactive)		
Algorithm	**Action**	
Step 1,2,3	Retrieve data and calculate driving force curve	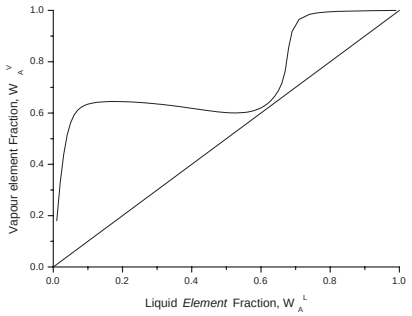
Step 4	Identify area of operation	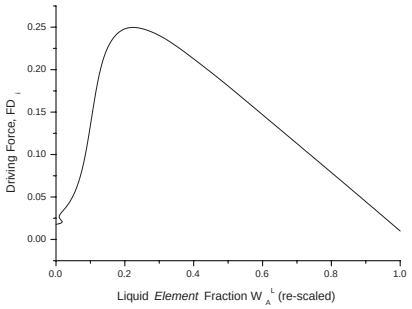
Step 5	Determine feed condition, q	$q = 0.05$
Step 6	Identify D, D_x	$D = 0.25$, $D_x = 0.20$
Step 6.1	Determine N_F	$N_F = 4$
Step 6.2	Determine RR_{min}	$RR_{min} = 0.2$
Validation		
Step 1	Optimisation of N_F, $N_{F,opt} = 4$	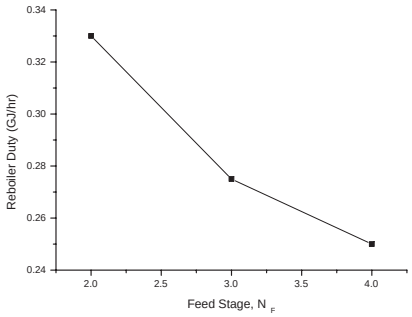
Step 2	Actual RR	$RR = 2.5$ (molar)

Table A.33: Application of algorithm D3 to example 24.

Sytem: Benzene synthesis from disproportionation of toluene to benzene and *o*-xylene		
Pressure, $P = 1$ atm, Number of stages, $N = 13$		
Algorithm	**Action**	
Step 1,2,3	Retrieve data and calculate driving force curve	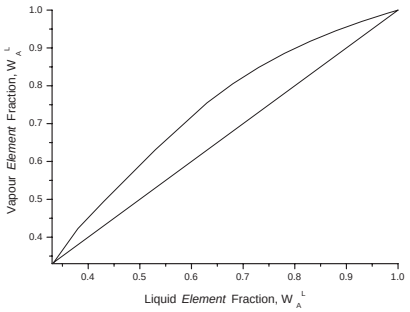
Step 4	Identify area of operation	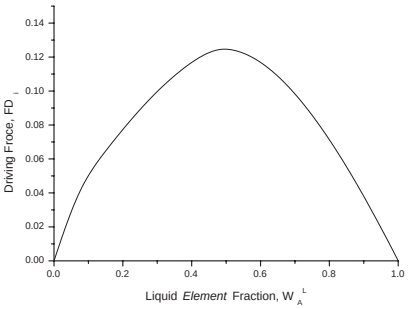
Step 5	Determine feed condition, q	$q = 0$
Step 6	Identify D, D_x	$D = 0.25$, $D_x = 0.20$
Step 6.1	Determine N_F	$N_F = 4$
Step 6.2	Determine RR_{min}	$RR_{min} = 0.2$
Validation		
Step 1	Optimisation of N_F, $N_{F,opt} = 4$	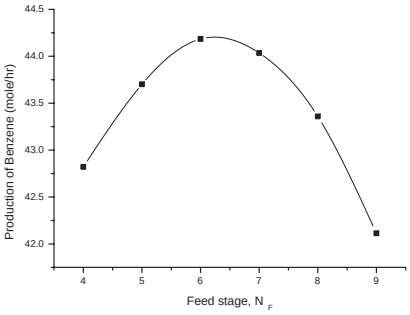
Step 2	Actual RR	$RR = 2.5$ (molar)

Table A.34: Application of algorithm D3 to example 10.

Feed: Benzene, Toluene, Xylenes (0.20, 0.65, 0.15)		
Pressure, $P = 0$ psig, Number of stages, $N_{main} = 50$, $N_{pre-frac} = 6$		
Desired products: Benzene Toluene, Xylenes (0.995, 0.98, 0.99)		
Algorithm	**Action**	
Step 1,2,3,4	Retrieve data and calculate driving force curve	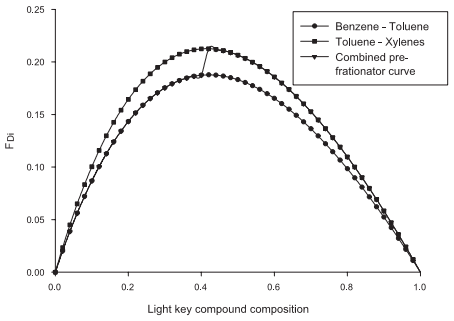
Step 6	Identify $D_{x,prefrac}$	$D_{x,prefrac} = 0.42$ (0.55 considering 90 % vapour feed)
Step 6	Determine $N_{F,prefrac}$	$N_F = 3$
Step 6	Determine distribution of main column segments, find N_S	$N_S = 24$
Step 6	Identify $D_{x,top}$, $D_{x,bot}$	$D_{x,top} = 0.57$ (vapour feed), $D_{x,bot} = 0.42$
Step 6	Determine $N_{F,top}$, $N_{F,bot}$	$N_{F,top} = 10$ (vapour feed), $N_{x,bot} = 39$ (38)

Table A.35: Application of algorithm D5 to example 25.

Validation	
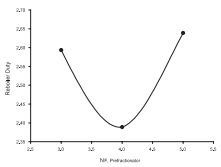	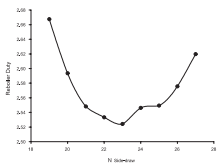
Optimum $N_{F,prefrac} = 4$	Optimum $N_S = 24$
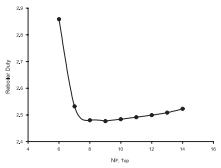	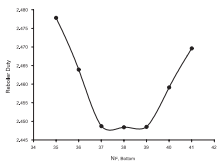
Optimum $N_{F,top} = 9$	Optimum $N_{F,bot} = 38$

Table A.36: Validation of algorithm D5 to example 25, see table A.38.

Feed: s-Butanol, i-Butanol, n-Butanol (0.33, 0.33, 0.33)		
Pressure, $P = 0$ psig, Number of stages, $N_{main} = 72$, $N_{pre-frac} = 20$		
Desired products: s-Butanol, i-Butanol, n-Butanol (0.98, 0.98, 0.98)		
Algorithm	**Action**	
Step 1,2,3,4	Retrieve data and calculate driving force curve	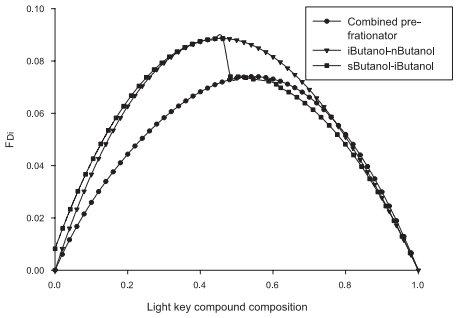
Step 6	Identify $D_{x,prefrac}$	$D_{x,prefrac} = 0.48$ (0.63 considering 50 % vapour feed)
Step 6	Determine $N_{F,prefrac}$	$N_F = 7$
Step 6	Determine distribution of main column segments, find N_S	$N_S = 41$
Step 6	Identify $D_{x,top}$, $D_{x,bot}$	$D_{x,top} = 0.55$ (vapour feed), $D_{x,bot} = 0.45$
Step 6	Determine $N_{F,top}$, $N_{F,bot}$	$N_{F,top} = 14$ (vapour feed), $N_{x,bot} = 57$

Table A.37: Application of algorithm D5 to example 26.

Validation	
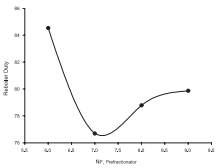	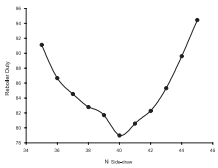
Optimum $N_{F,prefrac} = 7$	Optimum $N_S = 40$
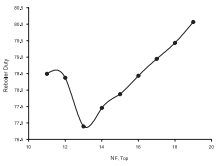	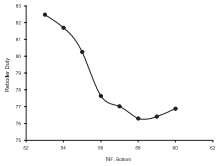
Optimum $N_{F,top} = 13$	Optimum $N_{F,bot} = 58$

Table A.38: Validation of algorithm D5 to example 25, see table A.37.

A.3 retrofit examples

System: $N = 60$, $N_F = 33$-38		
Algorithm	**Action**	
Step 1	Determine desired products	$X_{B,HK} = 0.995$, $X_{D,LK} = 0.995$
Step 2	Find $F_{Di\|Max}$	$F_{Di\|Max} \simeq 0.07$
Step 3	Find range of α	$\alpha \simeq 0.33$-0.34
Step 4	Find RR_{min}	$RR_{min} \simeq 6.4$
Step 5	Check for mixtures with these properties	
Validation		
α	$FD_{i\|max}$	Mixture, Pressure
1.33-1.34	$\simeq 0.074$	Butane-iButane, 5 atm.
1.33-1.38	$\simeq 0.080$	Cycloheptanol-Cycleoctanol, 5 atm.
1.24-1.85	$\simeq 0.065$	1,4Butanediol-1,3Butanediol, 15 atm.
1.22-1.34	$\simeq 0.07$	Diethyleneglycol-1,6Hexanediol, 3 atm.

Table A.39: Application of algorithm R1 to example 15.

List of definitions

BELSIM	Consulting and software company providing service to the chemical process industry
CAPEC	Computer Aided Process Engineering Center, at the Department of Chemical Engineering, Technical University of Denmark
Complex columns	Distillation columns where there are more than two products and/or more than one feed feed
DC	Disturbance Cost
DCN	Disturbance Condition number
DECHEMA	Society for Chemical Engineering and Biotechnology
DIPPR	Design Institute for Physical Properties, from the American Institute of Chemical Engineers
Driving force	Defined in this thesis as difference in composition between two co-existing phases
Extractive/azeotropic column	Distillation column where an entrainer (solvent) is employed as extractive agent, usually to overcome azeotropic composition
GCA	Group Contribution Approach - Property prediction based on the assumption that the group has the same properties as the the fragment of a molecule where it is a constituent part
HEN	Heat Exchanger Network - A network of heat exchangers in a process plant where the different heat exchangers supply/recieve energy from one another
Hybrid separation	A separation scheme comprising multiple separation units, and possibly multiple separation techniques
LP	Linear Programming - Solving of linear mathematical optimisation problem with contonous variables

MILP	Mixed Integer Linear Programming - Solving of linear mathematical optimisation problem with integer variables
MIMO	Multiple Input - Multiple Output
MINLP	Mixed Integer Non-linear Programming - Solving of non-linear mathematical optimisation problem with integer variables
MSA	Mass Separating Agent - Solvent, a compound that affects the liquid activity coefficients of a mixture, employed in this work to ease separation
NIST	National Institute of Standards and Technology
NLP	Non-linear Programming - Solving of non-linear mathematical optimisation problem with continous variables
Petlyuk column	Thermally (fully) coupled distillation, with a prefractionator and a main-fractionator operating with one condenser and one reboiler
Relative separability	Parameter used for modelling of differences in composition, as defined in equation 4.1
RGA	Relative Gain Array
SEN	State Equipment Network
Simple column	Distillation column where one feed splits in two products and key compounds are adjacent in relative volatility. It has one reboiler and one condenser
STN	State Task Network
Superstructure	Alternative candidate solutions to an optimisation problem

Nomenclature

α_B	Relative volatility of bottom product
α_D	Relative volatility of distillate product
α_F	Relative volatility of feed
α	Relative volatility
β	Relative separability
Λ	RGA matrix
μ_i^β	Chemical potential of component i in phase β
θ,φ,ϕ	Underwood's parameters
A	Product composition specification
B	Bottom flow
B	Product composition specification
C	Multiplication factor for RR_{min} to RR
C_i	Contribution of group i
D	Distillate flow
D	Largest driving force
D_s	Relative position of side-draw driving force
D_x	Relative position of largest driving force
D_y	Size of maximum driving force
F	Feed flow
F_x	Relative position of largest driving force for vapourized feed
F'_x	Relative position of largest driving force for mixed vapour liquid feed
FD_i	Driving force
$FD_{i\|max}$	Maximum driving force

G	Gibbs free energy
HK	Heavy key compound
LK	Light key compound
N	Number of stages
n	Number of equilibrium stages
N_F	Feed stage
N_i	Number of times group C_i occures in molecule
n_i^β	Number of species in phase β
N_P	Number of stages
N_R	Number of stages in rectifying section
N_S	NUmber of stages in stripping section
N_S	Side-draw stage
NC	Number of products
P	Pressure
p	Pressure
p^0	Vapour pressure
p_i	Property of component i
p_j	Property of component j
PF_{Di}	Primary driving force
q	Liquid fraction
RB	Reboil ratio
RR	Reflux ratio
RR_{min}	Minimum reflux ratio
S	Side-draw
S_R	Number of sequences
T	Temperature (K)
T_b	Bubble point temperature (K)

W_i^L	Element mole fration of cpmponent i in liquid phase
W_i^V	Element mole fration of cpmponent i in vapour phase
x_i	Liquid composition of compound i
x_i'	Liquid phase composition on solvent free basis
$x_{i\|max}$	Relative position of largest driving force
y_i	Vapour composition of compound i
y_i'	Vapour phase composition on solvent free basis
z_i	Feed composition of compound i

References

Abrams, D. S. and Prausnitz, J. M. (1975). Statistical thermodynamics of liquid mixtures: a new expression for the excess gibbs energy of partly or completely miscible systems. *AIChE J.*, **21**(1), 116–128.

Abufares, A. A. and Douglas, P. L. (1995). Mathematical Modelling and Simulation of an MTBE Catalytic Distillation Process using SPEEDUP and ASPENPLUS. *Trans Ichem. Eng.*, **273A**, 3.

Aggerwal, A. and Floudas, C. A. (1990). Synthesis of general distillation sequences. *Comput. Chem. Eng.*, **14**(6), 631–653.

Agrawal, R. (2000). Thermally coupled distillation with reduced number of intercolumn vapour transfers. *AIChE J.*, **46**(11), 2198–2210.

Agrawal, R. and Fidkowski, Z. T. (1999). New thermally coupled schemes For ternary distillation. *AIChE J.*, **45**(3), 485–496.

Agrawal, R. and Herron, D. M. (1998). Intermediate reboiler and condenser arrangement for binary distillation columns. *AIChE J.*, **44**(6), 1316–1324.

Agreda, V. H.; Partin, L. R. and Heise, W. H. (1990). High-Purity Methyl Acetate via Reactive Distillation. *Chem. Eng. Prog.*, **86**, 40.

Aguirre, P.; Espinosa, E.; Tarifa, E. and Scenna, N. (1997). Optimal thermodynamic approximation to reversible distillation of interheaters and intercoolers. *Ind. Eng. Chem. Res.*, **36**(11), 4882–4893.

Al-Rabiah, A. A.; Timmerhaus, K. D. and Noble, R. D. (1999). Modeling and simulation of several hybrid distillation systems for the ethane/ethylene separation. In *20. International Congress on Refrigiration, IIR/IIF*, Sydney, Australia.

Andrecovich, M. J. and Westerberg, A. W. (1985). An MILP formulation for heat integrated distillation sequence synthesis. *AIChE J.*, **31**(9), 1461–1747.

Bansal, V.; Perkins, J. D.; Pistikopoulos, E. N.; Ross, R. and van Schijndel, J. M. G. (2000a). Simultanous design and control optimisation under uncertainty. *Computers Chem. Engng.*, **24**, 261–266.

Bansal, V.; Ross, R.; Perkins, J. D. and Pistikopoulos, E. N. (2000b). The interactions of design and control: double-effect distilation. *J. of Process Control*, **10**, 219–227.

Barbosa, D. and Doherty, M. F. (1988a). Design and minimum-reflux calculations for single-feed reactive distillation columns. *Chem. Eng. Sci.*, **43**(7), 1523–1537.

Barbosa, D. and Doherty, M. F. (1988b). Design and minimum-reflux calculations for double-feed reactive distillation columns. *Chem. Eng. Sci.*, **43**(9), 2377–2389.

Barnicki, S. and Fair, J. R. (1990). Separation system synthesis: A knowledge based approach. 1. Liquid mixture separations. *Ind. Eng. Chem. Research*, **29**, 421–432.

Becker, H.; Godorr, S.; Kreis, H. and Vaughan, J. (2000). Die weltweit grösste Trennnwandkolonne mit Böden - Erfahrungen von der Konceptfindung bis zur Inbetriebnahme. *Linde - Berichte aus Technik und Wissenschaft*, **80**, 42–48.

Bekiaris, N. and Morari, M. (1996). Multiple steady states in distillation: ∞/∞ predictions, extensions, and implications for design, synthesis, and simulation. *Ind. Chem. Eng. Res.*, **35**(11), 4264–4280.

Berry, D. A. and Ng, K. M. (1997). Synthesis of crystallization-distillation hybrid processes. *AIChE J.*, **43**(7), 1751–1762.

Bessling, B.; Schembecker, G. and Simmrock, K. H. (1997). Design of processes with reactive distillation line diagrams. *Ind. Eng. Chem. Res.*, **36**(8), 3032–3042.

Biegler, L. T.; Grossmann, I. E. and Westerberg, A. W. (1997). *Systematic methods of chemical process design*. Prentice Hall PTR, New Jersey, first edition.

Bossen, B. S. (1995). *Simulation and optimisation of ammonia plants*. Ph.D. thesis, Department of Chemical Engineering, Technical University of Denmark.

Bossen, B. S.; Jørgensen, S. B. and Gani, R. (1993). Simulation, design and analysis of azeotropic distillation operations. *Ind. Eng. Chem. Res.*, **32**, 620–633.

Bristol, E. H. (1966). On a new measure of interactions for multivariable process control. *IEEE Trans. Auto. Control*, pages 133–134.

Brusis, D.; Frey, T.; Stichlmair, J.; Wagner, I. and Kuppinger, F. F. (2000). MINLP Optimisation of several process structures for the separation of azeotropic ternary mixtures. In S. Pierucci, editor, *European Symposium on Computer Aided Process Engineering - 10*, Florence, Italy, 7-10 May, 2000. Elsevier.

Carlberg, N. A. and Westerberg, A. W. (1989a). Temperature-heat diagrams for complex columns. 3. Underwood's method for the Petlyuk configuration. *Ind. Eng. Chem. Res.*, **28**, 1386–1397.

Carlberg, N. A. and Westerberg, A. W. (1989b). Temperature-heat diagrams for complex columns. 2. Underwood's method for side strippers and enrichers. *Ind. Eng. Chem. Res.*, **28**, 1379–1386.

Cerda, J. and Westerberg, A. W. (1981). Shortcut methods for complex distillation columns. 1. Minimum reflux. *Ind. Eng. Process Des. Dev.*, **20**, 546–557.

Chen, Y. and Fan, L. T. (1993). Synthesis of complex separation schemes with stream splitting. *Chem. Eng. Sci.*, **48**(7), 1251–1264.

Chilton, T. H. and Colburn, A. P. (1935). Distillation and absorption in packed columns - A convenient design and correlation method. *Ind. Eng. Chem.*, **27**(3), 255.

Constantinou, L. and Gani, R. (1994). New Group-Contribution Method for the Estimation of Properties of Pure Compounds. *AIChE J.*, **10**, 1697–1710.

Doherty, M. F. and Buzad, G. (1992). Reactive distillation by design. *Trans IChemE*, **70**, 448–458.

Doherty, M. F. and Caldarola, G. A. (1985). Design and synthesis of homogenous azeotropic distillation 3. Sequencing of Columns for Azeotropic and Extractive Distillations. *Ind. Eng. Chem. Fundam.*, **24**, 474–485.

Douglas, J. M. (1985). A hierachical decision procedure for process synthesis. *AIChE J.*, **31**(3), 353–362.

Dünnebier, G. and Pantelides, C. C. (1999). Optimal design of thermally coupled distillation columns. *Ind. Eng. Chem. Res.*, **38**(1), 162–176.

Duran, M. A. and Grossmann, I. E. (1986). An outer-approximation algorithm for a class of mixed-integer nonlinear programs. *Mathematical Programming*, **36**, 307–339.

Düssel, R.; Groebel, M.; Janowsky, R. and Goedecke, R. (2001). Dividing wall column: 50 years old but still up t date? In *AIChE Spring Meeting 2001*. Houston, Texas, April. 23– 26.

Duvedi, A. and Achenie, L. E. K. (1997). On the Design of Environmentally Benign Refrigerant Mixtures: a Mathematical Programming Approach. *Computers Chem. Engng.*, **21**(8), 915–923.

Espininosa, J.; Scenna, N. and Pérez, G. (1993). Graphical procedure for reactive distillation systems. *Chem. Eng. Comm.*, **119**, 109.

Espininosa, J.; Aguirre, P. and Pérez, G. (1995). Some aspects in the design of multicomponent reactive distillation columns including nonreactive species. *Chem. Eng. Sci.*, **50**(3), 469–484.

Espininosa, J.; Aguirre, P. and Pérez, G. (1996). Some aspects in the design of multicomponent reactive distillation columns with reacting core: Mixtures containing inerts. *Ind. Eng. Chem. Res.*, **35**(12), 4537–4549.

Espininosa, J.; Aguirre, P.; Frey, T. and Stichlmair, J. (1999). Analysis of finishing reactive distillation columns. *Ind. Eng. Chem. Res.*, **38**(1), 187–196.

Fenske, M. R. (1932). Fractionation of Straight-Run Pennsylvania Gasoline. *Ind. Eng. Chem*, **24**, 482–485.

Fidkowski, Z. T. and Agrawal, R. (2001). Multicomponent thermally coupled systems of distillation columns at minimum reflux. *AIChE J.*, **47**(12), 2713–2724.

Fidkowski, Z. T. and Królikowski, L. (1987). Minimum energy requirements of thermally coupled distillation columns. *AIChE J.*, **33**(4), 643–653.

Fidkowski, Z. T.; Doherty, M. F. and Malone, M. F. (1993). Feasibility of separations for distillation of nonideal ternary mixtures. *AIChE J.*, **39**, 1303–1321.

Floudas, C. A. (1995). *Nonlinear and Mixed-Integer Optimization.* Oxford University Press, New York, first edition.

Foucher, E. R.; Doherty, M. F. and Malone, M. F. (1991). Automatic Screening of Entrainers For Homogeneous Azeotropic Distillation. *Ind. Eng. Chem. Res.*, **30**, 760–772.

Fredenslund, A.; Gmehling, J. and Rasmussen, P. (1977). *Vapour-Liquid Equilibria Using UNIFAC.* Elsevier, Amsterdam.

Freshwater, D. C. and Ziogou, E. (1976). Reducing energy requirements in unit perations. *Chem. Eng. Journal*, **11**, 215.

Friedler, F.; Fan, L. T.; Kalotai, L. and Dallos, A. (1998). A Combinatorial Approach for Generating Candidates Molecules with Desired Properties Based on Group Contribution. *Computers Chem. Engng.*, **22**(6), 809–817.

Gani, R. (2002). ICAS Documentation. CAPEC, Technical University of Denmark.

Gani, R. and Jørgensen, S. B. (1994). Multiplicity in numerical solution of nonlinear models. *Comput. Chem. Eng.*, **18**, 55.

Gani, R. and O'Connell, J. P. (1989). A Knowledge Based System For The Selection Of Thermodynamic Models. *Computers Chem. Engng.*, **13**(4–5), 397–404.

Gani, R.; Nielsen, B. and Fredenslund, A. (1991). A Group Contribution Approach to Computer Aided Molecular Design. *AIChE J.*, **37**(9), 1318–1332.

Geffrion, A. M. (1972). Generalized Benders Decomposition. *Juornal of Optimization*, **10**(4), 237–260.

Georgiadis, M. C.; Schenk, M.; Pistikopoulos, E. N. and Gani, R. (2002). The interactions of design, control and operability in reactive distillation systems. *Computers Chem. Engng.*, **26**, 735–746.

Gilliland, E. R. (1940). Multicomponent rectification, -Estimation of the number of theoretical plates as function of the reflux ratio. *Ind. Eng. Chem*, **32**, 1101–1106.

Glinos, K. N. and Malone, M. F. (1984). Minimum reflux, product distribution and lumping rules for multicomponent distillation. *Ind. Eng. Chem. Process Des. Dev.*, **23**, 764–768.

Glinos, K. N. and Malone, M. F. (1985). Design of side-stream distillation columns. *Ind. Eng. Chem. Process Des. Dev.*, **24**, 822–828.

Glinos, K. N. and Malone, M. F. (1988). Optimiality regions for complex column alternatives in distillation systems. *Chem. Eng. Res Des.*, **66**, 229–240.

Gmeling, J. and Onken, U. (1977). *Vapour liquid equilibrium data collection, DECHEMA chemistry data series, Vil. 1-8*. DECHEMA, Frankfurt.

Górak, A. and Hoffmann, A. (2001). Catalytic distillation in structured packings: Methyl acetate synthesis. *AIChE J.*, **47**(5), 1067–1076.

Grossmann, I. E. and Morari, M. (1983). Operability, reciliency and flexibility - Process design objectives for a changing world. In *Proceedings for the second international conference on Foundations of Computer-Aided Design*, pages 931–1010.

Gumus, Z. H. and Ciric, A. R. (1997). Reactive distillation column design with vapour/liquid/liquid equilibria. *Computers Chem. Eng.*, **21**.

Güttinger, T. E. and Morari, M. (1996). Multiple steady states in homogenous separation sequences. *Ind. Chem. Eng. Res.*, **35**(12), 4597–4611.

Güttinger, T. E.; Dorn, C. and Morari, M. (1997). Experimental study on multiple steady states in homogenous azeotropic distillation. *Ind. Chem. Eng. Res.*, **36**(3), 794–802.

Halvorsen, I. J. (2001). *Minimum energy requirements in complex distillation arrangements*. Ph.D. thesis, Department of Chemical Engineering, Technical University of Norway.

Harper, P. and Gani, R. (2000). Computer Aided Tools for Design/Selection of Environmentally Friendly Substances. In M. El-Halwagi and S. Sikdar, editors, *Process Design Tools for the Environment*, chapter 7. Taylor and Francis, Philadelphia.

Harper, P. M. (2000). *Multi-phase, multi-level framework for computer aided molecular design*. Ph.D. thesis, Department of Chemical Engineering, Technical University of Denmark.

Harper, P. M. and Hostrup, M. (2002). *ProPred Manual*. CAPEC Internal Report, Department of Chemical Engineering, Technical University of Denmark.

Heaven, D. L. (1970). *Optimum sequencing of distillation columns in multicomponent fractionation*. Master's thesis, University of California, Berkeley, CA. M.Sc. Thesis.

Hendry, J. E. and Hughes, R. R. (1972). Generating separation process flowsheets. *Chem. Eng. Prog*, **68**(6), 71–76.

Hernández, S. and Jiménez, A. (1999). Design of energy efficient Petlyuk systems. *Computers Chem. Eng.*, **23**, 1005–1010.

Hillier, F. S. and Lieberman, G. J. (1986). *Introduction to operations research*. Holden Day, San Francisco.

Hoch, P. M. and Eliceche, A. M. (1999). Energy savings in operation of distillation columns. In *PRESS'99. Second conference on process integration, modelling and optimisation for energy saving and pollution reduction*, pages 335–346.

Hömmerich, U. and Rautenbach, R. (1998). Design and optimisation of combined pervaporation/distillation processes for the production of MTBE. *J. membrane sci.*, **146**, 53–64.

Hostrup, M. (2001). *Integrated approach to computer aided process synthesis*. Ph.D. thesis, Department of Chemical Engineering, Technical University of Denmark.

Hostrup, M.; Harper, P. M. and Gani, R. (1999). Design Of Environmentally Benign Processes: Integration Of Solvent Design And Process Synthesis. *Computers and Chem. Eng.*, **23**, 1395–1414.

Hu, Z.; Chen, B. and Rippin, D. R. T. (1991). Synthesis of general distillation-based separation systems. In *AIChE Annual Meeting 1991*. Los Angeles, CA.

Hunek, J.; Gal, S.; Posel, F. and Glavić, P. (1989). Separation of an azeotropic mixture by reverse extractive distillation. *AIChE J.*, **35(7)**, 1207–1209.

Ismail, S. R.; Pistokopoulos, E. N. and Papalexandri, K. P. (1999). Modular representation synthesis framework for homogenous azeotropic separation. *AIChE J.*, **45**(8), 1701–1720.

Jaksland, C. (1996). *Seperation Process Design and Synthesis Based on Thermodynamic Insights*. Ph.D. thesis, Department of Chemical Engineering, Technical University of Denmark.

Jaksland, C. A.; Gani, R. and Lien, K. (1995). Separation process design and synthesis based on thermodynamic insights. *Chem. Eng. Sci.*, **50**(3), 511–530.

Joback, K. G. and Reid, R. C. (1987). Estimation of Pure-Component Properties from Group Contributions. *Chem. Engng. Commun.*, **57**, 233–243.

Joback, K. G. and Stephanopoulos, G. (1995). Searching Spaces of Discrete Solutions: The Design of Molecules Possessing Desired Physical Properties. *Advances in Chemical Engineering*, **21**, 257–311.

Julka, V. and Doherty, M. F. (1993). Geometric nonlinear analysis of multicomponent nonideal distillation: A simple computer-aided design procedure. *Chem. Eng. Sci.*, **48**(8), 1367–1391.

Kaibel, G.; Blass, E. and Köhler, J. (1990). Thermodynamics - guideline for the developments of distillation Column arrangements. *Gas Separation & Purification*, **4**, 109–114.

Kenig, E.; Jakobsson, K.; Banik, P.; Aittamaa, J.; Górak, A.; Koskinen, M. and Wettmann, P. (1999). An integrated tool for synthesis and design of reactive distillation. *Chem. Eng. Sci.*, **54**, 1347–1352.

Kenig, E.; Bäder, H.; Górak, A.; Adrian, T. and Schoenmakers, H. (2001). Investigation of ethyl acetate reactive distillation process. *Chem. Eng. Sci.*, **56**, 6185–6193.

Kim, Y. H. (2001). Rigorous design of fully thermally coupled distillation column. *J. Eng. Chem. Japan*, **34**(2), 236–243.

King, C. J. (1980). *Separation Processes*. McGraw-Hill, Inc., New York.

Kirkbride, C. G. (1944). *Petroleum Refiner*, **23**(9), 87–102.

Knapp, J. P. and Doherty, M. F. (1992). A new pressure-swing distillation process for separating homogenous azeotropic mixtures. *Ind. Eng. Chem. Res.*, **31**, 346.

Kocis, G. R. and Grossmann, I. E. (1989). Modelling and decomposition strategy for the MINLP optimization of process flowsheets. *Computers and Chem. Eng.*, **7**, 797–819.

Laroche, L.; Bekiaris, N.; Andersen, H. W. and Morari, M. (1992). The curious behaviour of homogenous azeotropic distillation. *AIChE Journal*, **38**(9), 1309–1328.

Lee, J. W.; Hauen, S. and Westerberg, A. W. (2000). Graphical methods for reaction distribution in a reactive distillation column. *AIChE Journal*, **46**(6), 1218–1233.

Lestak, F.; Deak, G. and Fónyo, Z. (1989). Comparison of a group method with the empiracal correlation based on limiting flows and stage requirements for distillation. *Hung. J. Ind. Chem.*, **17**, 81–92.

Levy, S. G. and Doherty, M. F. (1986). Design and synthesis of homogenous azeotropic distillation 4. Minimum reflux calculations for multiple feed columns. *Ind. Eng. Chem. Fundam.*, **25**, 269–279.

Lewin, D. R. (1996). A simple tool for disturbance resiliency diagnosis and feedforward control design. *Computers Chem. Eng.*, **20**, 13–25.

Linstrom, P. J. and Mallard, W. G. (2001). The NIST Chemistry webbook: A chemical data resource on the internet. *J. Chem. Eng. data*, **46**, 1059–1063.

Lydersen, A. L. (1955). Estimation of Critical Properties of Organic Compounds. Technical Report 3, Univ. Wisconsin Coll. Eng., Madison, Wisconsin, USA.

Lyman, L. J.; Reehl, W. F. and Rosenblatt, D. H., editors (1990). *Handbook of Chemical Property Estimation Methods, Environmental Behavior of Organic Compounds*. American Chemical Society, Washington DC.

Magnussen, T.; Michelsen, M. L. and Fredenslund, A. (1979). Azeotropic distillation using UNIFAC. *Inst. Chem. Eng. Symp. Ser.*, **56**.

Malone, M. F. and Doherty, M. F. (1995). Separation system synthesis for nonideal liquid mixtures. *AIChE Symposium series*, **91**, 9–18.

Marcoulaki, E. C. and Kokossis, A. C. (1998). Molecular Design Synthesis Using Stochastic Optimisation as a Tool for Scoping and Screening. *Computers chem. Engng.*, **22**(Suppl.), S11–S18.

Marrero, J. (1998). *Quick-Guide for ProCAMD*. CAPEC Internal Report, Department of Chemical Engineering, Technical University of Denmark.

Marrero, J. and Gani, R. (2001). Group-Contribution based estimation of pure component properties. *FLUID*, **183**.

Martin, H. Z. and Brown, G. G. (1939). *Trans. AIChE*, **35**, 679–708.

McCabe, W. L. and Thiele, E. W. (1925). Grahical Design of Fractionating Columns. *Ind. Eng. Chem.*, **17**(6), 605–611.

McCarthy, E.; Fraga, E. S. and Ponton, J. W. (1998). An automated procedure for multicomponent product separation synthesis. *Computers chem. Engng.*, **22**, 77–88.

McDonough, J. A. and Holland, C. D. (1961). Determination of the conditions at minimum reflux when the components are most and least volatile components. *Chem. Eng. Sci.*, **16**(3).

Meiers, R.; v. Watzdorf, R. and Marquardt, W. (1995). Näherungsverfahren zur auslegung von Destillationskolonnen mit Seitenströmen. *Chem.-Ing. Tech.*, **67**, 612–615.

Monroy, R.; Pérez-Cisneros, E. S. and Alvarez, J. (2000). High purity ethylene glycol reactive distillation column. *Chem. Eng. Sci.*, **55**, 4925.

Myasnikov, S. K.; Uteshinsky, A. D.; Kasymbekov, B. A. and Kulov, N. N. (2002). CHISA 2002 Proceedings volume.

Nemhauser, G. L. and Wolsey, L. A. (1988). *Integer and combinatorial optimisation*. John Wiley, New York.

Nielsen, T. L.; Abildskov, J.; Harper, P. M.; Papaeconomou, I. and Gani, R. (2001). The CAPEC database. *J. Chem. Eng. data*, **46**, 1041–1044.

Nikolaides, I. P. and Malone, M. F. (1987). Approximate design of multiple feed/side-stream distillation systems. *Ind. Eng. Chem. Res.*, **26**, 1839–1845.

Nishida, N.; Stephanopolous, G. and Westerberg, A. W. (1981). A review of process synthesis. *AIChE J.*, **27**(3), 321–348.

Oliver, E. D. (1966). *Diffusional Separation Processes: Theory, Design and Evaluation*. John Wiley and Sons, New York.

Peng, D. Y. and Robinson, D. (1976). A new two-constant equation of state. *Ind. Eng. Chem. Fundam.*, **15**, 59–64.

Pérez-Cisneros, E. S.; Gani, R. and Michelsen, M. L. (1997). Reactive separation systems - I. Computation of physical and chemical equilibrium. *Chem. Eng. Sci.*, **52**(4), 527–543.

Peterson, E. J. and Partin, L. R. (1997). Temperature sequences for categorizing all ternary distillation boundary maps. *Ind. Eng. Chem. Res.*, **36**(5), 1799–1811.

Petlyuk, F. B. (1997). Simple methods for predicting feasible sharp separations of azeotropic mixtures. *Theoretical Foundations of Chem. Eng.*, **32**(3), 245–253.

Petlyuk, F. B. and Danilov, R. Y. (1998). Sharp distillation of azeotropic mixtures in a two-feed column. *Theoretical Foundations of Chem. Eng.*, **33**(9), 233–242.

Petlyuk, F. B. and Danilov, R. Y. (2001). Theory of distillation trajectory bundles and its application to the optimal design of separation units:Distillation trajectory bundles at finite reflux. *Trans IChemE*, **79**(Part A), 733–746.

Petlyuk, F. B.; Platonov, V. M. and Slavinskii, D. M. (1965). Thermodynamically optimal method for separating multicomponent mixtures. *International Chem. Eng.*, **5**(3), 555–561.

Petrochemical processes '97 (1997). Benzene production - Petrochemical processes '97. *Hydrocarbon Processing*, page pp. 112.

Pham, H. N. and Doherty, M. F. (1990a). Design and Synthesis of heterogenous azeotropic distillation: I. Heterogenous phase diagrams. *Chem. Eng. Sci.*, **45**(7), 1823–1836.

Pham, H. N. and Doherty, M. F. (1990b). Design and Synthesis of heterogenous azeotropic distillation: II. Residue curve maps. *Chem. Eng. Sci.*, **45**(7), 1837–1843.

Pham, H. N. and Doherty, M. F. (1990c). Design and Synthesis of heterogenous azeotropic distillation: III. Column sequences. *Chem. Eng. Sci.*, **45**(7), 1845–1854.

Pistikopoulos, E. N. and Stefanis, S. K. (1998). Optimal Solvent Design for Environmental Impact Minimization. *Computers Chem. Engng.*, **22**(6), 717–733.

Poling, B. E.; Prausnitz, J. M. and O'Connell, J. (2000). *The Properties of Gasses and Liquids*. McGraw-Hill, New York, fifth edition.

Ponchon, M. (1921). *Tech. Moderne*, **13**(20), 55.

Pressly, T. G. and Ng, K. M. (1998). A break-even analysis of distillation-membrane hybrids. *AIChE J.*, **44**(1), 93–105.

ProVision User's Guide (1994). *Simulation Science Inc.*. Brea, CA, USA.

Renon, H. and Prausnitz, J. M. (1968). *AIChE J.*, **14**, 135.

Rév, E.; Szitkai, E. Z.; Mizsey, P. and Fónyo, Z. (2001). Energy savings of integrated and coupled distillation systems. *Computers Chem. Engng.*, **2**, 119–140.

Reyes, J. A.; Lómez, A. G. and Marcilla, A. (2000). Graphical concepts to orient the minimum reflux ratio calculation on ternary mixtures distillation. *Ind. Eng. Chem. Res.*, **39**, 3912–3919.

Robinson, C. S. and Gilliland, E. R. (1950). *Elements of Fractional Distillation*. McGraw-Hill, New York.

Rong, B.; Kraslawski, A. and Nyström, L. (2000). The synthesis of thermally coupled distillation flowsheets for separations of five-component mixtures. *Computers Chem. Eng.*, **24**, 247–252.

Rooks, R. E.; Malone, M. F. and Doherty, M. F. (1996). A geometric design method for side-stream distillation columns. *Ind. Eng. Chem. Res.*, **35**, 3653–3664.

Rudd, H. (1992). Thermal coupling for energy efficiency. *Suppl. to The Chemical Engineer*, pages 14–15.

Safrit, B. T. and Westerberg, A. W. (1997). Algorithm for generating the distillation regions for azeotropic multicomponent mixtures. *Ind. Eng. Chem. Res.*, **36**, 1827–1840.

Sander, U. and Soukop, P. (1988). Design and operation of a pervaporation plant for ethanol dehydration. *J. membrane sci.*, **36**, 463–475.

Sano, T.; Hasagawa, M.; Kawakami, Y. and Yanagishita, H. (1995). Separation of MeOH / Methyl-tert-Butyl Ether Mixture by Pervaparation using silicate membrane. *Journal of membrane science*, **107**, 193.

Savarit, R. (1922). *Arts et Metiers.*, pages 65, 142, 178, 241, 266, 307.

Scheibel, E. (1946). Multi component tray calculations based on equilibrium curve of key components. *Ind. Eng. Chem.*, **38**, 397–399.

Seader, J. D. and Henley, E. J. (1998). *Separation Process Principles*. John Wiley and Sons, New York.

Seider, W. D.; Seader, J. D. and Lewin, D. R. (1999). *Process Design Principles*. John Wiley and Sons, New York.

Shah, P. B. and Kokossis, A. C. (1997). Conceptual programming: Towards the development of new targeting and screening technology using engineering and optimisation methods. In *AIChE Topical conference on separation science and technologies*, New York.

Shah, P. B. and Kokossis, A. C. (2001). Knowledge based models for the analysis of complex separation processes. *Computers Chem. Eng.*, **25**, 867–878.

Shiras, R. N.; Hanson, D. N. and Gibson, C. H. (1950). Calculation of minimum reflux in distillation columns. *Ind. Eng. Chem.*, **42**(5), 871–876.

Siirola, J. J. (1995). An industrial perspective on process synthesis. In *AIChE symposium series*, volume 91, pages 222–234.

Skogestad, S. and Morari, M. (1987). The ffect of disturbance directions on closed-loop performance. *Ind. Eng. Chem. Res.*, **26**, 2029–2035.

Smith, L. A. and Huddleston, M. N. (1982). New MTBE Design - Now Commercial. *Hydrocarbon Processing*, **3**, 121.

Smith, R. (1995). *Chemical process design*. McGraw-Hill Int. Editions, New York, first edition.

Soave, G. (1972). Equilibrium constants from a modified Redlich-Kwong equation of state. *Chem. Eng. Sci.*, **27**, 1197–1203.

Stepanski, M. and Haller, U. (2000). Economic recovery of meta-xylene. *Sulzer Technical Review*, **3**, 8–9.

Stephanoloulos, G. and Westerberg, A. W. (1976). Studies in process synthesis - II, Evolutionary synthesis of optimal process flowsheets. *Chem. eng. Sci.*, **31**, 195.

Stephanopoulos, G. (1984). *Chemical process control - An introduction to theory and practice*. John Wiley, New York.

Stichlmair, J. G. and Herguijuela, J.-R. (1992). Separation regions and processes of zeotropic and azeotropic ternary distillation. *AIChE J.*, **38**(10), 1523–1535.

Stichlmair, J. G.; Fair, J. R. and Bravo, J. L. (1989). Separation of azeotropic mixtures via enhenced distillation. *Chem. Eng. Prog*, **85**, 63–69.

Stitt, E. H. (2002). Reactive distillation for toluene disproportionation: a technical and economic evaluation. *Chem. Eng. Sci.*, **57**, pp. 1537.

Szitkai, Z.; Lelkes, Z.; Rev, E. and Fonyo, Z. (2002). Optimisation of hybrid ethanol dehydration systems. *Chemical Engineering and Processing*, **41**, 631–646.

Taylor, R. and Krishna, R. (2000). Review - Modelling reactive distillation. *Chem. Eng. Sci.*, **55**, 5183–5229.

Tedder, D. W. and Rudd, D. F. (1978). Parametric studies in industrial distillation: PArt 1. Design comparisons. *AIChE Journal*, **24**(2), 303–315.

Terranova, B. E. and Westerberg, A. W. (1989). Temperature-heat diagrams for complex columns. 1. Intercooled/interheated distillation columns. *Ind. Eng. Chem. Res.*, **28**, 1374–1379.

Thomson, G. H. and Larsen, A. H. (1996). DIPPR: Satisfying industry needs. *J. Chem. Eng. data*, **41**, 930–934.

Thomson, R. W. and King, C. J. (1972). Systematic synthesis of separation schemes. *AIChE J.*, **18**(5), 941–948.

Triantafyllou, C. and Smith, R. (1992). The design and optimisation of fully thermally coupled distillation columns. *Trans IChemE*, **70**(Part A), 118–132.

Ung, S. and Doherty, M. F. (1995). Vapour-liquid phase equilibrium in systems with multiple chemical reactions. *Chem. Eng. Sci.*, **50**(1), 23–48.

Vaidyanathan, R. and El-Halwagi, M. (1994). Computer-Aided Design of High Performance Polymers. *Journal of Elastomers and Plastics*, **26**(3), 277–293.

van Dongen, D. B. and Doherty, M. F. (1985). Design and synthesis of homogenous azeotropic distillation 1. Problem formulation for a single column. *Ind. Eng. Chem. Fundam.*, **24**, 454–463.

van Krevelen, D. W. (1990). *Properties of Polymers: Their Correlation with Chemical Structure; Their Numerical Estimation and Prediction from Additive Group Contributions*. Elsevier, Amsterdam, third edition.

Venkatasubramanian, V.; Chan, K. and Caruthers, J. M. (1995). Genetic Algorithmic Approach for Computer-Aided Molecular Design. *ACS Symposium Series*, **589**, 396–414.

Wahnschafft, O. M. and Westerberg, A. W. (1993). The product composition regions of azeotropic distillation columns 2. Separability in two-feed columns and entrainer selection. *Ind. Eng. Chem. Res.*, **32**, 1108–1120.

Wahnschafft, O. M.; Jurian, T. P. and Westerberg, A. W. (1991). SPLIT: A separation process designer. *Comput. Chem. Eng.*, **15**, 565.

Wahnschafft, O. M.; Koehler, J. W.; Blass, E. and Westerberg, A. W. (1992a). The product composition regions of single-feed azeotropic distillation columns. *Ind. Eng. Chem.*, **31**, 2345–2362.

Wahnschafft, O. M.; Rudulier, J. P. L.; Blania, P. and Westerberg, A. W. (1992b). SPLIT: II Automated synthesis of hybrid liquid separation systems. *Comput. Chem. Eng.*, **16**, 305.

Wahnschafft, O. M.; Rudulier, J. P. L. and Westerberg, A. W. (1993). A problem decomposition approach for the synthesis of complex separation processes with recycling. *Ind. Eng. Chem. Res.*, **32**, 1121.

Wakeham, W. A.; Cholakov, G. S. and Stateva, R. P. (2001). Consequences of property erors on the design of distillation columns. *FLUID*, **185**, 1–12.

Widagdo, S. and Seider, W. D. (1996). Azeotropic Distillation. *AIChE Journal*, **42**(1), 96–130.

Wilson, G. M. (1964). *J. Am. Chem. Soc.*, **86**, 127.

Wolff, E. A. and Skogestad, S. (1995). Operation of integrated three-product (Petlyuk) distillation columns. *Ind. Eng. Chem. Res.*, **34**(6), 2094–2113.

Yeomans, H. and Grossmann, I. E. (1999). Nonolinear disjunctive programming model for synthesis of heat integrated distillation sequences. *Computers Chem. Engng.*, **23**, 1135–1151.

Zhou, M.; Xu, C. and Yu, G. (1995). Adsorptive distillation - Novel hybrid separation process. *Progress in Natuaral Science*, **3**(1), 291–298.

Index